Heavy-ion collisions.
The Quark Gluon Plasma

A. Marin

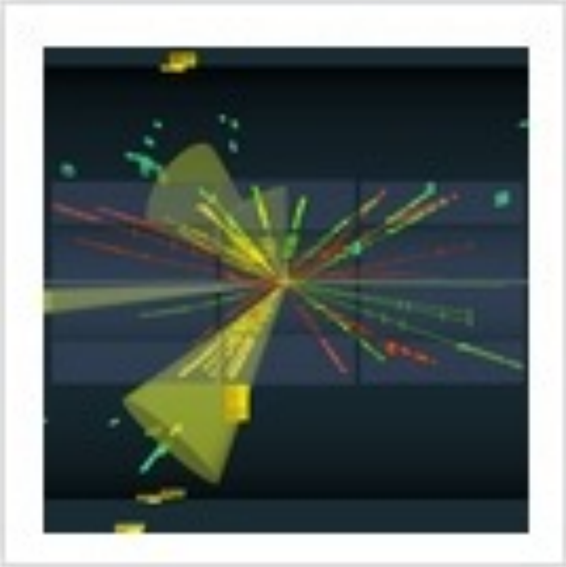

TAE 2024- International Workshop on High Energy Physics
Benasque Science Center, Sep 1-14, 2024

GSI

Table of Contents

- Introduction. History of HIC.
- The LHC experiments: ALICE, LHCb, CMS and ATLAS

Physics observables:

- Global properties
- Heavy quarks and high p_T
- Quarkonia
- Photons and dileptons

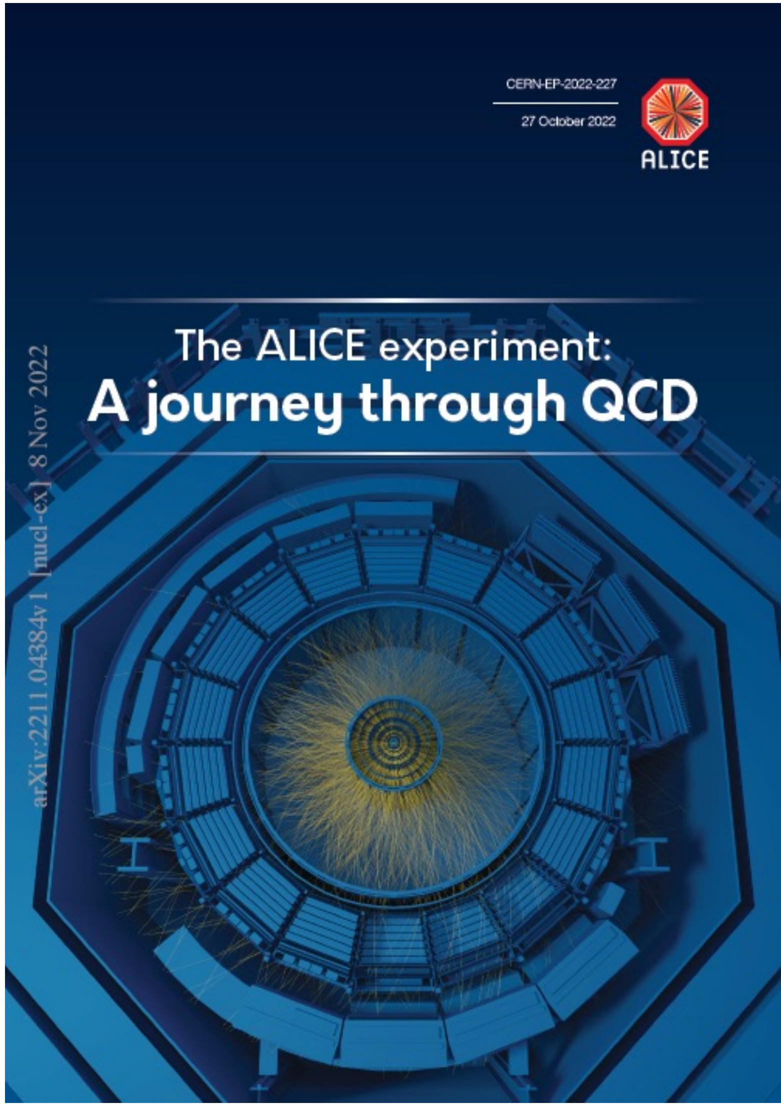

EPJC (2024) 84:813

Bibliography

- Ultra-relativistic Heavy-Ion Collisions. Ramona Vogt.
- Introduction to High-Energy Heavy-Ion Collisions, C.Y. Wong, World Scientific, 1994
- The Physics of the Quark-Gluon Plasma, S. Sarkar, H. Satz and B. Sinha, Lecture notes in physics, Volume 785, 2010
- Heavy Ions, F. Bellini, CERN Summer Student Lectures 2024
- Heavy-Ion Physics, K. Reygers, HASCO Summer School 2024
- Modern aspects of Quark Gluon Plasma, Stachel, Braun-Munzinger, Reygers, SS2023 Uni Heidelberg
- A journey through QCD, ALICE Collaboration, arXiv: 2211.04384, EPJC (2024) 84:813

Goals of High Energy Heavy-Ion Collisions

- Understand two basic properties of the strong interaction: (de)confinement, chiral symm. breaking/restoration

- Probe conditions quark-hadron phase transition in primordial Universe (few μsec after the Big Bang)

- Study the phase diagram of QCD matter: produce and study the QGP

Quantum Chromodynamics (QCD)

- QCD:

Gauge field theory describing the strong interaction of colored quarks and gluons

- QCD potential

$$V = -\frac{4}{3}\frac{\alpha_s}{r} + kr$$

  - Asymptotic freedom at short distance:
    for large Q exchange processes

  - Confinement at large distance:
    ordinary matter (colorless hadrons)

Phys. Rev. D 110, 030001 (2024)

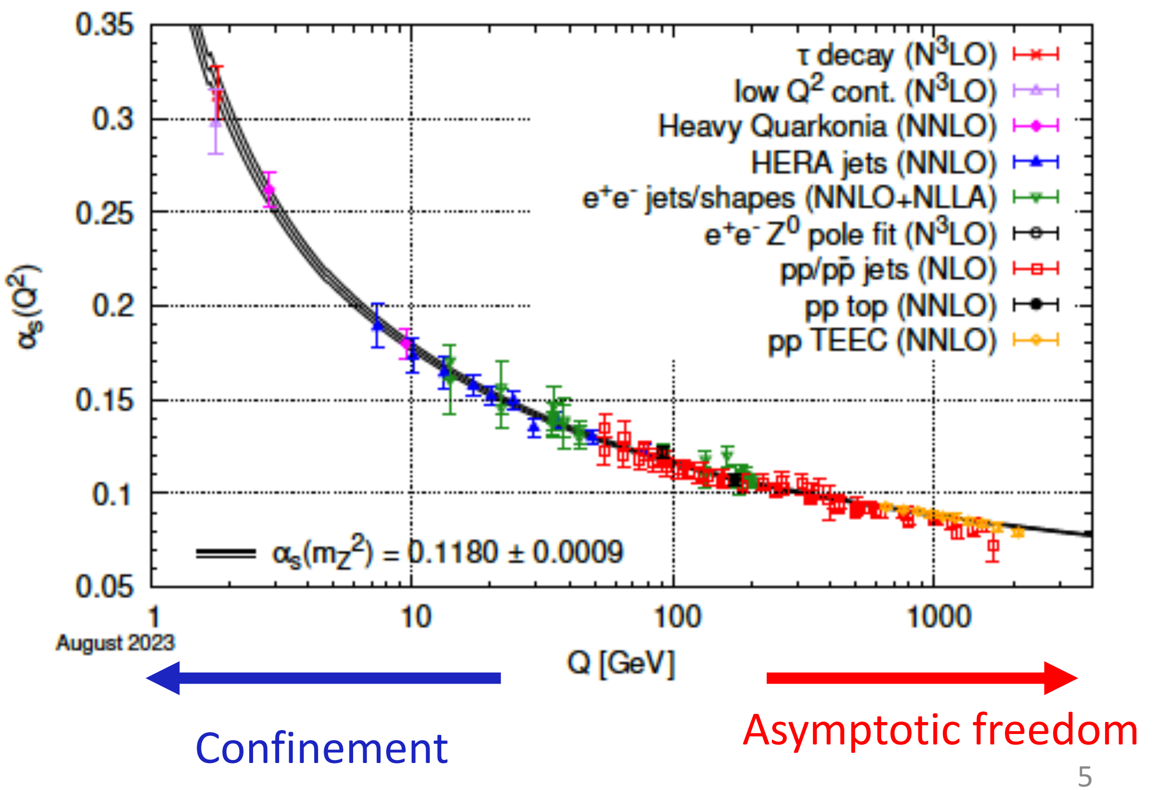

Lattice QCD: Pressure and energy density

A. Bazavov, et al, PRD90, 094503 (2014)

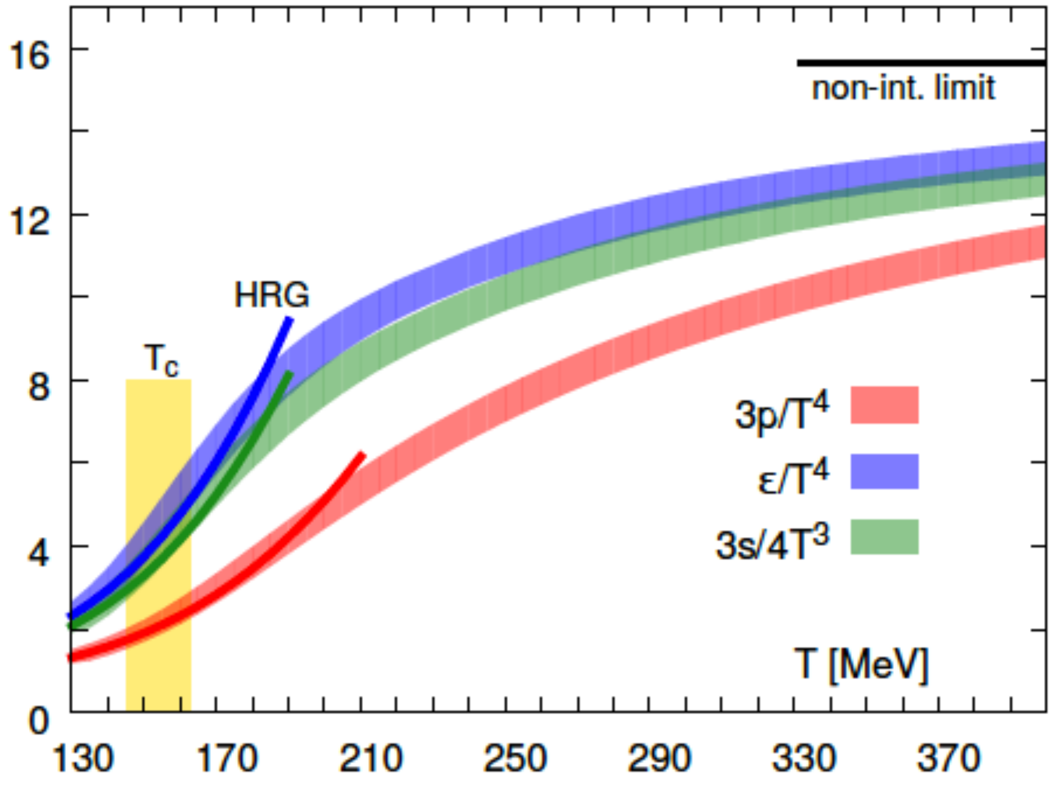

Allows for calculations in the non-perturbative regime of QCD
(2+1) flavor QCD
Two light (u,d) + one heavir quark (s)

Transition to QGP (cross-over):

T_c = 156.5 ± 1.5 MeV, ε_c = 0.42 ± 0.06 GeV/fm^3

Hot QCD Collaboration, PLB 795 (2019) 15

Above T_c the energy goes into more degrees of freedom

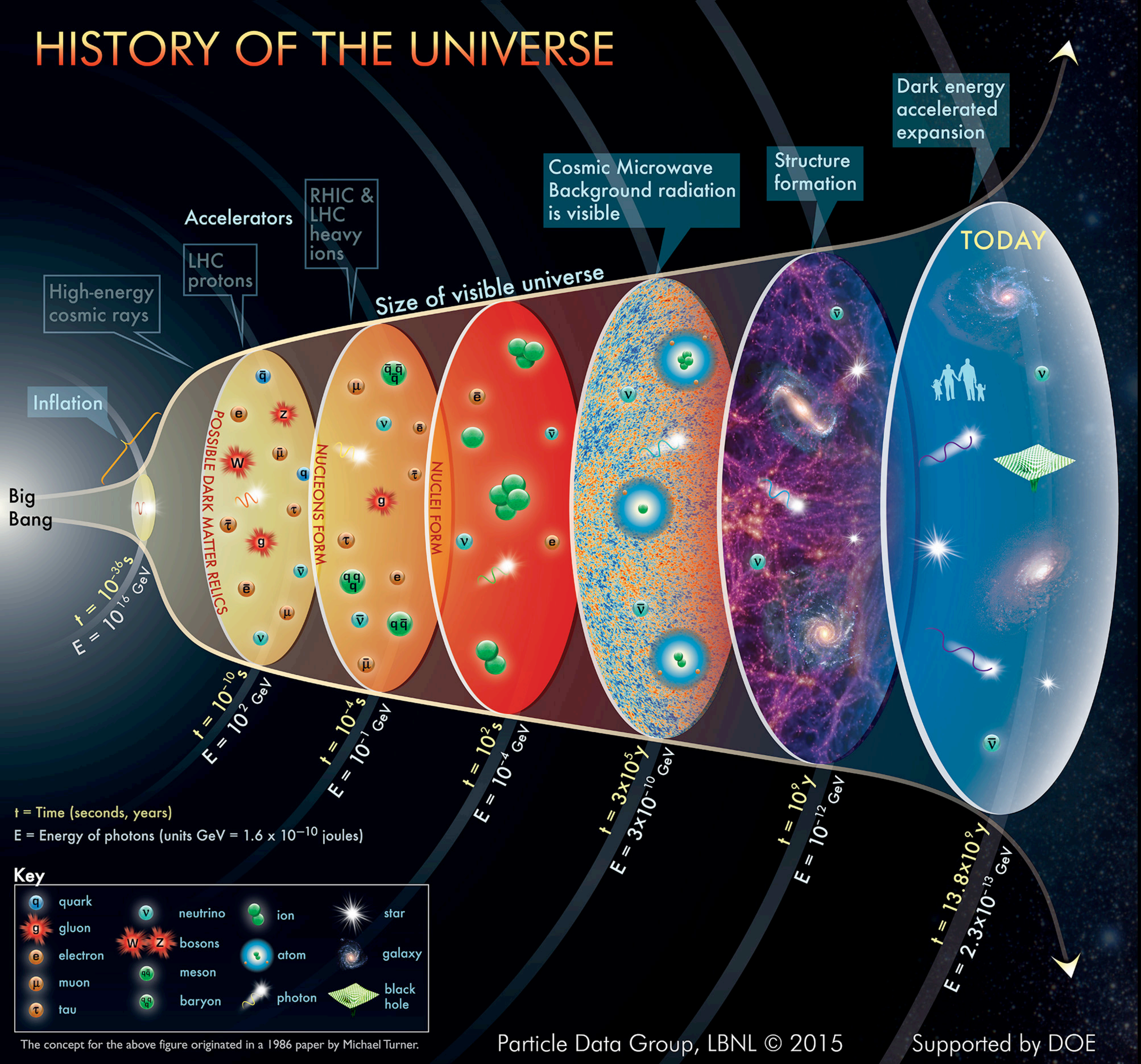

Transitions in the early universe

Electroweak transition:

T ~ 100 GeV, t ~10^{-12} s

QCD transition:

T ~ 150 MeV, t ~10^{-5} s

Phase transitions in the early and the present universe, Ann. Rev. Nucl. Part. Sci. 56, 441-500 (2006)

QGP in the laboratory

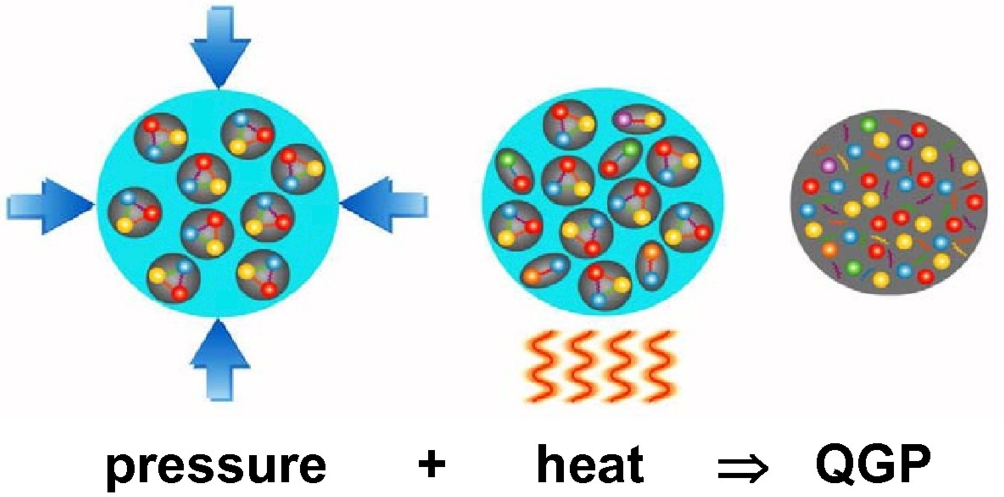

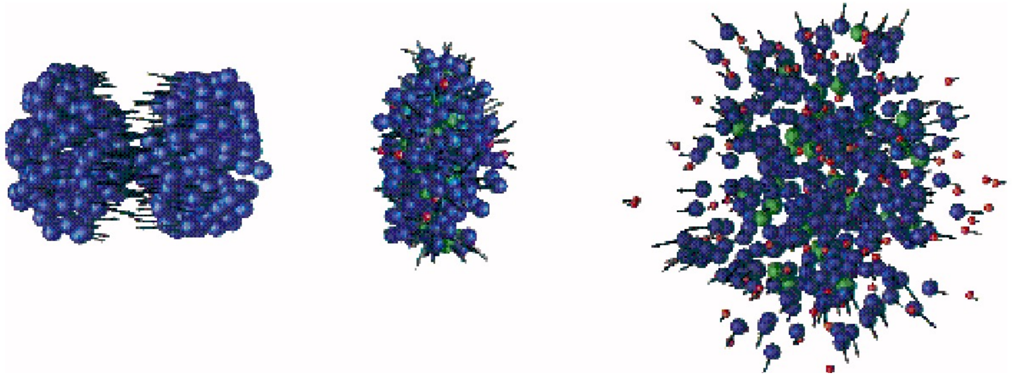

Key parameters:
Bombarding energy and
collision centrality

Nature

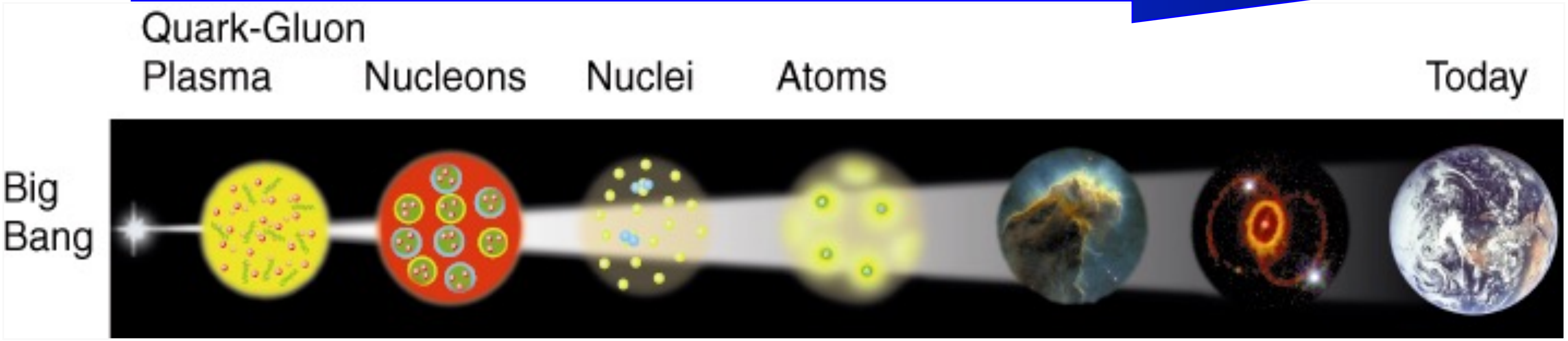

10 $^{-6}$ sec   10 $^{-4}$ sec   3 min   15 Mil Years

Experiment

Time evolution of heavy-ion collisions

Courtesy C. Shen

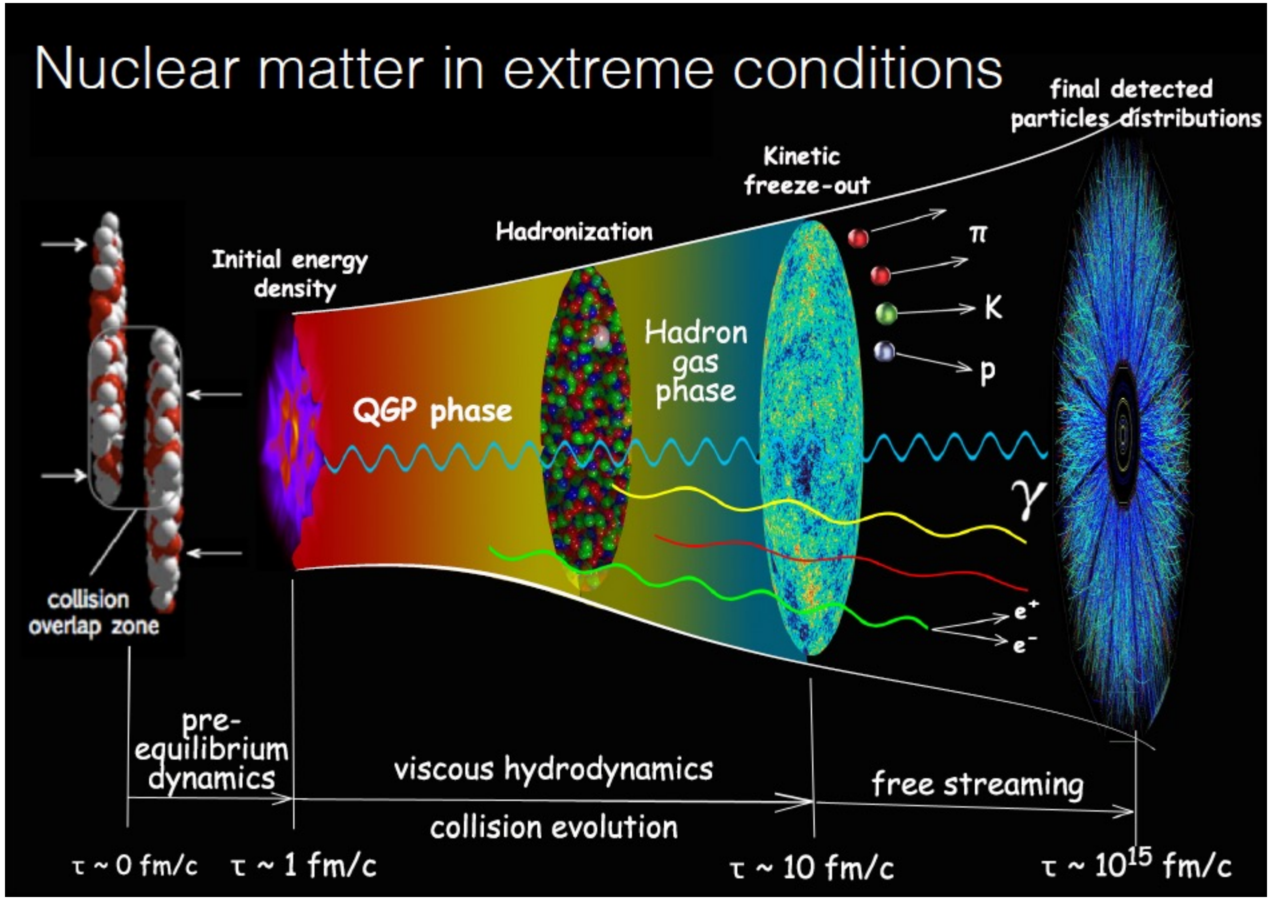

1. Initial Nuclei Collide
2. Partons are Freed from Nuclear Wavefunction
3. Partons interact and potentially form a QGP
4. System expands and cools off
5. System Hadronizes and further Re-Scatters
6. Hadrons and Leptons stream towards our detectors

Study different probes

↓

Collect information at each stage

↓

Characterize the QGP and hadron gas phase

AA collisions
pA and pp : control and reference systems

History of Heavy Ion Collisions

- Bevalac (LBL)
  - fixed target (1975-1986) $\sqrt{s}$ <2.4 GeV
- SIS (GSI)
  - fixed target (1989-) $\sqrt{s}$ <2.7 GeV
- AGS (BNL)
  - fixed target (1986-1998) $\sqrt{s}$ <5 GeV
- SPS (CERN)
  - fixed target (1986-2003) $\sqrt{s}$ <20 GeV
- RHIC (BNL)
  - collider (2000-) $\sqrt{s}$ <200 GeV
- LHC (CERN)
  - collider (2008-) $\sqrt{s}$ <5500 GeV
- FAIR (GSI)
  - fixed target (2027-) $\sqrt{s}$ <9 GeV

"Livingston plot"
J. Schukraft nucl-ex/0602014

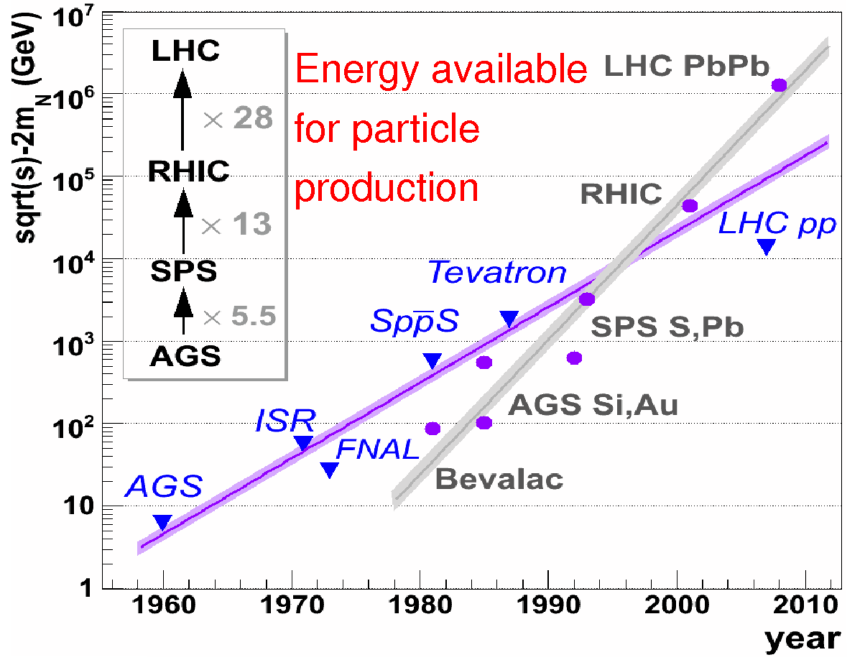

Energy doubling every ~4 (1.7) years for p (ion) beams.

Exploration of the QCD phase diagram

EPJC (2024) 84:813

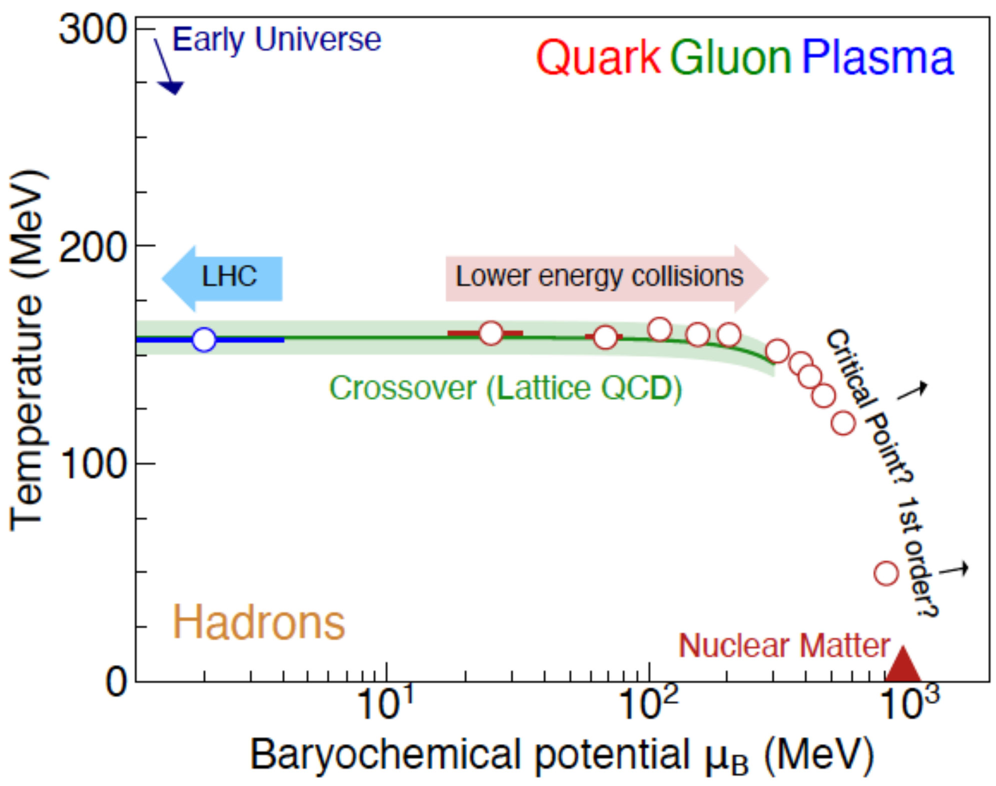

Heavy-ion collisions

↓

Explore and characterize phase diagram of QCD matter

QGP

- quarks and gluons are deconfined
- hot and dense thermalized medium
- strongly interacting
- existed few μs after the Big Bang
- predicted by lattice QCD above a critical energy density

Heavy ion collisions at LHC

	SPS	RHIC	LHC
$\sqrt{s_{NN}}$ (GeV)	17	200	2760(5500)
dN_{ch}/dy	430	730	1584
τ^0_{QGP} (fm/c)	1	0.2	0.1
T/T_c	1.1	1.9	3.0-4.7
ε (GeV/fm^3)	3	5	>18
τ_{QGP} (fm/c)	≤2	2-4	≥10
τ_f (fm/c)	~10	20-30	15-60
V_f(fm^3)	few 10^3	few 10^4	few 10^5

faster
hotter
denser
longer

bigger

LHC: Entering a new regime

C W Fabjan 2008 J. Phys. G: Nucl. Part. Phys. 35, 104038

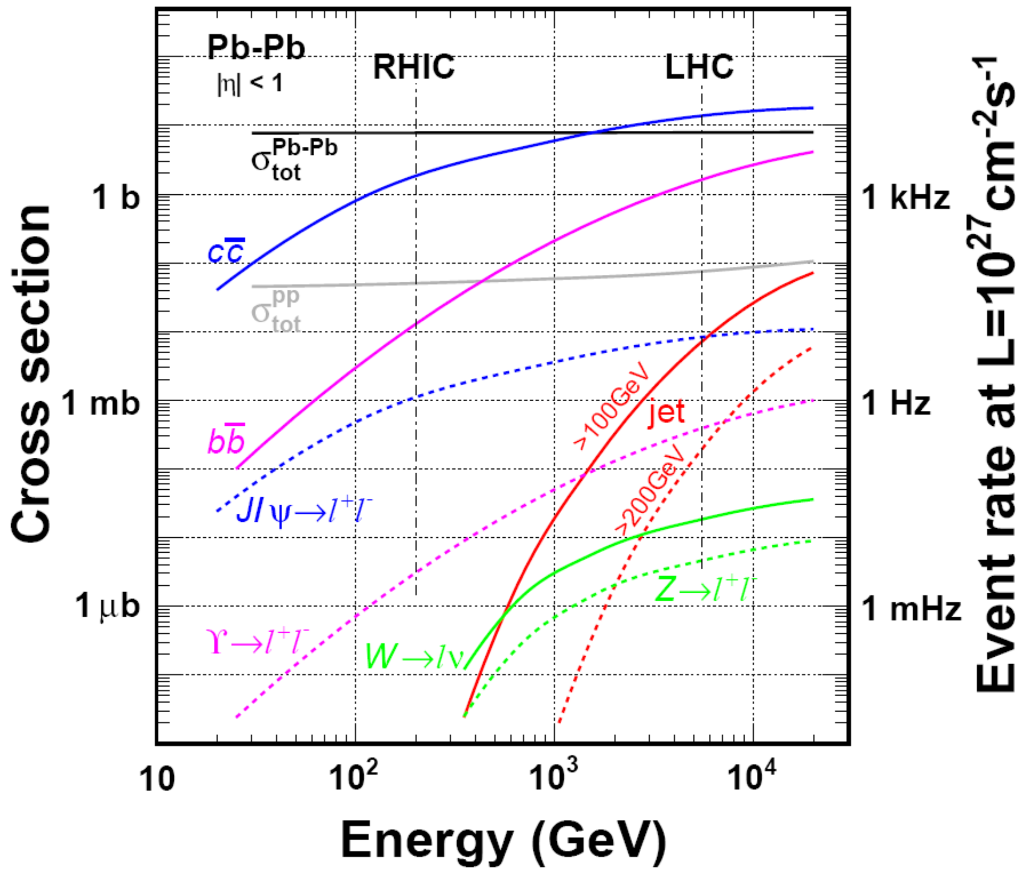

Cross-sections of interesting probes expected to increase by factors

~ 10 (cc) to

~ 10^2 (bb) to

~ > 10^5 (very high p_T jets) ;

Hard probes of the medium accessible at LHC

Direct photons are abundantly produced at LHC

The LHC

The Large Hadron Collider

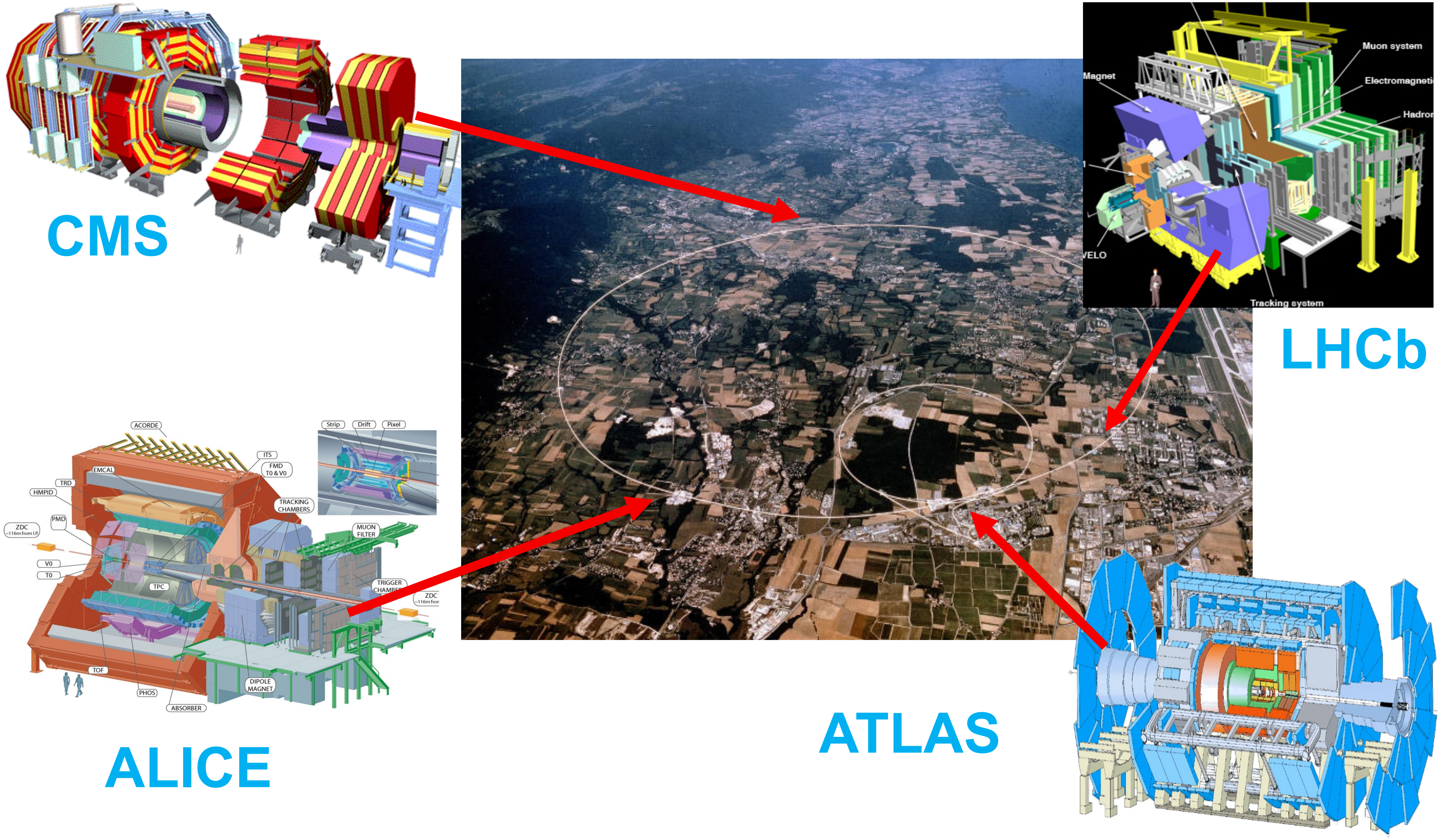

LHC experiments

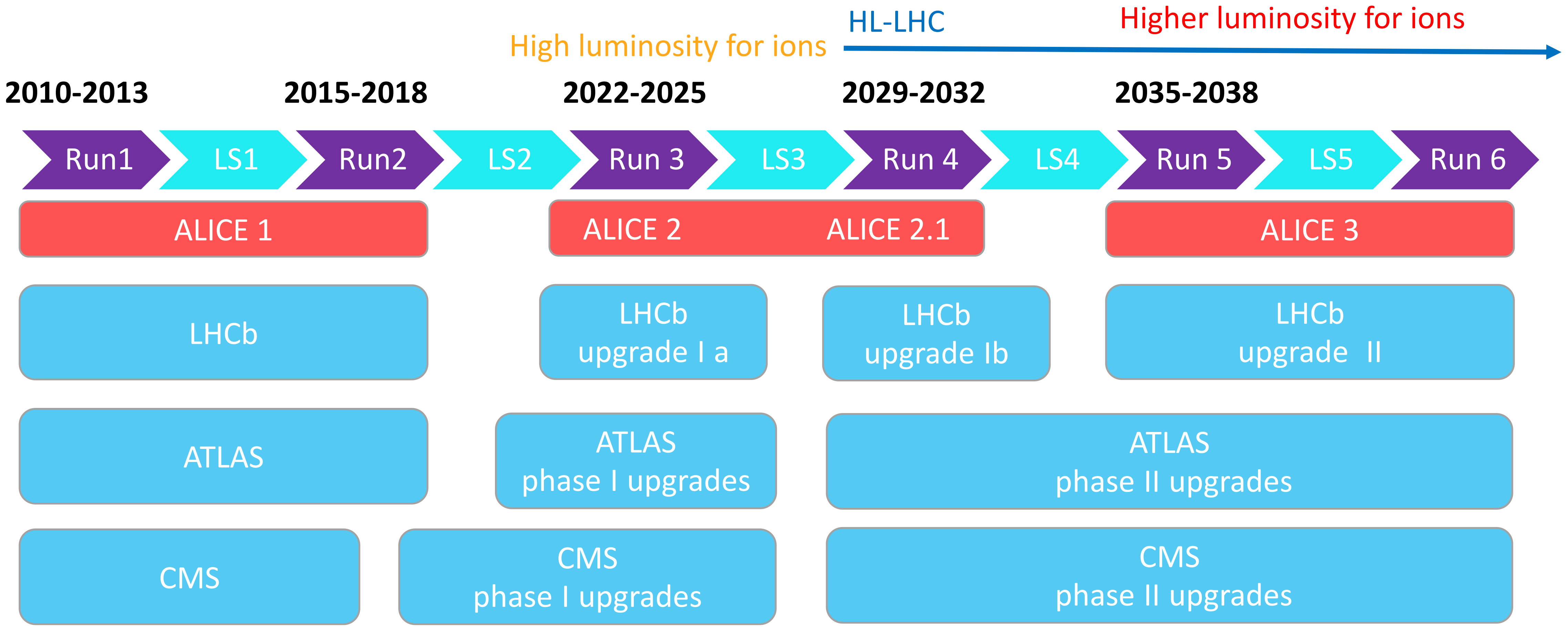

Available energy √s for Fixed Target and Collider experiments

Fixed Target experiment:

m_1, E_1^{lab} → $m_2, p_2^{lab} = 0$

$$\sqrt{s} = \sqrt{m_1^2 + m_2^2 + 2E_1^{lab} m_2} \approx \sqrt{2E_1^{lab} m_2}$$

$E_1^{lab} >> m_1, m_2$

Collider experiment:

m_1, E_1^{lab} → ← m_2, E_2^{lab}

$$\sqrt{s} = \sqrt{m_1^2 + m_2^2 + 2E_1^{lab} E_2^{lab} + 2 p_1^{lab} p_2^{lab}} = 2E_1^{lab}$$

$p_1 = -p_2$

$m_1 = m_2$

Kinematics, notations, conventions

$c=\hbar=1$

$\hbar c=197.3269631$ MeV.fm

$$\frac{1eV}{k_B}=\frac{1.60217653(14)\times10^{-19}J}{1.3806505(24)\times10^{-23}J/K}=11604.505(20)K$$

$$y=\frac{1}{2}\ln\left(\frac{E+p_z}{E-p_z}\right)=\tanh^{-1}\left(\frac{p_z}{E}\right)\underset{p>>m}{\approx}-\ln\tan\left(\frac{\theta}{2}\right)$$

$$E=m_T\cosh y$$

$$p_x, p_y, p_z=m_T\sinh y$$

$$m_T=\sqrt{m^2+p_x^2+p_y^2}$$

$$y=\frac{1}{2}\ln\left[\frac{\sqrt{p_T^2\cosh^2\eta+m^2}+p_T\sinh\eta}{\sqrt{p_T^2\cosh^2\eta+m^2}-p_T\sinh\eta}\right]$$

$$\eta=\frac{1}{2}\ln\left[\frac{\sqrt{p_T^2\cosh^2 y-m^2}+m_T\sinh y}{\sqrt{p_T^2\cosh^2 y-m^2}-m_T\sinh y}\right]$$

$$\frac{dN}{d\eta dp_T}=\sqrt{1-\frac{m^2}{m_T^2\cosh^2 y}}\frac{dN}{dydp_T}$$

Pb+Pb collision at LHC at $\sqrt{s}_{NN}$=2.76TeV

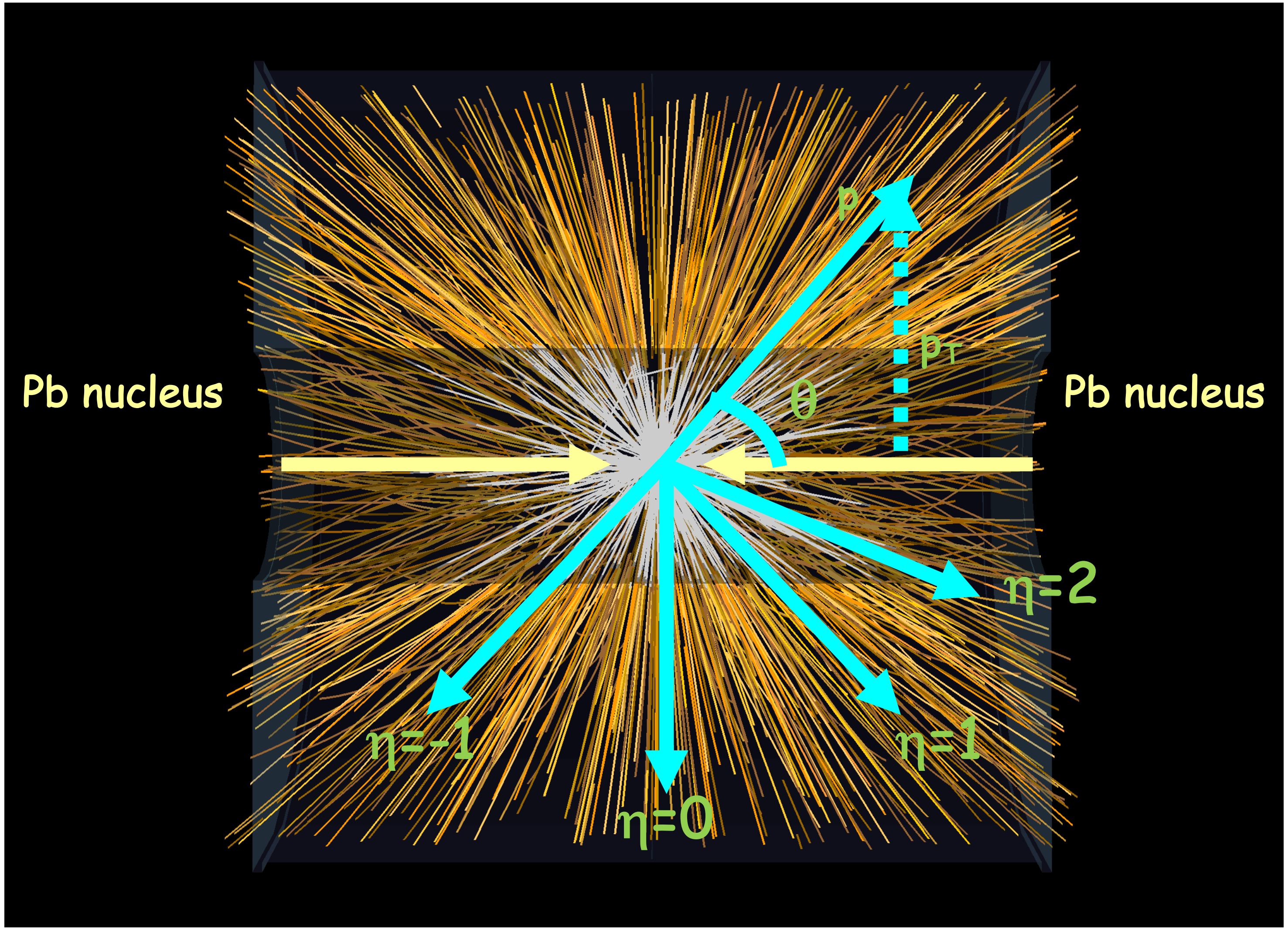

The ALICE 2 detector

Continuous readout
Central barrel | η | < 0.9
Tracking
PID
Calorimeters

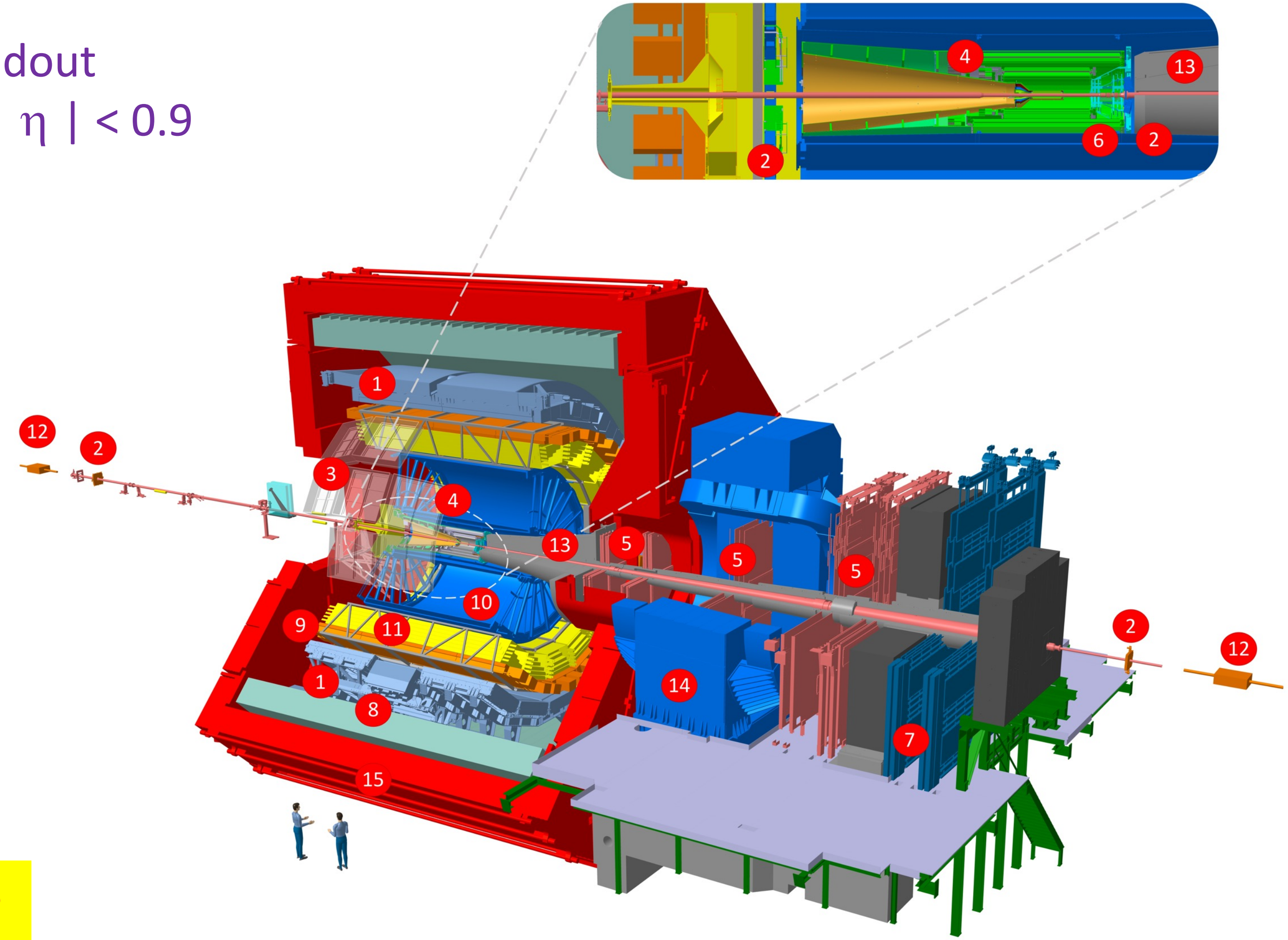

1. **EMCAL |** Electromagnetic Calorimeter
2. **FIT |** Fast Interaction Trigger
3. **HMPID|** High Momentum Particle Identification Detector
4. **ITS|** Inner Tracking System
5. **MCH|** Muon Tracking Chambers
6. **MFT|** Muon Forward Tracker
7. **MID|** Muon Identifier
8. **PHOS/CPV|** Photon Spectrometer
9. **TOF|** Time Of Flight
10. **TPC|** Time Projection Chamber
11. **TRD|** Transition Radiation Detector
12. **ZDC|** Zero Degree Calorimeter
13. **Absorber**
14. **Dipole Magnet**
15. **L3 Magnet**

Size: 16 x 26 meters
Weight: 10,000 tons

ALICE PID and reconstruction capabilities

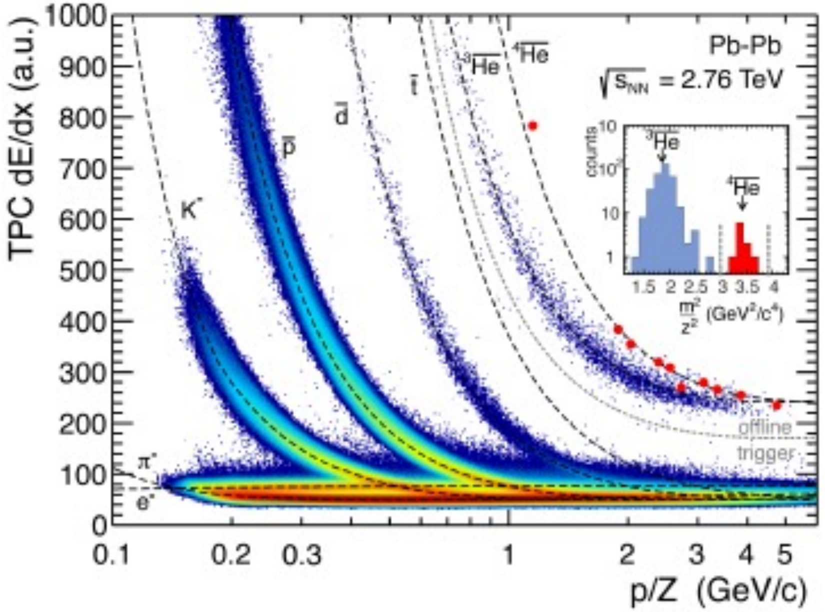

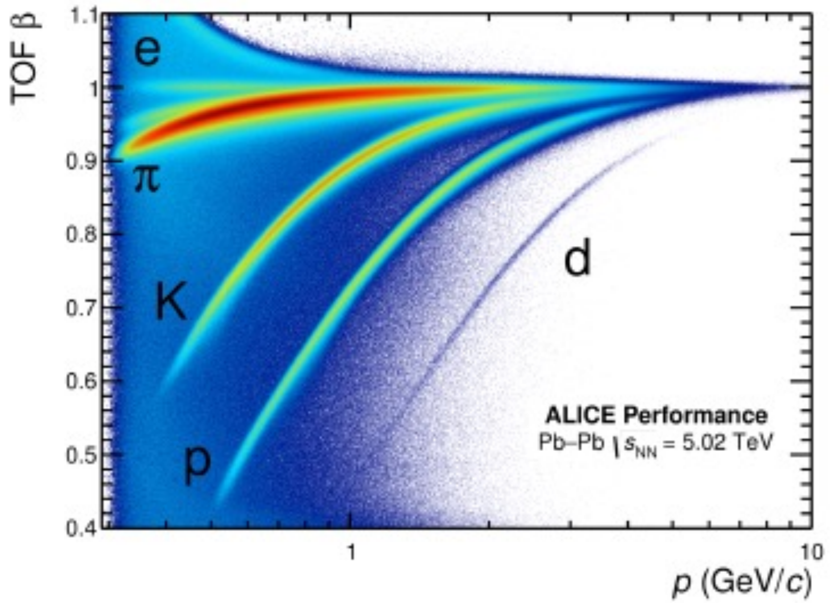

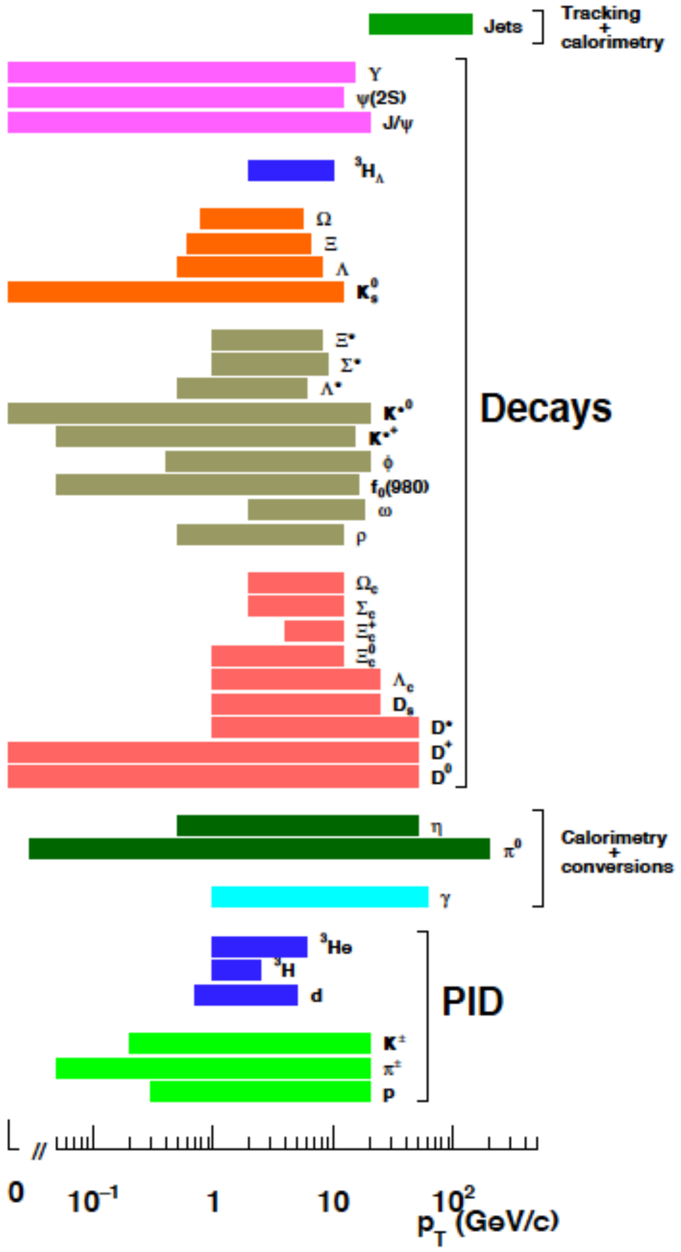

The ALICE Collaboration

40 countries,
172 institutes,
2033 members

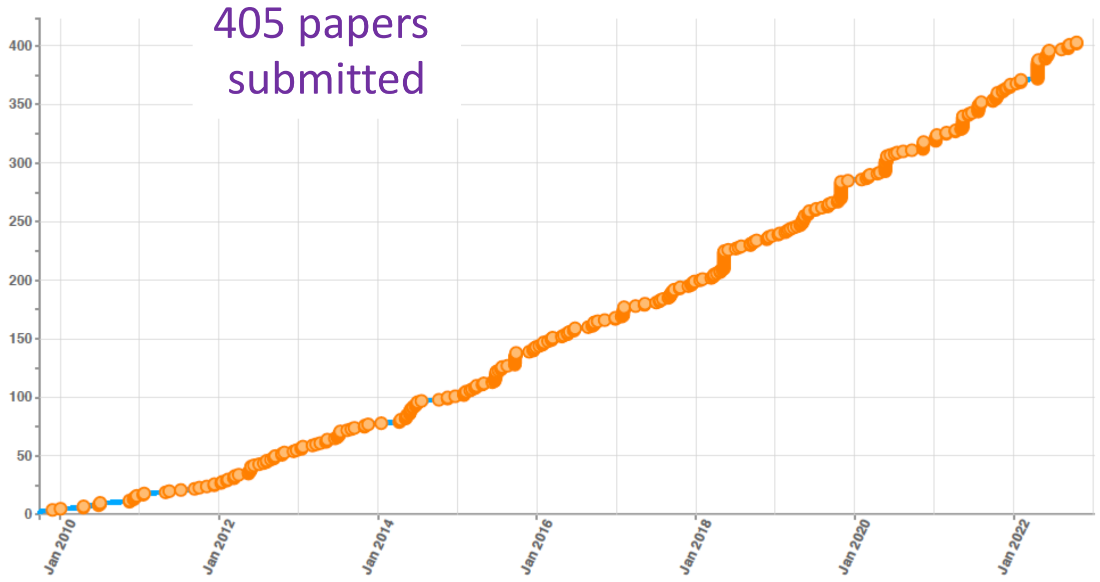

Run 1 Run 2

System	Year(s)	$\sqrt{s_{NN}}$ (TeV)	L_{int}
Pb-Pb	2010,2011 2015,2018	2.76 5.02	75 μb^{-1} 800 μb^{-1}
Xe-Xe	2017	5.44	0.3 μb^{-1}
p-Pb	2013 2016	5.02 5.02, 8.16	15 nb^{-1} 3 nb^{-1}, 25 nb^{-1}
pp	2009-2013 2015,2017 2015-2018	0.9,2.76, 7,8 5.02 13	200 μb^{-1}, 100 mb^{-1} 1.5 pb^{-1},2.5 pb^{-1} 1.3 pb^{-1} 36 pb^{-1}

ALICE Run 3: Pb-Pb @ $\sqrt{s_{NN}}$ = 5.36 TeV and pp @ $\sqrt{s}$ = 13.6 TeV

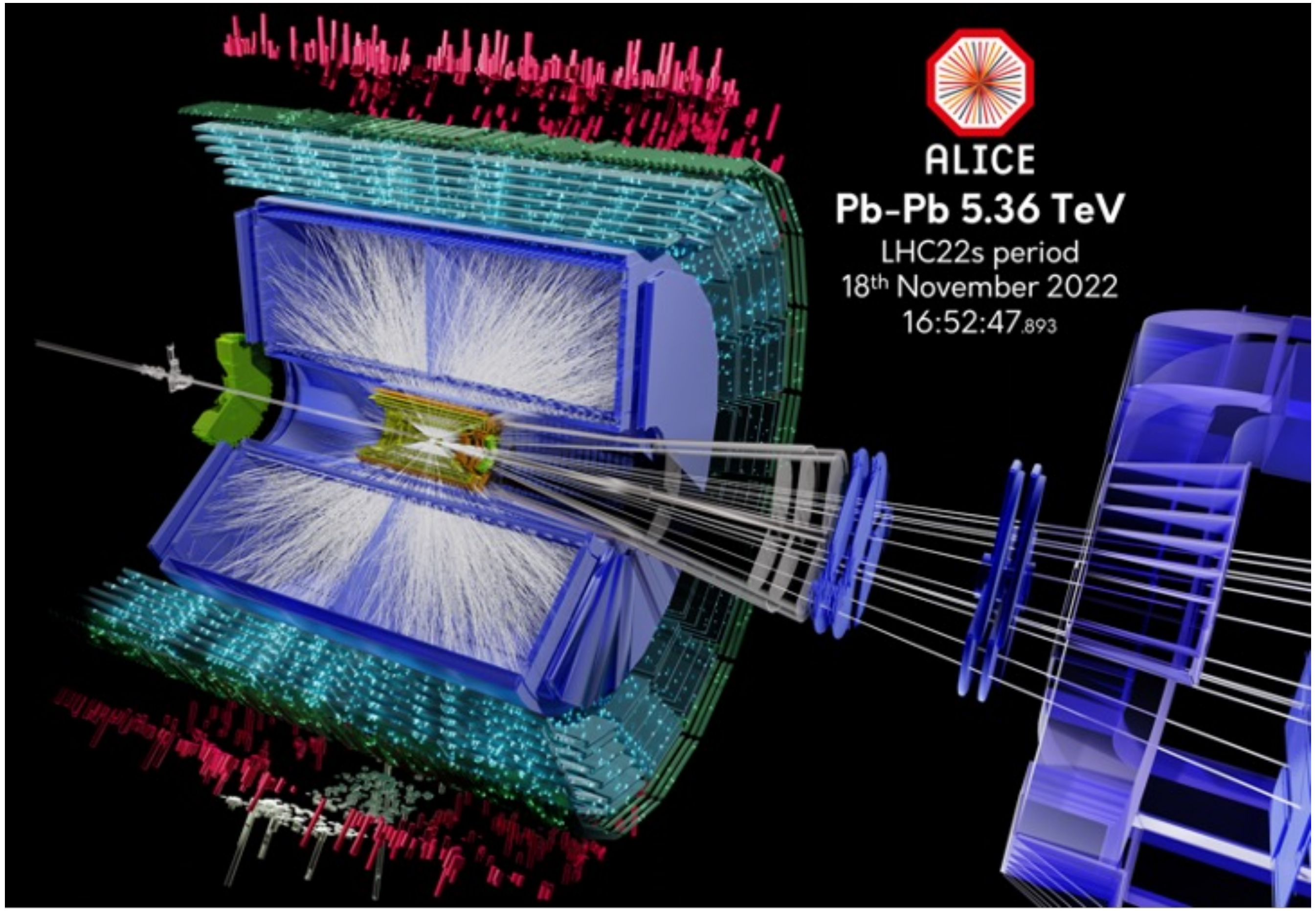

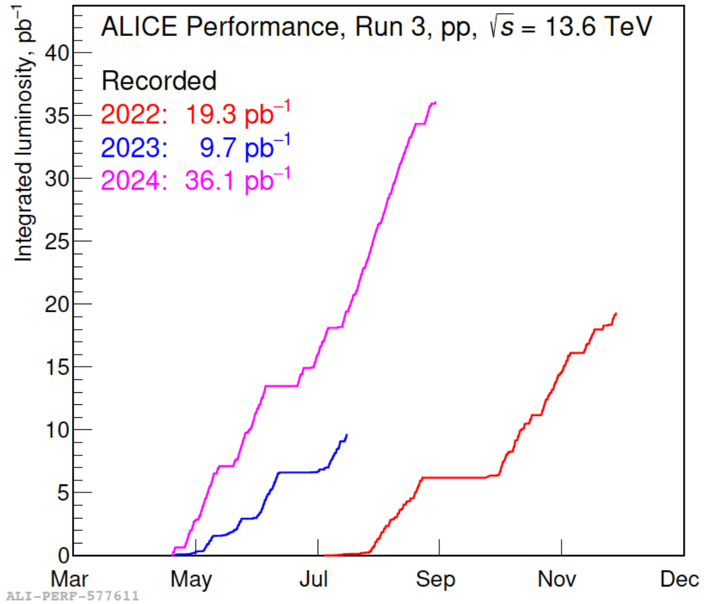

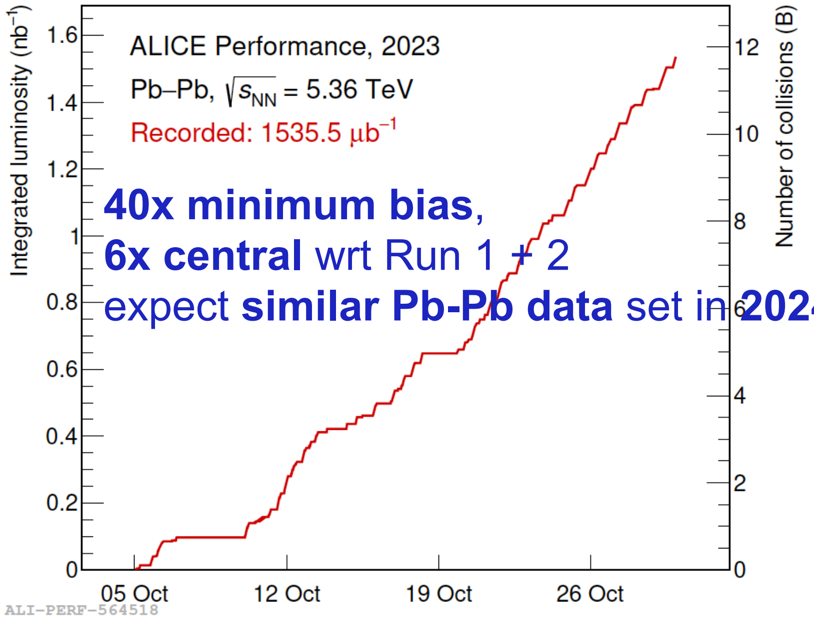

40x minimum bias,
6x central wrt Run 1 + 2
expect **similar Pb-Pb data** set in **2024**

ALICE centrality determination

ALICE-PUBLIC-2018-011

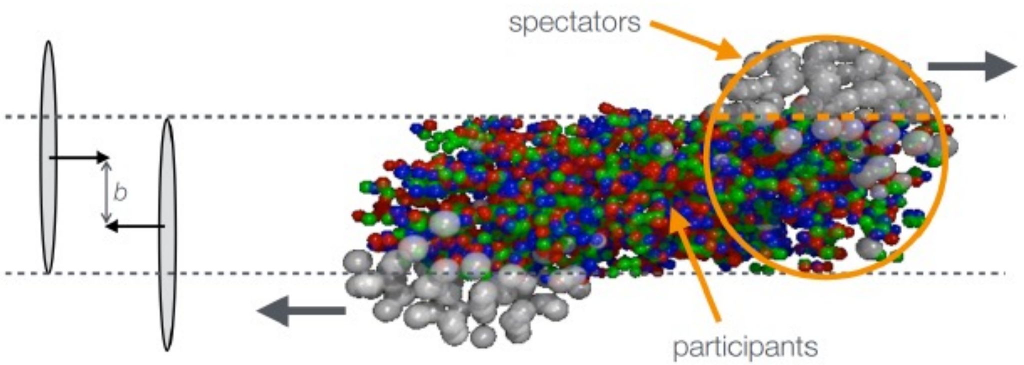

N_{coll}: number of inelastic nucleon-nucleon collisions#
N_{part}: number of nucleons that underwent at least one inelastic collision

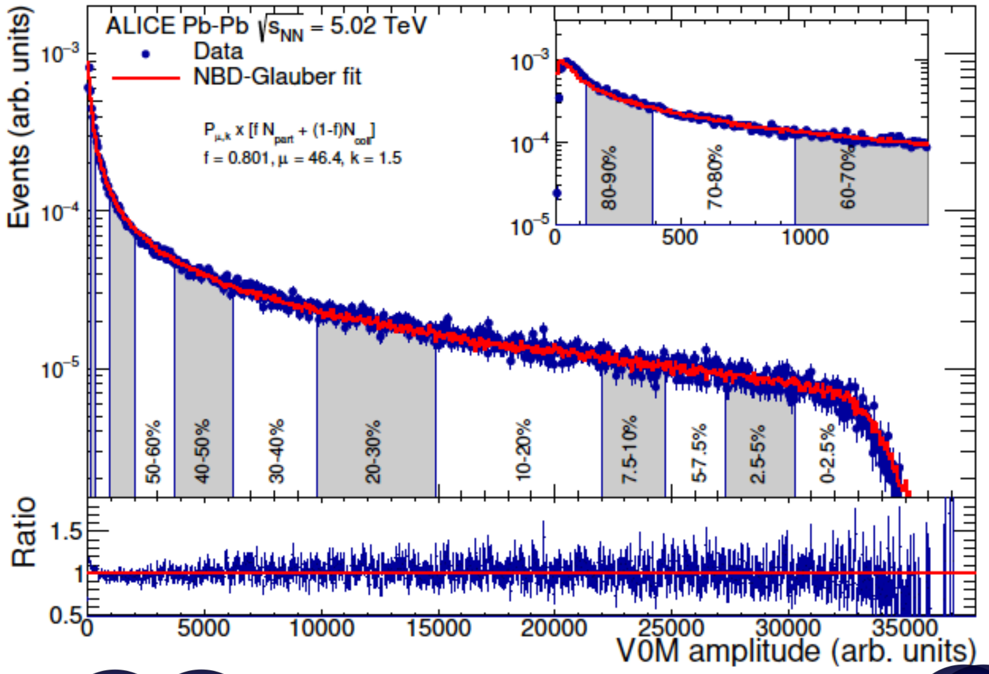

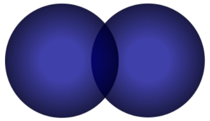

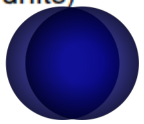

Centrality	$\langle N_{part}\rangle$	RMS	(*sys.*)	$\langle N_{coll}\rangle$	RMS	(*sys.*)	$\langle T_{PbPb}\rangle$ (1/mbarn)	RMS (1/mbarn)	(*sys.*) (1/mbarn)
0-1%	401.9	7.55	0.46	1949	87	21.1	28.83	1.29	0.177
1-2%	393.9	10.2	0.496	1844	81.3	20.1	27.28	1.2	0.171
2-3%	384.4	11.7	0.752	1755	80.8	20.3	25.96	1.19	0.2
3-4%	373.9	12.5	0.762	1673	79.9	18.8	24.75	1.18	0.18
4-5%	362.9	13	0.738	1593	77.6	17.8	23.57	1.15	0.178

Global properties

Charged-particle production

PRL 116 (2016) 222302

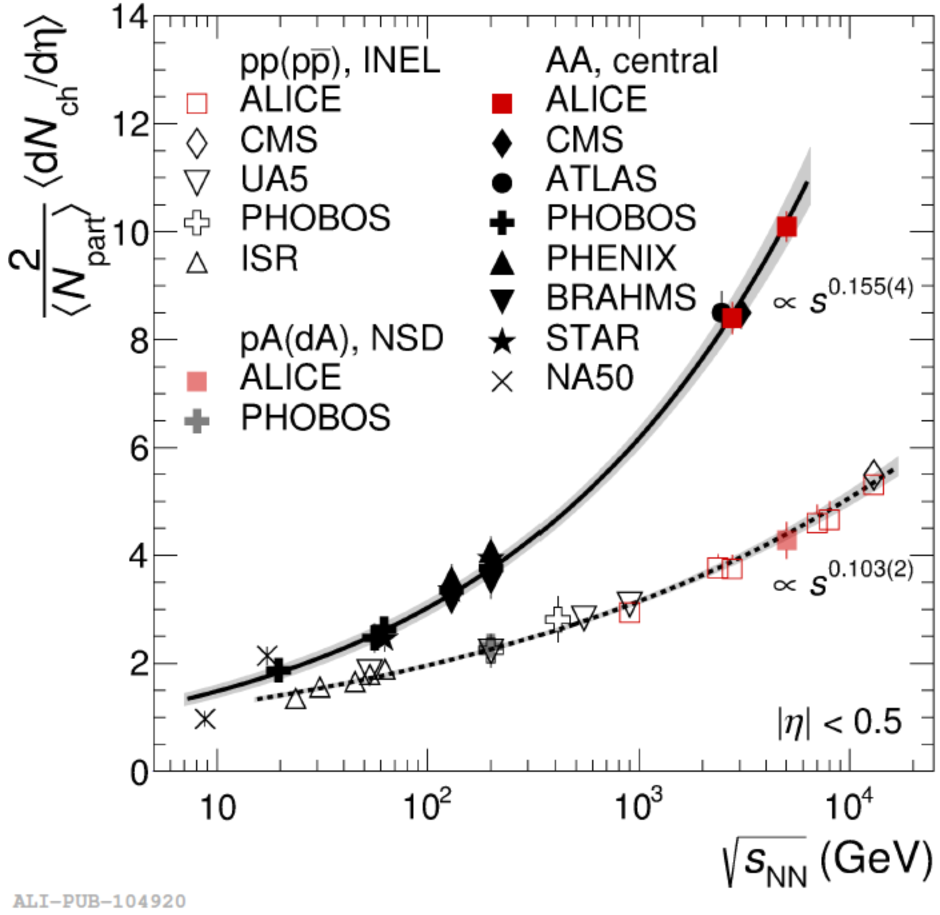

Increase of charged-particle production in nuclear collisions much faster with √s than in pp

More of the available energy used for particle production in heavy-ion collisions

Charged particles pseudorapidity density

EPJC (2024) 84:813

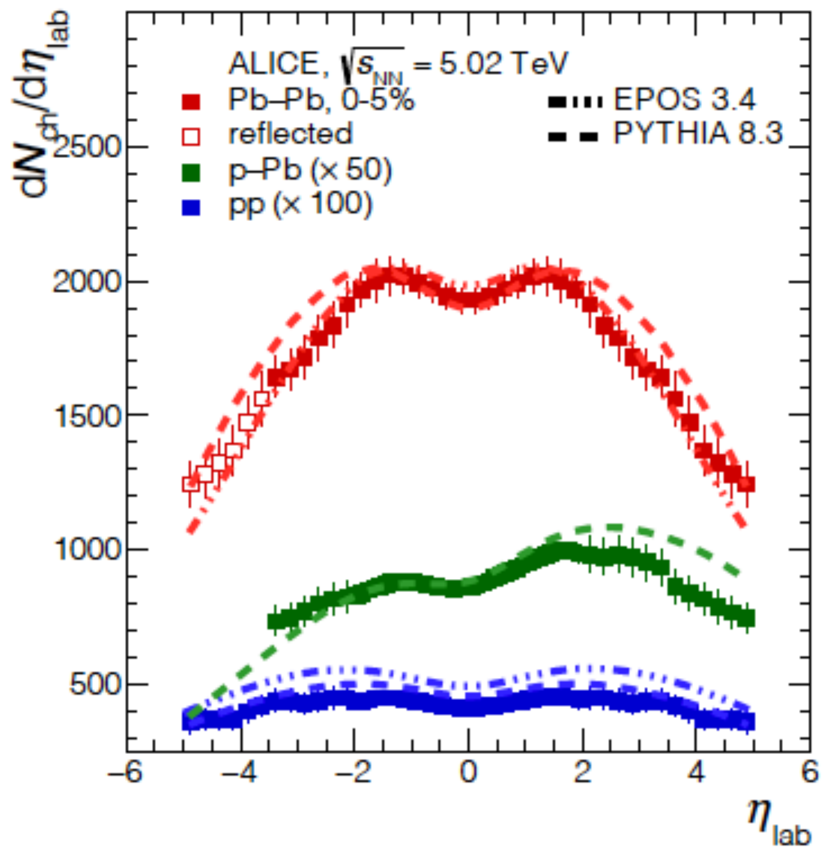

Different level of agreement of models depending on η and system

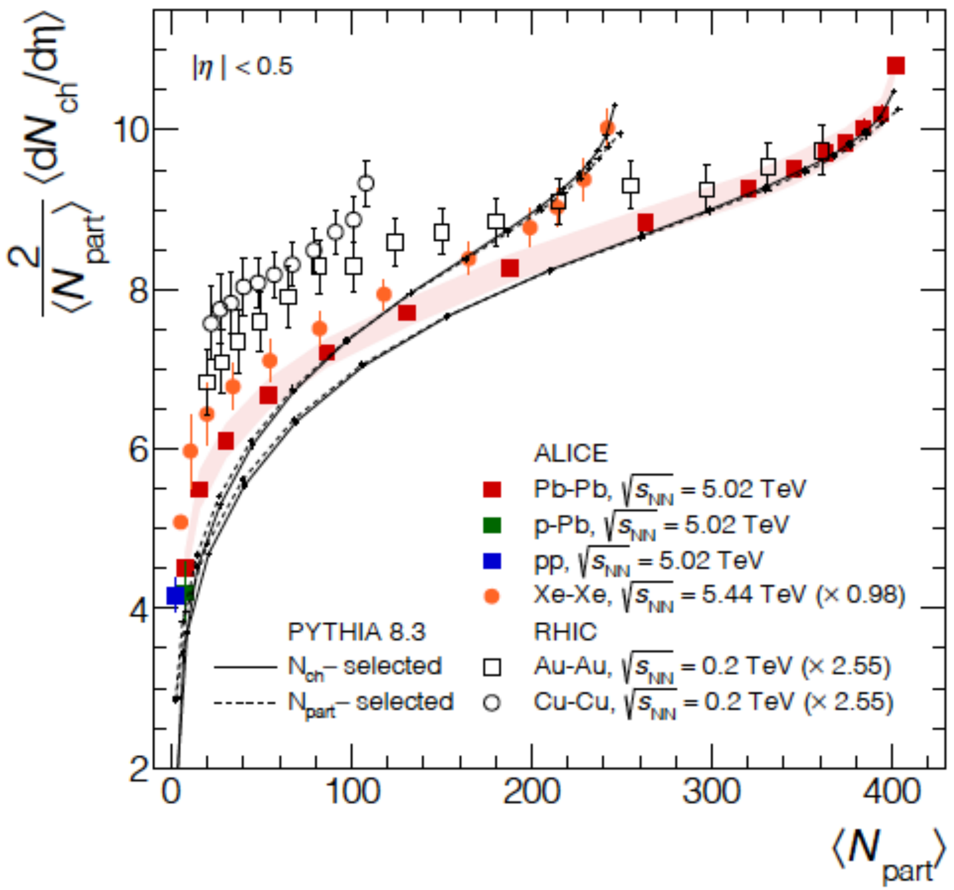

Hints of separation between RHIC and LHC for $<N_{part}>$ <100
Steep increase for most central 5% in the different systems

Initial energy density

$$\varepsilon_{Bj} = \frac{1}{\pi R^2}\frac{1}{\tau_0}\frac{dE_T}{dy}$$

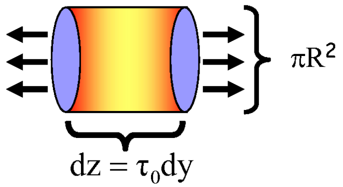

Phys. Rev. C 100, 024902 (2019)

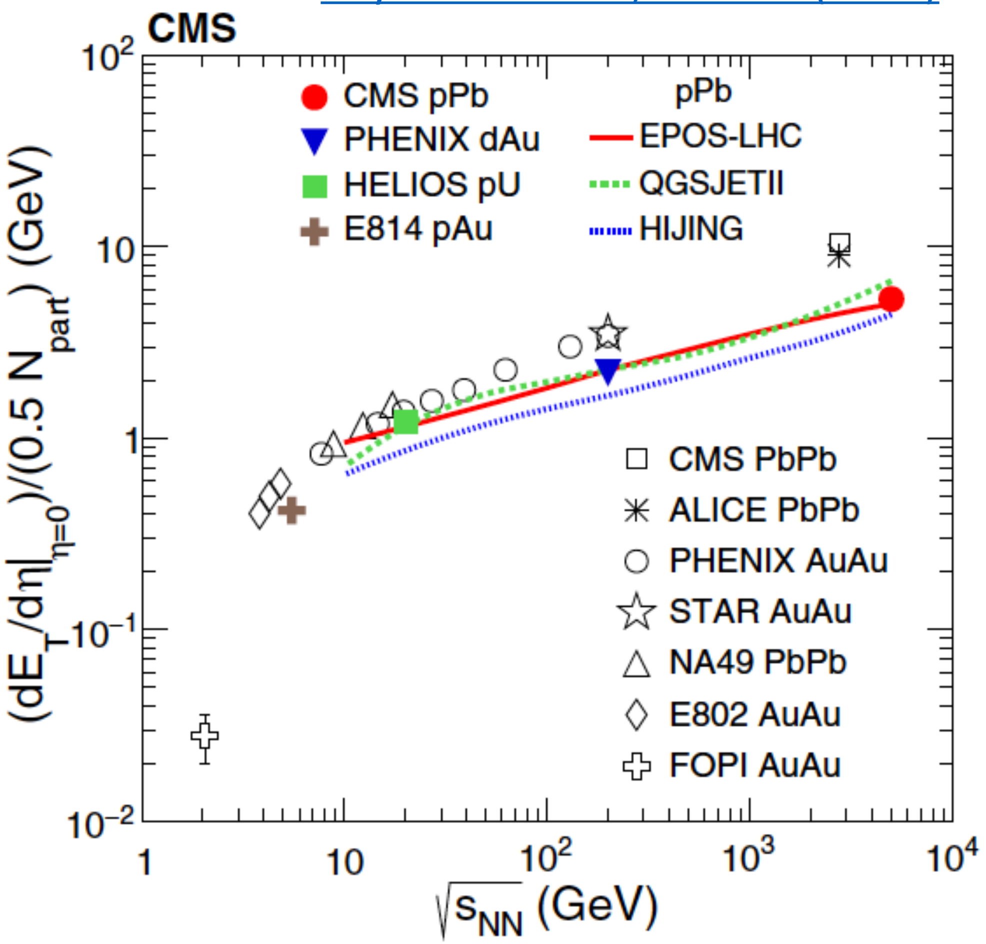

arXiv:2211.04384

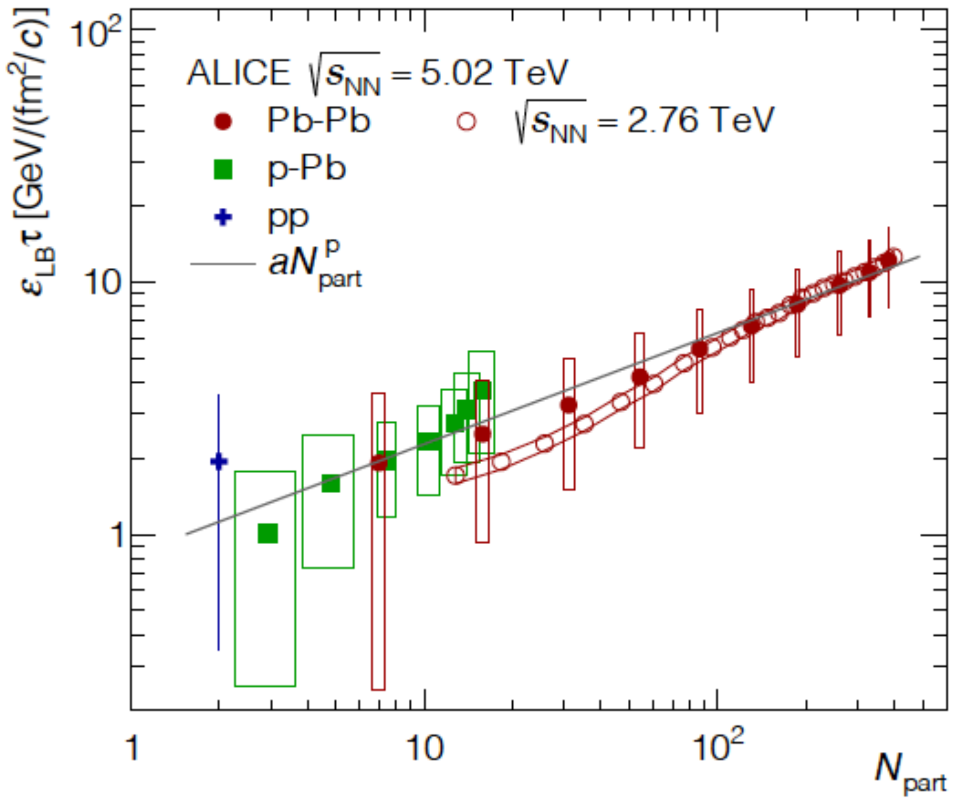

A factor ~10 increase from pp, peripheral pPb to Pb--Pb

Change in slope at $\sqrt{s_{NN}}$ ~ 10 GeV

Stronger energy density increase for AA than pA

Identified particle production

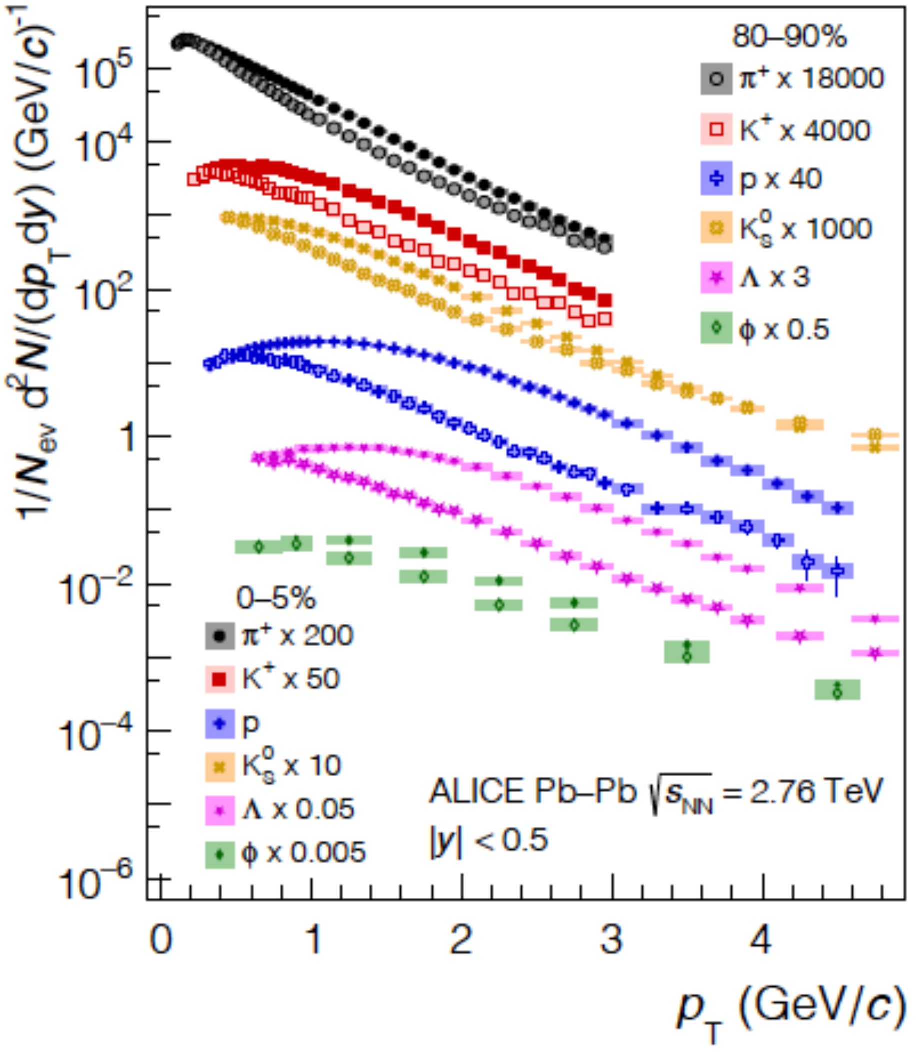

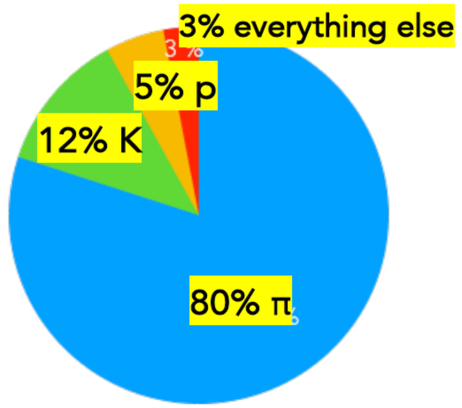

- π, K and p are the most abundant hadronic species produced in the collision
- Bulk of particles are soft and composed by light flavour hadrons
- Collective motion is observed

Particle production in Pb-Pb

PRC 101 (2020) 044907

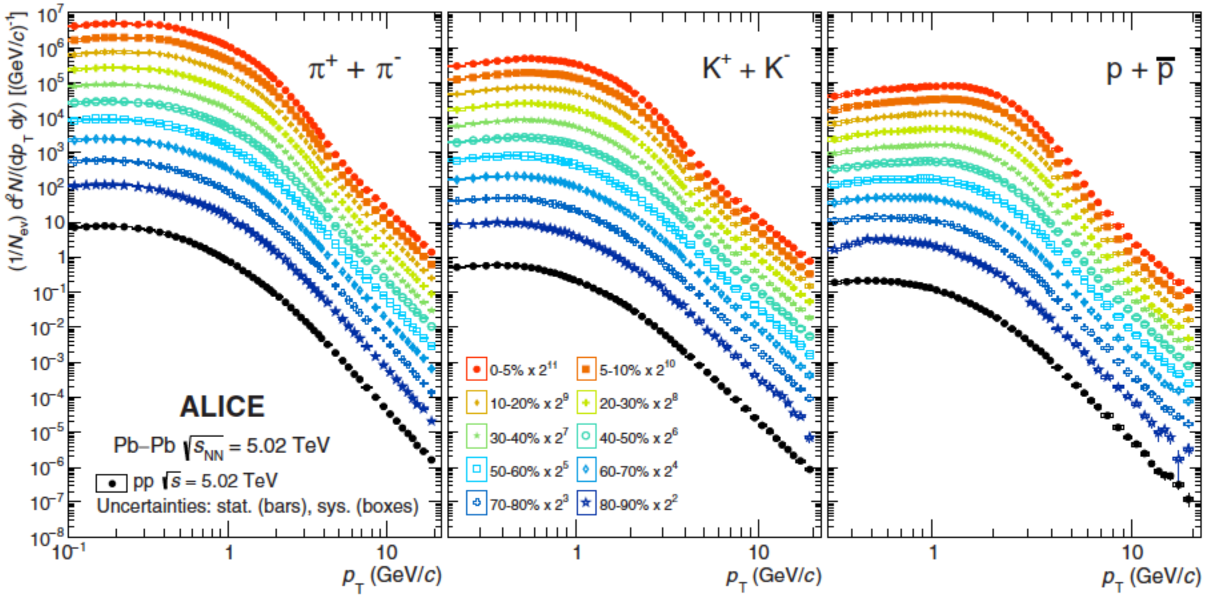

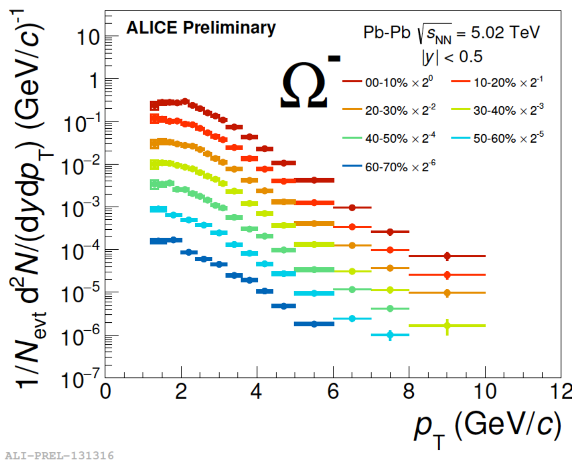

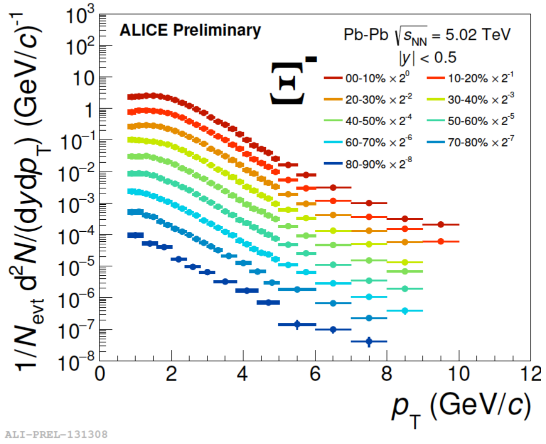

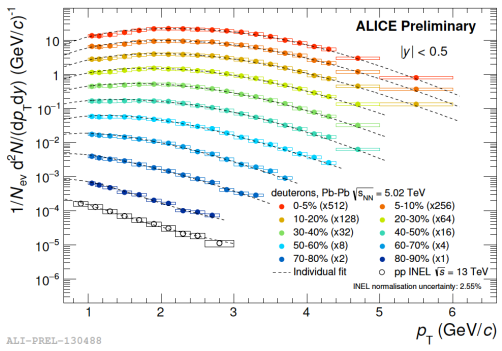

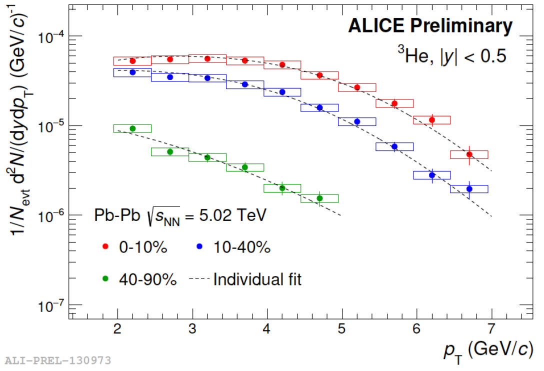

- precise p_T and centrality differential measurements of various light-flavour particle species at highest Pb-Pb collision energy
- large number of multiplicity dependent measurements in pp and p-Pb

Identified particle spectra

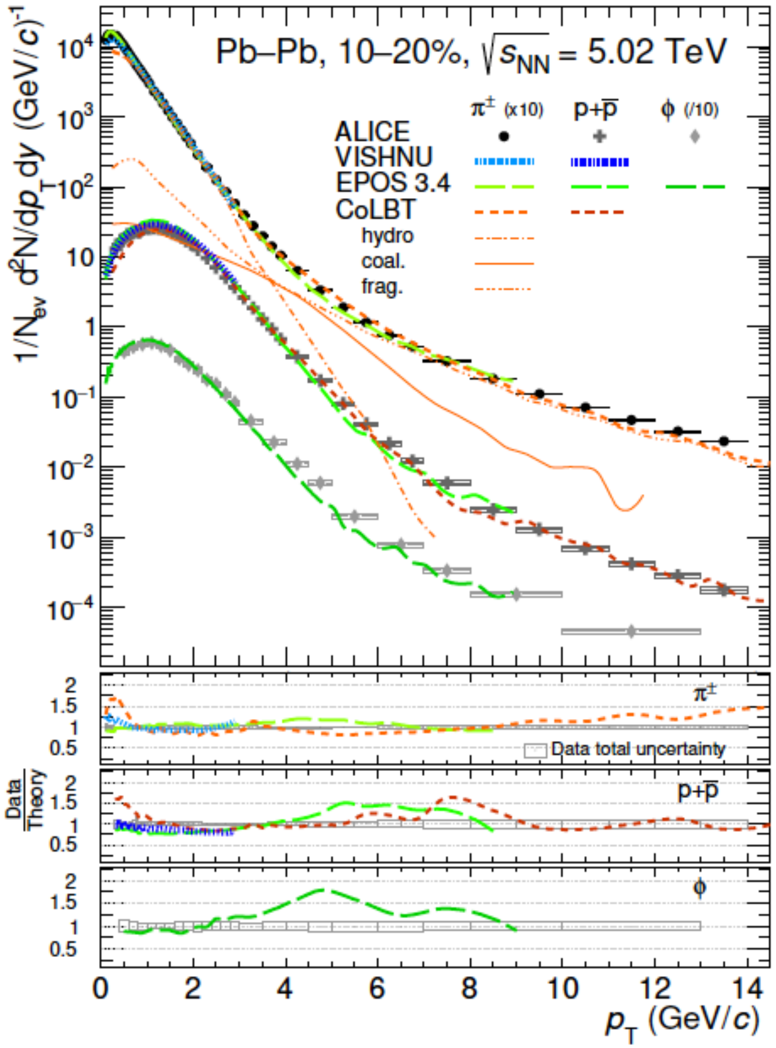

Hydro gives a good description of the data at low p_T

Coalescence important in the intermediate p_T and

Fragmentation at higher p_T

Statistical hadronization model (SHM)

- Assume chemically equilibrated system at freeze-out (constant T_{ch} and μ)
- Composed of non-interacting hadrons and resonances
- Given T_{ch} and μ 's, particle abundances (n_i's) can be calculated in a grand canonical ensemble

Partition function: $$\ln Z_i = \frac{V g_i}{2\pi^2} \int_o^\infty \pm p^2 dp \ln(1 \pm \exp(-(E_i - \mu_i)/T))$$

Particle densities: $$n_i = \frac{g}{2\pi^2} \int_0^\infty \frac{p^2 dp}{e^{(E_i(p)-\mu_i)/T} \pm 1}, \quad E_i = \sqrt{p^2 + m_i^2}$$

- Obey conservation laws: Baryon Number, Strangeness, Isospin

$$\mu = \mu_B B_i + \mu_S S_i + \mu_{I3} I_i^3, \qquad V\sum_i n_i B_i = Z + N, \qquad V\sum_i n_i S_i = 0, \qquad V\sum_i n_i I_i^3 = \frac{Z - N}{2}$$

- Short-lived particles and resonances need to be taken into account

Measure particle ratios → Extract T_{ch} and μ → Calculate particle ratios
Compare particle abundancies
Predict

SHM yields

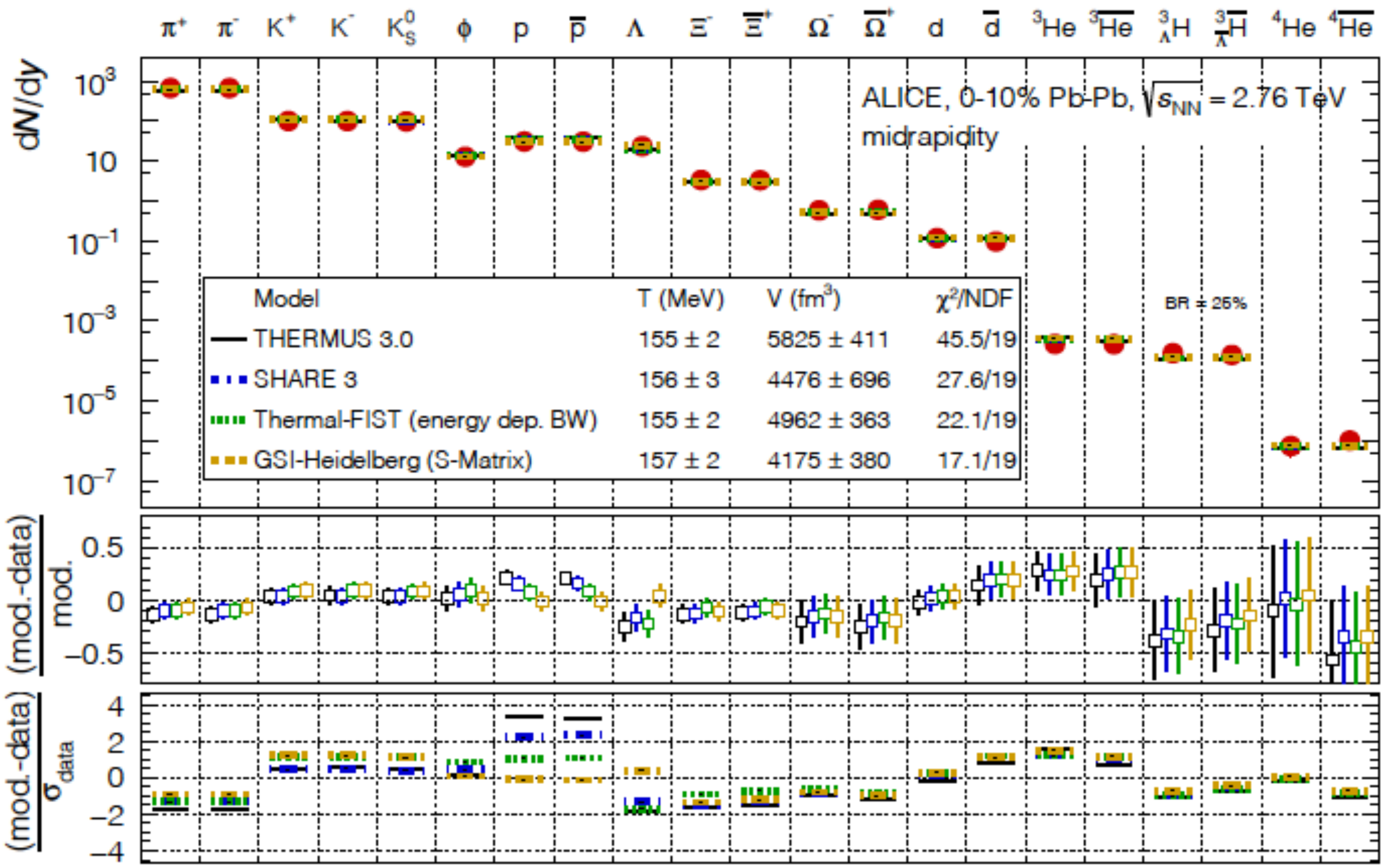

π⁺ π⁻ K⁺ K⁻ K⁰S ϕ p p̄ Λ Ξ⁻ Ξ̄⁺ Ω⁻ Ω̄⁺ d d̄ ³He ³H̄e ³ΛH ³Λ̄H̄ ⁴He ⁴H̄e
dN/dy
ALICE, 0-10% Pb-Pb, √sNN = 2.76 TeV
midrapidity
Model T (MeV) V (fm³) χ²/NDF
THERMUS 3.0 155 ± 2 5825 ± 411 45.5/19
SHARE 3 156 ± 3 4476 ± 696 27.6/19
Thermal-FIST (energy dep. BW) 155 ± 2 4962 ± 363 22.1/19
GSI-Heidelberg (S-Matrix) 157 ± 2 4175 ± 380 17.1/19
BR = 25%
(mod.-data)/mod.
(mod.-data)/σdata

Statistical hadronization model

Nature 561 (2018) 321

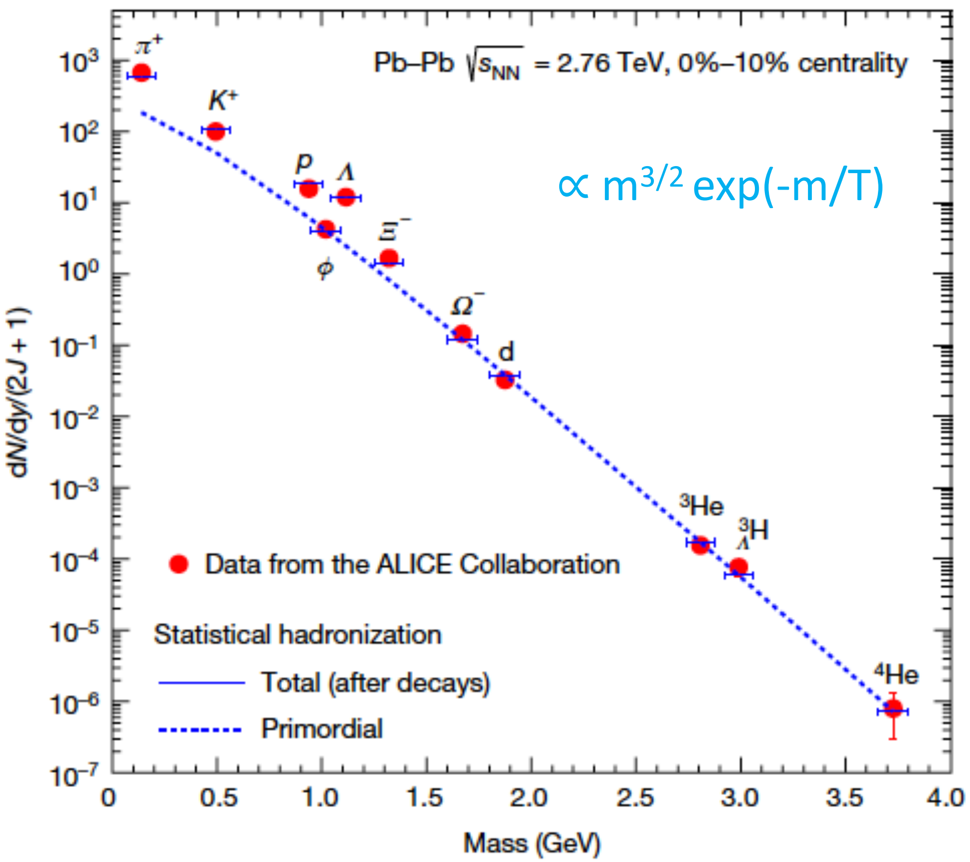

Predict yields at a given T

PRL133,092301(2024)

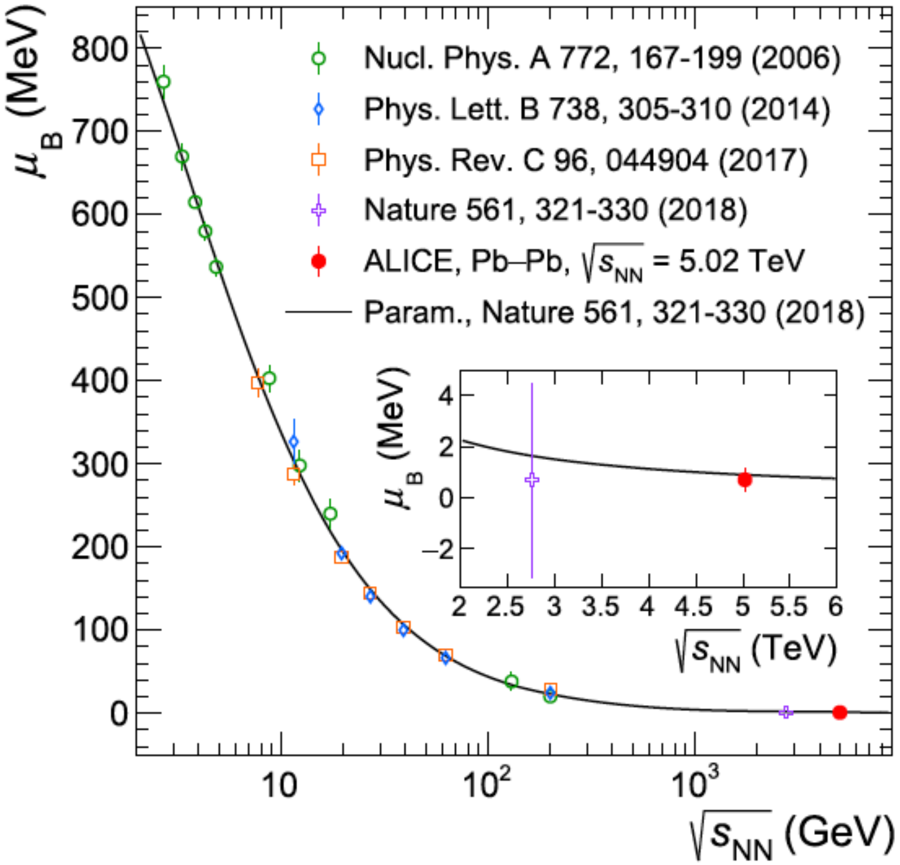

Smooth evolution of μ_B with $\sqrt{s_{NN}}$

Strangeness enhancement

Phys. Rev. Lett. **48**, 1066 (1982)

Strangeness Production in the Quark-Gluon Plasma

Johann Rafelski and Berndt Müller
Institut für Theoretische Physik, Johann Wolfgang Goethe-Universität, D-6000 Frankfurt am Main, Germany

(Received 11 January 1982)

Rates are calculated for the processes $gg \to s\bar{s}$ and $u\bar{u}, d\bar{d} \to s\bar{s}$ in highly excited quark-gluon plasma. For temperature $T \geq 160$ MeV the strangeness abundance saturates during the lifetime ($\sim 10^{-23}$ sec) of the plasma created in high-energy nuclear collisions. The chemical equilibration time for gluons and light quarks is found to be less than 10^{-24} sec.

In the QGP:

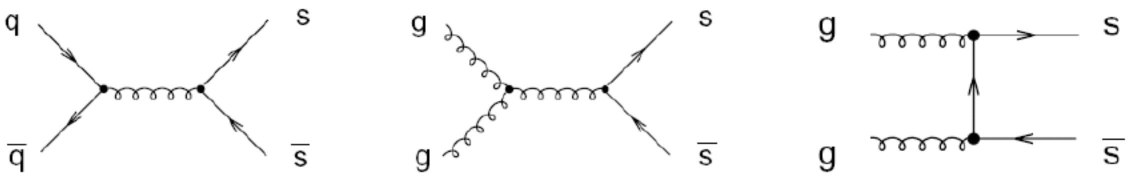

$$Q_{QGP} \approx 2m_s \approx 200 \text{ MeV}$$

In collisions of hadrons:

Example 1: $p + p \to p + K^+ + \Lambda, \quad Q = m_\Lambda + m_{K^+} - m_p \approx 670 \text{ MeV}$

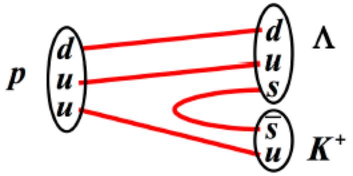

associated production of strangeness

Example 2: $p + p \to p + p + \Lambda + \bar{\Lambda}, \quad Q = 2m_\Lambda \approx 2230 \text{ MeV}$

Integrated particle yields

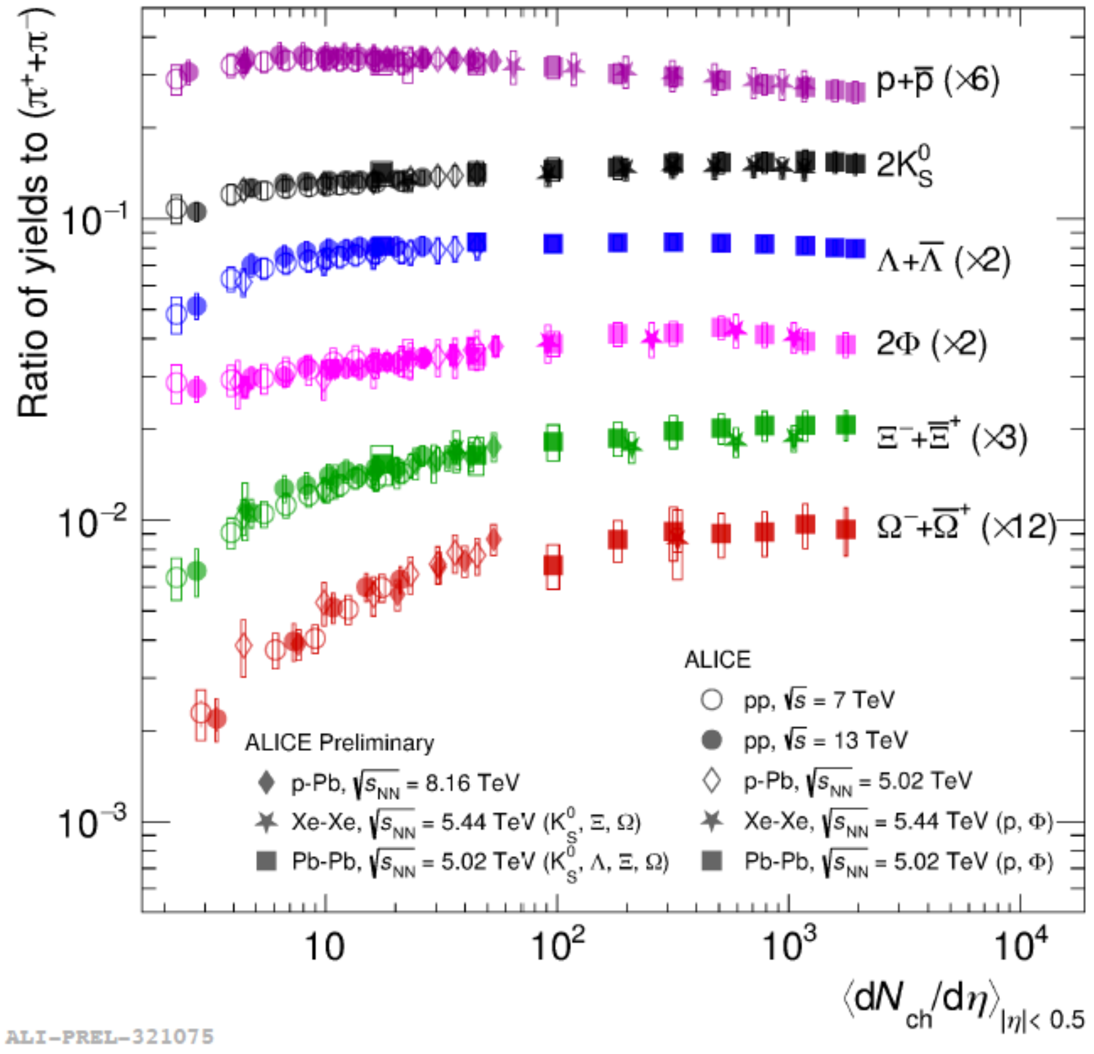

|S| = 0

|S| = 1

|S| = 1

|S| = 0 (hidden)

|S| = 2

|S| = 3

- Continuous evolution of strangeness production between different collision systems and energies
- Hadron chemistry driven by multiplicity
- Magnitude of strangeness enhancement grows with strange quark content:

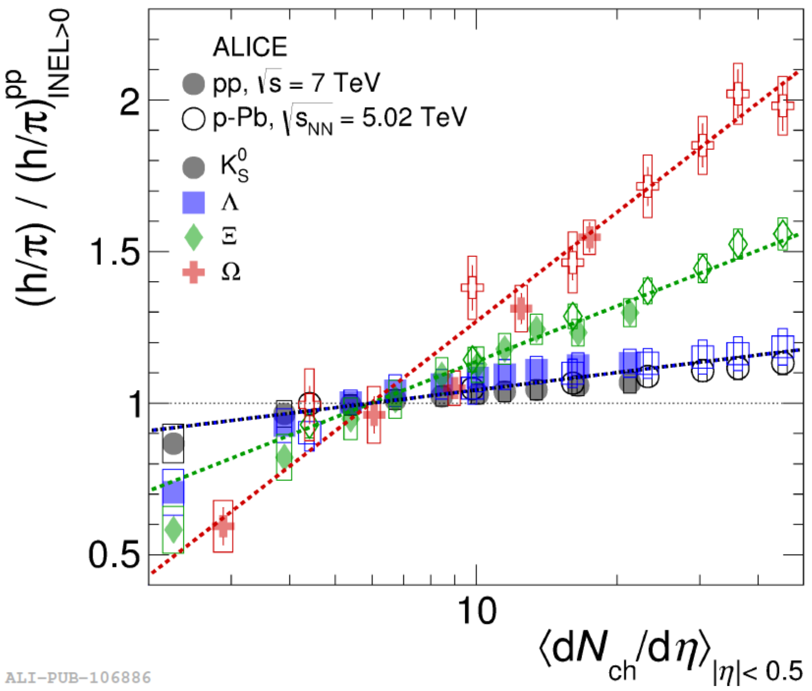

Nature Physics 13 (2017) 535

Radial flow

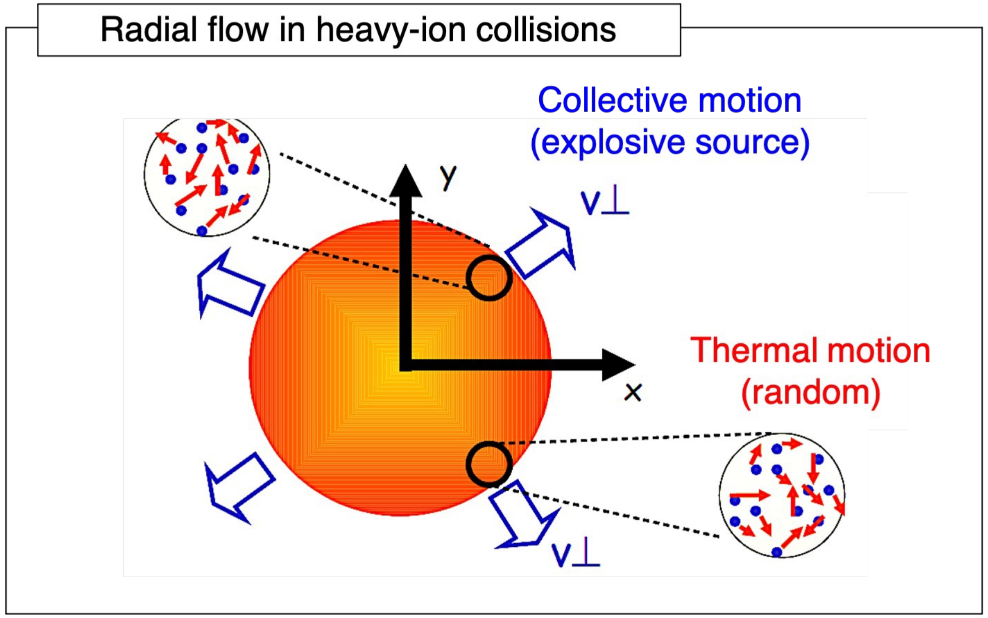

Collective motion is superimposed to the thermal motion of particles

Spectral shape different for particles with different mass
Main parameter: expansion velocity β

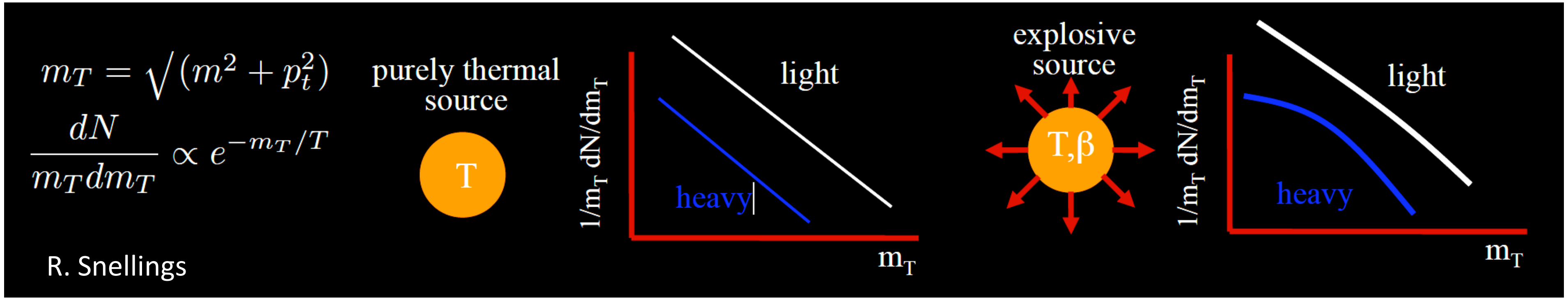

Radial Flow

PRC 101 (2020) 044907

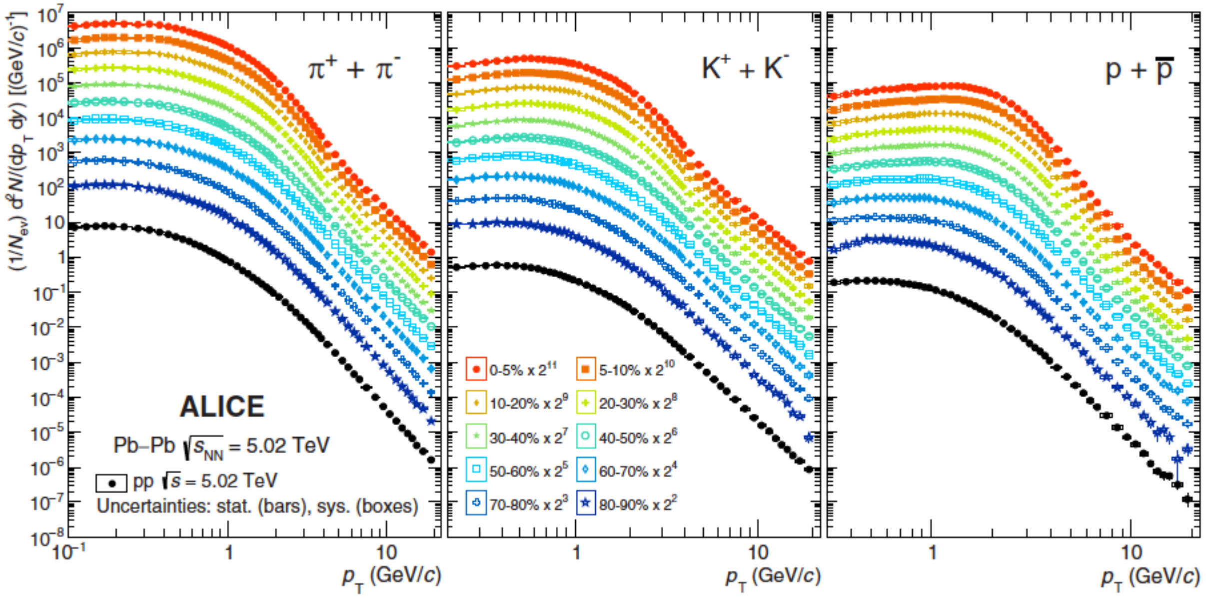

Blast-wave: A hydrodynamic inspired description of spectra

EPJ C 80(2020)693

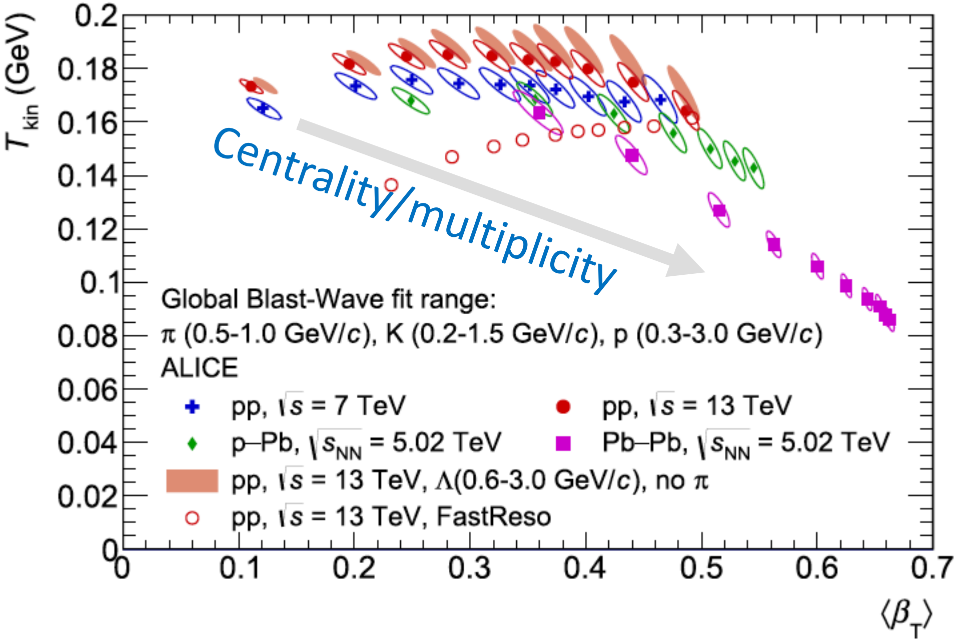

$$E\frac{d^3N}{dp^3} \propto \int_0^R m_T I_0\left(\frac{p_T \sinh(\rho)}{T_{kin}}\right) K_1\left(\frac{m_T \cosh(\rho)}{T_{kin}}\right) r\, dr.$$

The velocity profile ρ is given by

$$\rho = \tanh^{-1} \beta_T = \tanh^{-1}\left[\left(\frac{r}{R}\right)^n \beta_s\right],$$

- ⟨ β_T ⟩ increases with centrality
- Similar evolution of fit parameters for pp and p-Pb
- Thermalization in pp?
- At similar multiplicities, <β_T> is larger for smaller systems

Anisotropic flow

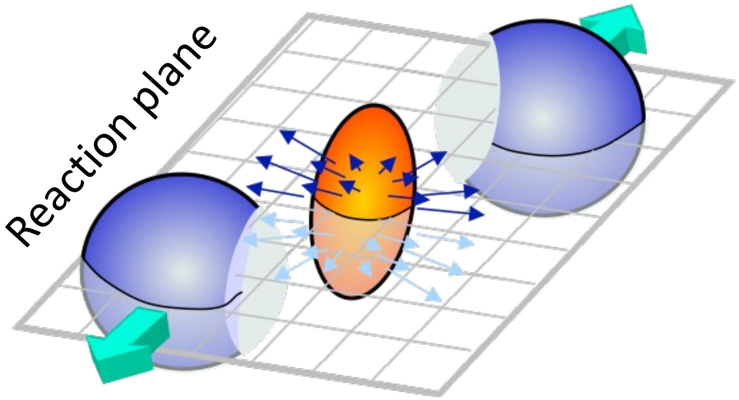

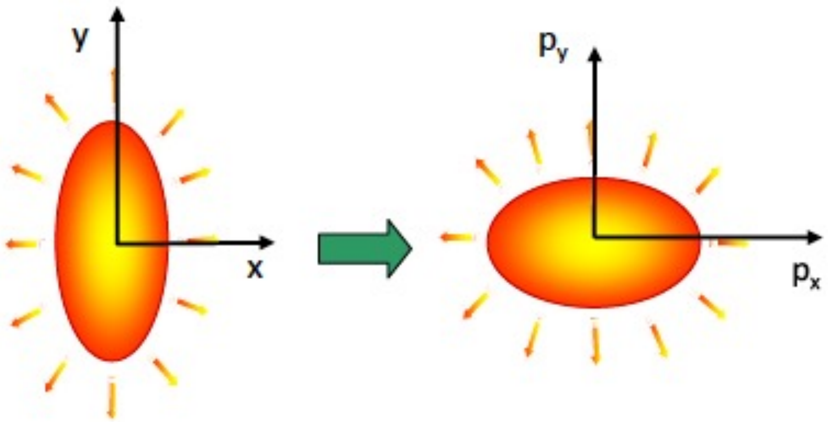

Initial spatial anisotropy → Strong pressure gradients → Anisotropy of produced particles

Fourier analysis of particle distribution:
v_1 : directed flow
v_2 : elliptic flow
v_3 : triangular flow ...

Sensitivity to early expansion

$$\frac{\mathrm{d}N}{\mathrm{d}\varphi} \propto 1 + 2\sum_{n=1}^{\infty} v_n \left[\cos(n(\varphi - \Psi_n)\right]$$

Elliptic flow in Pb-Pb, and in pp, p-Pb

arXiv: 2206.04587

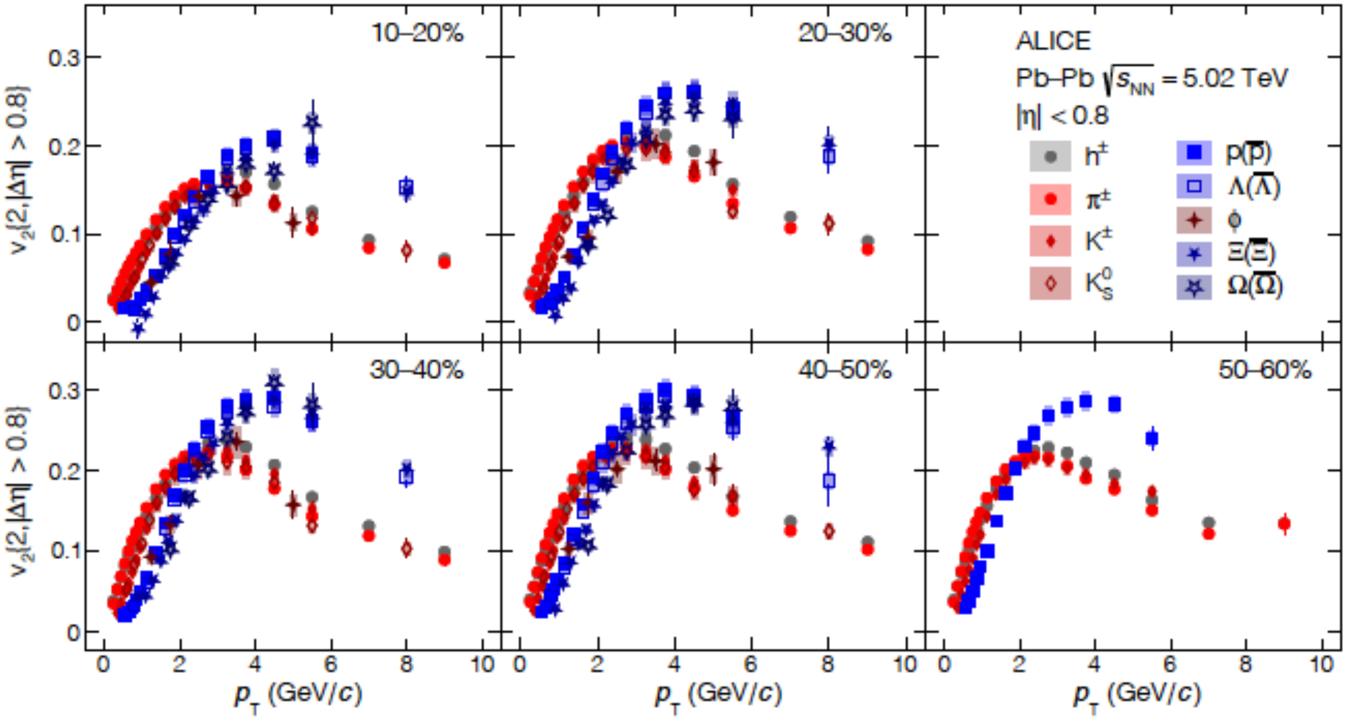

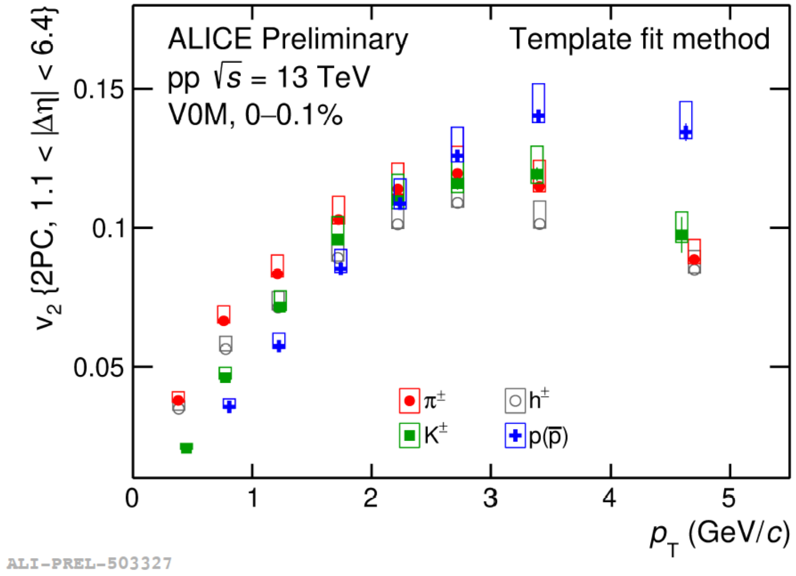

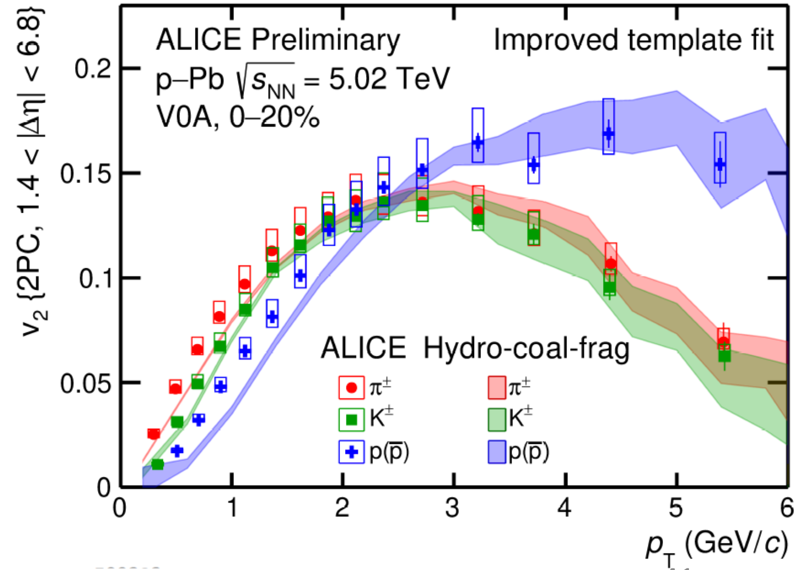

Low p_T:
Mass ordering
→ hydrodynamic flow
Intermediate p_T:
Baryon vs meson grouping : in Pb-Pb, and high multiplicity pp & p-Pb
→ quark-level flow + recombination

v_2 excitation function

PRL105(2010)252302, arXiv2211.04384

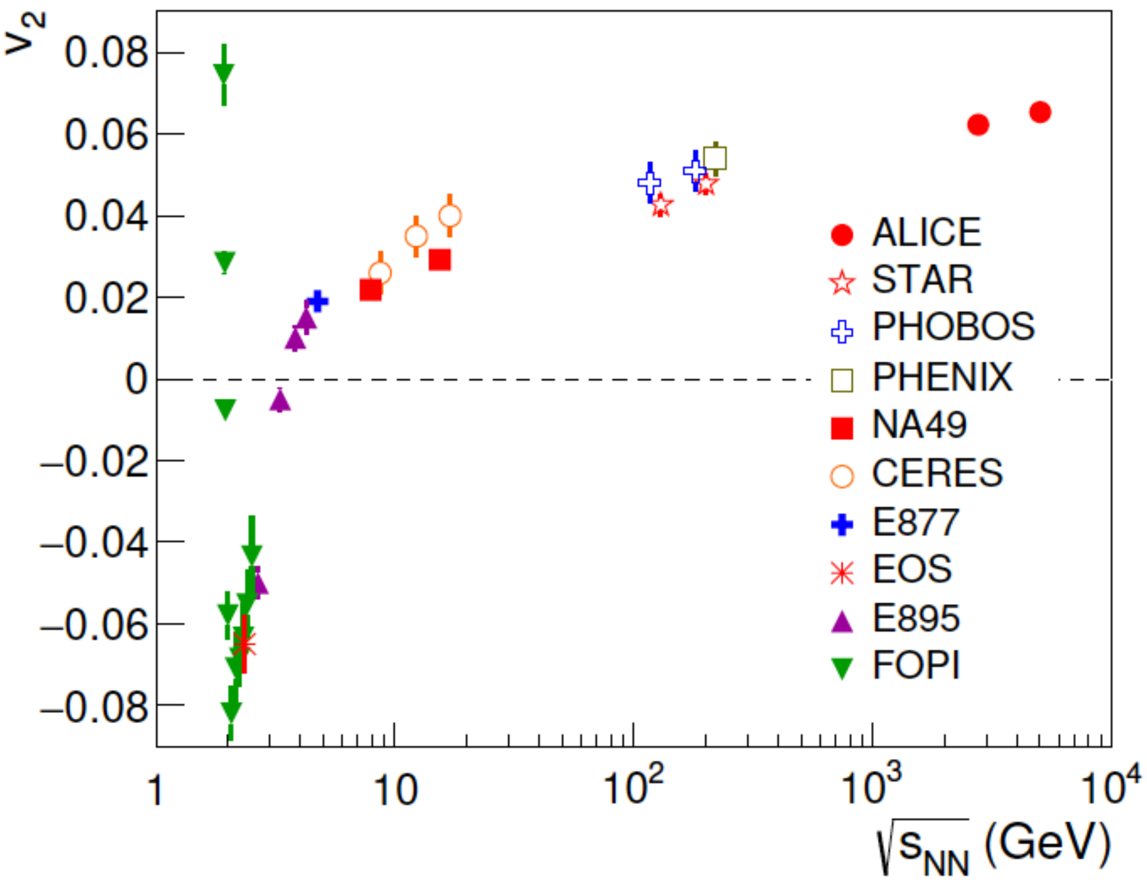

•$\sqrt{s}_{NN}$ < 2 GeV:
In-plane, rotation-like emission

•2 < $\sqrt{s}_{NN}$ < 4 GeV:
Onset of expansion and presence of spectator
matter inhibits in plane
particle emission ("squeezeout")

•$\sqrt{s}_{NN}$ > ~ 4 GeV:
Initial eccentricity
leads to pressure
gradients that cause
positive v_2

30% larger v_2 at LHC compared to RHIC

Hydrodynamics

Energy momentum conservation and current conservation

$$\nabla_\mu T^{\mu\nu} = 0 \qquad \nabla_\mu J^\mu_B = 0$$

Corrections for bulk and shear viscosity, and charge diffusion

$$T^{\mu\nu} = \epsilon u^\mu u^\nu - (P - \zeta\Theta)\Delta^{\mu\nu} - 2\eta\sigma^{\mu\nu}$$

$$J^\mu = q u^\mu + \kappa \nabla^\mu_\perp (\mu/T)$$

Shear viscosity

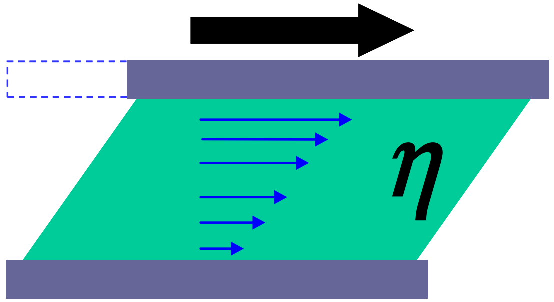

Bulk viscosity

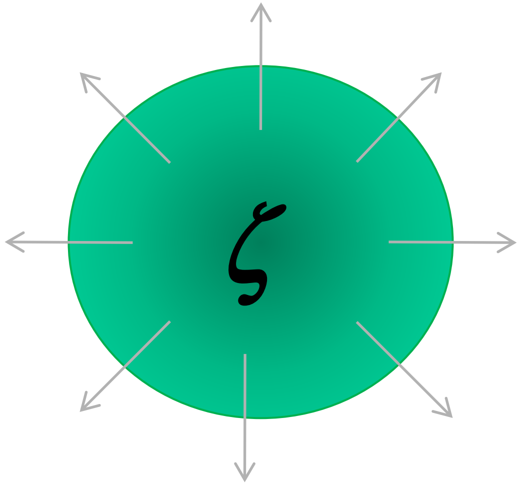

Higher order flow coefficients in Pb-Pb: v_n

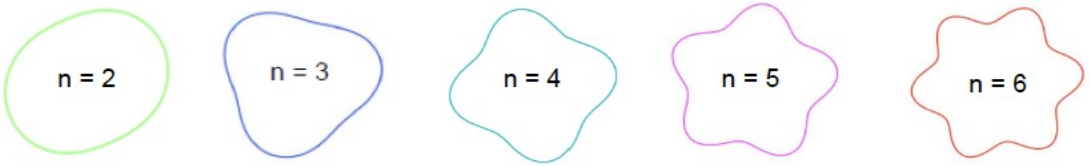

PRC95, 064913 (2017)

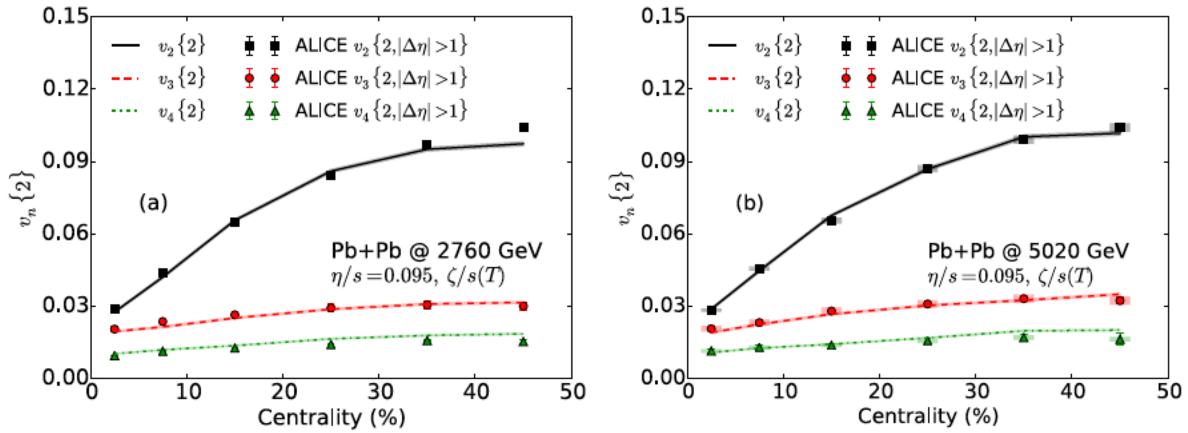

IP-Glasma+MUSIC+UrQMD

Inclusion of bulk and shear viscosity

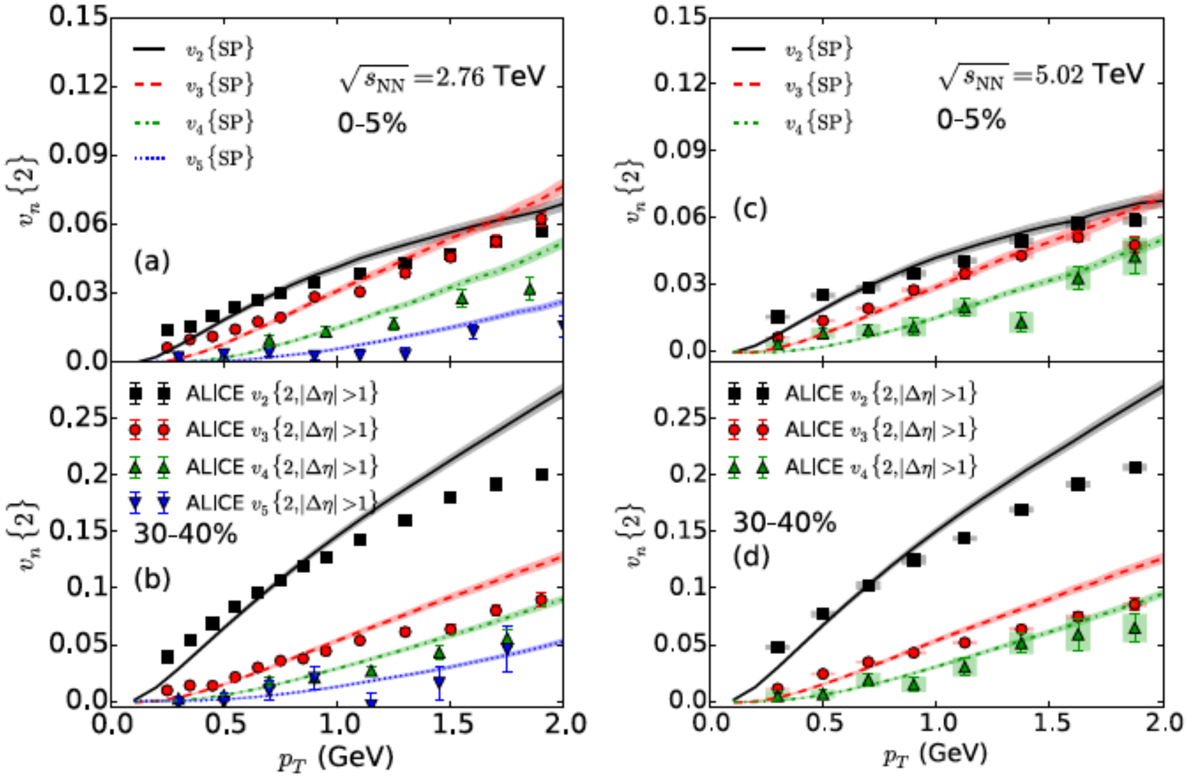

Good description of data by viscous hydrodynamics

Constraining initial condition and QGP medium properties

Nature 15(2019)1113
Phys. Rev. C 101, 024911 (2020)

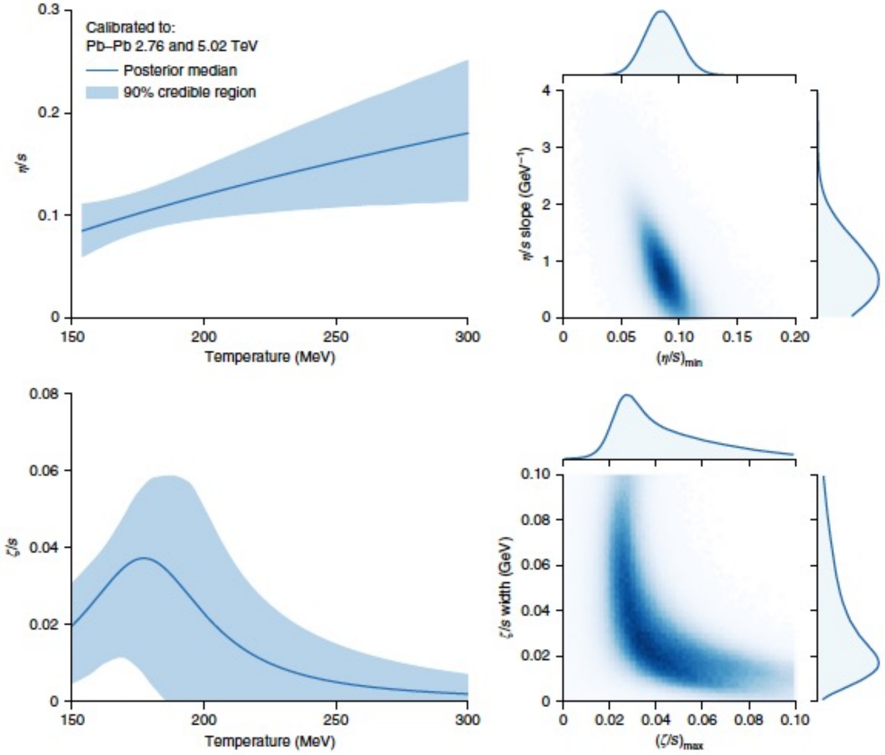

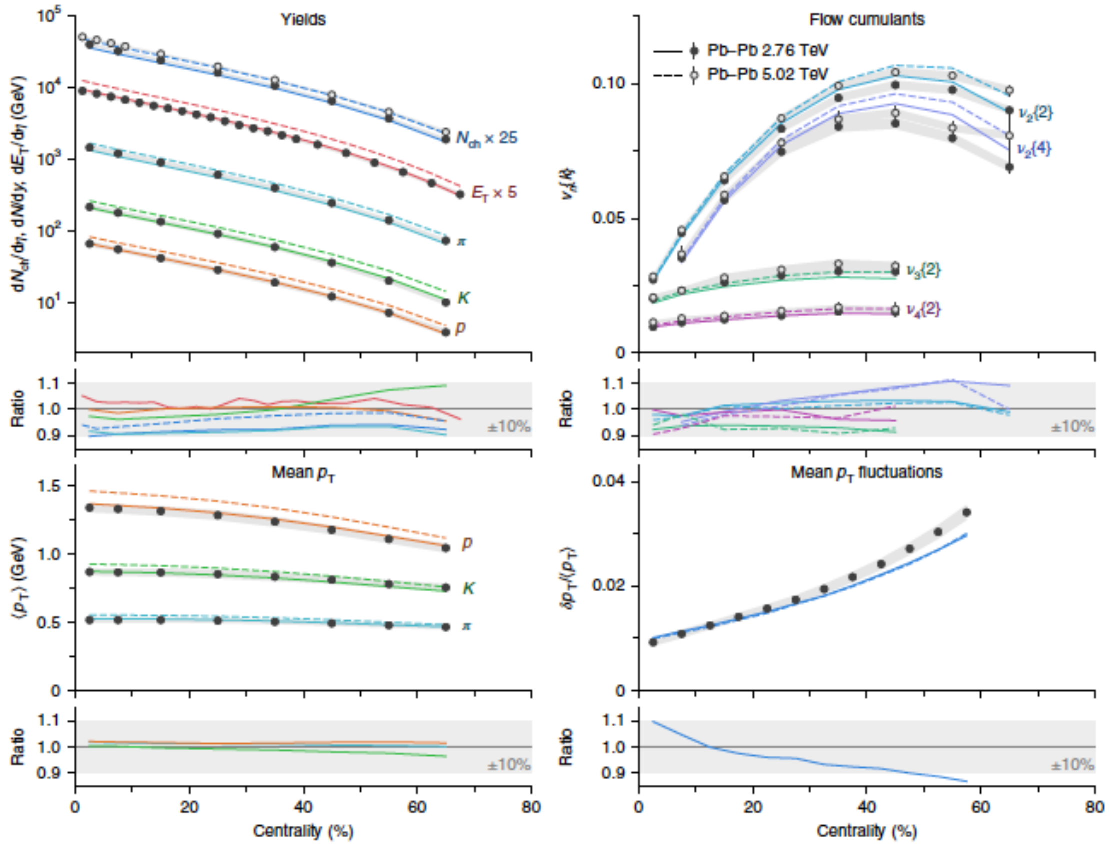

- near T_c, shear viscosity/entropy density close to AdS/CFT lower bound $1/4\pi$ rising with temperature in QGP
- bulk viscosity/entropy density peaks near T_c

Constraining initial condition and QGP medium properties

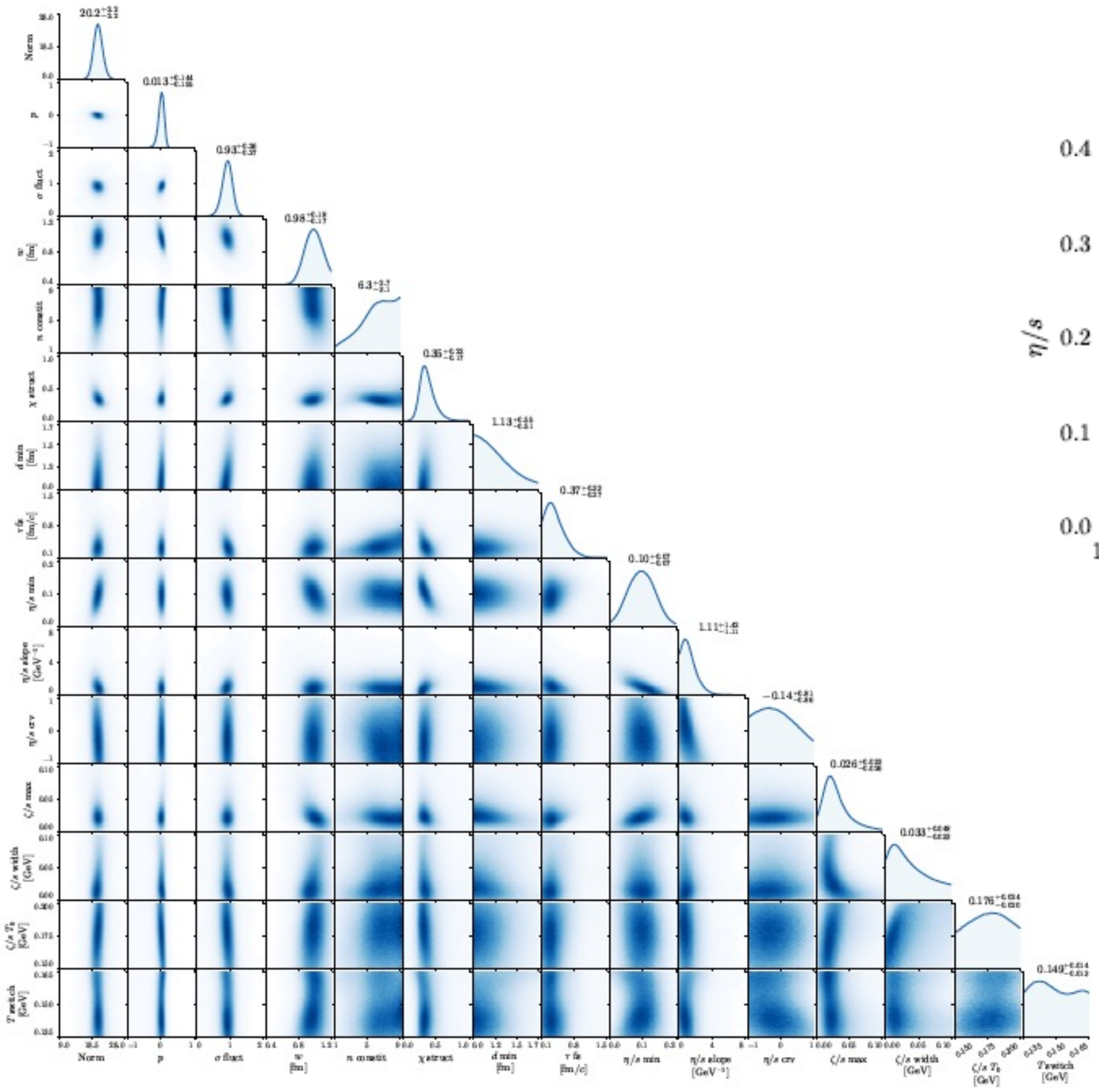

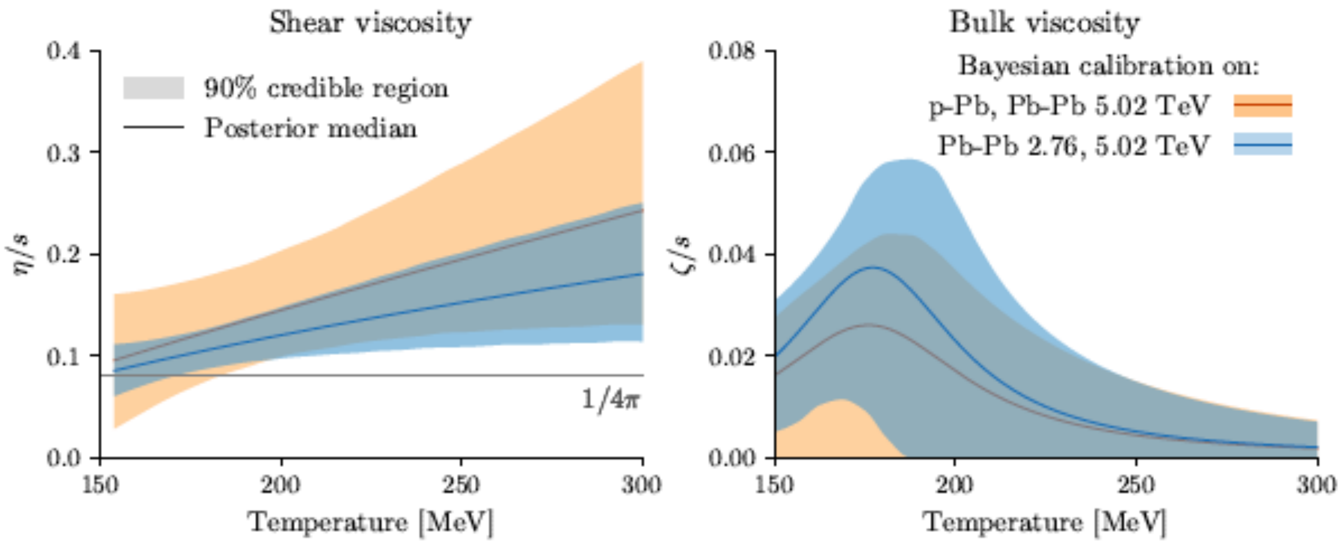

Phys. Rev. C 101, 024911 (2020)

Accessing initial conditions: v_2 - $[p_T]$ correlations

PLB 834 (2022) 137393

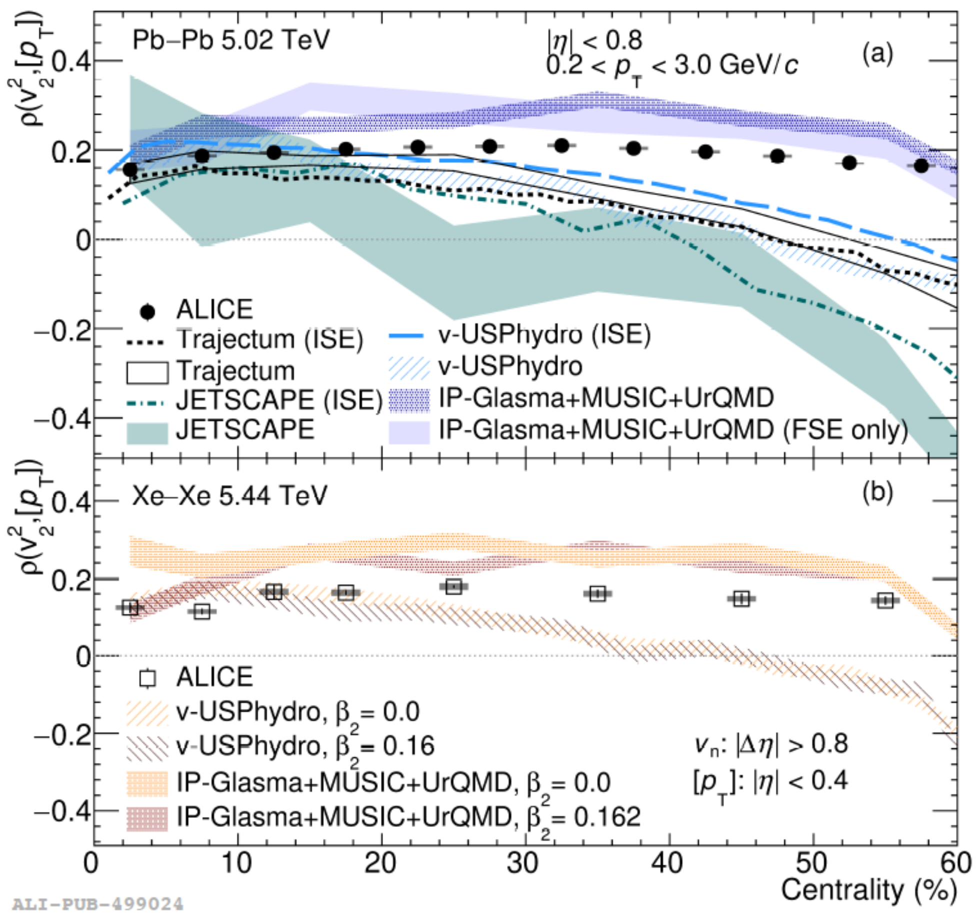

$$\rho(v_n^2, [p_T]) = \frac{Cov(v_n^2, [p_T])}{\sqrt{Var(v_n^2)}\sqrt{c_k}},$$

- positive correlation observed
- almost no centrality dependence

Initial conditions:
Trento ↔ IP - Glasma

IP-Glasma closer to data than Trento

including these data in the Bayesian global fitting
→ better constraint on the initial state in nuclear collisions
(Prerequisite for study of QGP transport properties)

Two-particle transverse momentum correlator G_2

PLB 804 (2020) 135375

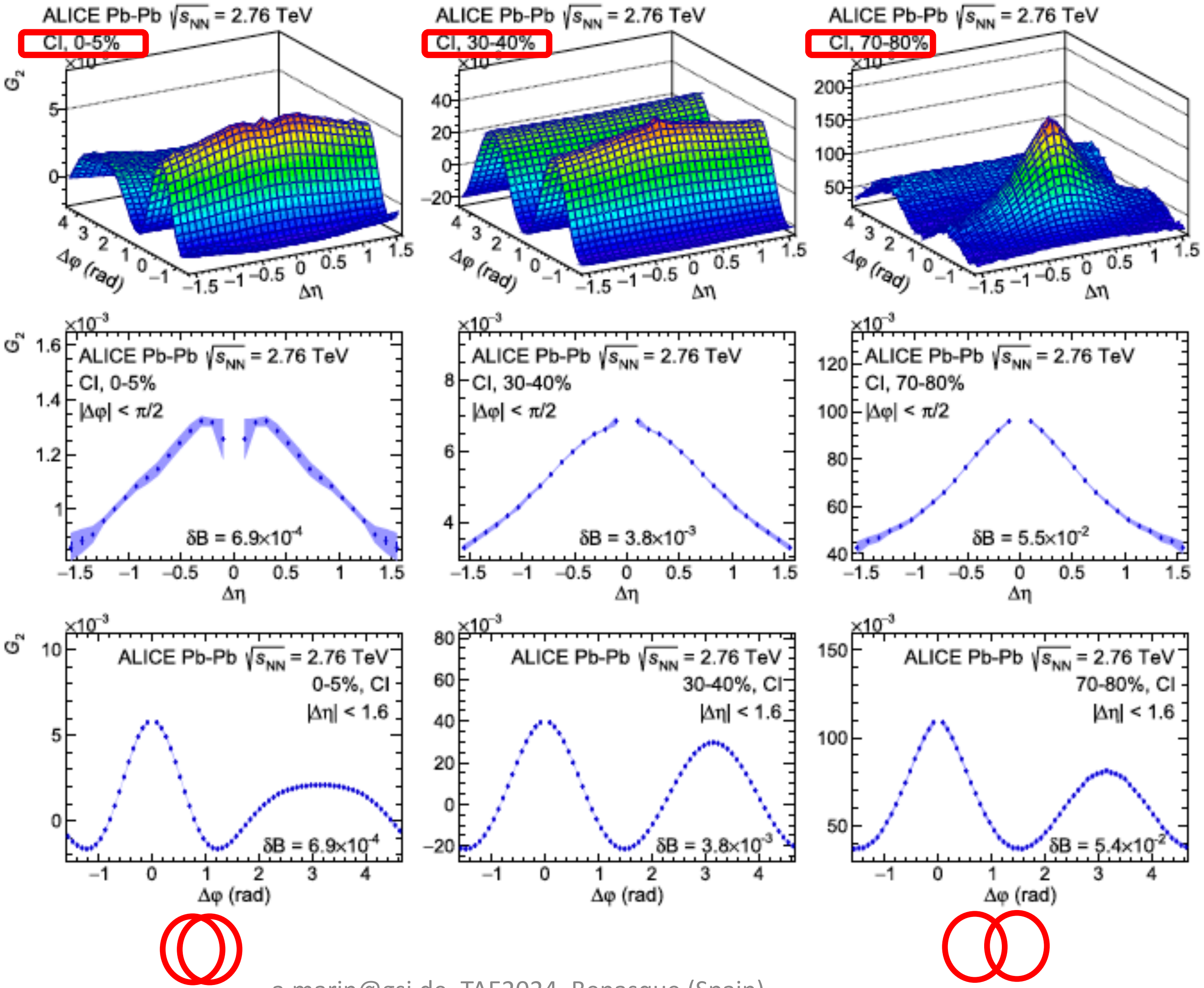

Extraction of QGP transport characteristics

$$G_2(\Delta\eta, \Delta\varphi) = \frac{1}{\langle p_T \rangle^2} \left[\frac{\langle \sum_i^{n_{1,1}} \sum_{j \neq i}^{n_{1,2}} p_{T,i}\, p_{T,j} \rangle}{\langle n_{1,1} \rangle \langle n_{1,2} \rangle} - \langle p_{T,1} \rangle \langle p_{T,2} \rangle \right]$$

- Sensitive to momentum currents transfer
- The longitudinal dimension provides fingerprints of this transfer
- The reach of the transfer ⇒ proxy for the shear viscosity η/s

Longitudinal width evolution with collision centrality ⇒ η/s

$$\sigma_c^2 - \sigma_0^2 = \frac{4}{T_c} \frac{\eta}{s} \left(\tau_0^{-1} - \tau_{c,f}^{-1} \right)$$

Gavin, Abdel-Aziz, PRL 97 162302 (2006)
Sharma, Pruneau, PRC 79 024905 (2009)
STAR, PLB 704, 467–473 (2011)

G_2 widths evolution: Pb-Pb, p-Pb and pp

PLB 804 (2020) 135375

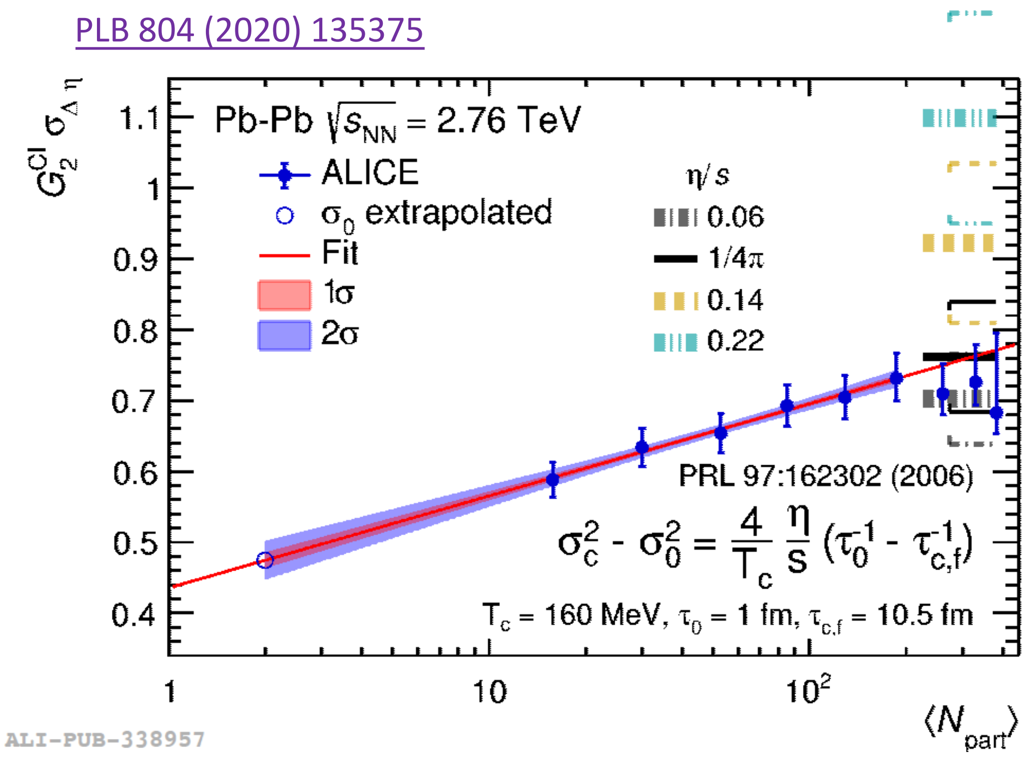

arXiv: 2211.08979

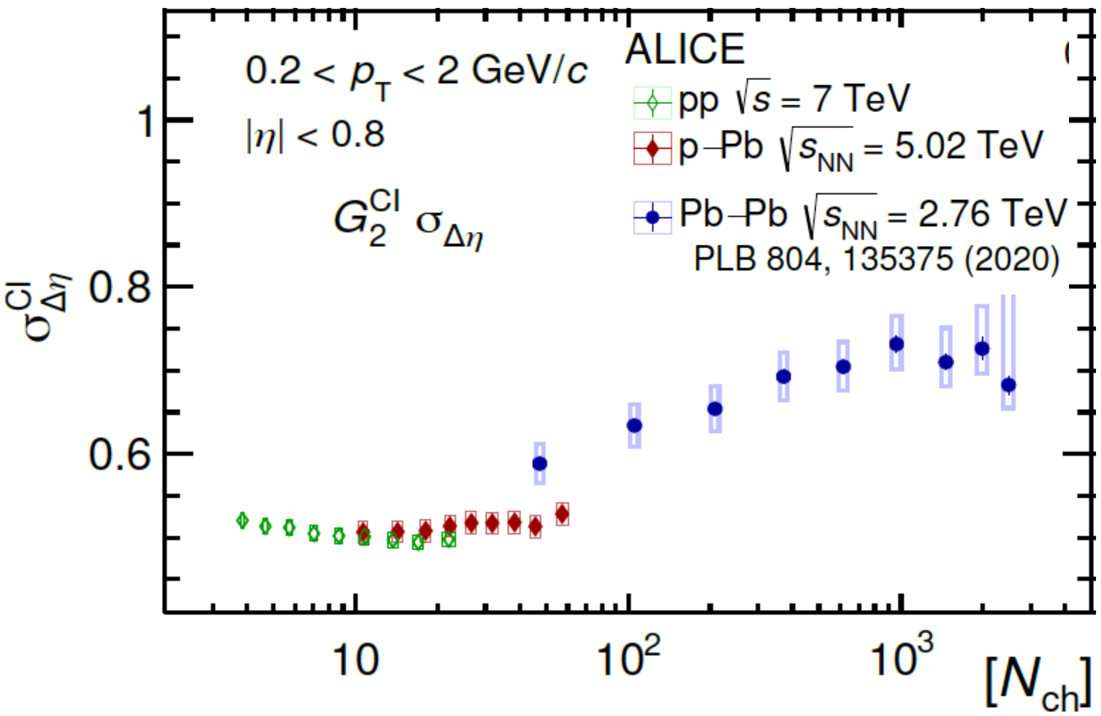

Data seem to favour small η/s values

V. Gonzalez *et al.*
EPJC 81 (2021) 5, 465

No evidence for shear viscous effects in pp & p–Pb based on $G_2^{CI}\sigma_{\Delta\eta}$
- System lifetime too short for viscous forces to play a significant role?

ALICE constraints on shear and bulk viscosity

arXiv: 2211.04384

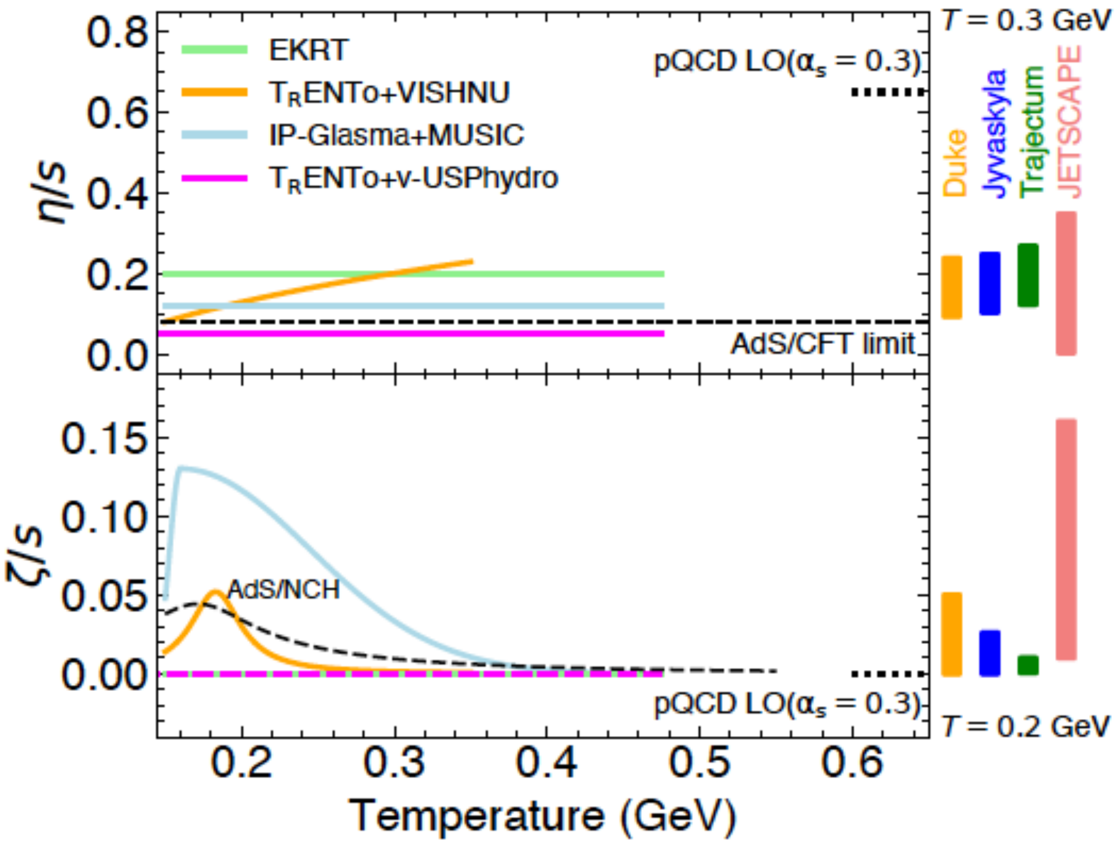

Probing Hot QCD Matter with hard probes

Hard Probes:

"highly penetrating observables (particles, radiation) used to explore properties of matter that cannot be viewed directly!"

p_T , m > 2 GeV >> Λ_{QCD}

Hard probes

p+p:
- parton scattering → fragmentation → jet
- can be calculated in perturbative QCD
- collinear factorization

A+A:
- partons traversing medium lose energy
  gluon radiation, elastic collisions
- energy loss different for g, light/heavy quarks
  (color factor, dead cone effect)

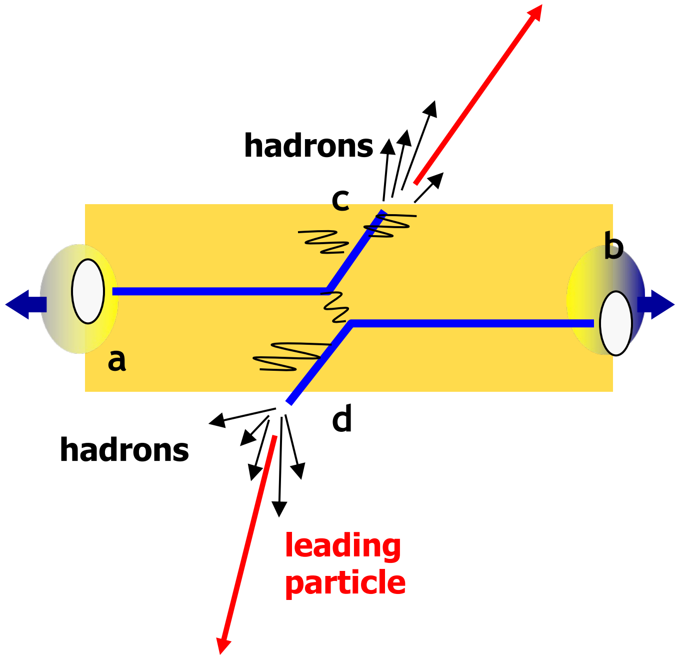

X.-N. Wang, M. Gyulassy, Phys. Rev. Lett. ***68*** *(1992) 1480*

Goal: Use in-medium energy loss to measure medium properties

$$\frac{d\sigma_{pp}^{h}}{dy\,d^{2}p_{T}} = K\sum_{abcd}\int dx_a dx_b f_a(x_a,Q^2) f_b(x_b,Q^2) \frac{d\sigma}{d\hat{t}}(ab\rightarrow cd)\frac{D^{0}_{h/c}}{\pi z_c}$$

Parton distribution function	Matrix element	Fragmentation function
measured in DIS initial state (saturation?)	pQCD	e^+e^- final state (energy loss?)

Medium modifications

The Physics of the Quark-Gluon Plasma

$$R_{AA}(\sqrt{s_{NN}}, p_T, y, m; b) = \frac{\text{"hot/dense QCD medium"}}{\text{"QCD vacuum"}} \propto \frac{\Phi_{AA}(\sqrt{s_{NN}}, p_T, y, m; b)}{\Phi_{pp}(\sqrt{s}, p_T, y, m)}$$

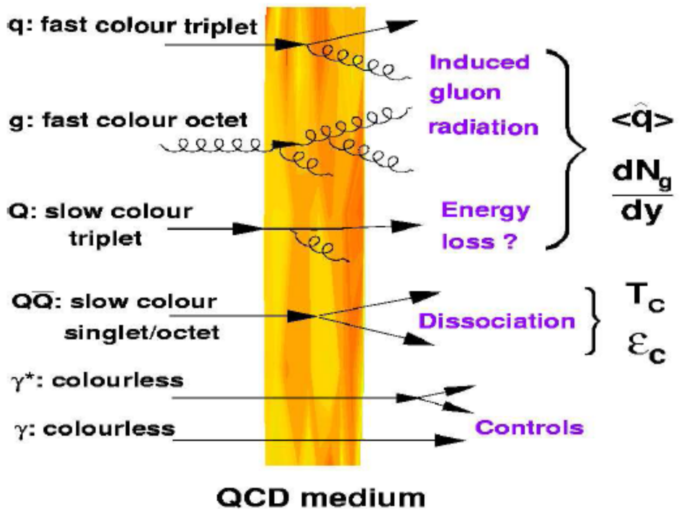

Figure 3. Examples of hard probes whose modifications in high-energy *AA* collisions provide direct information on properties of QCD matter such as the $\langle\hat{q}\rangle$ transport coefficient, the initial gluon rapidity density dN^g/dy, and the critical temperature and energy density.

Any observed *enhancements* and/or *suppressions* in the $R_{AA}(s_{NN}, p_T, y, m; b)$ ratios can then be directly linked to the properties of strongly interacting matter.

Measurement in pp collisions is essential/ mandatory

Medium modifications: R_{AA}

$$R_{AA}(p_t) = \frac{1}{\langle N_{coll} \rangle} \times \frac{dN_{AA}/dp_t}{dN_{pp}/dp_t}$$

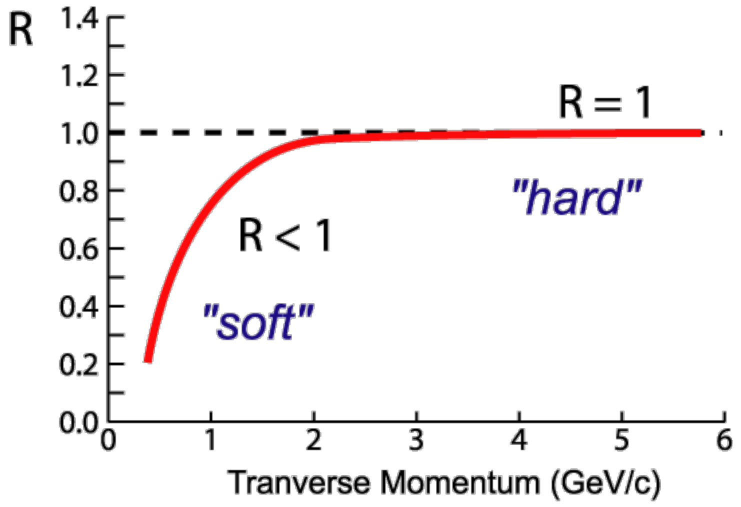

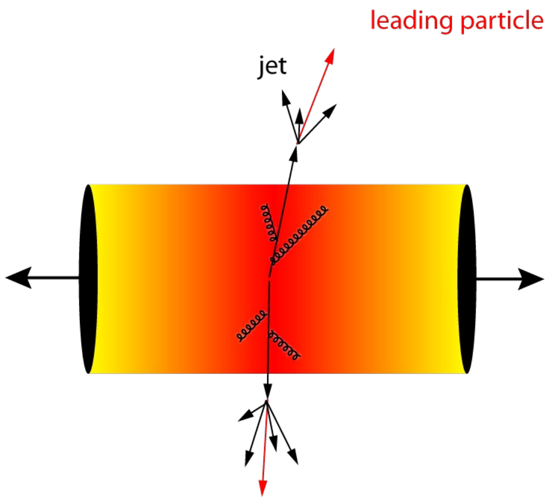

No "Effect":

- R < 1 at small momenta
- R = 1 at higher momenta where hard processes dominate

Suppression:

- R < 1

$$\Delta E(\varepsilon_{QGP}; C_R, m, L)$$

$$\Delta E_g > \Delta E_{c \approx q} > \Delta E_b$$

$$R_{AA}^{\pi} < R_{AA}^{D} < R_{AA}^{B}$$

Measurement in pp collisions is essential/mandatory.

Measurement in p-Pb (cold nuclear matter effects) collisions as control experiment

Goal: Use in-medium energy loss to measure medium properties

Discovery of jet quenching at RHIC

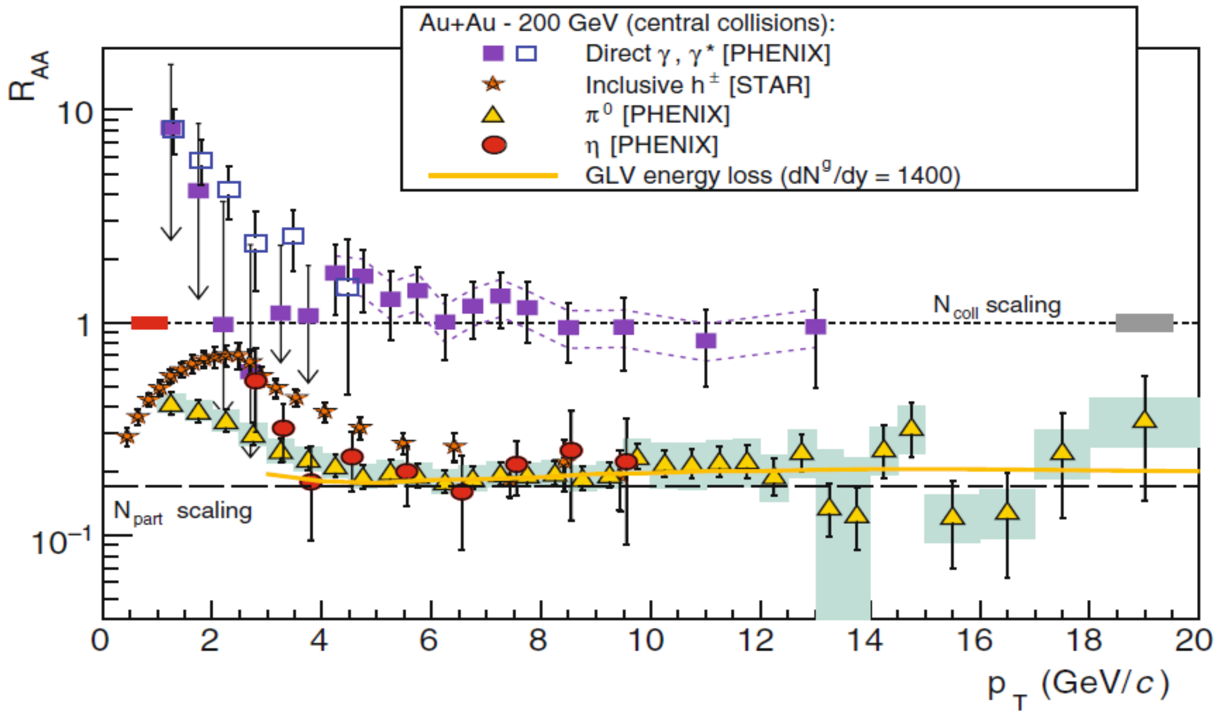

PHENIX: Phys.Rev.Lett.88:022301, 2002
PHENIX: Phys.Rev.Lett.91:072301, 2003
PHENIX: Phys.Rev.Lett.94:232301, 2005
STAR: Phys.Rev.Lett.89:202301,2002
STAR: Phys.Rev.Lett.90:082302,2003
STAR: Phys.Rev.Lett.91:172302,2003

R_{AA}^{γ} ~=1

$R_{AA}^{\pi^0,\eta}$ ~=0.2

- Hadrons are suppressed, direct photons are not
- The hadron spectra at RHIC from p+p, Au+Au and d+Au collisions establish existence of parton energy loss from strongly interacting, dense QCD matter in central Au-Au collisions

$$\varepsilon_{\text{loss}} \approx 1 - R_{AA}^{1/(n-2)}$$

https://wiki.bnl.gov/TECHQM/index.php/Main_page
Theory-Experiment Collaboration on Hot Quark Matter

<q^> = 4 – 13 GeV2 / fm
dNg/dy~1400+-200
S. Bass et al. PRC79 (2009) 024901

Discovery of jet quenching at RHIC

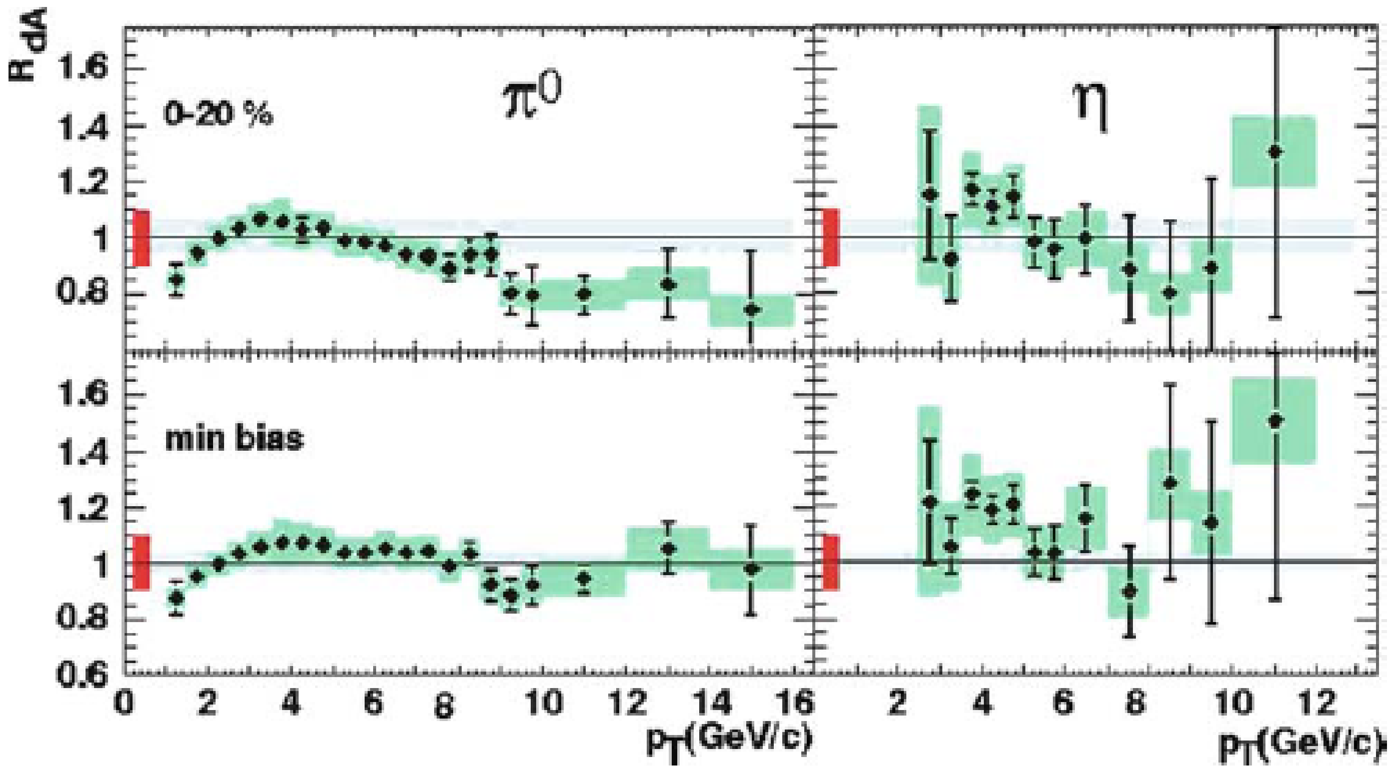

Fig. 14 Nuclear modification factors for high-p_T π^0 (*left*) and η (*right*) mesons at midrapidity in dAu collisions at $\sqrt{s_{NN}}$ = 200 GeV [143, 144] compared to pQCD calculations [145, 146] with EKS98 [147] nuclear PDFs

No suppression in dAu. Evidence for final state effect.

Charged particles R_{AA}

JHEP11(2018)013

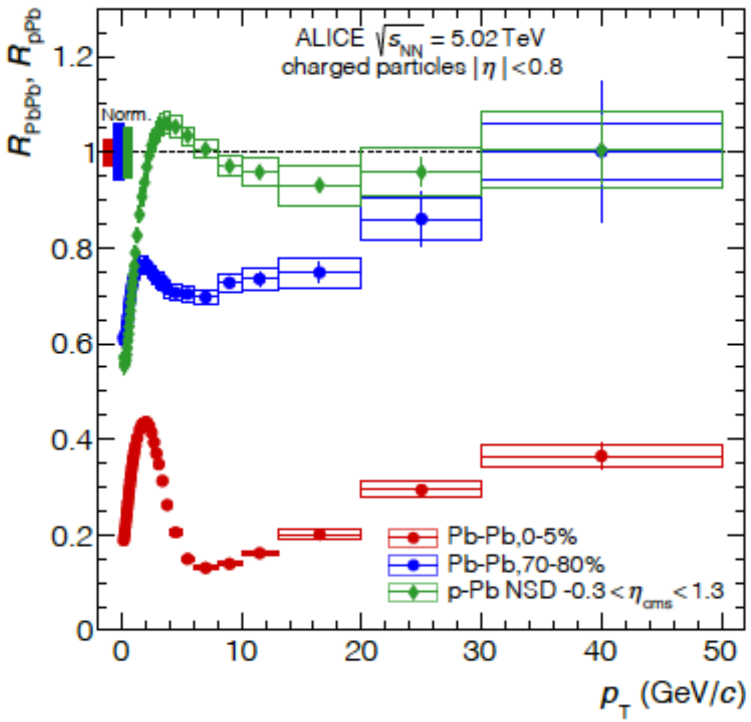

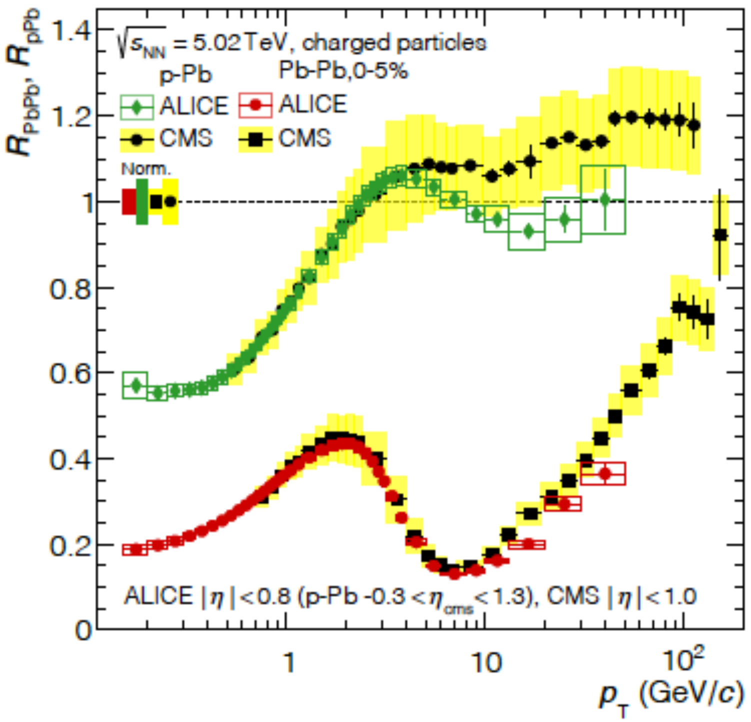

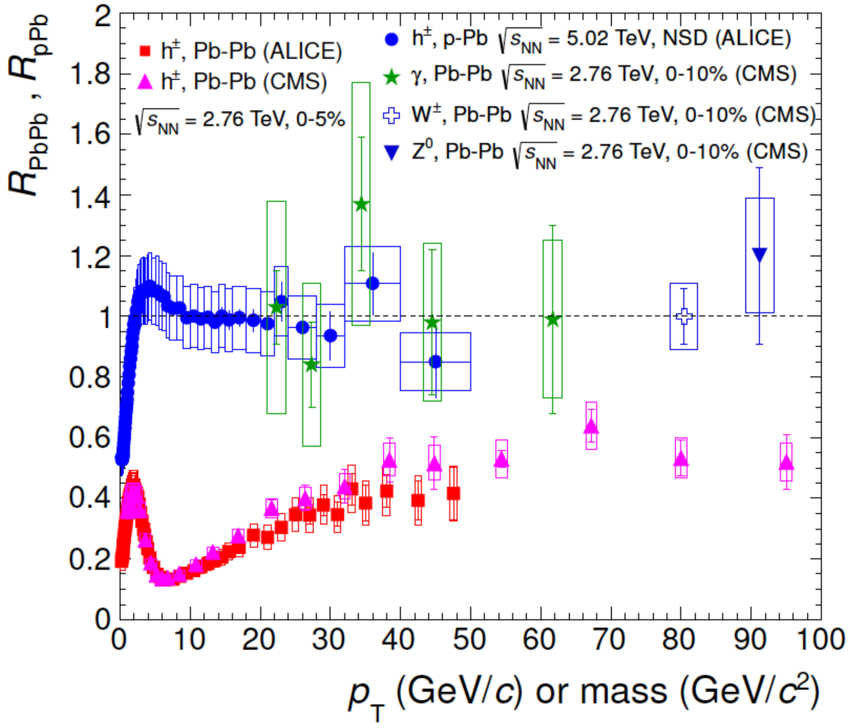

R_{pPb} ~1: small cold-nuclear effects
R_{PbPb} <1: suppression
Larger for more central Pb--Pb collisions

Colorless probes are unaffected:
γ, and W, Z bosons

Open heavy-flavor production: D^0, D^+, D^{*+}

JHEP 01 (2022) 174

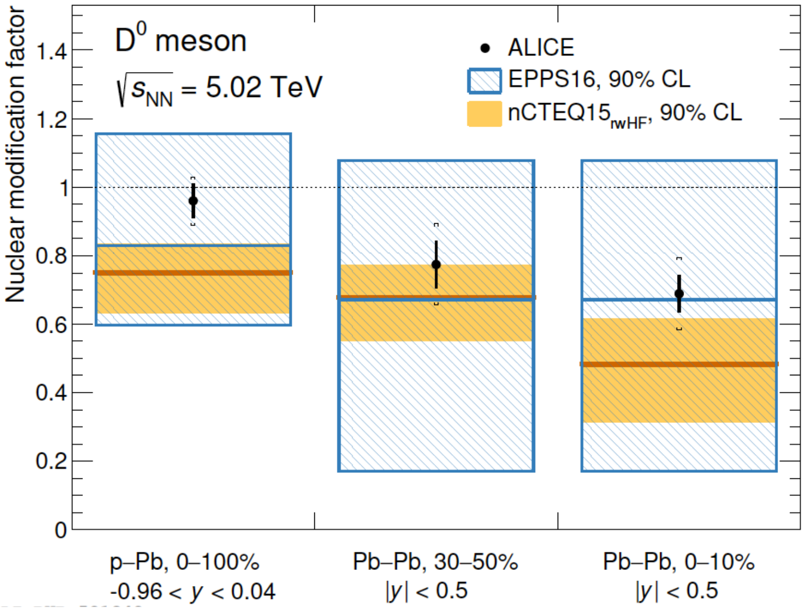

Charm quark flows

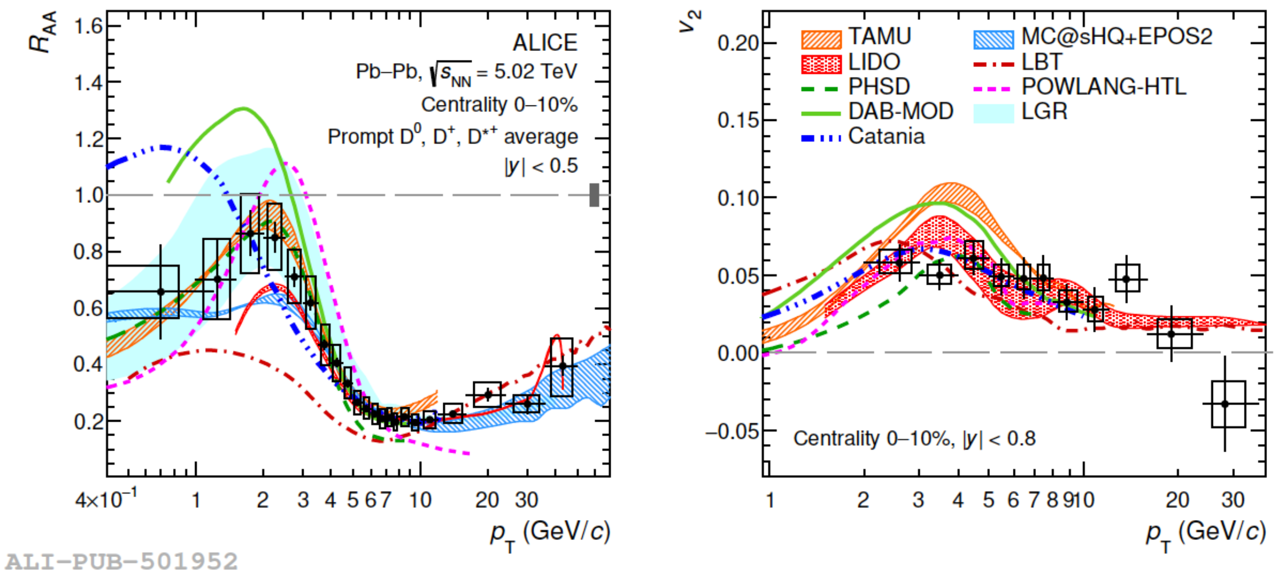

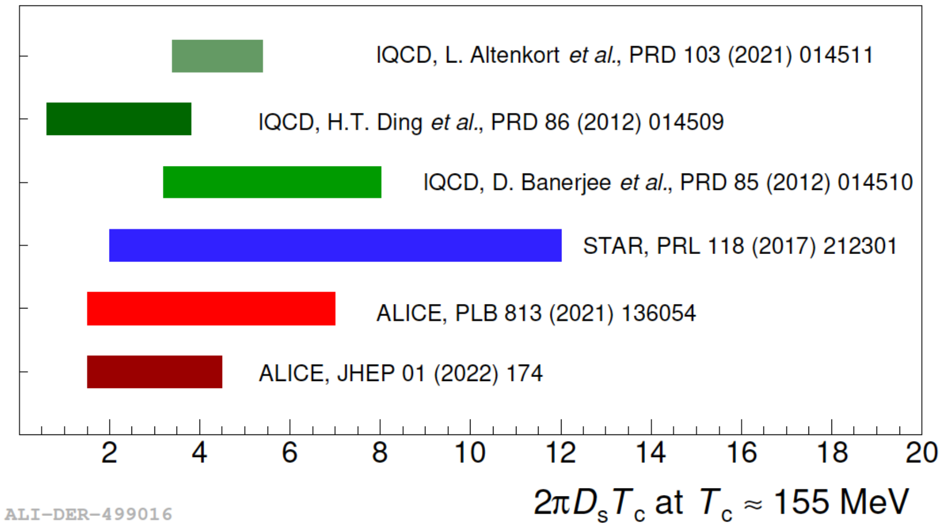

Precise R_{AA} and elliptic flow (v_2, v_3) non-strange D mesons
→ constraints on to charm quark energy loss models

- Intermediate and high p_T :

Radiative energy loss important

- Low/intermediate p_T :

Charm-quark hadronisation via recombination essential

Spatial diffusion coefficients:

$1.5 < 2\pi D_s T_c < 4.5$ → relaxation time of τ_{charm} ~ 3-8 fm/c

Charm Diffusion coefficient: T dependence

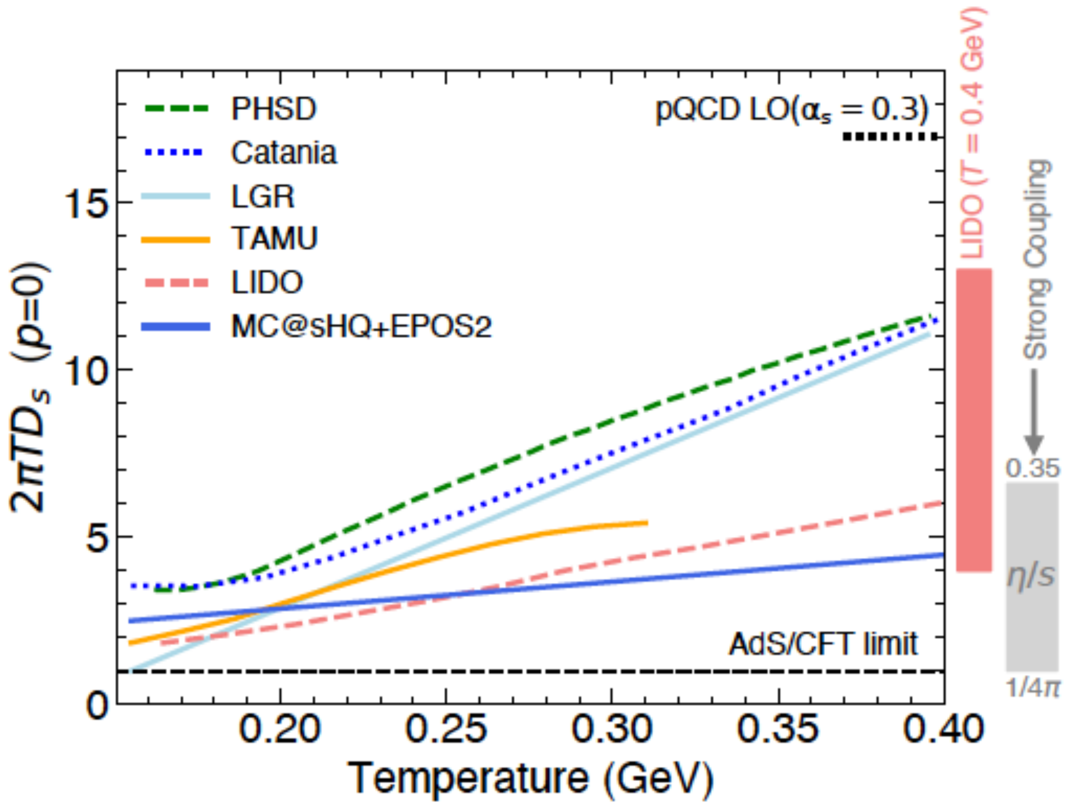

Temperature dependence of D_s constrained by ALICE measurement for various models

Probing ΔE dependence of parton species

JHEP01(2022)174

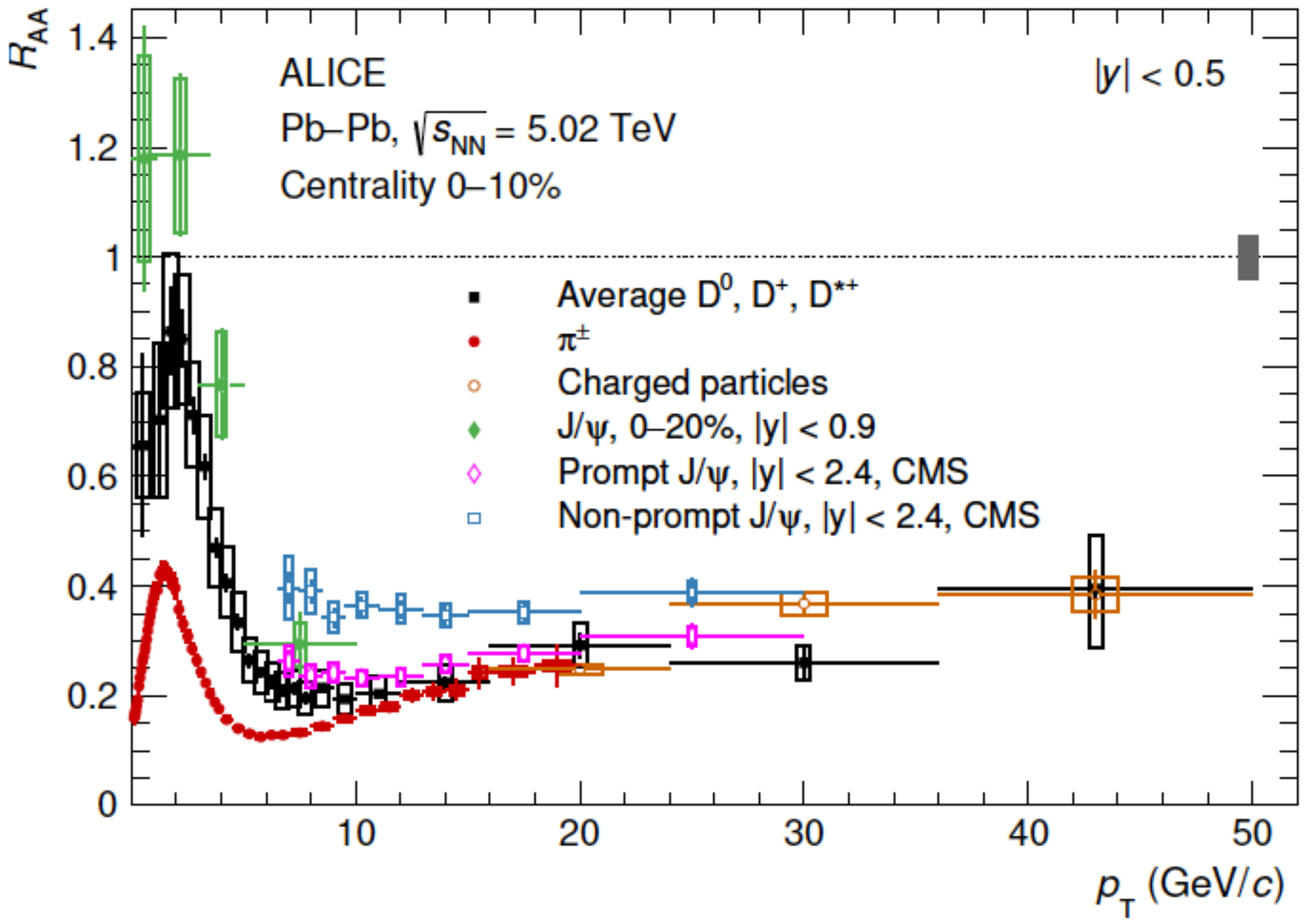

Beauty:
B→J/Ψ+X

Charm:
Prompt J/Ψ
Prompt D

Light-hadrons:
Pions
Charged particles

$$R_{AA}^{\pi} < R_{AA}^{D} < R_{AA}^{B}$$

v_2 across particle species

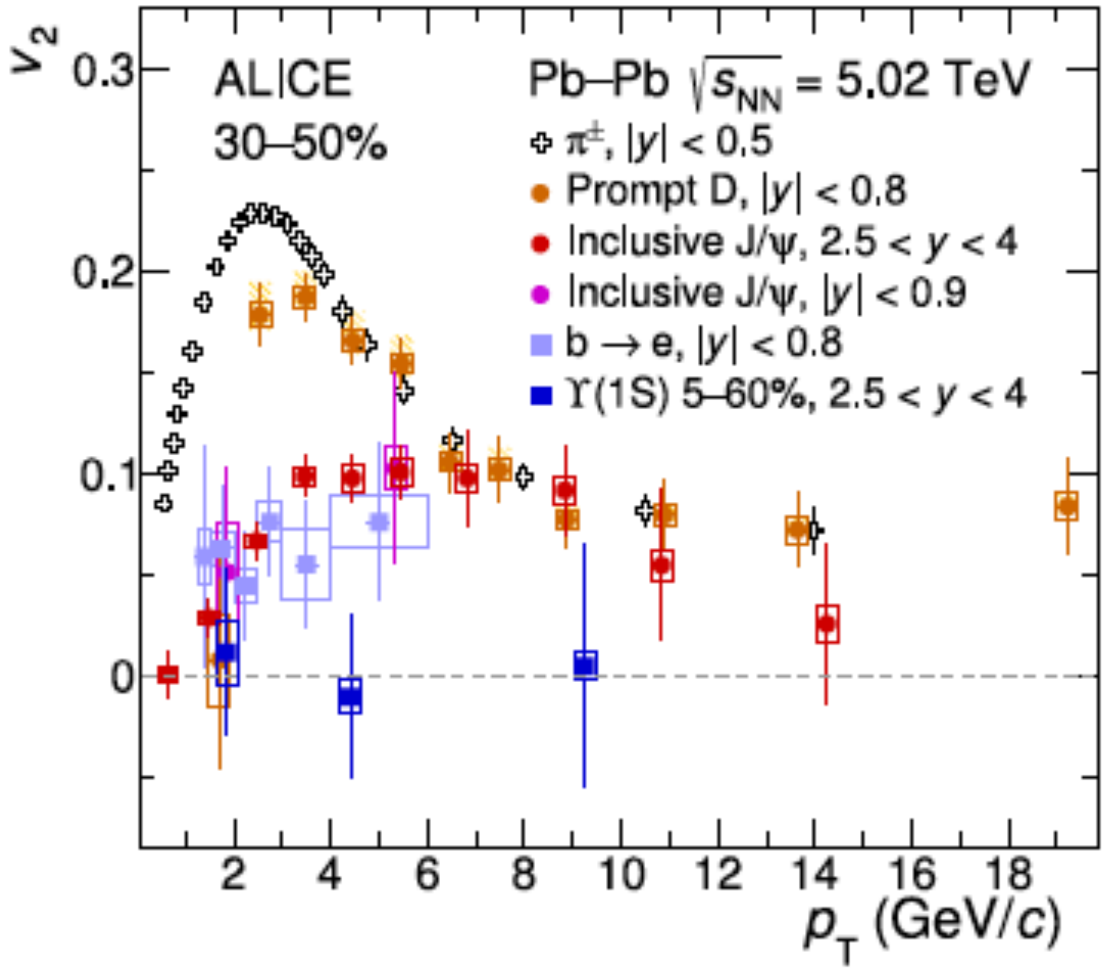

Clear quark flavor hierarchy observed in the low p_T

Significant v_2 for open and hidden charm hadrons

Open beauty hadrons exhibit flow

Quark-mass dependence of energy loss

Prompt D^0: c→ D^0

Non prompt D^0: b→ c → D^0

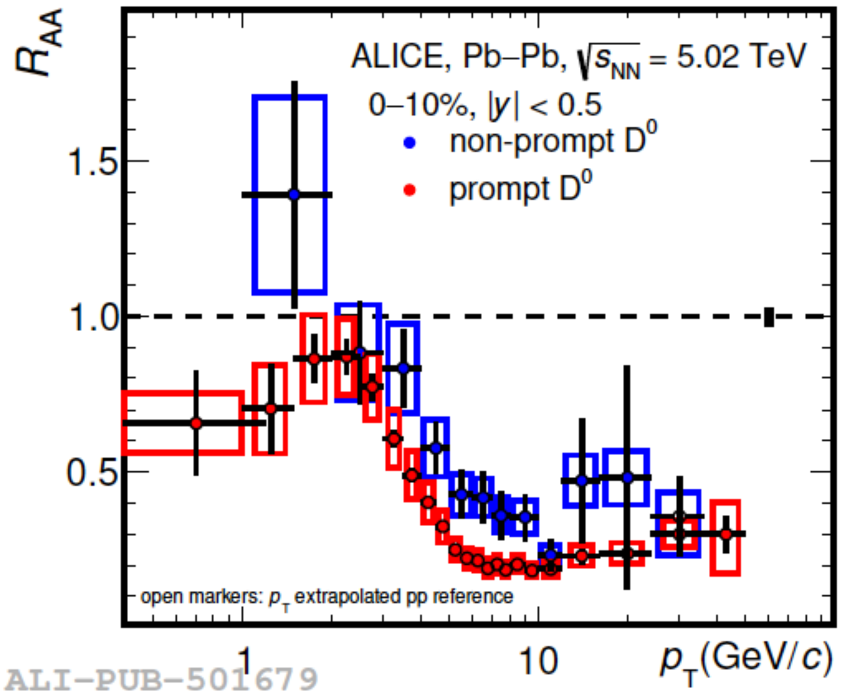

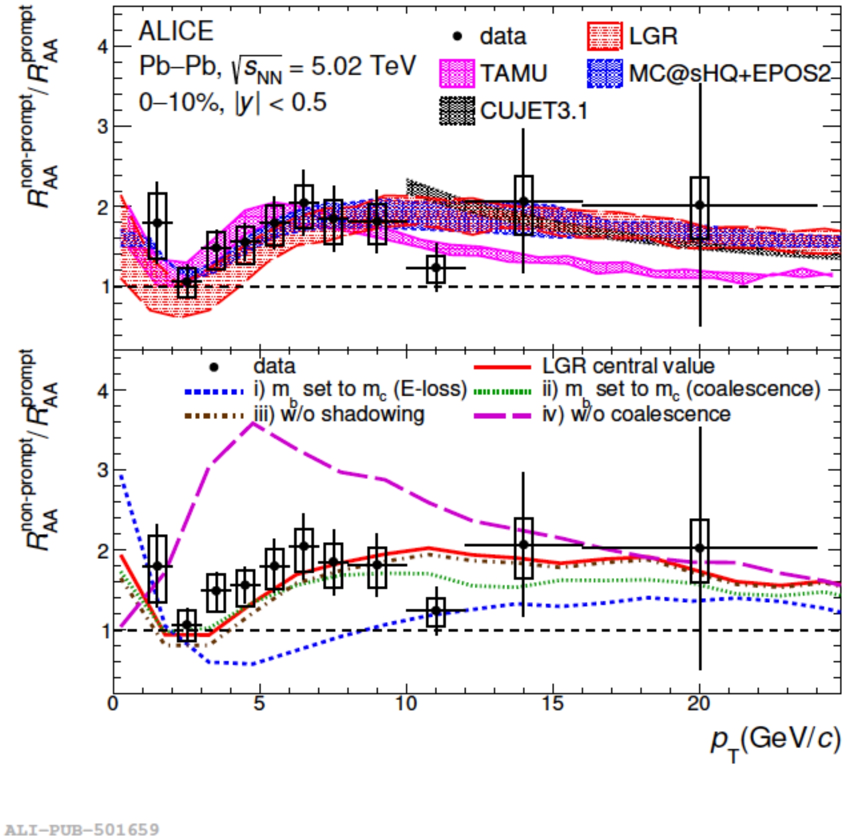

Energy loss predicted to depend on QGP density, but also on quark mass $\Delta E_c > \Delta E_b$

Less suppression for (non-prompt) D mesons from B decays than prompt D mesons

- Data described by models that include collisional and radiative energy loss, and recombination
- Valley structure at low p_T mainly due to formation of D via quark coalescence

Jet transport coefficient

PRC104, 024905 (2021)

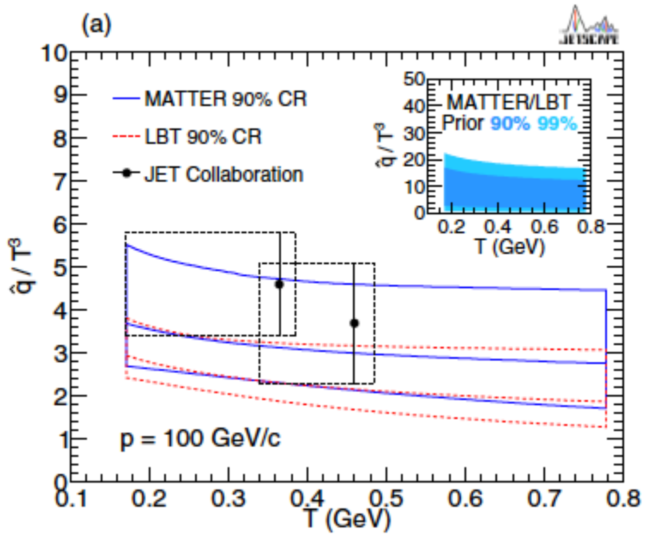

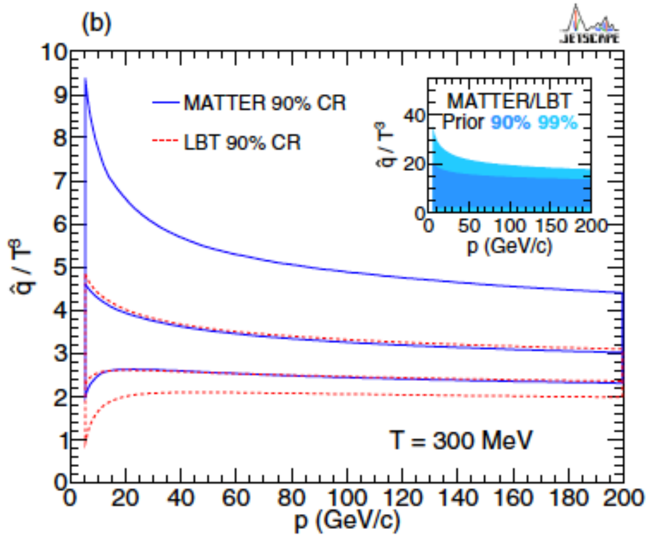

arXiv: 2211.04384

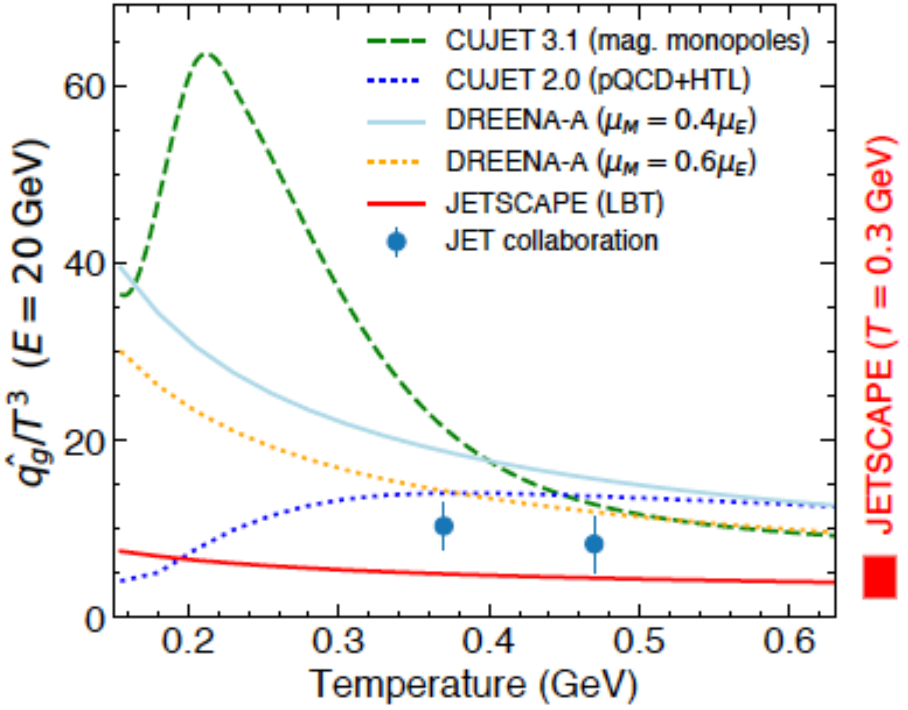

Quarkonia

Quarkonia

Quarkonia are heavy quark antiquark bound states, i.e. ccbar and bbar.
Stable with respect to strong decay into open charm or bottom.
$M_{ccbar} < 2M_D$ and $M_{bbbar} < 2M_B$

State	J/ψ	χ_c	ψ'	Υ	χ_b	Υ'	χ_b'	Υ''
Mass (GeV)	3.10	3.53	3.68	9.46	9.99	10.02	10.36	10.36
ΔE (GeV)	0.64	0.20	0.05	1.10	0.67	0.54	0.31	0.20
Radius (fm)	0.25	0.36	0.45	0.14	0.22	0.28	0.34	0.39

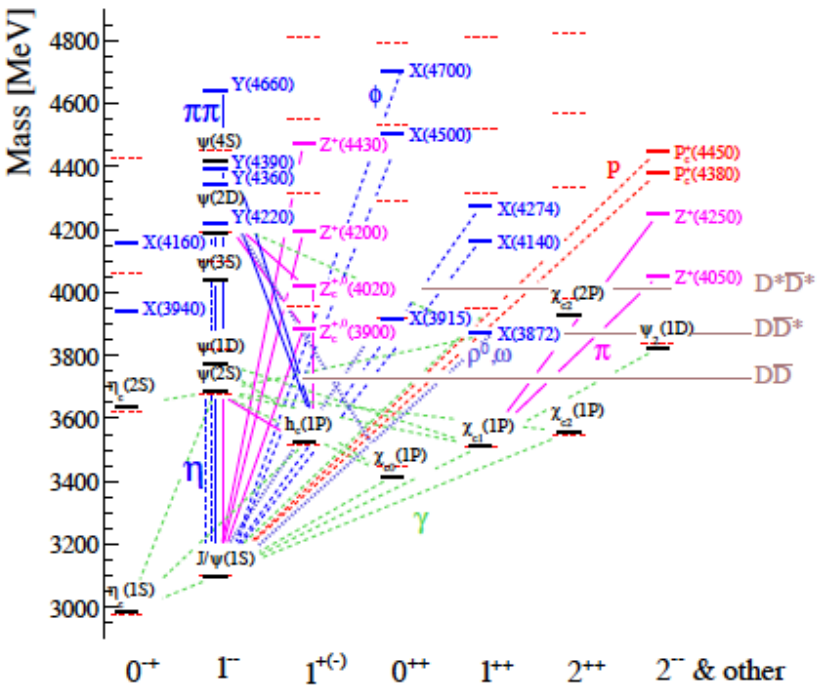

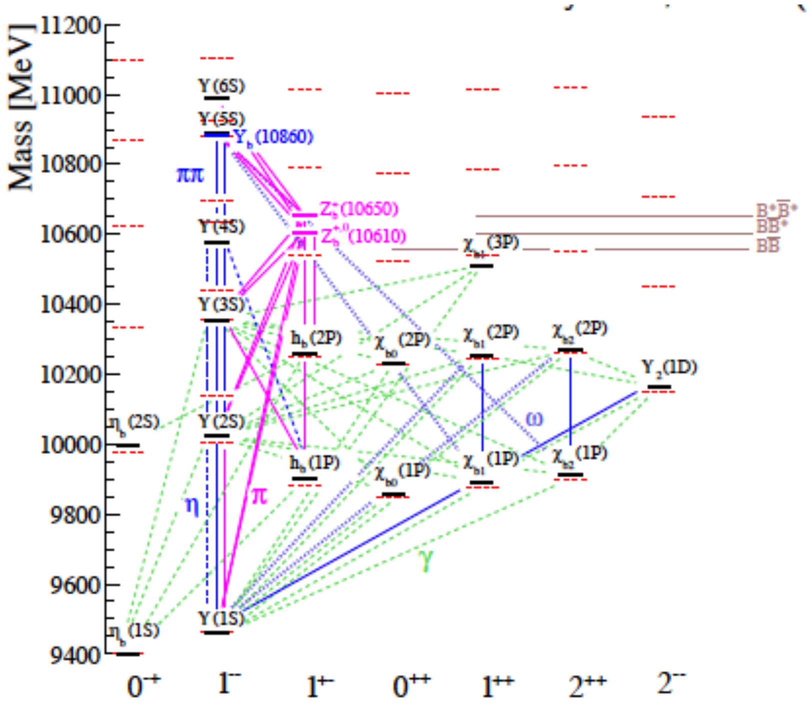

Quarkonia in Heavy-Ion Collisions

Quarkonia (J/Ψ, Υ):
26 years ago: Matsui & Satz (Phys. Lett. B178(1986) 416)
color screening in deconfined matter → J/Ψ suppression = "smoking gun"

- Sequencial dissociation versus T in QGP (Matsui/Satz)

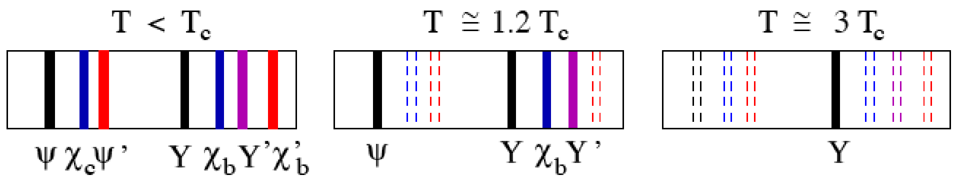

Can be used as thermometer of the medium

PRD 64 (2001) 094015

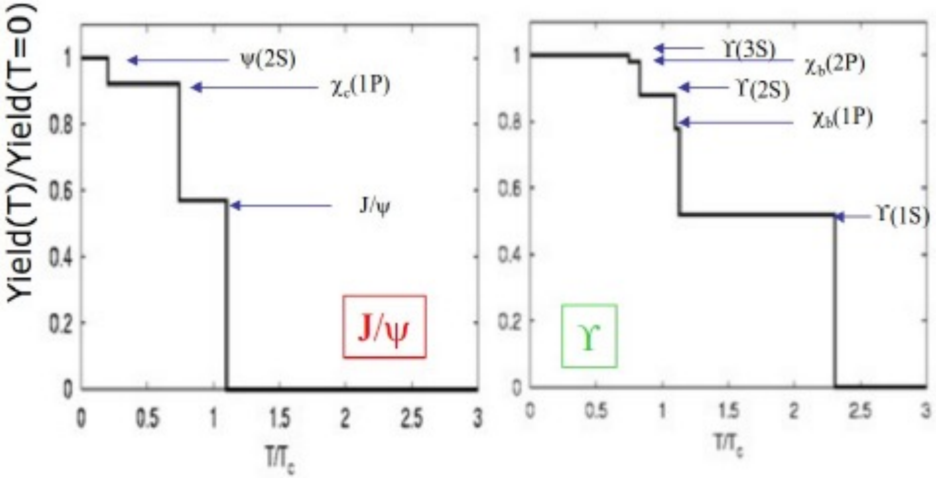

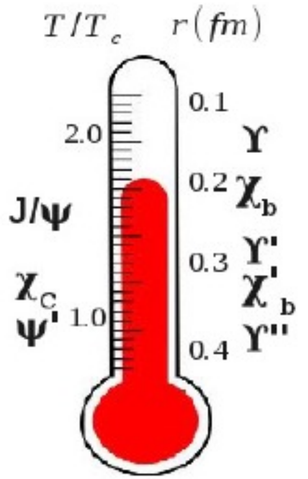

Recombination

PLB 490 (2000) 196
NPA 789 (2006) 334
PLB 652 (2007) 259

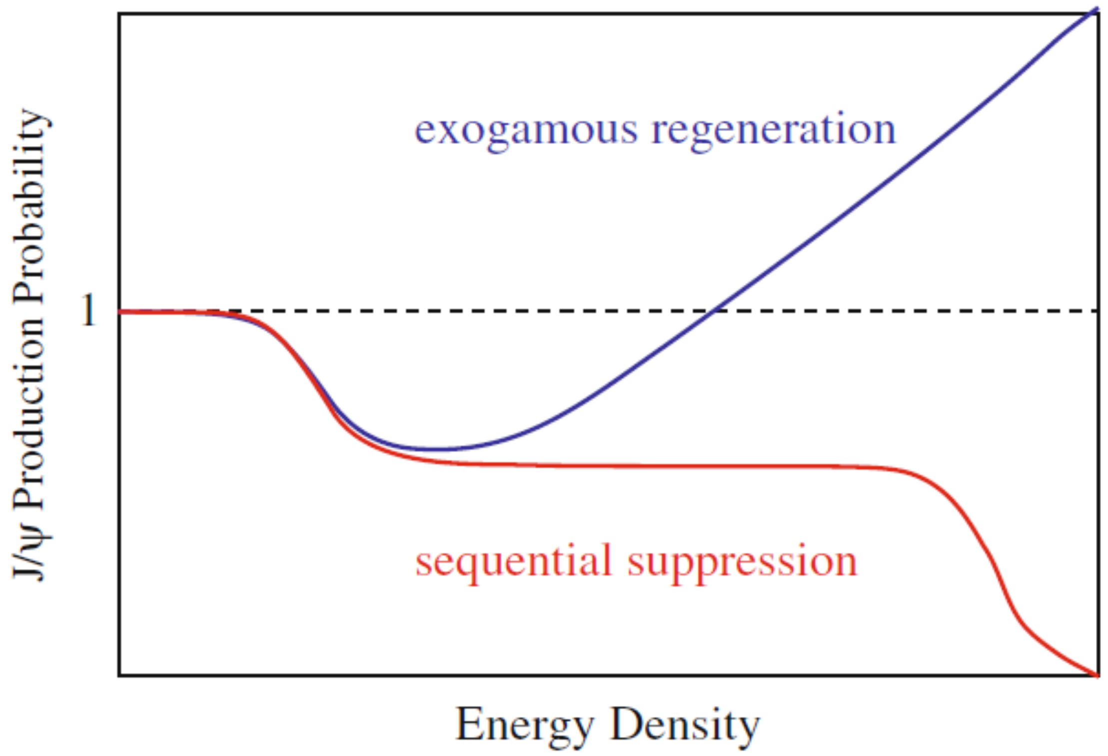

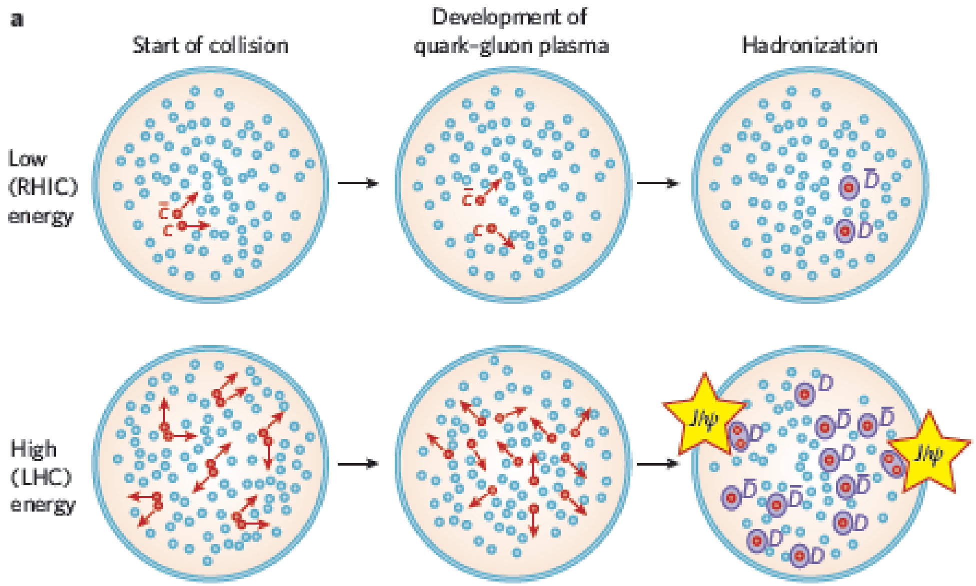

Total ccbar cross section in pp collisions needs to be known

Where does all the charm goes?

Total ccbar cross section in pp collisions needs to be known

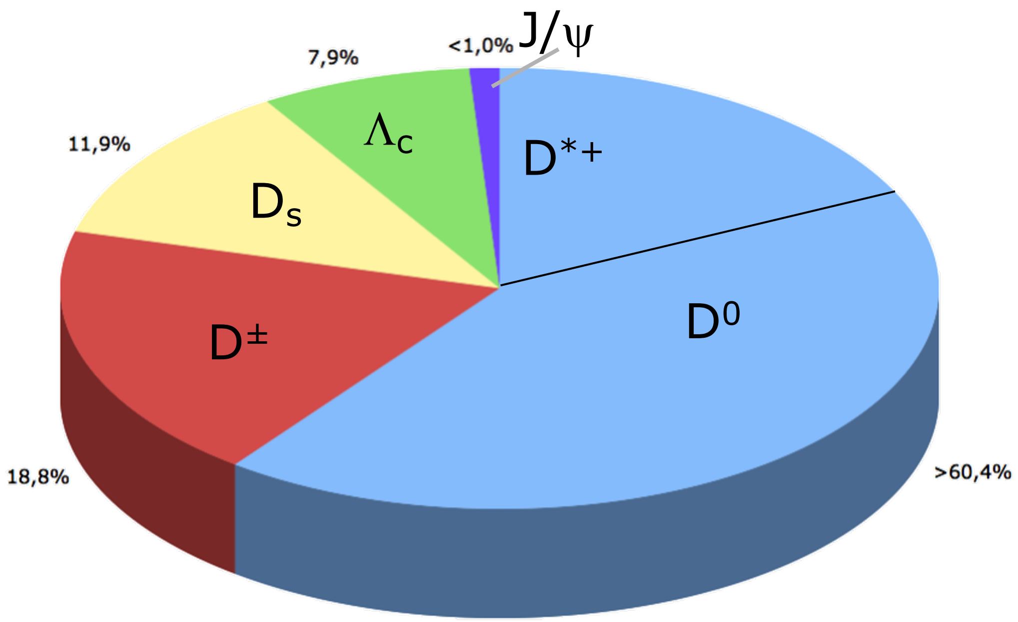

PRD 105 (2022) L011103

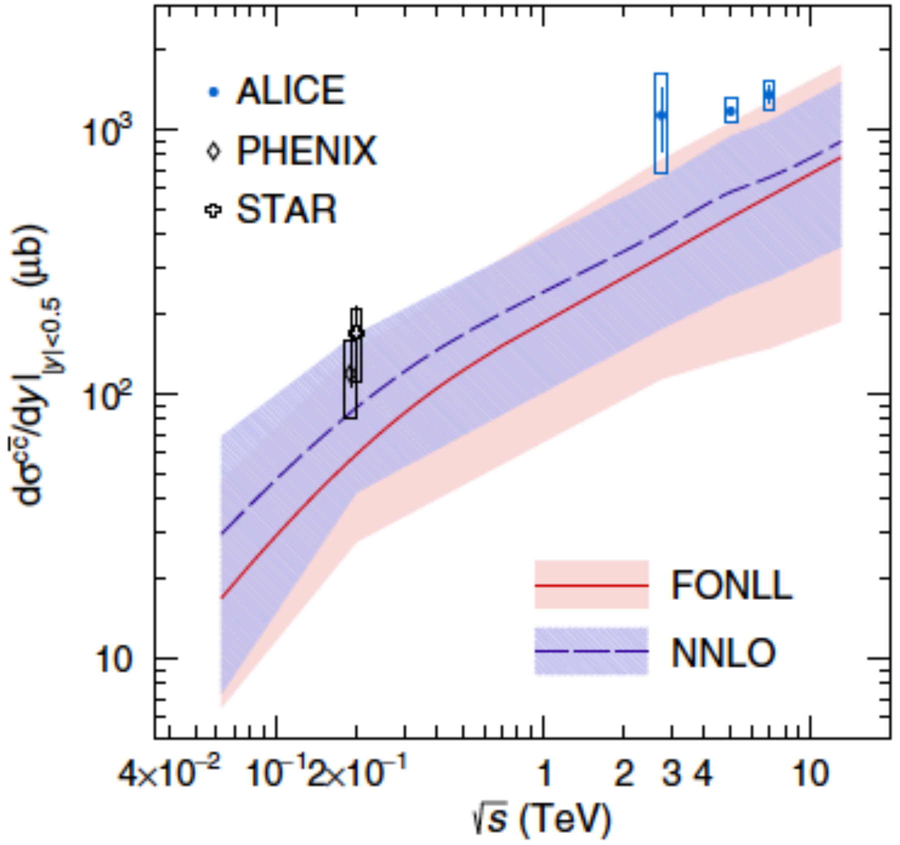

~40% increase driven by observed baryon enhancement

Data on the upper edge of FONLL and NNLO calculations

J/Ψ suppression: Energy and centrality dependence

arXiv: 2211.04384

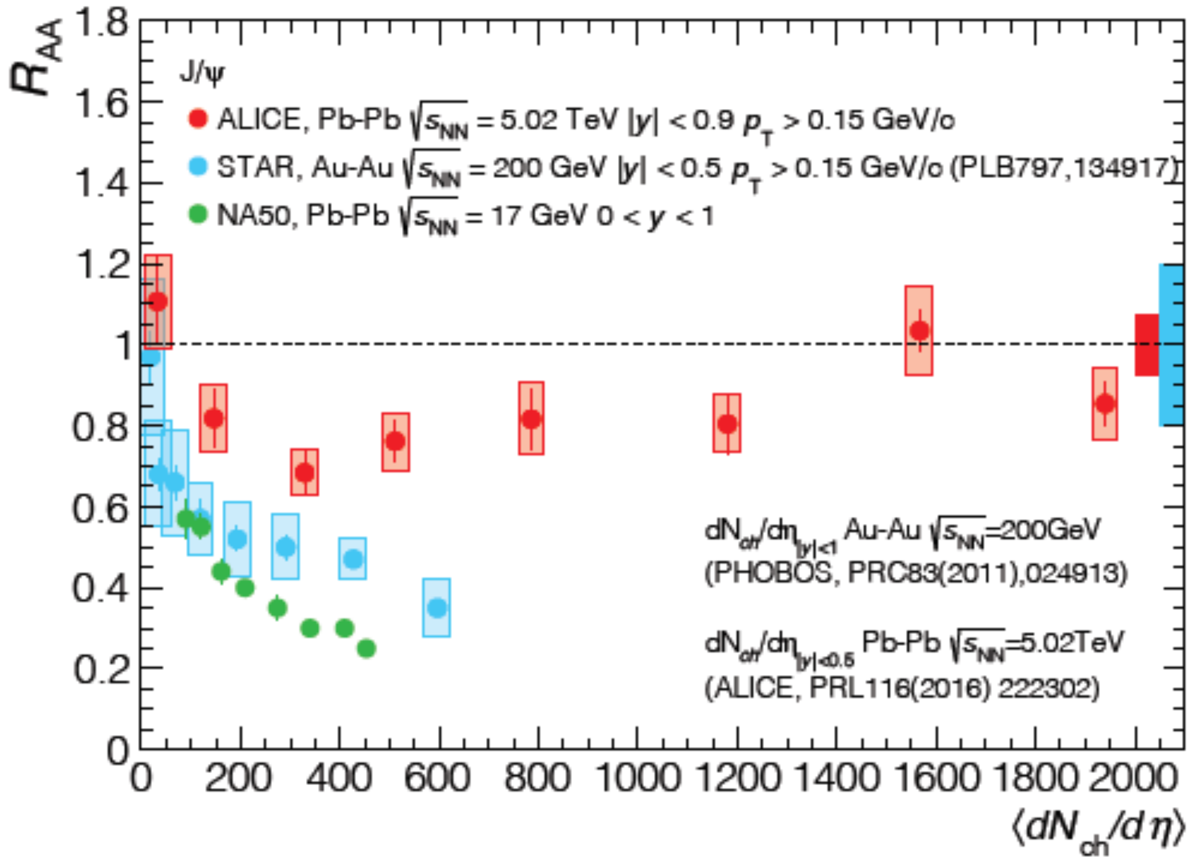

RHIC:

R_{AA} (J/Ψ) decreases with centrality at RHIC

LHC:

R_{AA}(J/Ψ) ~ 1 in central Pb--Pb

Less suppression in more central Pb--Pb collisions

Less suppression than at RHIC

Charmonium dissociation and regeneration

$$R_{AA} = \frac{1}{\langle N_{coll} \rangle} \frac{dN/dp_T|_{PbPb}}{dN/dp_T|_{pp}}$$

J/ψ suppression due to color screening in the QGP

reduced at low p_T and central rapidity by $c\bar{c}$ regeneration

~ 100 $c\bar{c}$ pairs per central Pb-Pb

P. Braun-Munzinger & J. Stachel, Nature 448 (2007) 302

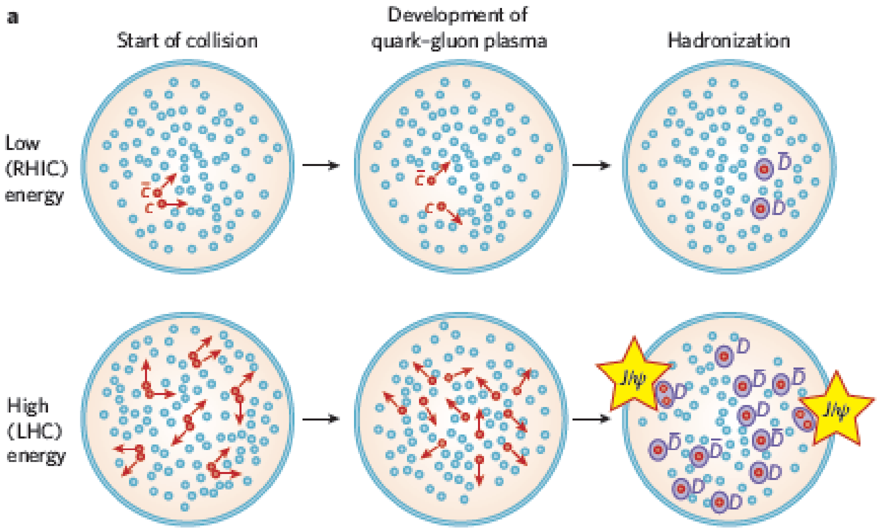

PLB 805 (2020) 135434

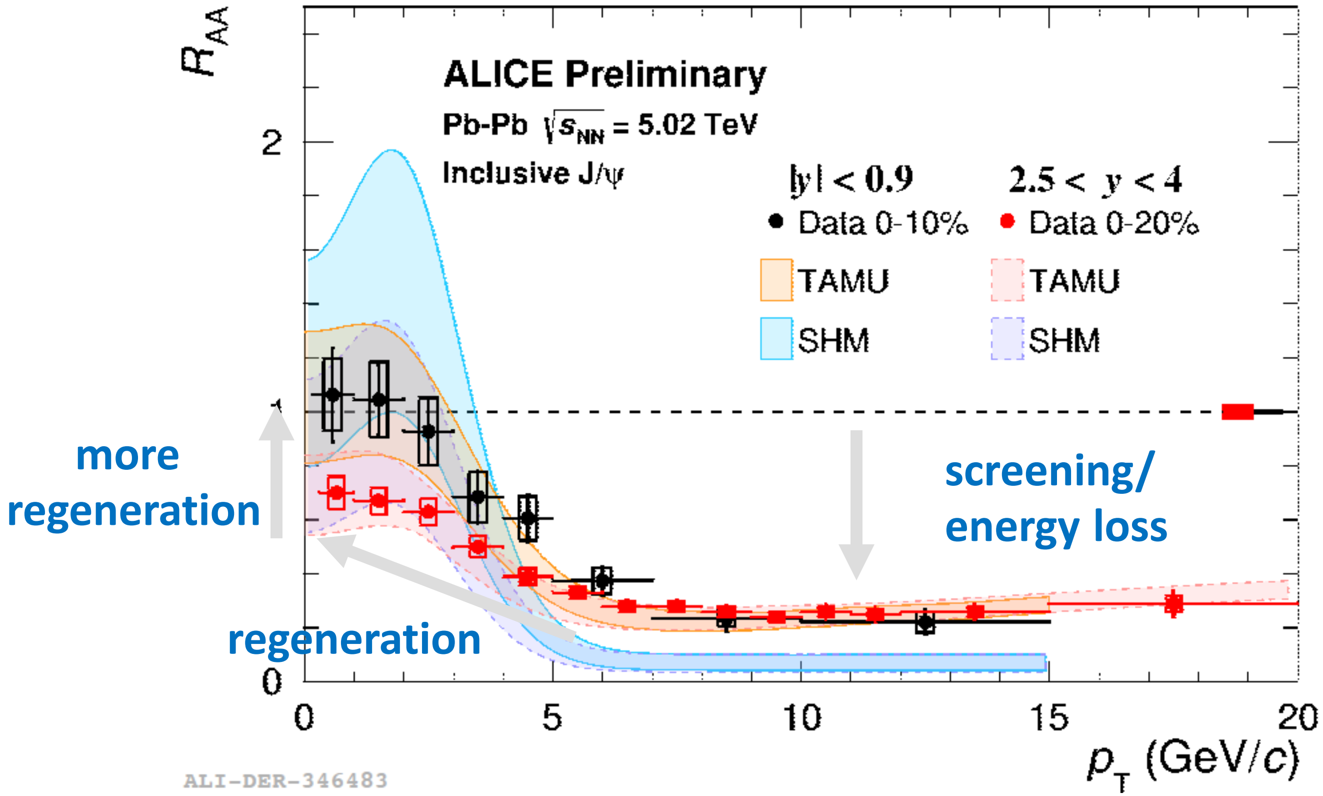

Charmonium dissociation and regeneration

- J/ψ suppression due to color screening in the QGP

Reduced at low p_T and central rapidity by $c\bar{c}$ regeneration

~ 100 $c\bar{c}$ pairs per central Pb-Pb

- New result: measured $\psi(2S)$ ~ x 10 lower binding energy !
- To pin down the role of these two mechanisms

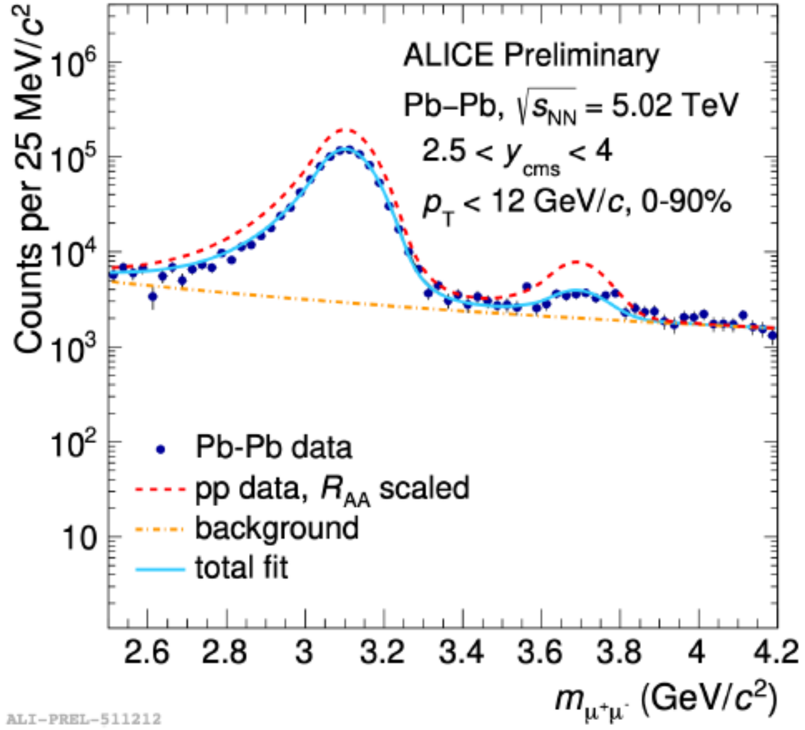

arXiv: 2210.08893

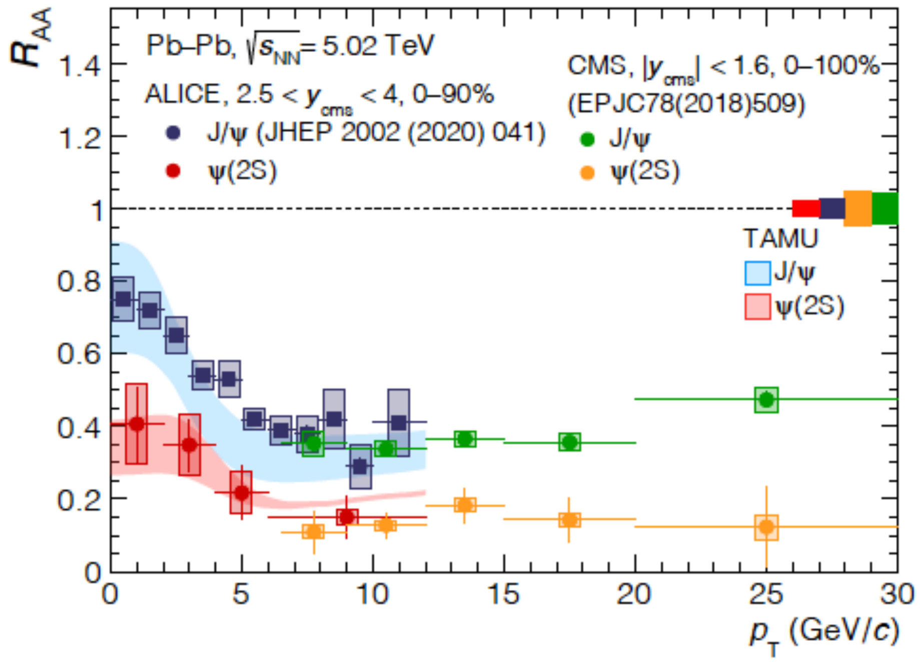

$\psi(2S)$ x2 more suppressed than J/ψ
Hint of regeneration at low p_T

Bottomonia Υ(nS)

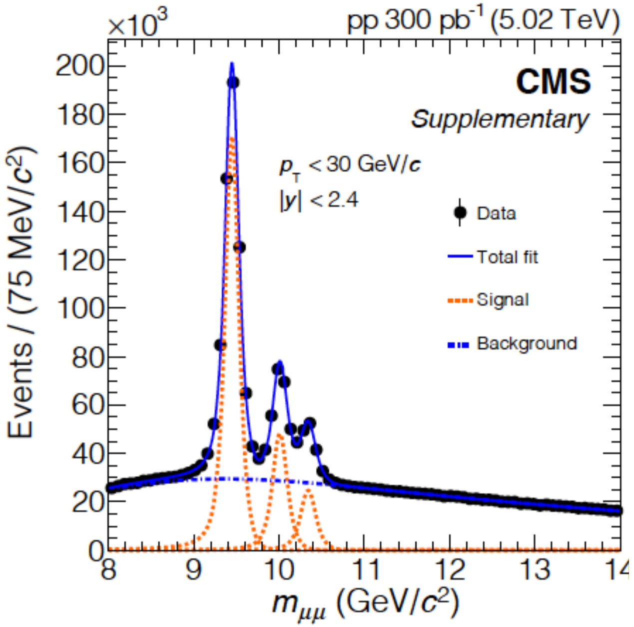

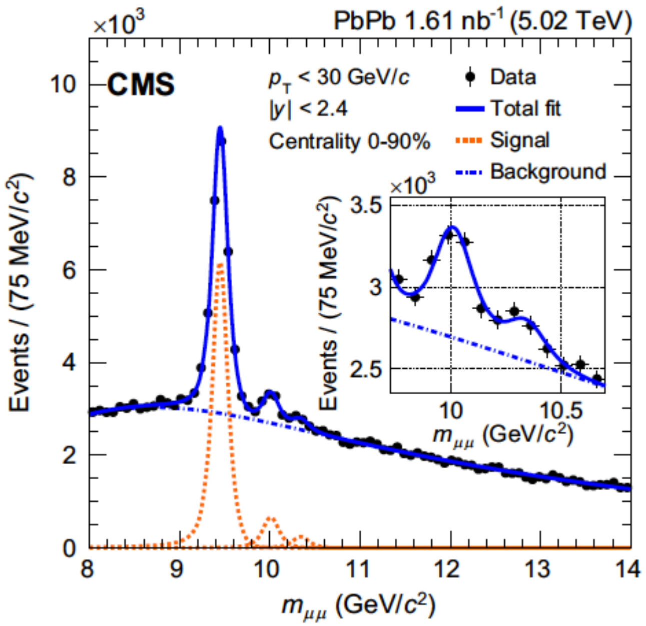

PRL133 (2022)022302

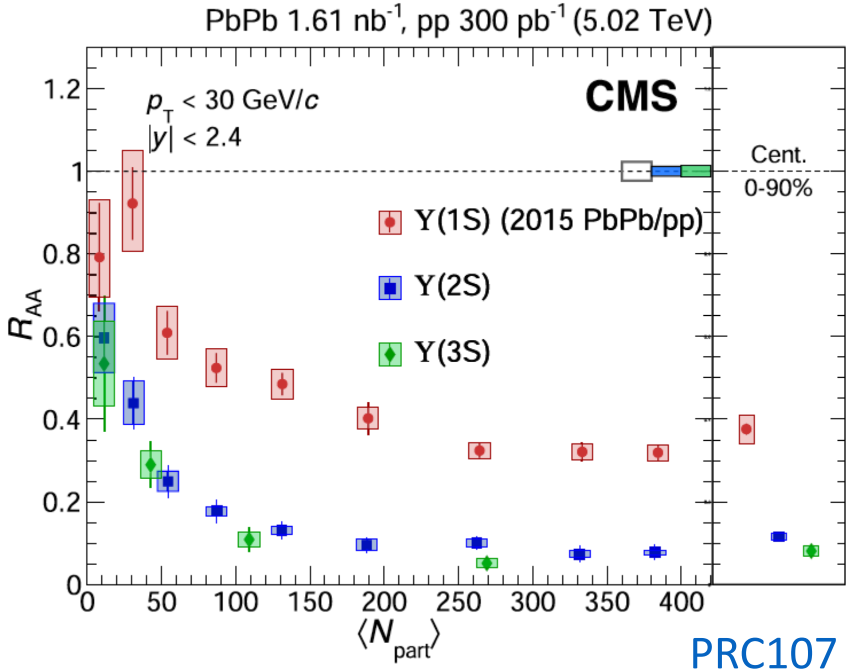

Suppression mechanism observed for bottomonium family

Courtesy R. Bailache

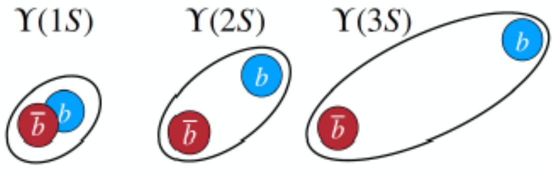

PRC107 (2023)054912

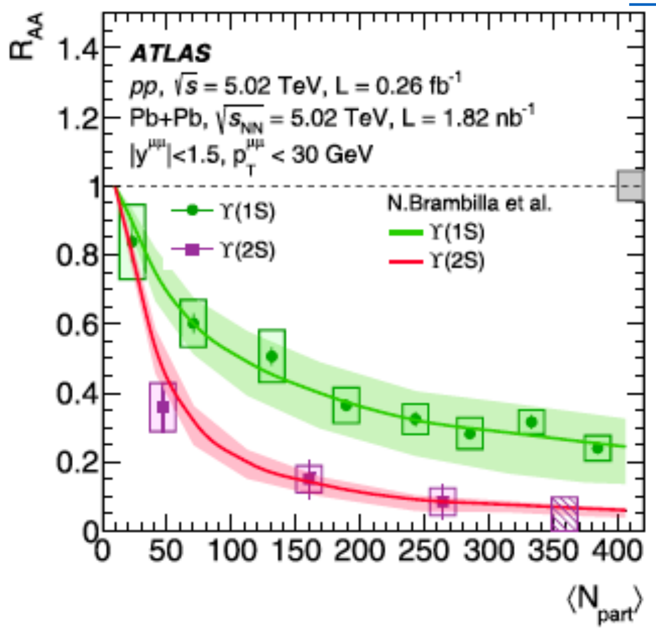

$R_{AA}(1S) > R_{AA}(2S) > R_{AA}(3S)$

Electromagnetic radiation

Thermal electromagnetic radiation

Thermal emission rates:

Dileptons: $\frac{dR_{ee}}{d^4q} = \frac{-\alpha^2}{\pi^3 M^2} f^B(q_0;T)\, \rho_{em}(M,q;\mu_B,T)$

Depends on the mass and on q

Photons: $q_0\frac{dR_\gamma}{d^3q} = \frac{-\alpha}{\pi^2} f^B(q_0;T)\, \rho_{em}(M=0,q;\mu_B,T)$

$M \rightarrow 0$, depends only on q

Photons: p_T
Dileptons: M, p_T

p_T : sensitive to temperature and expansion velocity, affected by "Doppler" blue shift

M: only sensitive to temperature (Lorentz invariant)

Dileptons

A. Drees Nucl. Phys. A830 (2009) 435

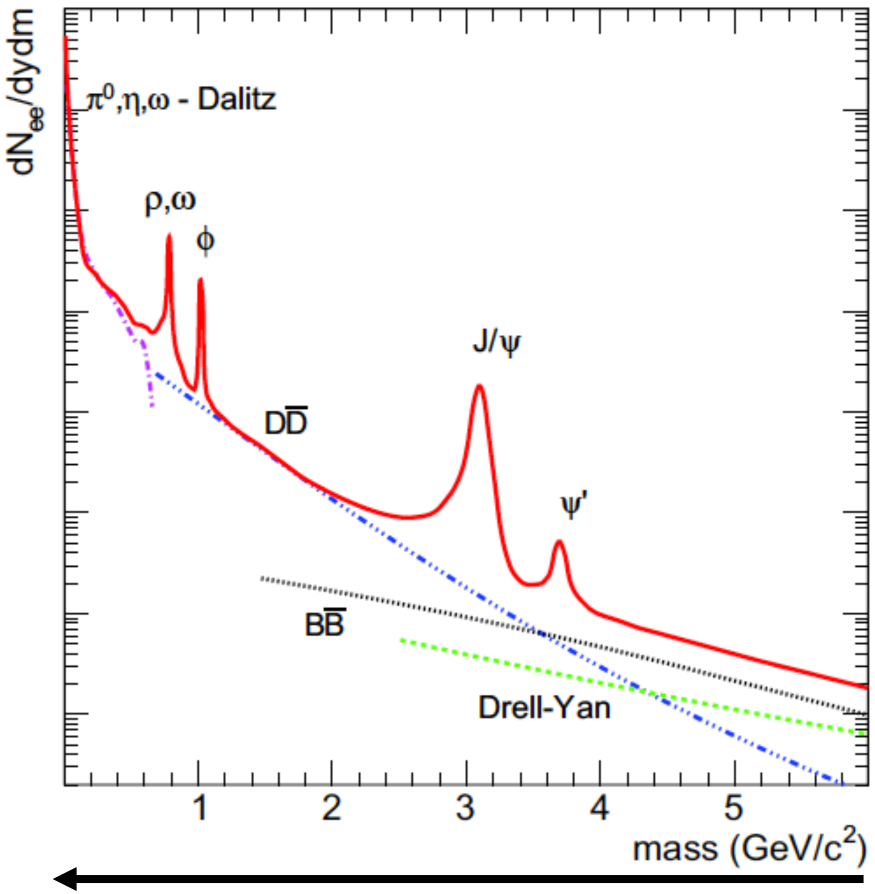

Late Probed time scale Early

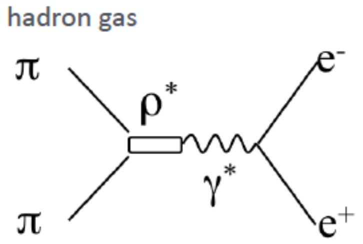

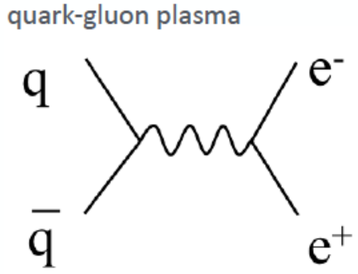

Invariant mass allows separation of different collision stages:

- **M < 1 GeV:** hadronic

hadrons in medium, in medium modifications of vector mesons, chiral symmetry restoration

- **M > 1 GeV:** partonic

early temperature, partonic collectivity, thermal radiation

Dileptons: Signal and background

R. Bailhache, HP2023

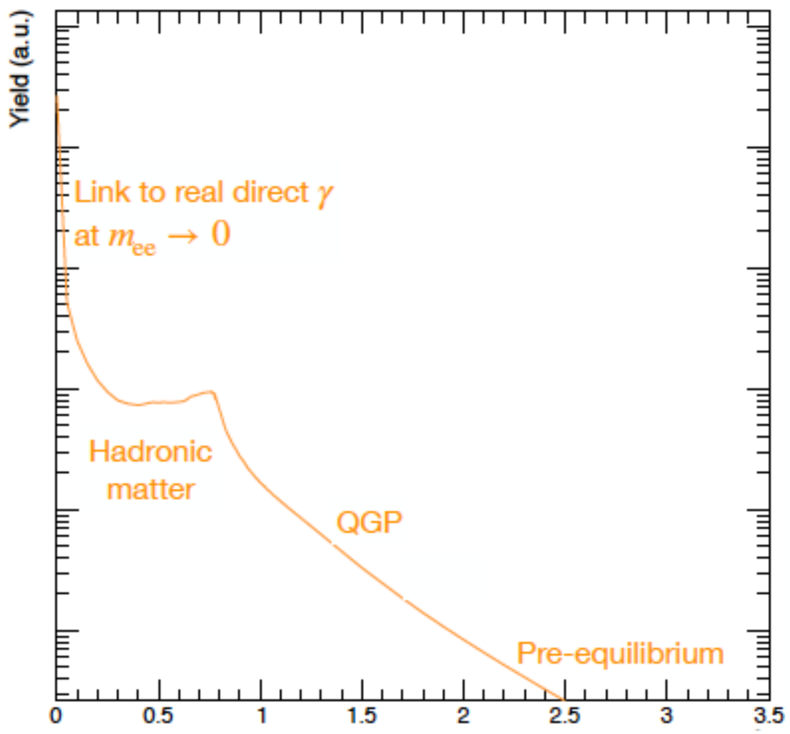

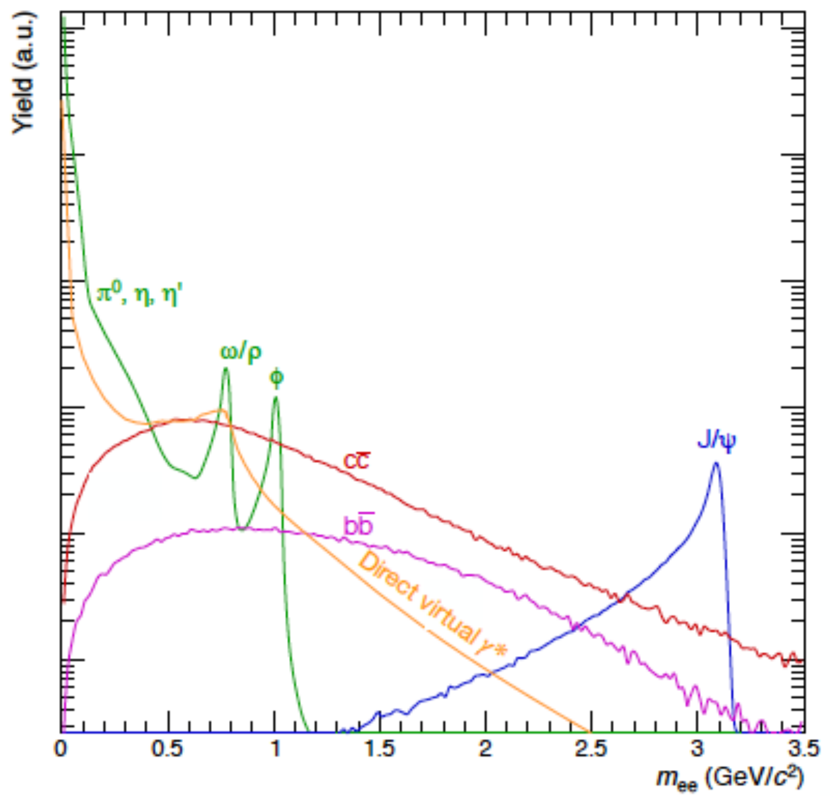

- Radiation from hot-hadronic matter
  Sensitive to in-medium spectral function of ρ meson
- Invariant mass not affected by radial flow
  → Access to average QGP temperatures without blue-shift

Large combinatorial and physics backgrounds

Dielectron production in central Pb—Pb at $\sqrt{s_{NN}}$ = 5.02 TeV

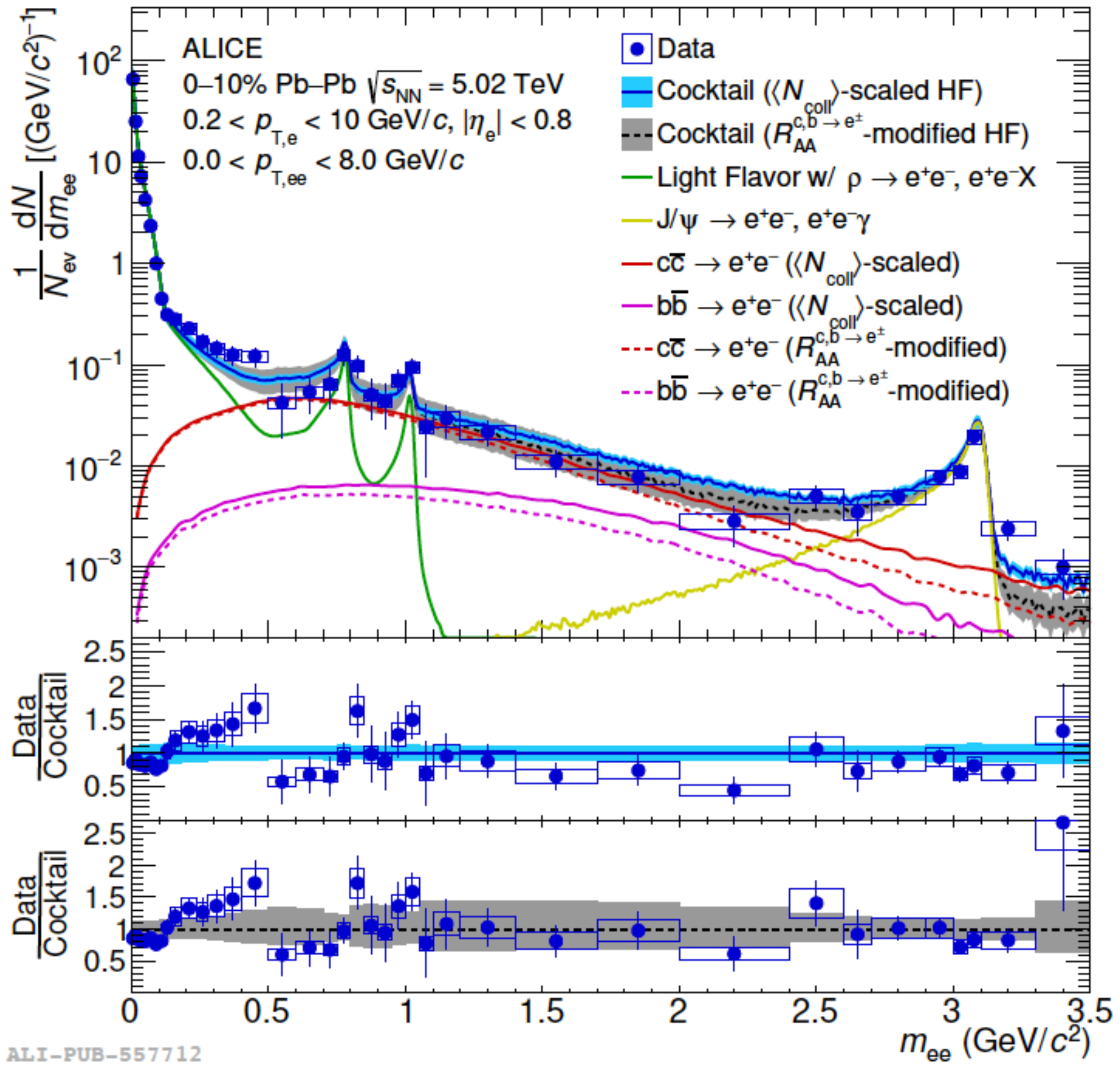

arXiv: 2308.16704

Comparison to hadronic cocktail, including:

- N_{coll} -scaled HF measured in pp at $\sqrt{s}$ = 5.02 TeV

Phys. Rev. C 102 (2020) 055204

⟶ Vacuum baseline

- Include measured R_{AA} of $c/b \longrightarrow e^{\pm}$

Phys. Lett. B 804 (2020) 135377

⟶ Modified-HF cocktail

Intermediate-mass region (IMR) from 1.1 < m_{ee} < 2.7 GeV/c^2

⟶ Consistent with HF suppression & therm. radiation from QGP

Indication for an excess at lower mass

⟶ Compatible with thermal radiation from HG

Excess mass spectrum: central Pb—Pb at $\sqrt{s_{NN}}$ = 5.02 TeV

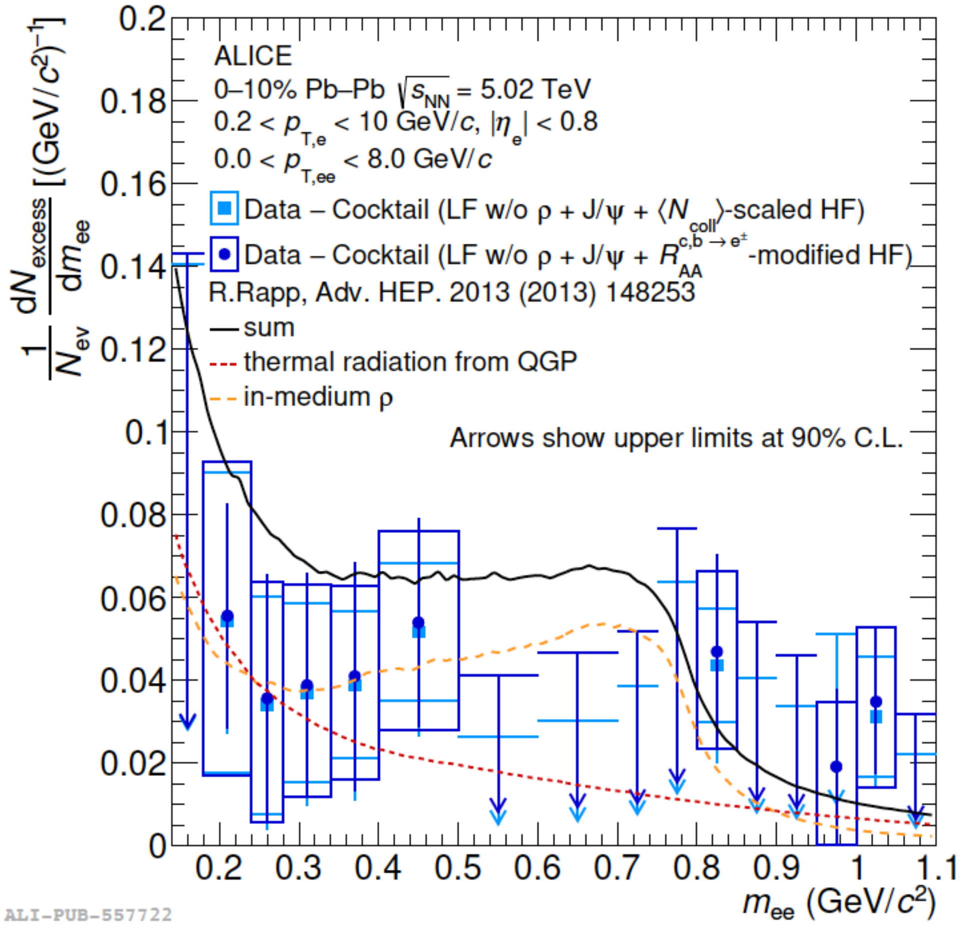

Significance of excess in $0.18 < m_{ee} < 0.5$ GeV/c^2

1.8 σ w.r.t. N_{coll}-scaled cocktail
1.5 σ w.r.t. R_{AA}-modified cocktail

Compared with sum of 2 contributions:

- ρ meson produced thermally in hot hadronic matter
- Thermal radiation from QGP

Consistent with thermal radiation from hadronic matter via $\pi^+\pi^- \to \rho \to e^+e^-$ in $0.18 < m_{ee} < 0.5$ GeV/c^2

NA60 In-In $\sqrt{s_{NN}}$=17.3 GeV : Inclusive excess mass spectrum

Eur. Phys. J. C 59 (2009) 607-623
CERN Courier 11/ 2009, 31-35
Chiral 2010 **,** AIP Conf.Proc. 1322 (2010) 1-10

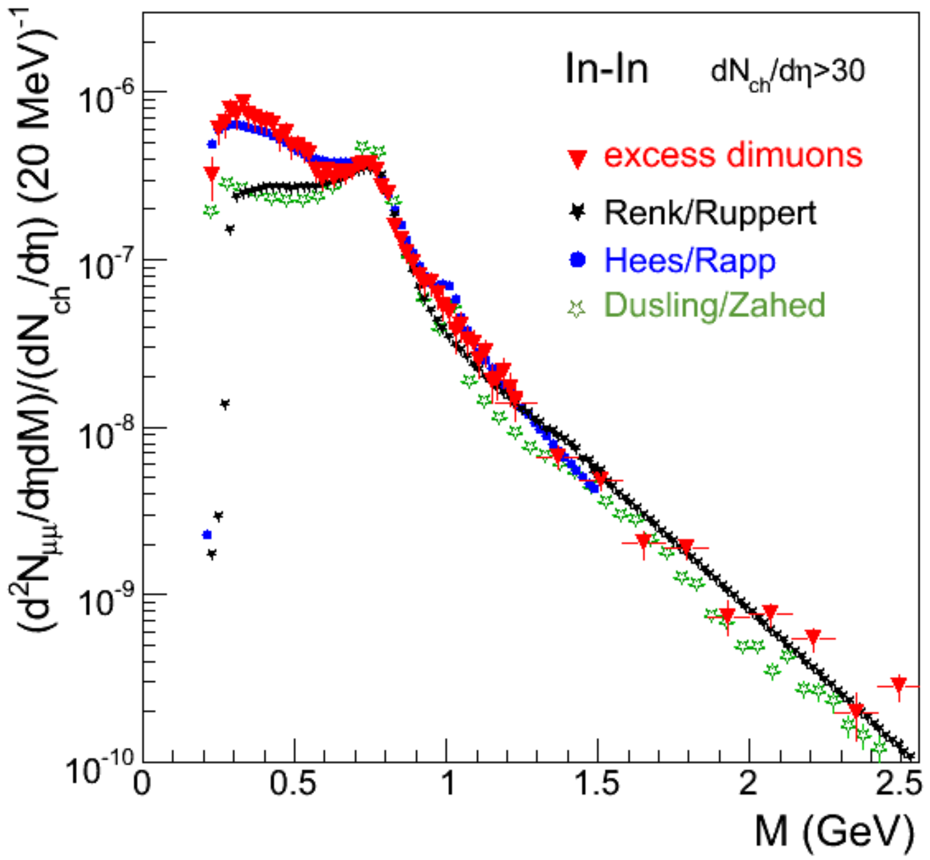

all known sources subtracted
integrated over p_T
fully corrected for acceptance
absolutely normalized to $dN_{ch}/d\eta$

M < 1 GeV
ρ dominates, 'melts' close to T_c
best described by H/R model

M > 1 GeV, QGP thermometer
~ exponential fall-off

$$dN/dM \propto M^{3/2} \times \exp(-M/T)$$

range 1.1-2.0 GeV: T=205±12 MeV
1.1-2.4 GeV: T=230±10 MeV
$T>T_c$: partons dominate
only described by R/R and D/Z models

Photon sources

- **Decay photons:**
  - π^0, η, ω
- **Direct photons:**
  - Hard:
    - Direct:
      - qg Compton Scattering
      - q$\bar{q}$ Annihilation
    - Fragmentation
  - Pre-equilibrium
  - Thermal:
    - QGP
    - Hadron Gas
  - Hard+thermal:
    - Jet-γ-conversion:
      - $q_{hard} + q_{QGP} \rightarrow \gamma + q$
      - $q_{hard} + q_{QGP} \rightarrow \gamma + g$
    - Medium induced γ bremss.

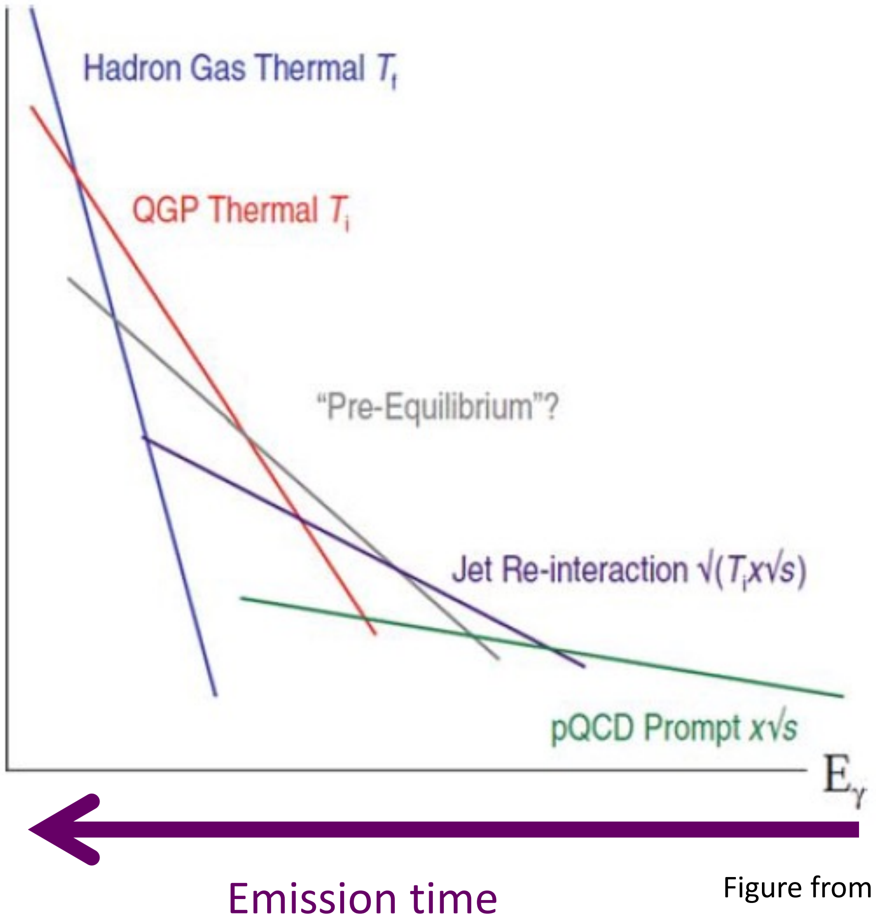

Figure from P. Stankus

Large background from neutral meson decays.
Difficult measurement

Photon production: Feynman diagrams

QGP:

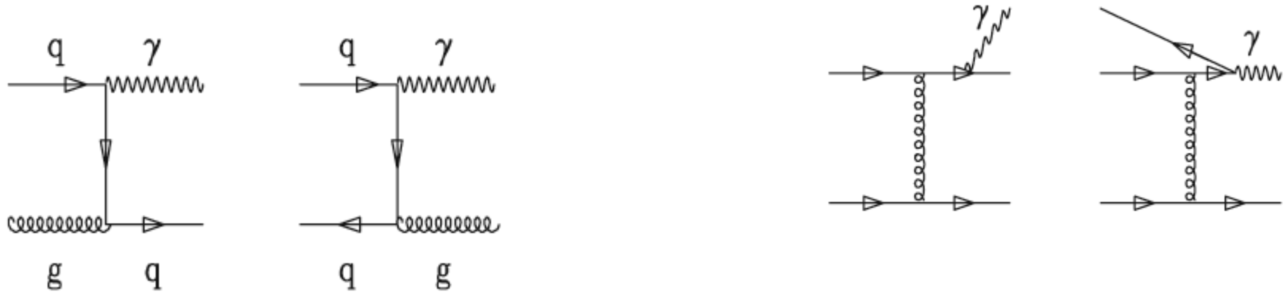

Hadron gas:

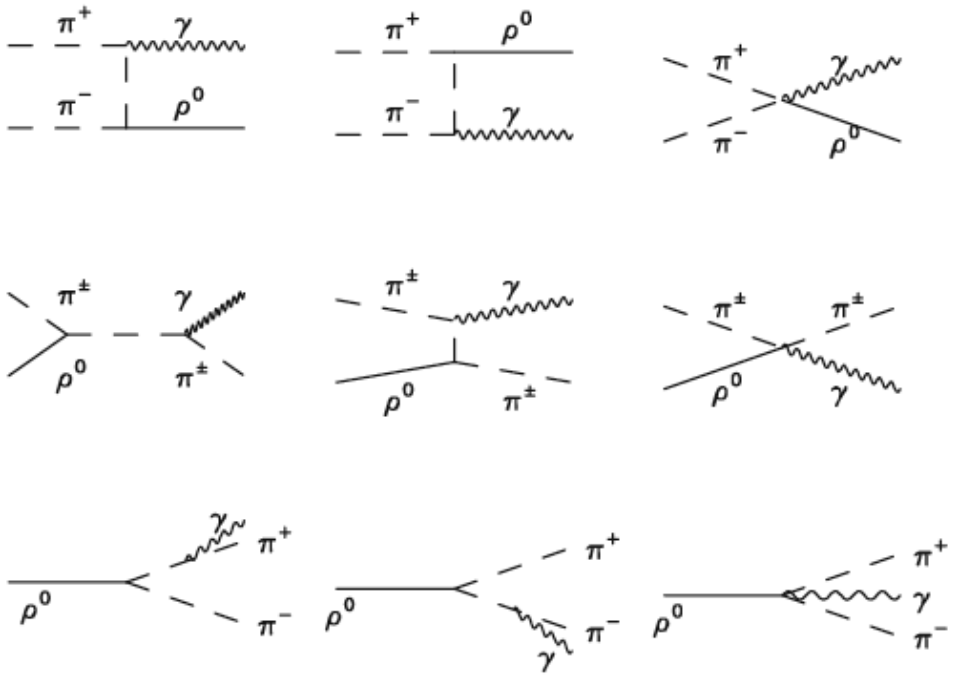

Methods to measure direct photons

- Statistical subtraction method
  - Measure inclusive photons and subtract photons from hadron decays
- Virtual photons ($\gamma^* \rightarrow e^+e^-$): PHENIX
- Isolation + (shower shape in case calorimeter is used)
- Tagging method
  - Remove decay photons by tagging decay photons
- Hanbury Brown-Twiss Method
  - Bose-Einstein correlation expected for direct photons
  - Direct photon yield from correlation strength

Direct photons: statistical subtraction method and double ratio

Subtraction method:

$$\gamma_{direct} = \gamma_{inc} - \gamma_{decay} = (1 - \frac{\gamma_{decay}}{\gamma_{inc}}).\gamma_{inc} = (1 - \frac{1}{R_\gamma}).\gamma_{inc}$$

Inclusive photons: All produced photons

Decay photons: Calculated from measured particle spectra with photon decay channels (π^0, η,...)

Double ratio:

$$\frac{\gamma_{inc}}{\pi^0} / \frac{\gamma_{decay}}{\pi^0_{param}} \sim \frac{\gamma_{inc}}{\gamma_{decay}}$$

>1 if direct photon signal

Advantage: Cancellation of uncertainties

To obtain γ direct spectrum add systematic uncertainties of the inclusive photon spectrum which canceled in the double ratio

Rγ at RHIC by PHENIX

PRC 109 (2024) 044912

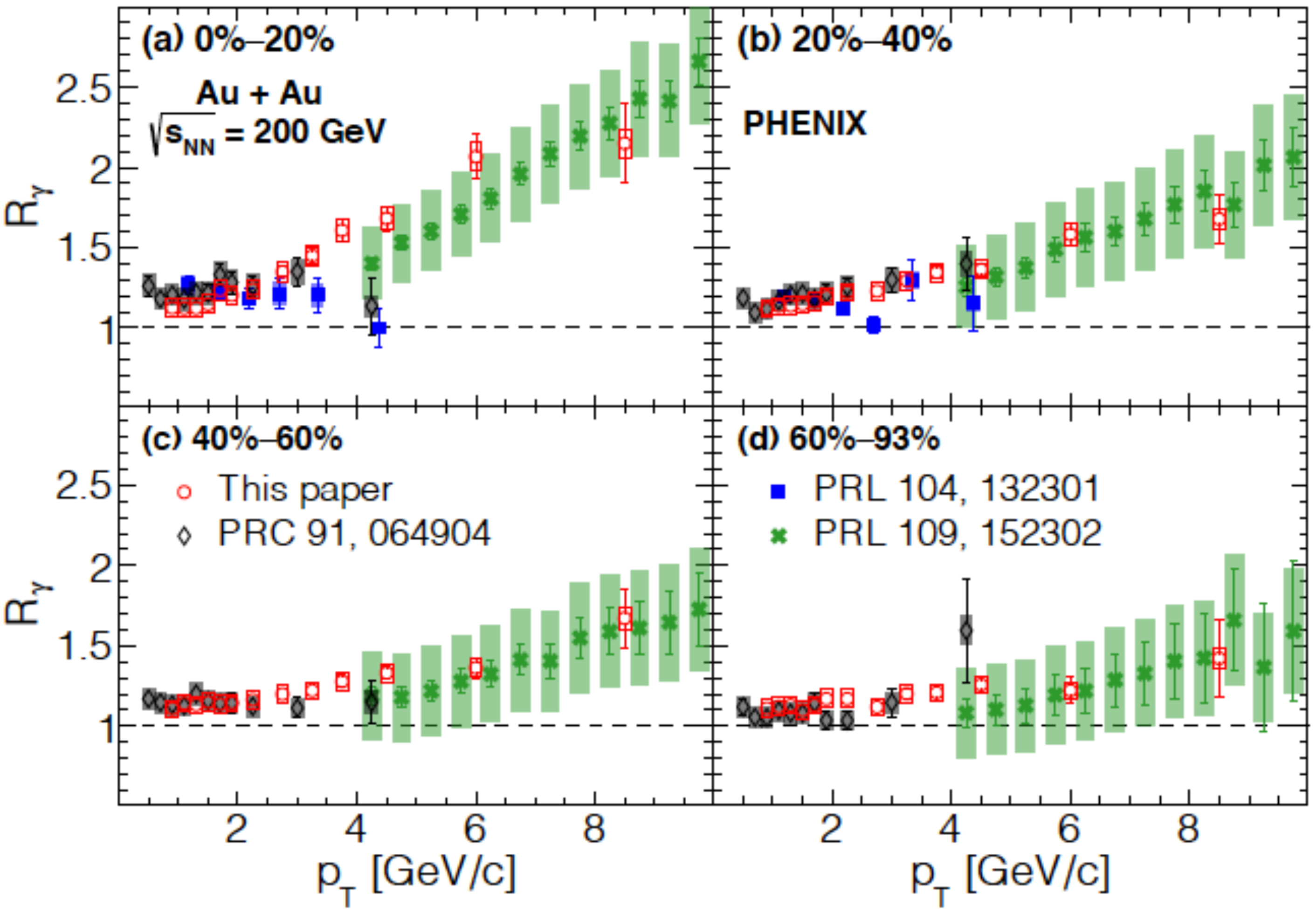

Thermal emission at RHIC

Direct photon puzzle

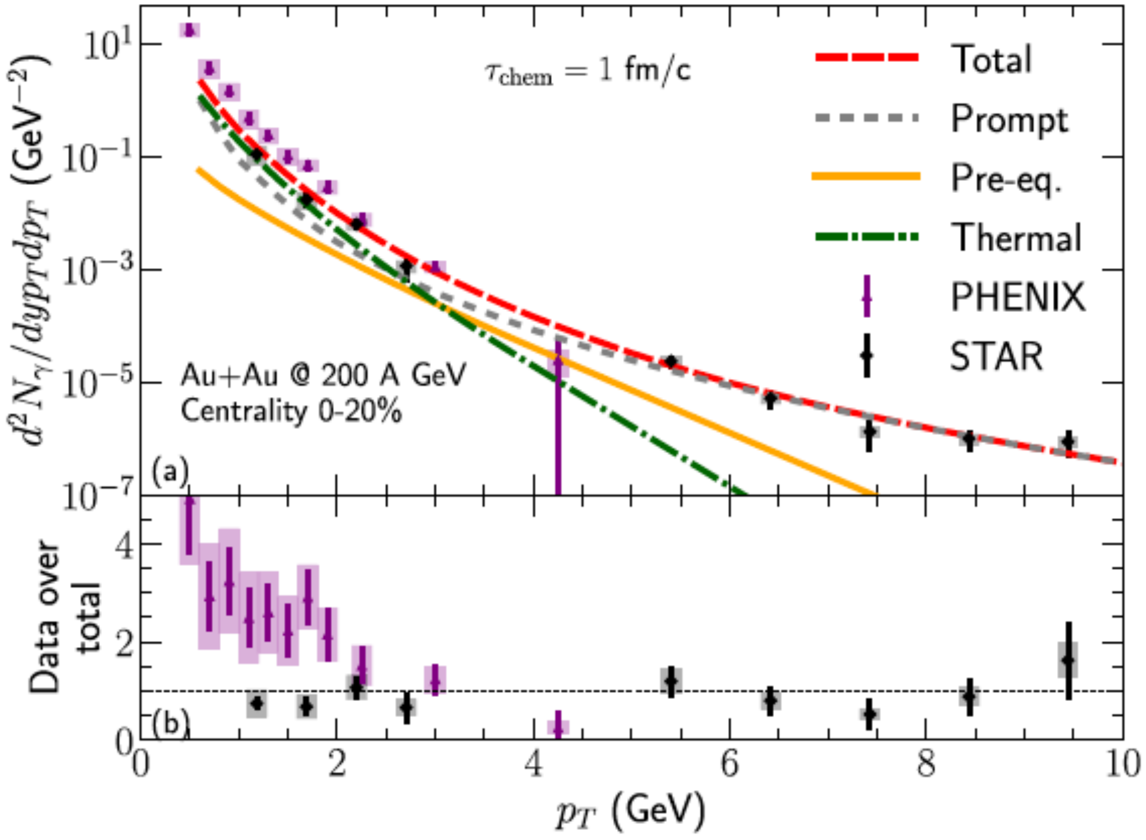

Phys. Rev C 105 (2022) 014909

Measured direct photon yield above model predictions at RHIC

… but

discrepancy PHENIX and STAR

QGP thermal emission

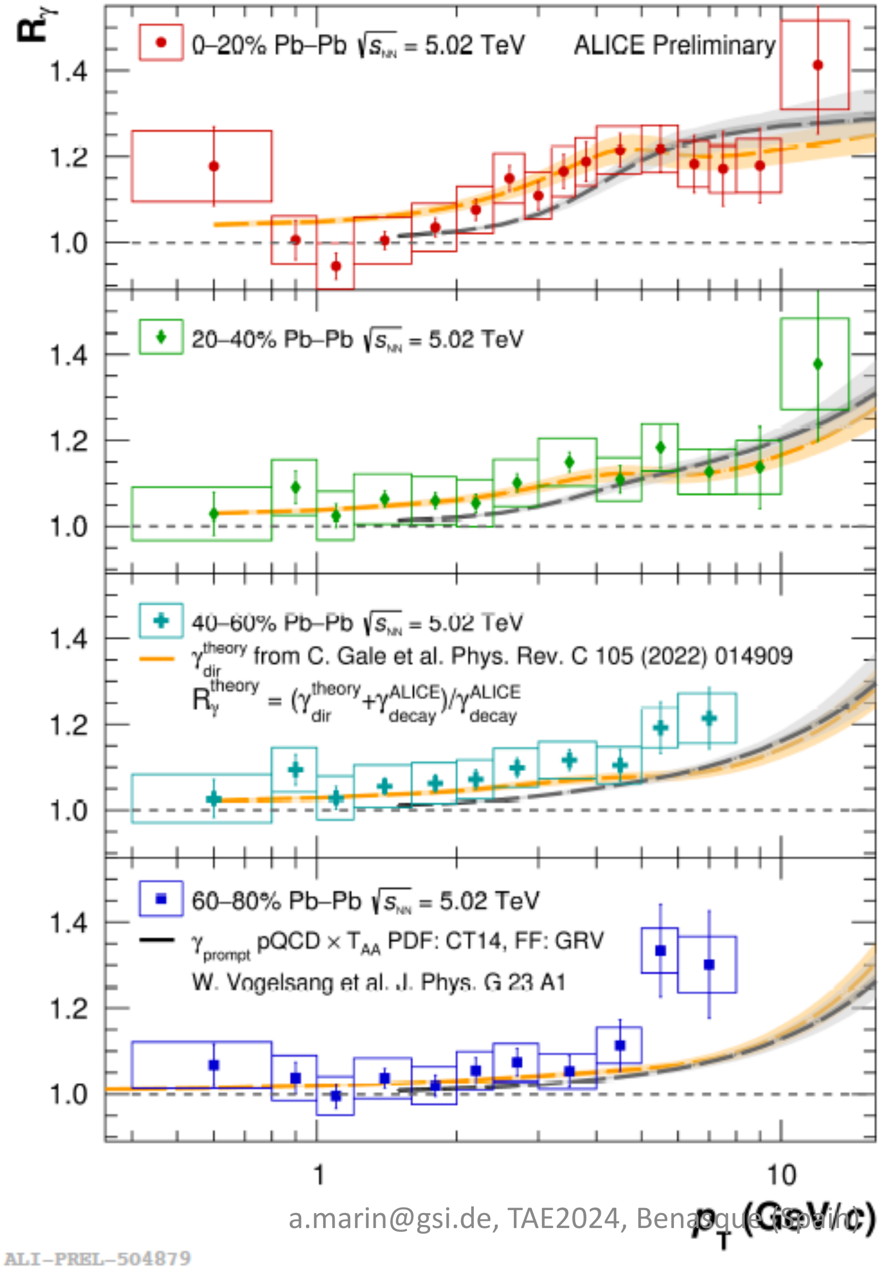

$$R_\gamma = N_{\gamma,\mathrm{inc}}/N_{\gamma,\mathrm{dec}} \approx \left(\frac{N_{\gamma,\mathrm{inc}}}{\pi^0}\right)_{\mathrm{meas}} / \left(\frac{N_{\gamma,\mathrm{dec}}}{\pi^0}\right)_{\mathrm{sim}}$$

$$R_\gamma^{\mathrm{pQCD}} = 1 + N_{coll} \cdot \frac{\gamma_{\mathrm{pQCD}}}{\gamma_{\mathrm{decay}}}$$

At low p_T :

- thermal radiation should dominate
- R_γ is close to 1 → small thermal and pre-equilibrium photon contribution
- Models with thermal and pre-equilibrium photons, can describe the data better than the calculation including only prompt photons

For p_T > 3 GeV/c:

- can be attributed to prompt (hard scattering) photons
- data is consistent with NLO pQCD calculation of prompt photons in pp collisions, scaled with T_{AA}
  Calculation by W. Vogelsang, using PDF: CT14, FF: GRV

QGP thermal emission

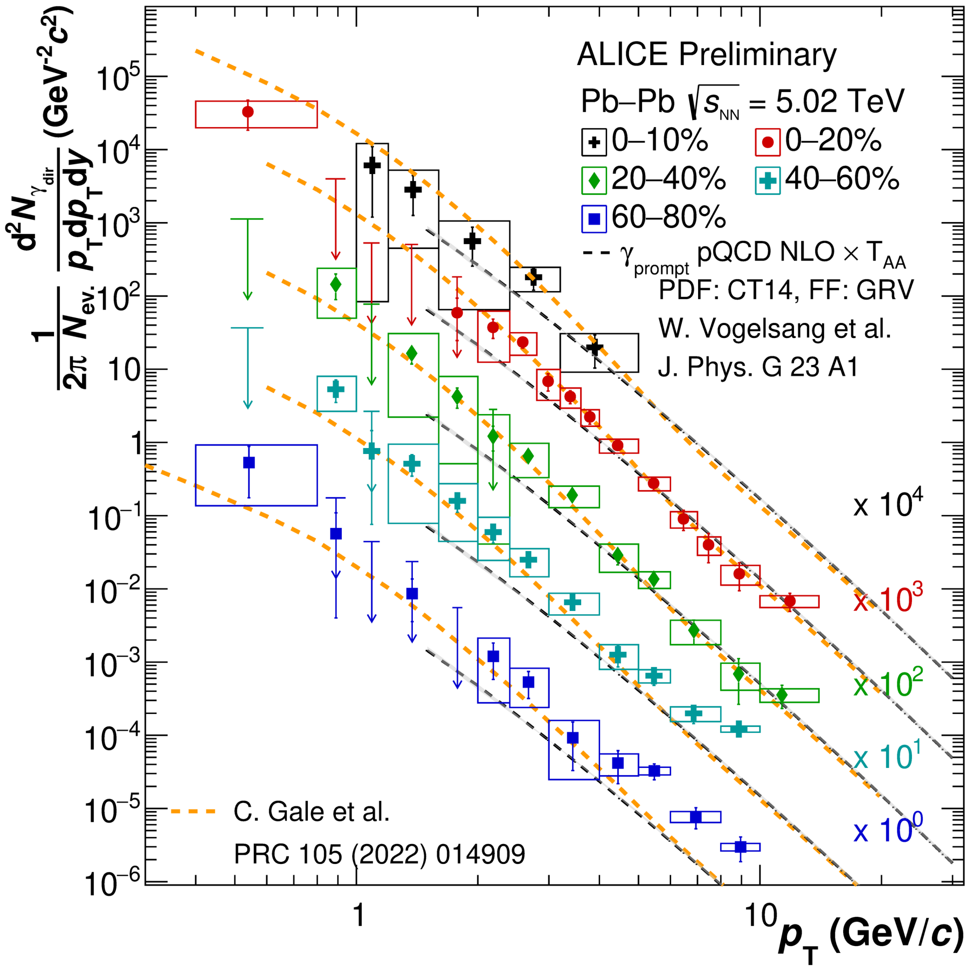

$$N_{\gamma,\mathrm{dir}} = N_{\gamma,\mathrm{inc}} - N_{\gamma,\mathrm{dec}} = \left(1 - \frac{1}{R_\gamma}\right) \cdot N_{\gamma,\mathrm{inc}}$$

$$\gamma_{\mathrm{dir}} = \frac{\gamma^*_{\mathrm{dir}}}{\gamma^*_{\mathrm{incl}}} \cdot (\gamma_{\mathrm{incl}})_{\mathrm{real}}$$

New measurement of direct γ in Pb-Pb at 5.02 TeV

- Virtual γ method, 0-10% centrality
- Real γ (conversion method), other centralities

Low p_T ($p_T \lesssim$ 3 GeV/c) – “thermal” photons

- consistent with model with pre-equilibrium and thermal photons

High p_T ($p_T \gtrsim$ 3 GeV/c) – prompt photons

- consistent with pQCD expectations

Virtual photon method

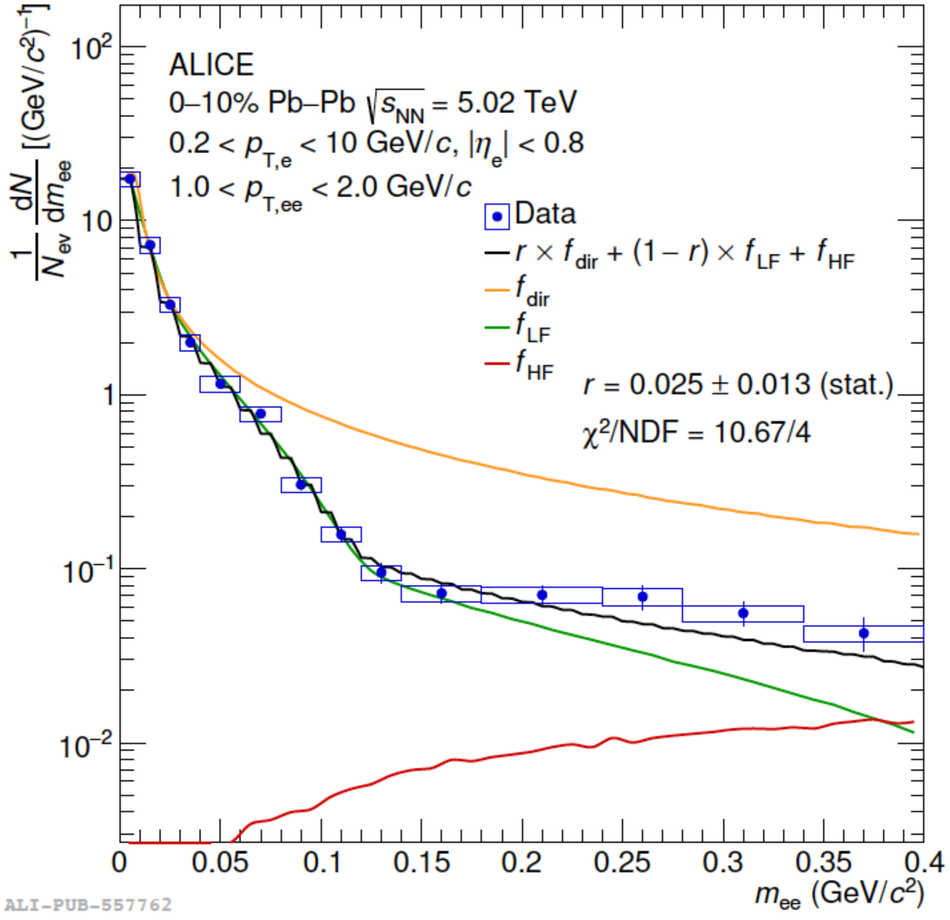

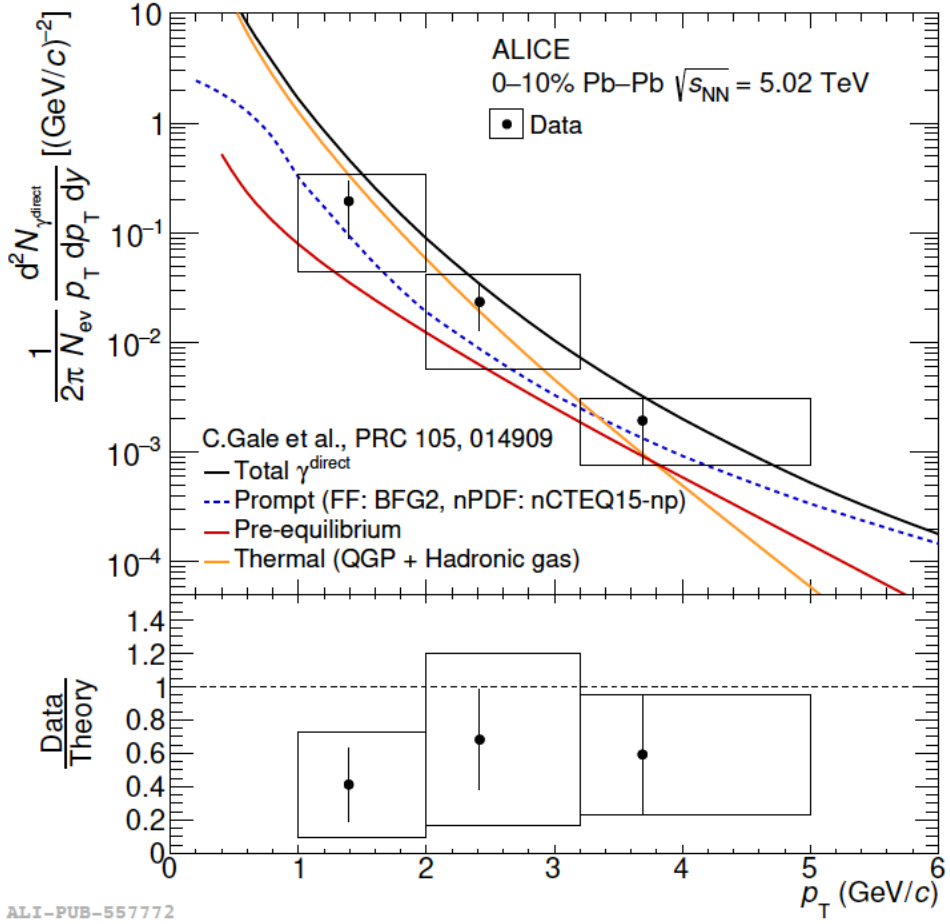

QGP thermal emission: Pb-Pb at $\sqrt{s_{NN}}$ = 2.76 TeV

$$N_{\gamma,\mathrm{dir}} = \left(1 - \frac{1}{R_\gamma}\right) \cdot N_{\gamma,\mathrm{inc}}$$

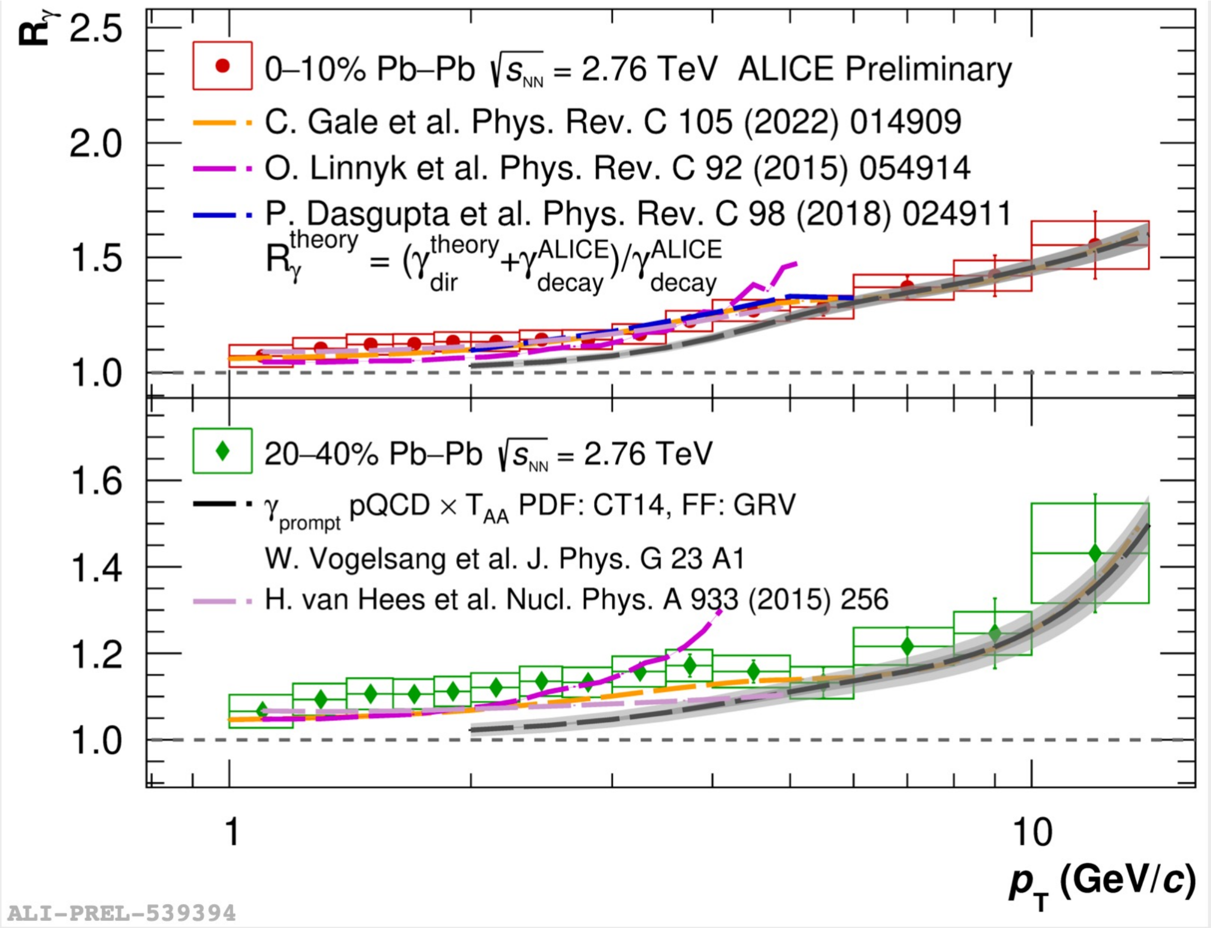

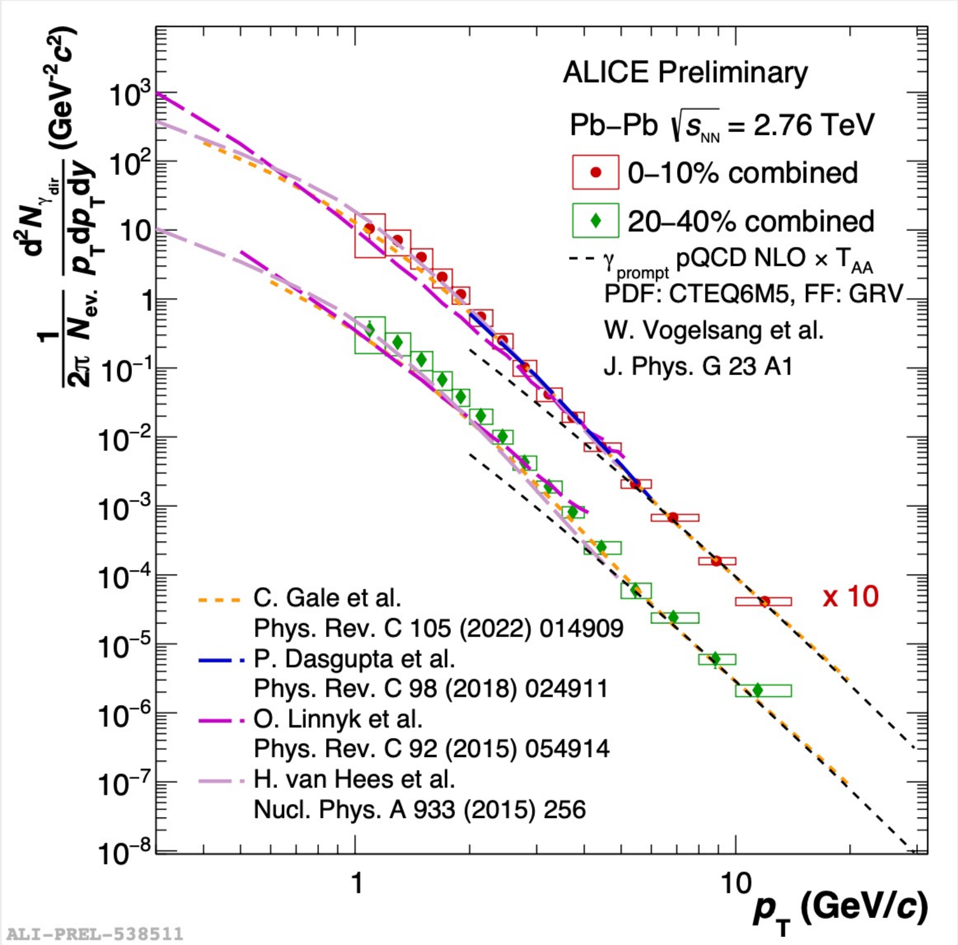

- Excess beyond known prompt yield 1 < p_T < 4 GeV/c
- Models that include thermal +(pre-equilibrium) + prompt photons are able to describe the data
- Not yet possible to discriminate among different models

HP2023, improved material budget

Direct photon puzzle in yields?

Ratio between direct photon production and their respective state-of the-art model calculation

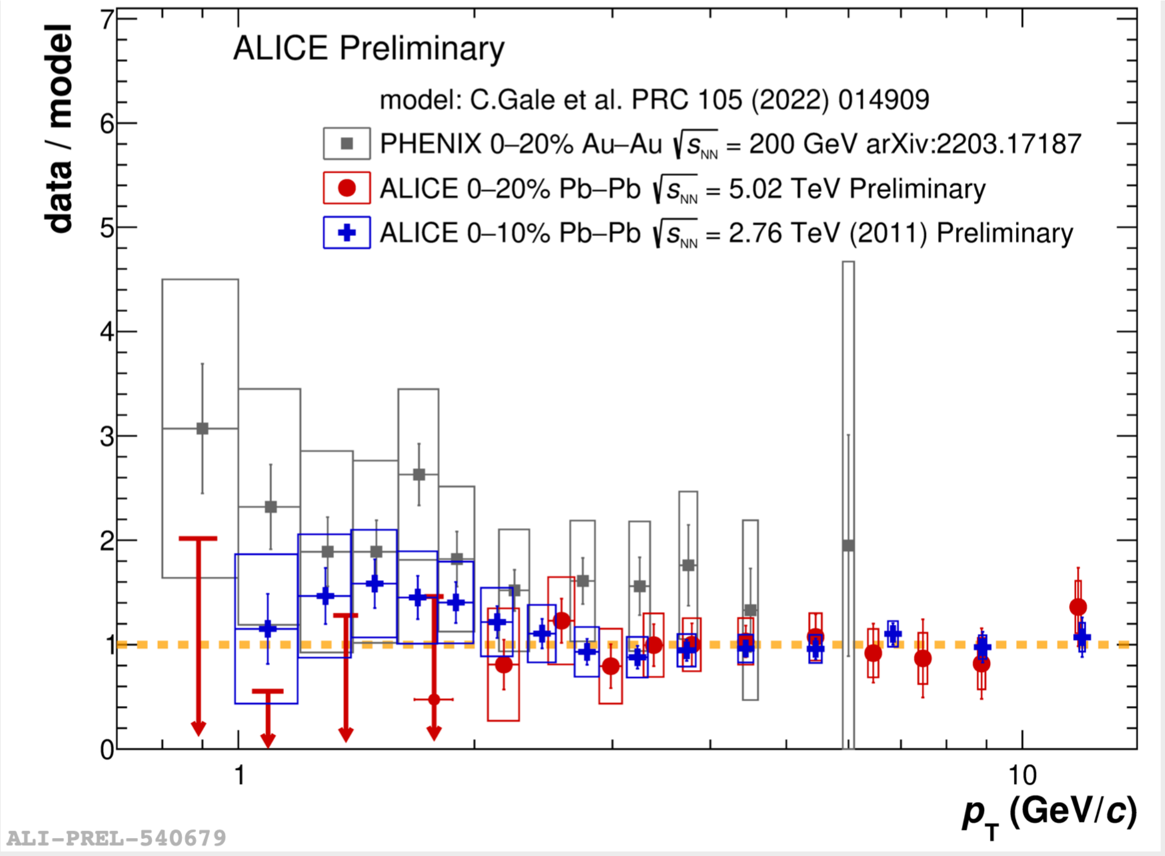

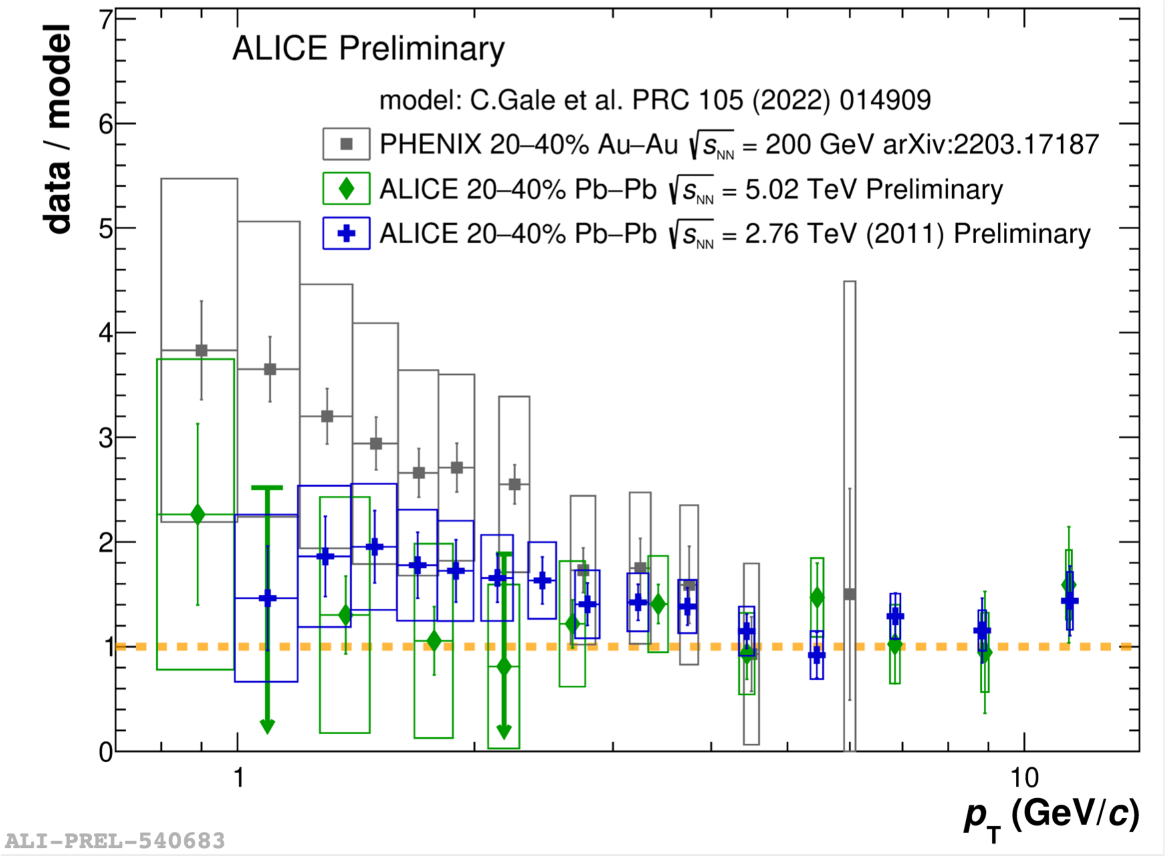

Good agreement between ALICE data and model predictions
Slight tension at low p_T for the PHENIX data
Future: puzzle involving direct photon flow?

Direct γ v_{2}: RHIC, LHC and models

Direct photon puzzle

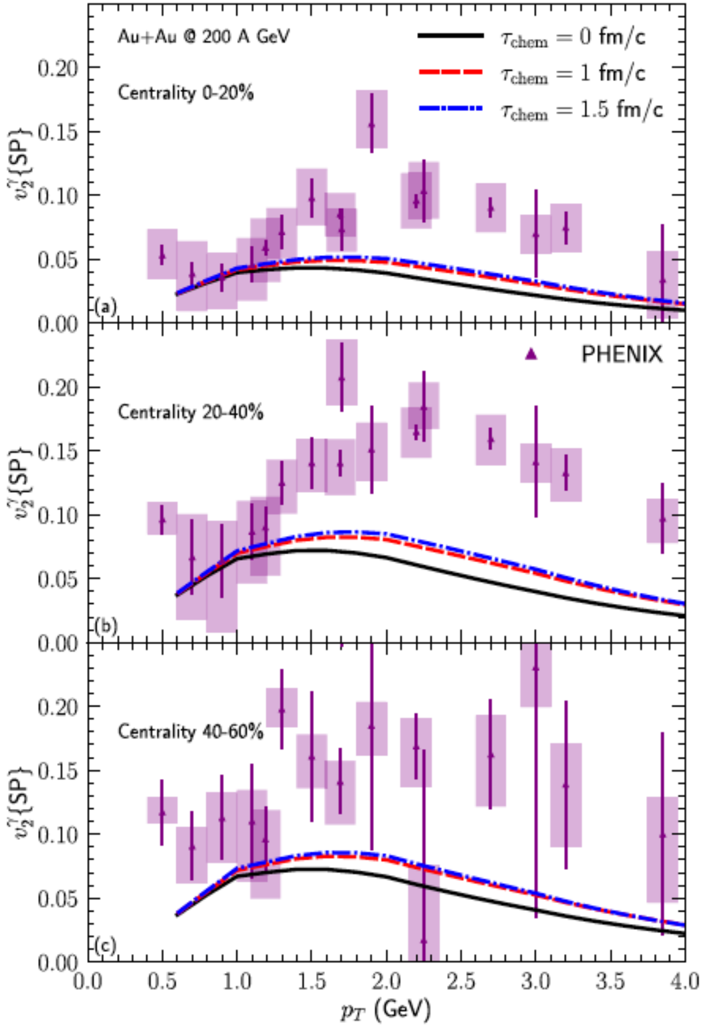

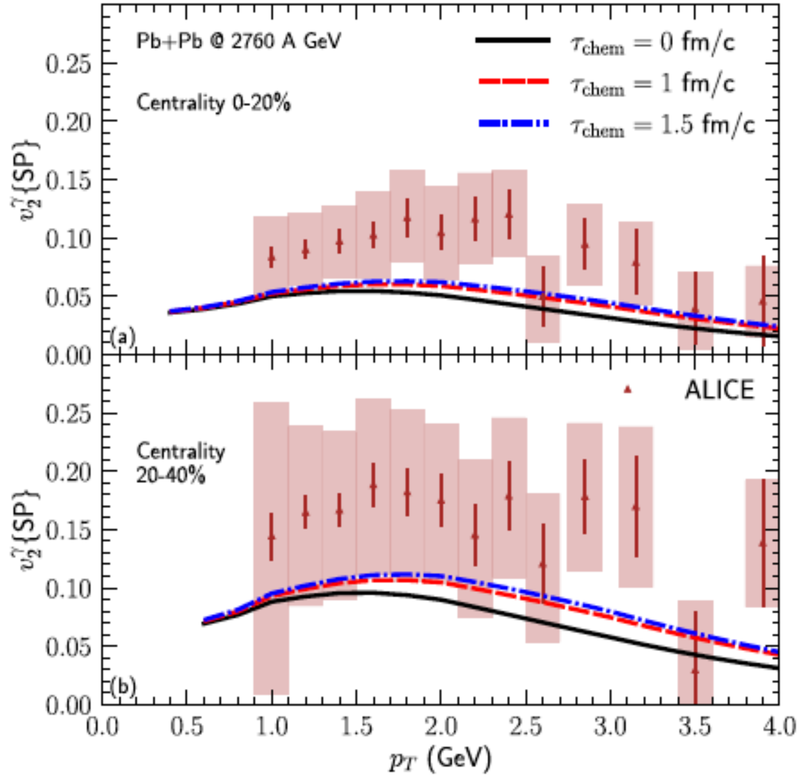

$v_2^{dir} \approx v_2^{\pi}$ but not puzzle within exp. uncertainties

large v_2 values not reproduced by models

Thermal emission: RHIC and LHC

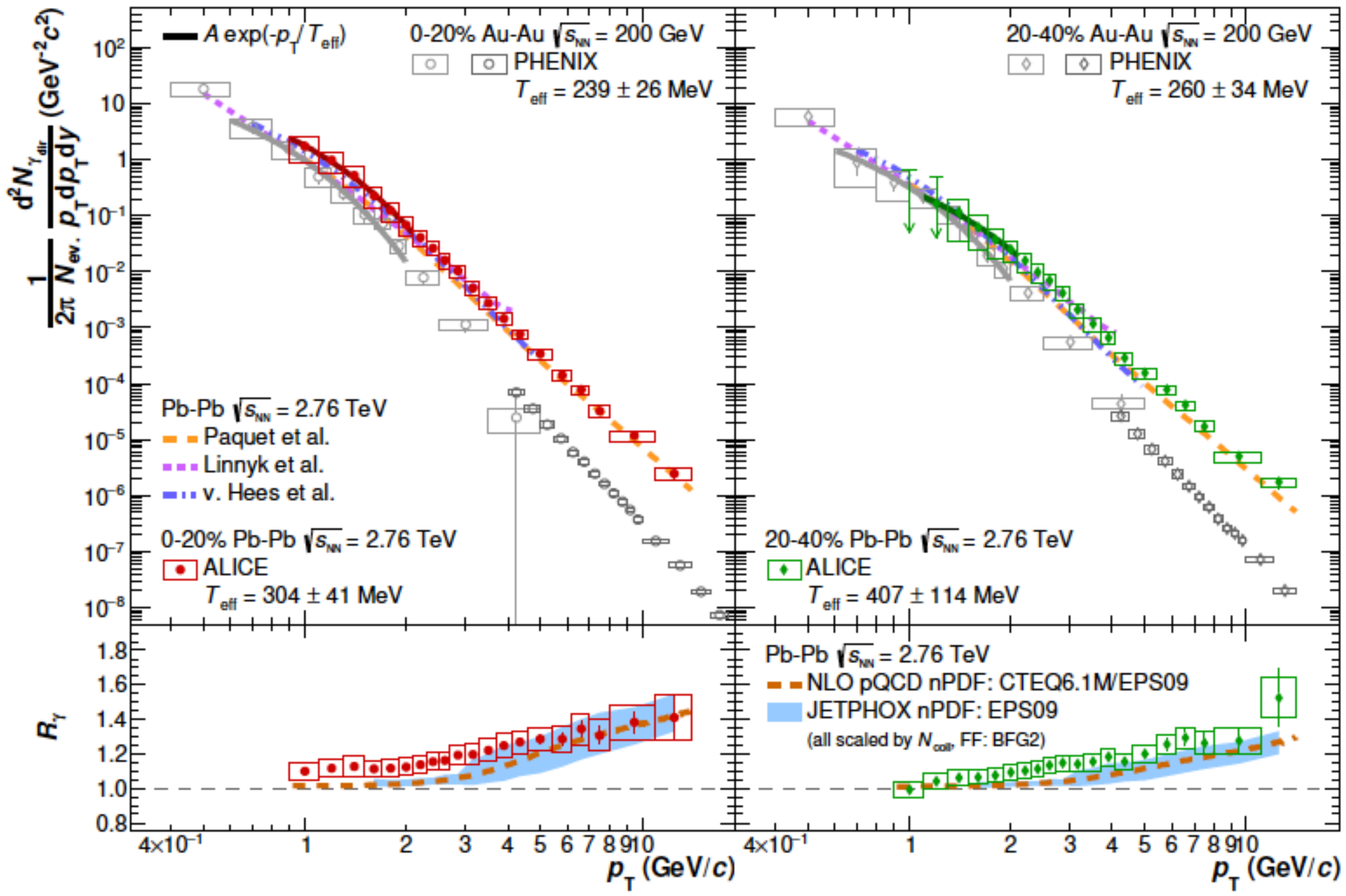

Increase in the effective temperature from RHIC to LHC

Conclusions

- Detailed insights into QGP properties gained during LHC Run1 and Run 2
- Run 3 ongoing after LS2 upgrades

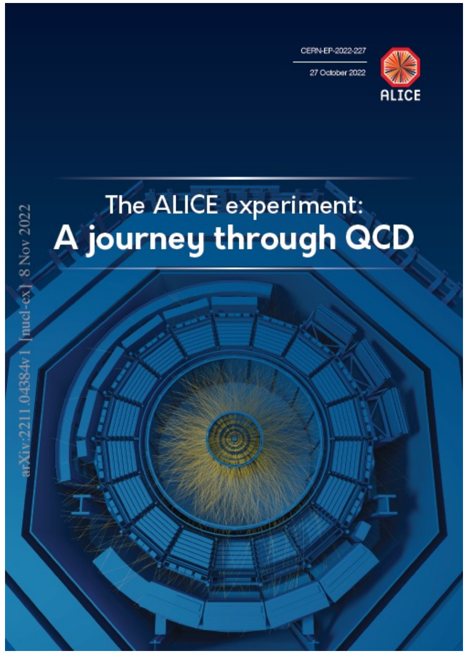

ALICE beyond Run 4

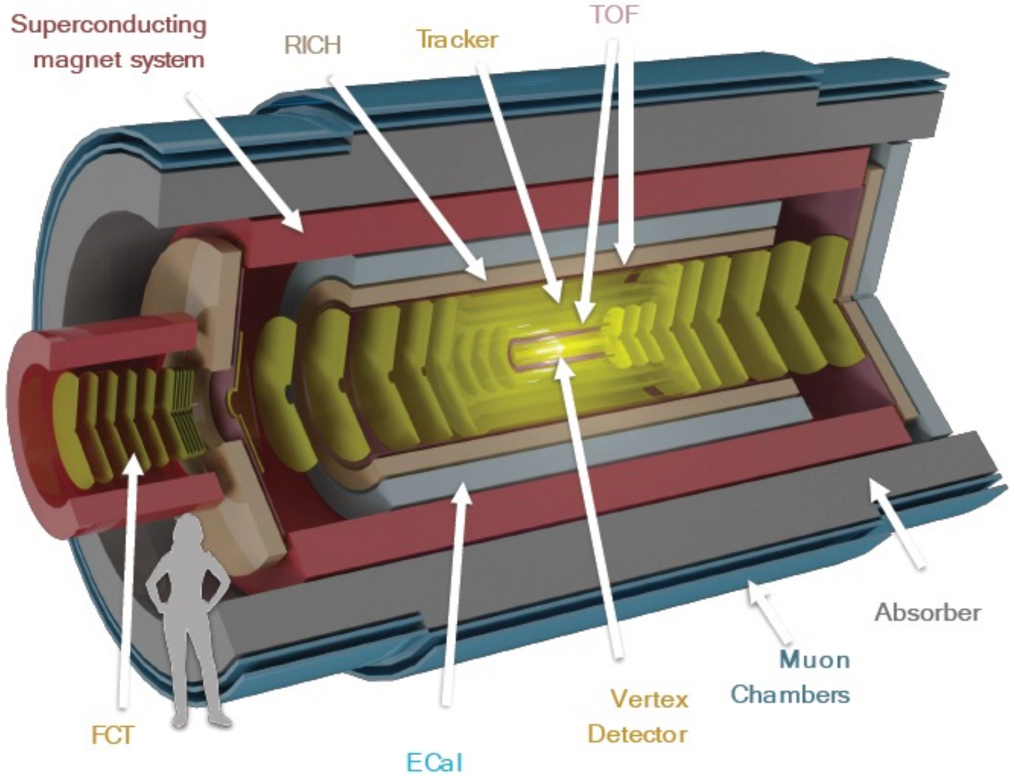

- Letter of Intent for ALICE 3: CERN-LHCC-2022-009 , arXiv: 2211.02491

Recommendation to proceed with R&D

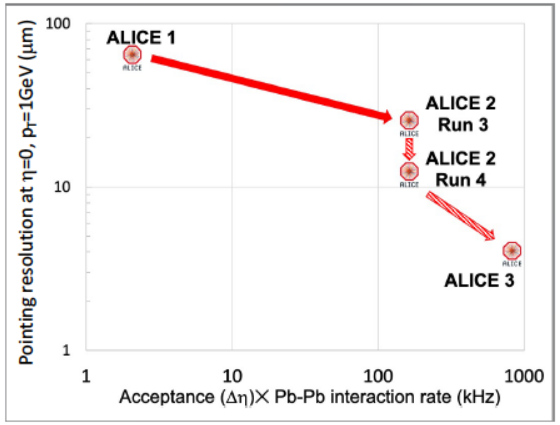

Extra slides

Direct photons

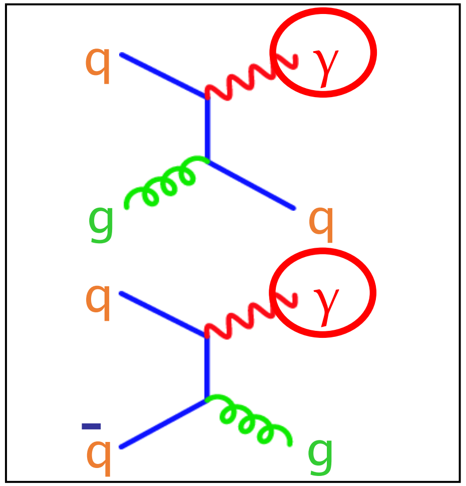

qg Compton Scattering

qq Annihilation

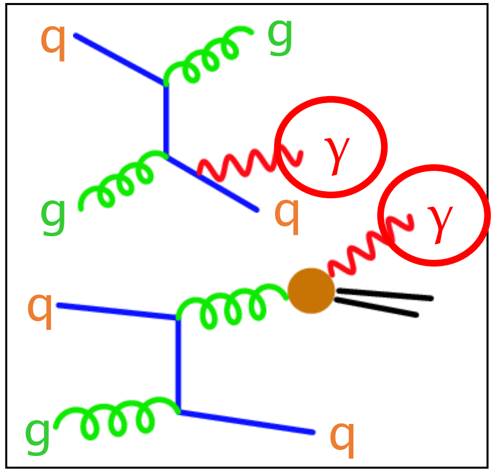

Bremsstrahlung, fragmentation

Cocktail generator: γ_{decay}

- γ $_{decay}$: obtained using a cocktail generator
- Fit to the measured π^0, η measured or parametrized from Kaons
- Other mesons using m_T-scaling,

PLB 754 (2016) 235

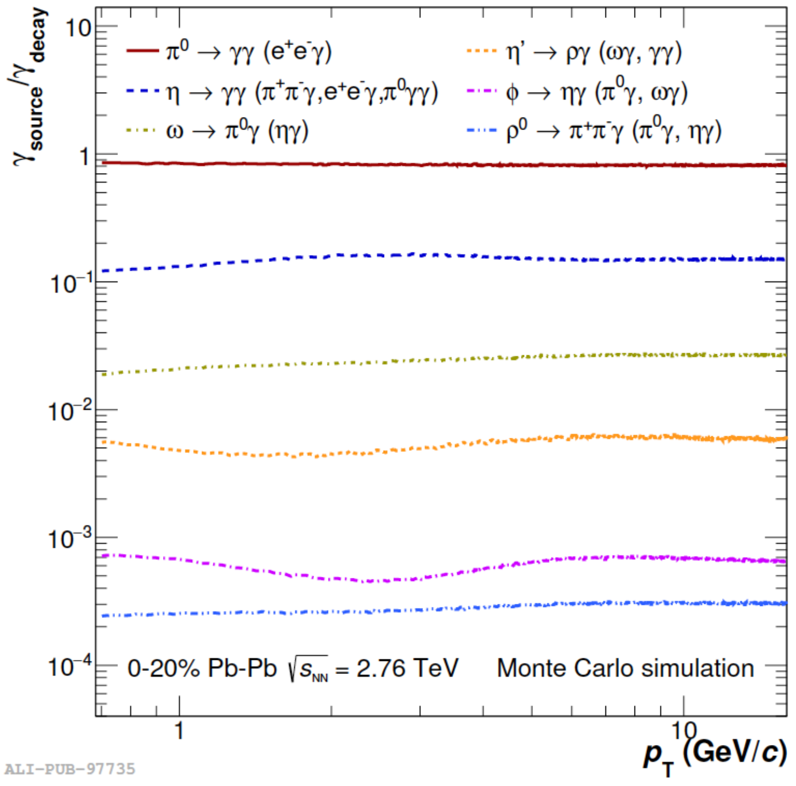

The Idea: Kroll-Wada formula

Relation between photon production and associated e^+e^-:

$$\frac{1}{N_\gamma}\frac{dN_{ee}}{dm_{ee}} = \frac{2\alpha}{3\pi}\sqrt{1-\frac{4m_e^2}{m_{ee}^2}}(1+\frac{2m_e^2}{m_{ee}^2})\frac{1}{m_{ee}}S$$

$$S = \left|F(m_{ee}^2)\right|^2 (1-\frac{m_{ee}^2}{M^2})^3$$

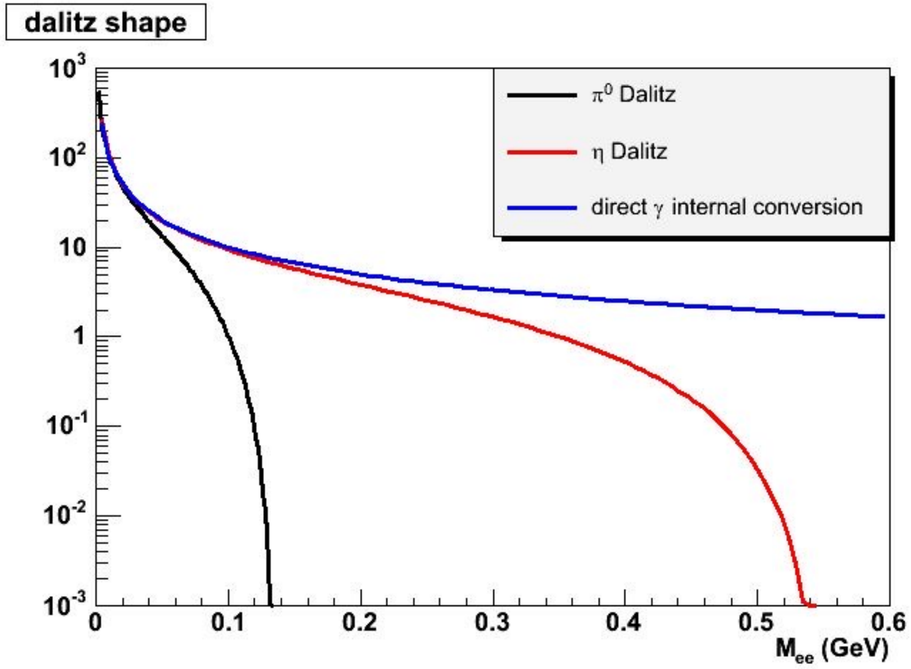

- S=1 for direct photons and m_{ee}>>p_T
- Any source of real γ produces virtual γ with very low mass

Direct photons at RHIC

Phys. Rev. Lett.104 (2010) 132301

$$f(m_{ee}) = (1-r) f_{cocktail}(m_{ee}) + r f_{direct}(m_{ee})$$

$$dN^{dir}(p_T) = r.dN^{incl}(p_T)$$

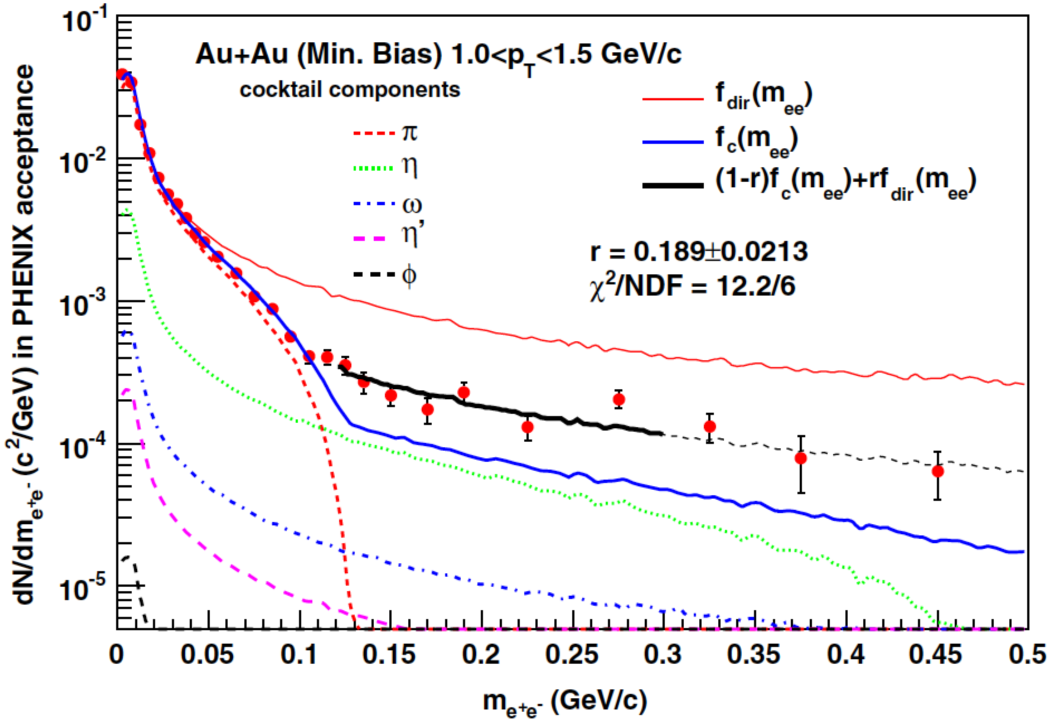

Cocktail normalized to data for $m_{ee} < 0.03$ GeV/c^2

Fit range: $0.12 < m_{ee} < 0.3$ GeV/c^2

Direct photons at RHIC

PHENIX Coll.:
Phys. Rev. Lett. 104(2010) 132301

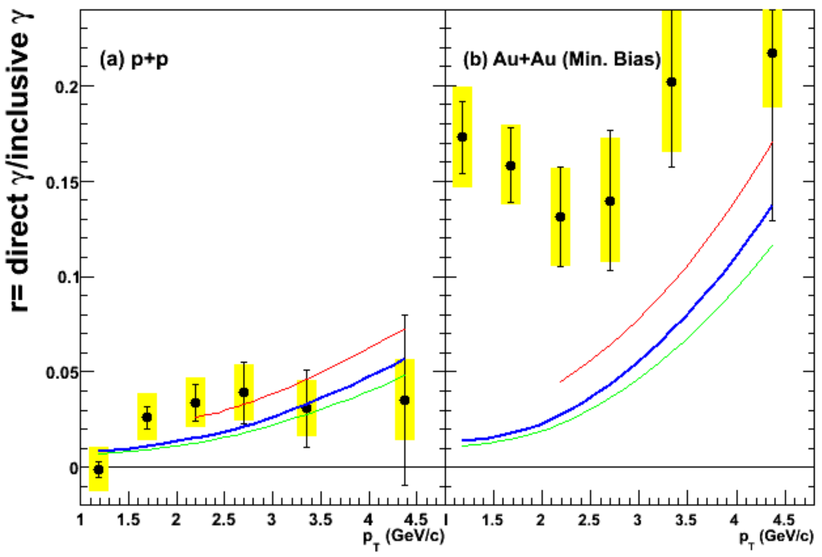

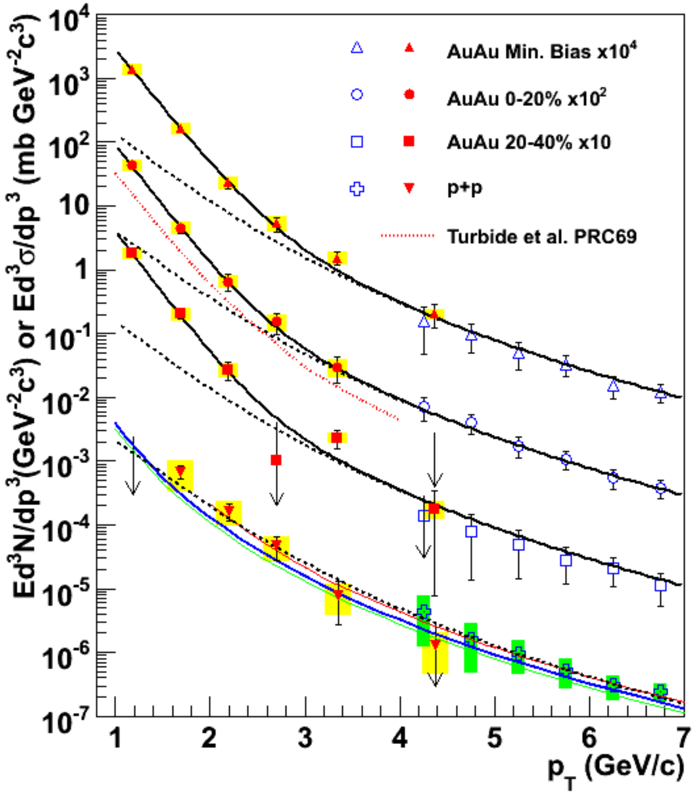

- pp consistent with NLO pQCD calculations
- AuAu larger than calculation for p_T<3.5GeV/c

Excess exponential in p_T (0-20%):

T = 221 ± 23 (stat) ± 18 (sys) MeV

Jet quenching: extended reach in p_T and R

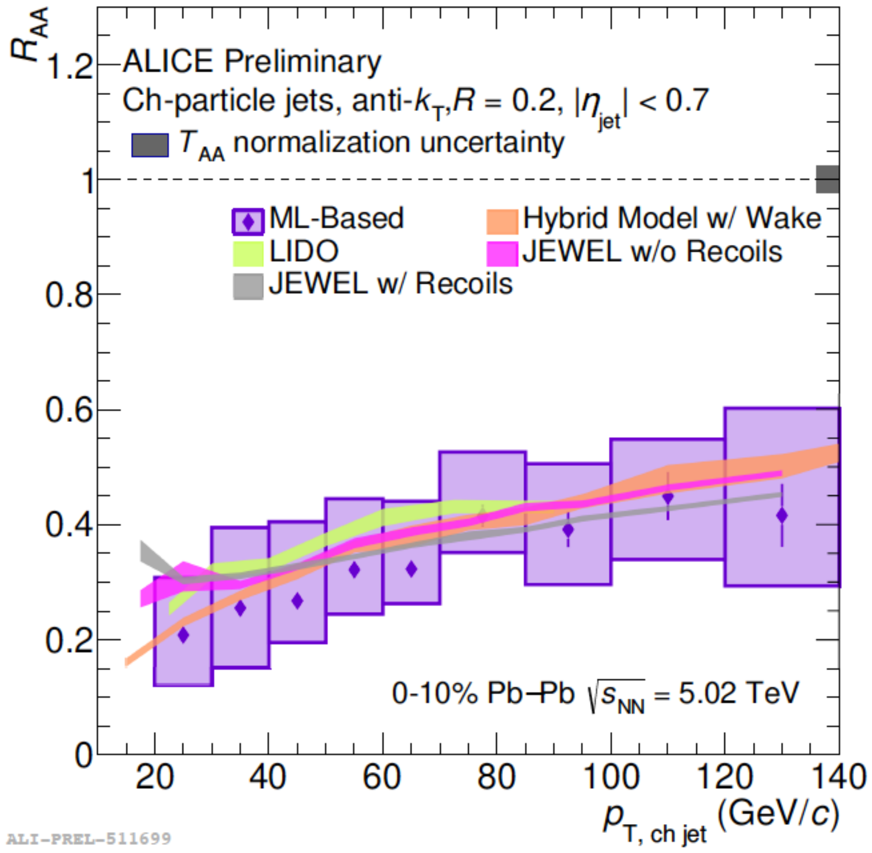

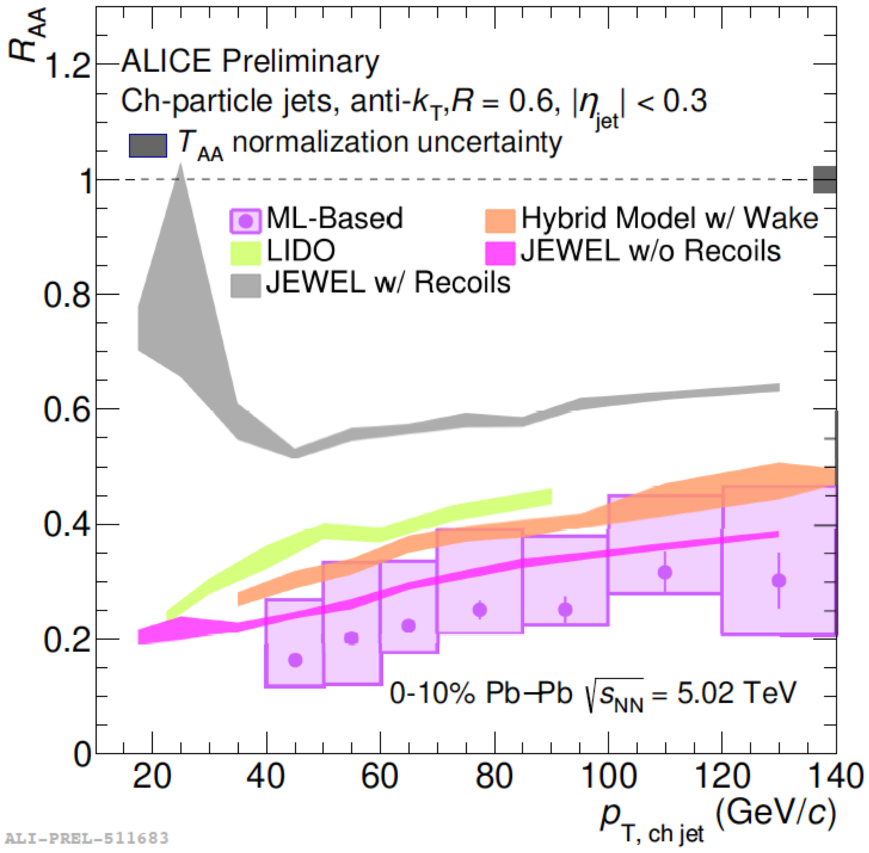

New ML method to subtract underlying Pb-Pb event fluctuations from jet energy: 2x better energy resolution

- Large reduction (factor 3-4) of jet yields, down to p_T = 20 GeV/c
- Lost energy not recovered within the jet “cone”
- Suppression may be even larger for large-cone (R=0.6) low-p_T jets

Microscopic structure of the QGP: acoplanarity

$$\Delta_{\mathrm{recoil}}(p_{\mathrm{T,jet}}, \Delta\varphi) = \frac{1}{N_{\mathrm{trig}}} \frac{\mathrm{d}^3 N_{\mathrm{jet}}}{\mathrm{d}\eta_{\mathrm{jet}}\, \mathrm{d}p_{\mathrm{T,jet}}\, \mathrm{d}\Delta\varphi}\Bigg|_{p_{\mathrm{T}}^{\mathrm{trig}} \in \mathrm{TT}_{\mathrm{Sig}}} - c_{\mathrm{Ref}} \cdot \frac{1}{N_{\mathrm{trig}}} \frac{\mathrm{d}^3 N_{\mathrm{jet}}}{\mathrm{d}\eta_{\mathrm{jet}}\, \mathrm{d}p_{\mathrm{T,jet}}\, \mathrm{d}\Delta\varphi}\Bigg|_{p_{\mathrm{T}}^{\mathrm{trig}} \in \mathrm{TT}_{\mathrm{Ref}}}$$

$$I_{\mathrm{AA}} = \frac{\Delta_{\mathrm{recoil}}(\mathrm{Pb-Pb})}{\Delta_{\mathrm{recoil}}(\mathrm{pp})}$$

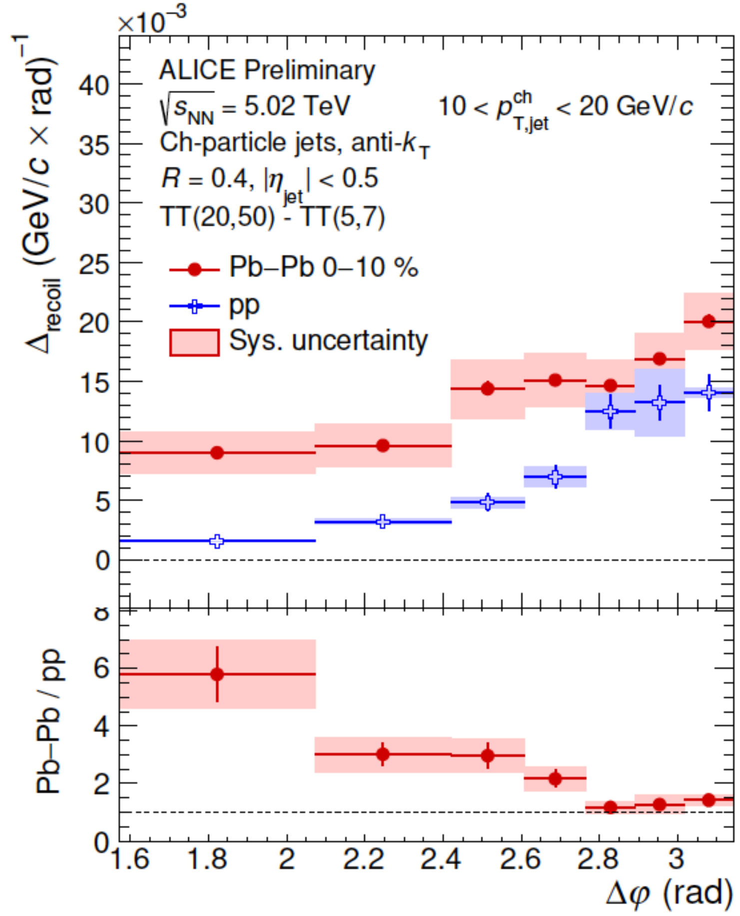

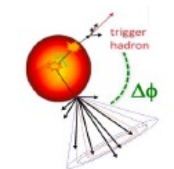

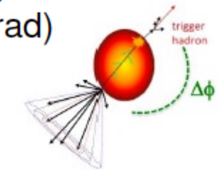

Δϕ broadening for larger R and small jet p_{T}

Scattering on QGP constituents?

Medium response to energy loss ?

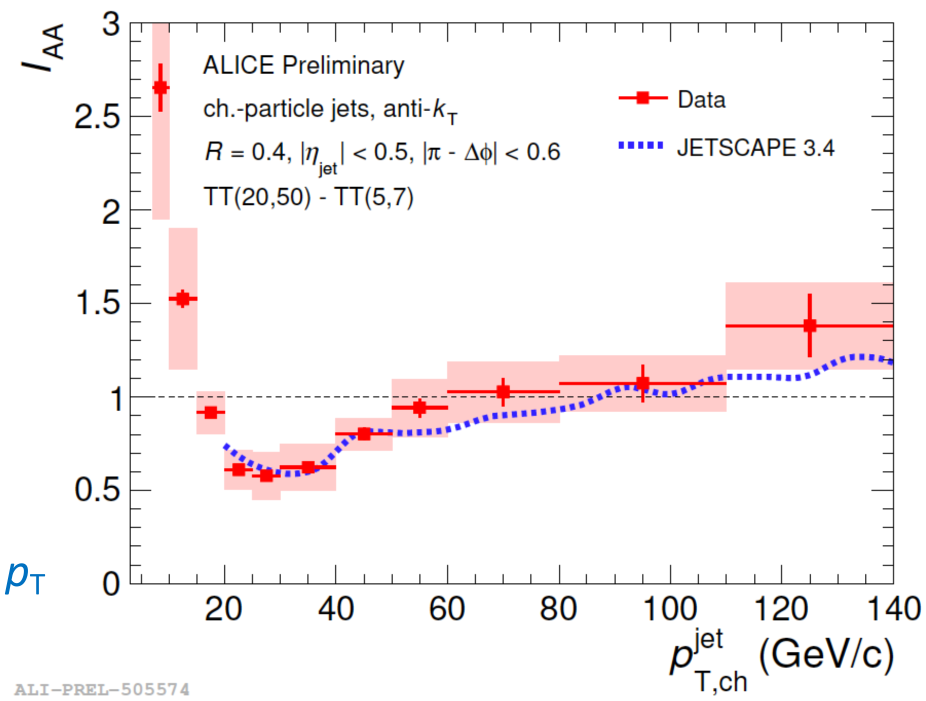

Hint of energy recovery at low jet momenta

Exploring angular dependence: groomed jet radius

PRL 128 (2022) 102001

$$z_g \equiv \frac{p_{T,\mathrm{subleading}}}{p_{T,\mathrm{leading}} + p_{T,\mathrm{subleading}}}$$

$$\theta_g = \frac{\sqrt{\Delta y^2 + \Delta\varphi^2}}{R}$$

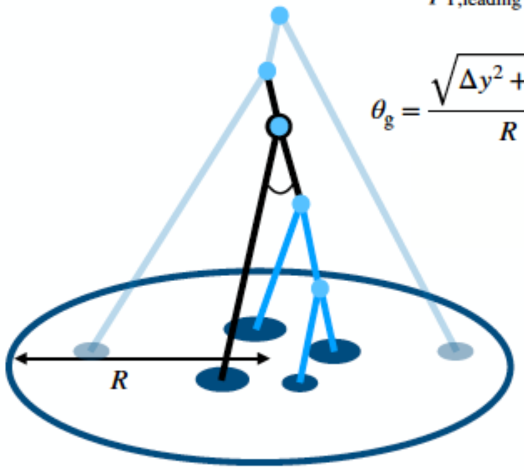

Grooming condition: $z > z_{cut}$

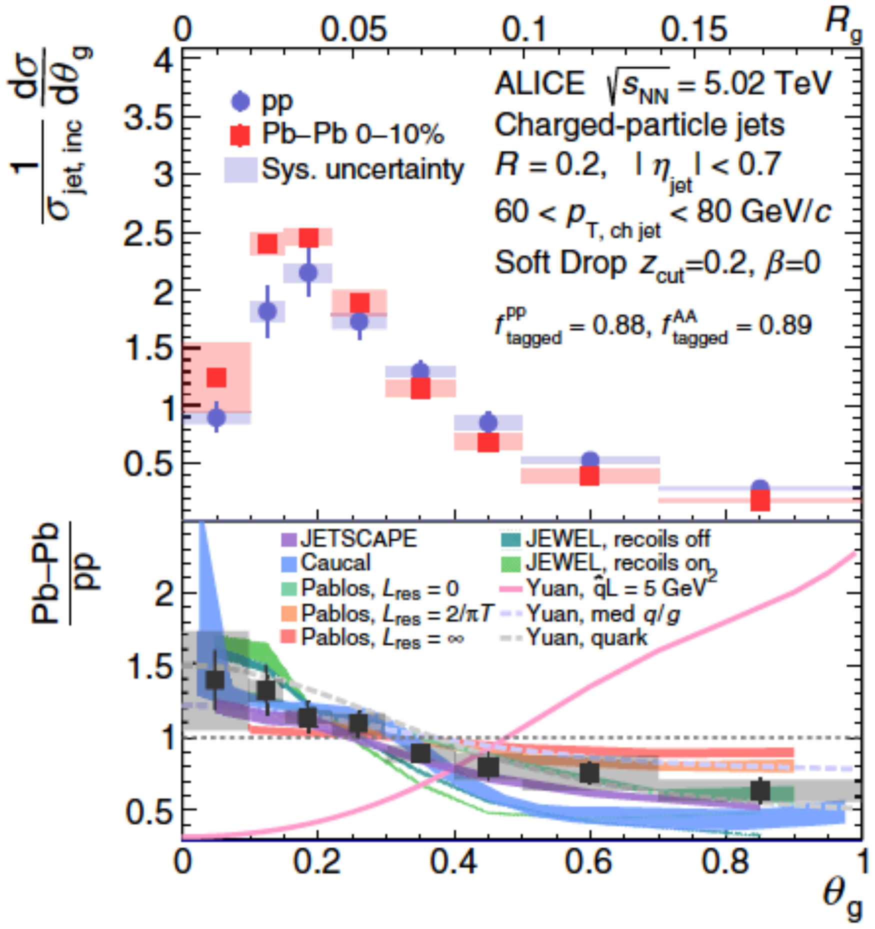

- Suppression of large angles
- Enhancement of small angles

First experimental evidence for modification of angular scale of groomed jets in HIC

Dead- cone effect now exposed by ALICE

Reduction of gluon radiation from heavy quarks at small angles

Dokshitzer, Khoze, Troian, J. Phys. G17 (1991) 1602

$$R(\theta) = \frac{1}{N^{\mathrm{D^0\,jets}}} \frac{\mathrm{d}n^{\mathrm{D^0\,jets}}}{\mathrm{d}\ln(1/\theta)} \Big/ \frac{1}{N^{\mathrm{inclusive\,jets}}} \frac{\mathrm{d}n^{\mathrm{inclusive\,jets}}}{\mathrm{d}\ln(1/\theta)} \Bigg|_{k_{\mathrm{T}},E_{\mathrm{Radiator}}}$$

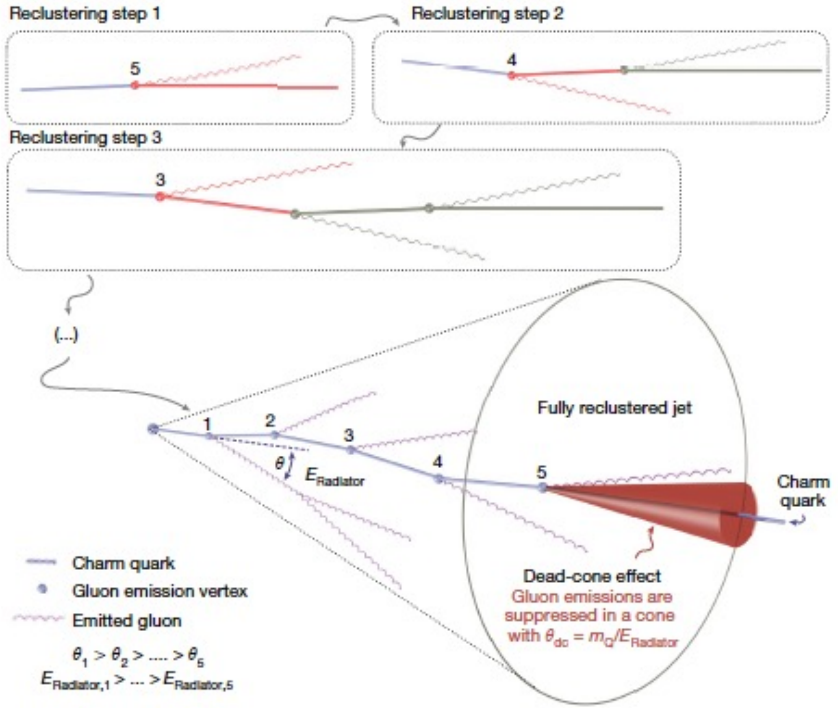

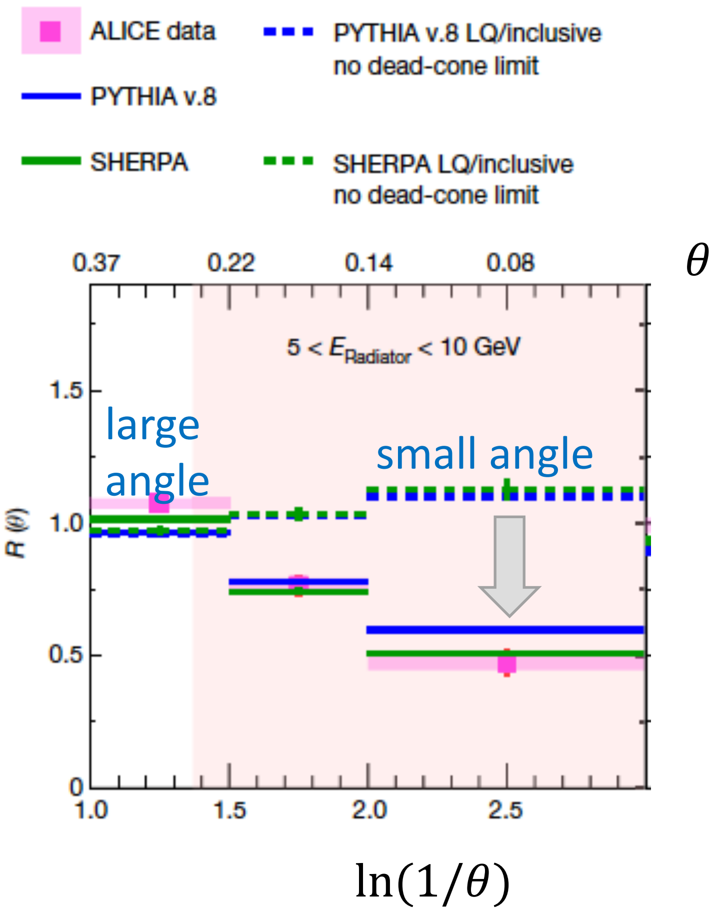

First direct observation using jet iterative declustering and Lund plane analysis of jets that contain a soft D^0 meson

Nature 605 (2022) 7910, 440

Charm splitting function in jets

arXiv: 2208.04857

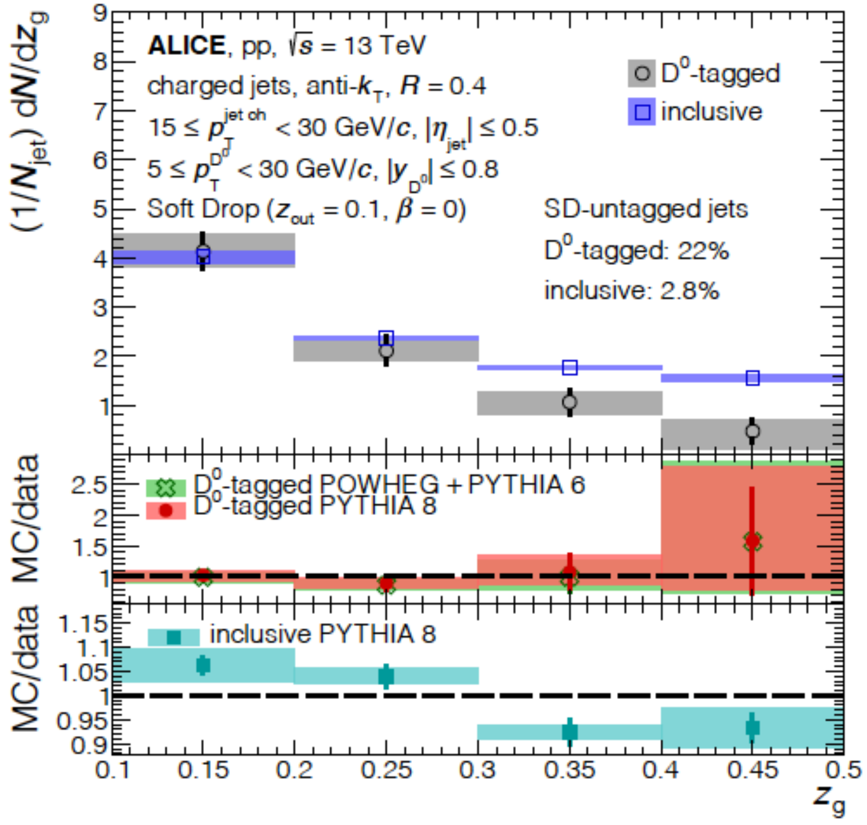

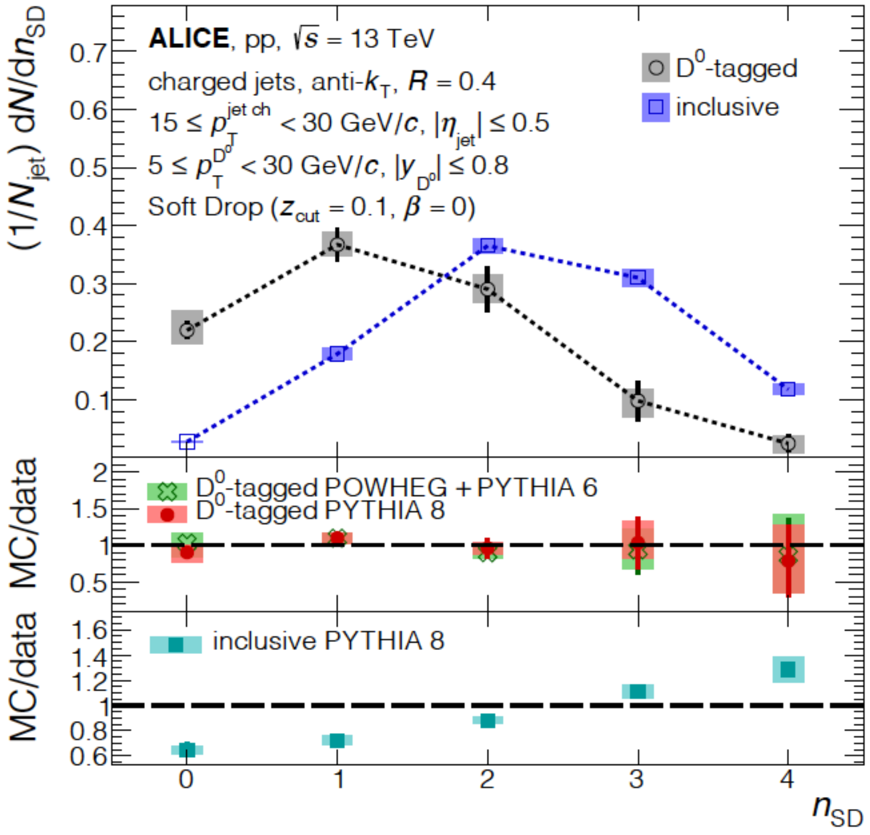

Charm-tagged jets → first direct experimental constraint of the splitting function of heavy-flavour quarks

- z_g distribution appears steeper than that of light quarks and gluons
- heavy-flavour quarks on average have fewer perturbative emissions compared to light quarks and gluons

ALICE 3 detector

CERN-LHCC-2022-009

arXiv 2211.02491

- Compact, ultra-lightweight all-silicon tracker → σ_{p_T}/p_T ~1-2%.
- Vertex detector with unprecedent pointing resolution σ_{DCA} ~ 10 μm (p_T = 0.2 GeV/c)
- Large acceptance $|\eta| < 4$, $p_T > 0.02$GeV/c
- Particle identification → $\gamma, e^{\pm}, \mu^{\pm}, K^{\pm}, \pi^{\pm}$
- Fast readout and online processing

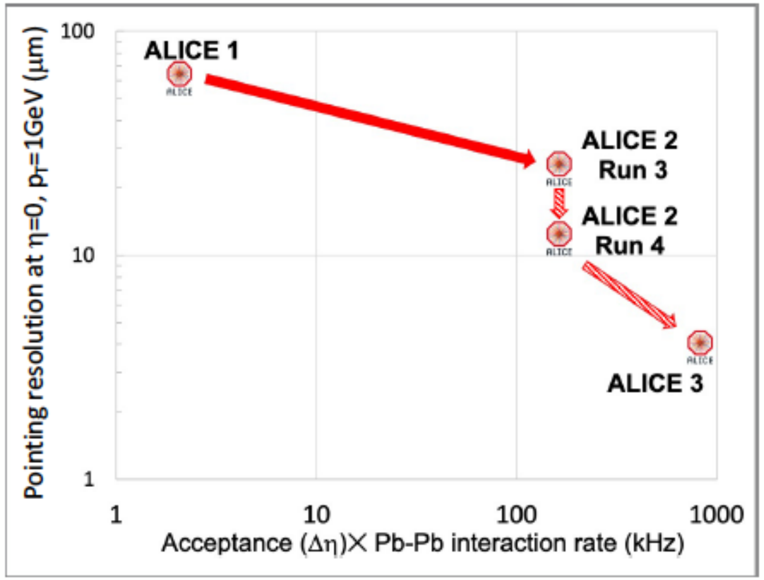

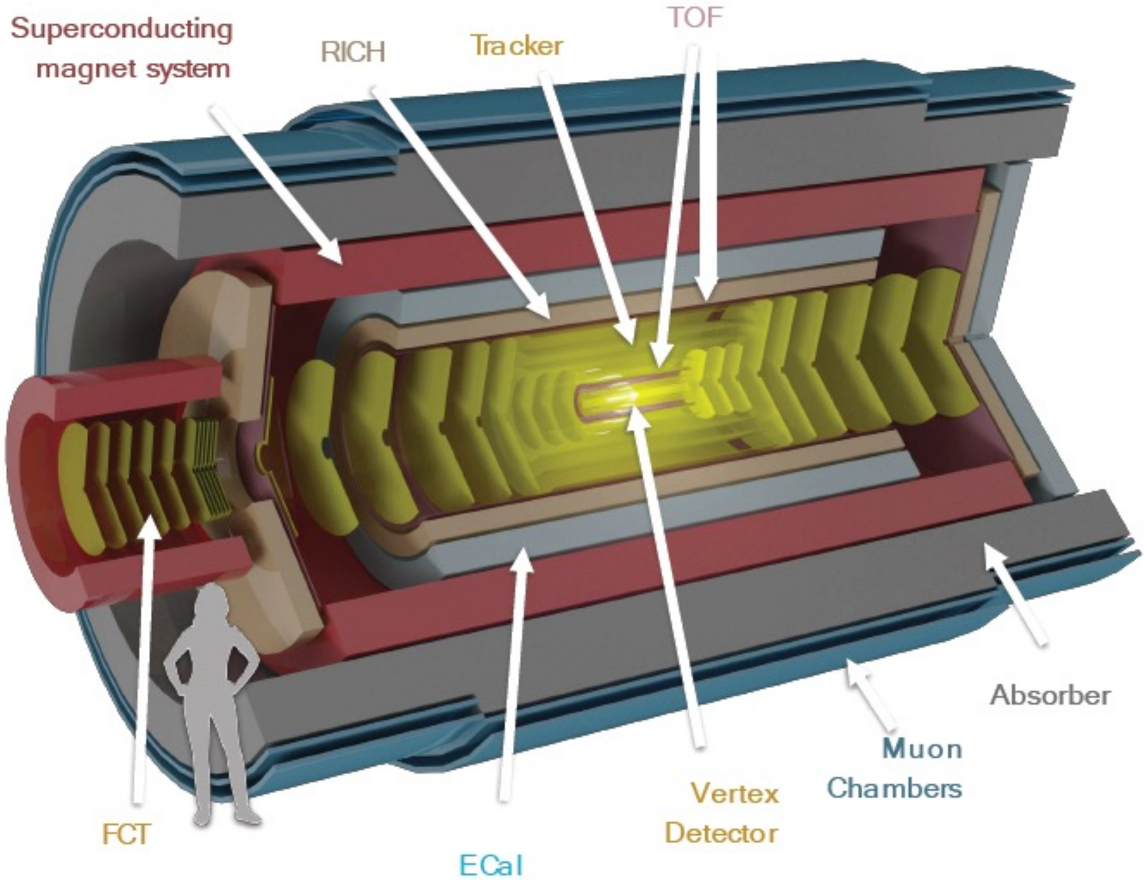

Physics reach improves dramatically!

ALICE 3 : Physics topics

- Precision differential measurements of dileptons
  - Evolution of the quark-gluon plasma
  - Mechanisms of chiral symmetry restoration in the QGP

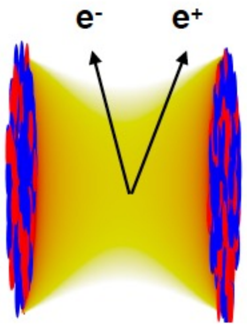

- Systematic measurements of (multi-) heavy-flavoured hadrons down to low p_T
  - Transport properties in the QGP down to thermal scale
  - Mechanisms of hadronization from the QGP

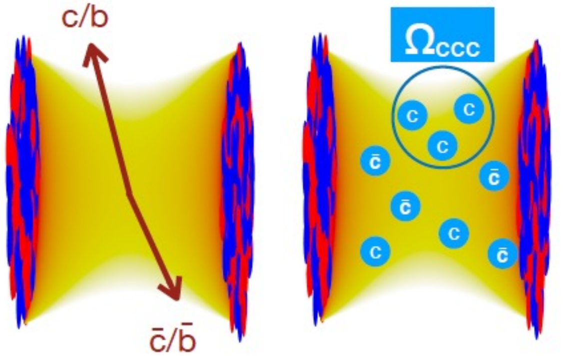

- Hadron interaction and fluctuation measurements
  - Existence and nature of heavy-quark exotic bound states and interaction potential
  - Search for super-nuclei (light nuclei with c)
  - Search for critical behaviour in event-by-event fluctuations of conserved charges

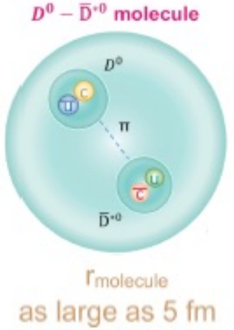

Electromagnetic radiation

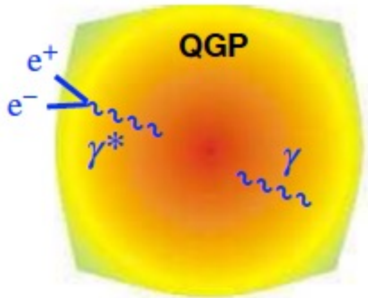

- Average T of the QGP with e^+e^- using thermal dielectron m_{ee} spectrum for m_{ee}> 1.1 GeV/c^2 (QGP radiation dominated)

- Requirements:
  - Good e PID down to low p_T
  - Small detector material budget (γ background)
  - Excellent pointing resolution (heavy-flavour decay electrons)

Possible with ALICE 3 due to excellent pointing resolution and small material budget

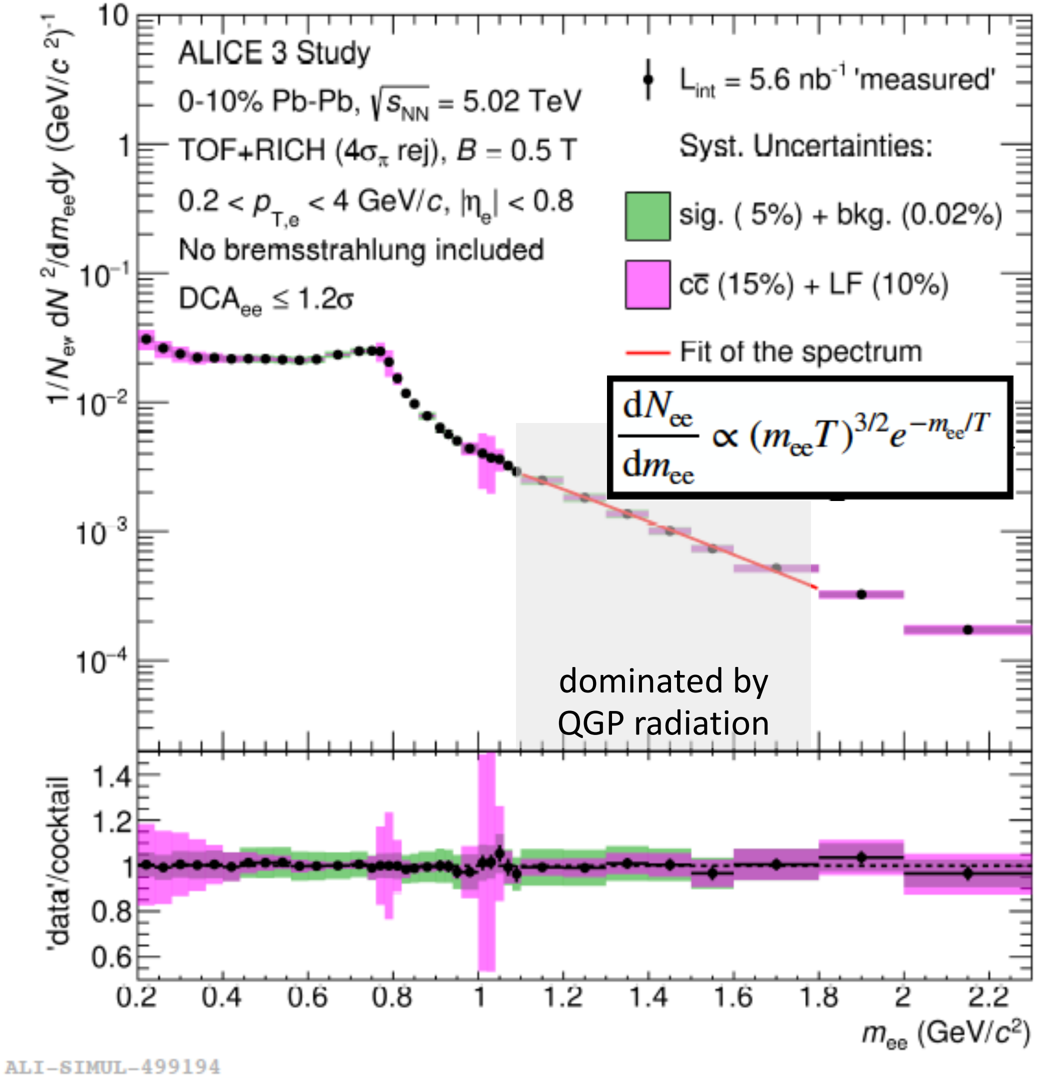

R. Rapp, Adv. High Energy Phys. 2013 (2013) 148253
P.M Hohler and R. Rapp, Phys. Lett. B 731 (2014) 103
ALICE CERN-LHCC-2022-009

Chiral symmetry restoration

Study chiral symmetry restoration (CSR) mechanisms using thermal dielectron spectrum $m_{ee} < 1.2$ GeV

ALICE 3 access to CSR mechanisms like ρ-a_1 mixing

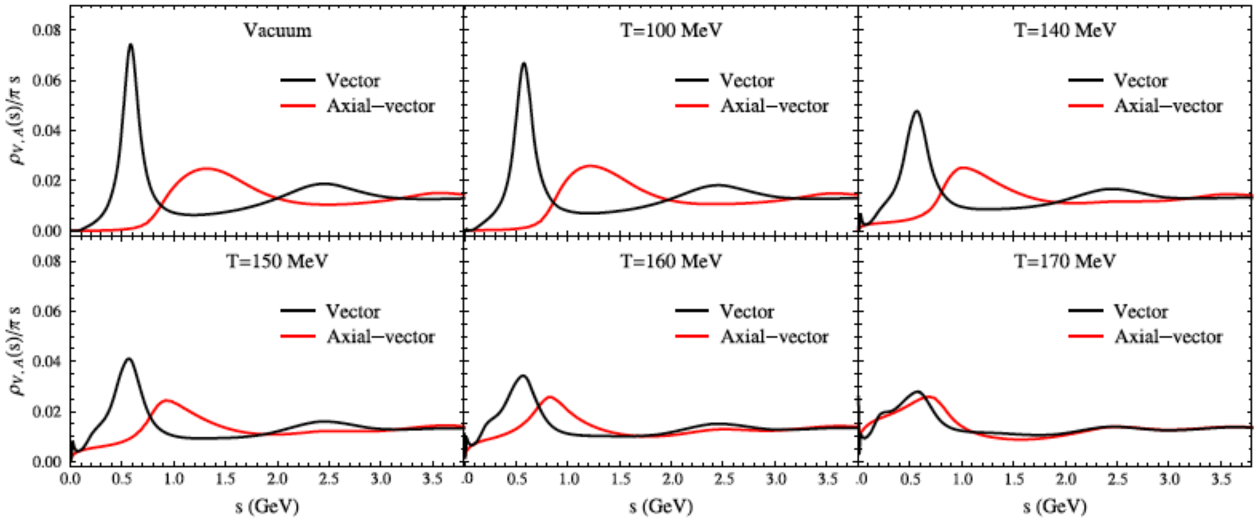

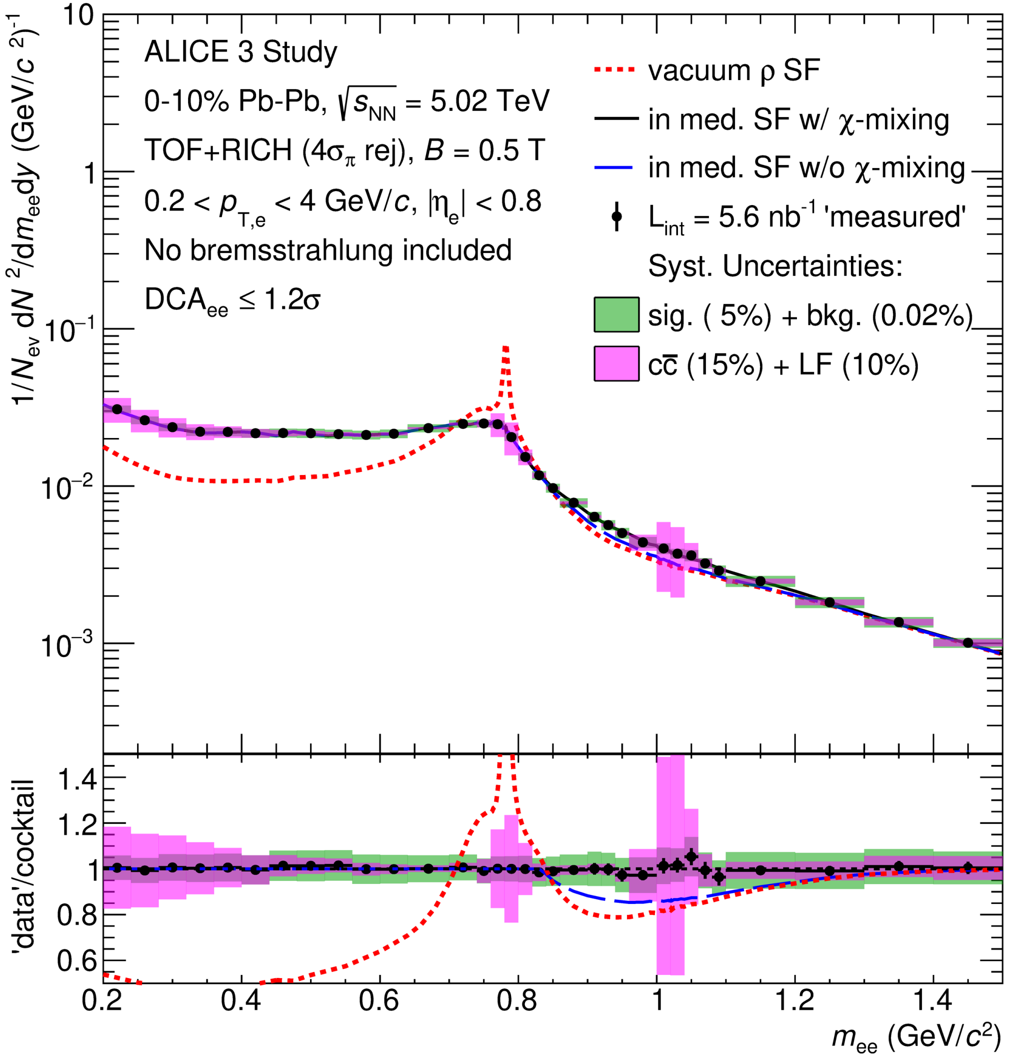

Electromagnetic radiation

ALICE 3:

- Probe time dependence of T

Double differential spectra: T vs mass, $p_{T,ee}$

- Access time evolution of flow

Dilepton v_2 vs mass and p_{Tee} possible

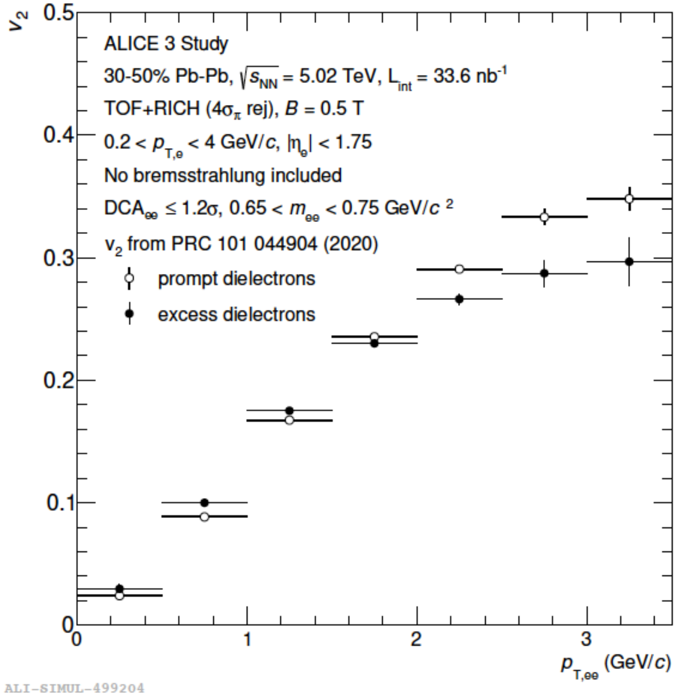

Expected statistical errors of T as a function of $p_{T,ee}$

ALICE 3 projection, one month Pb-Pb

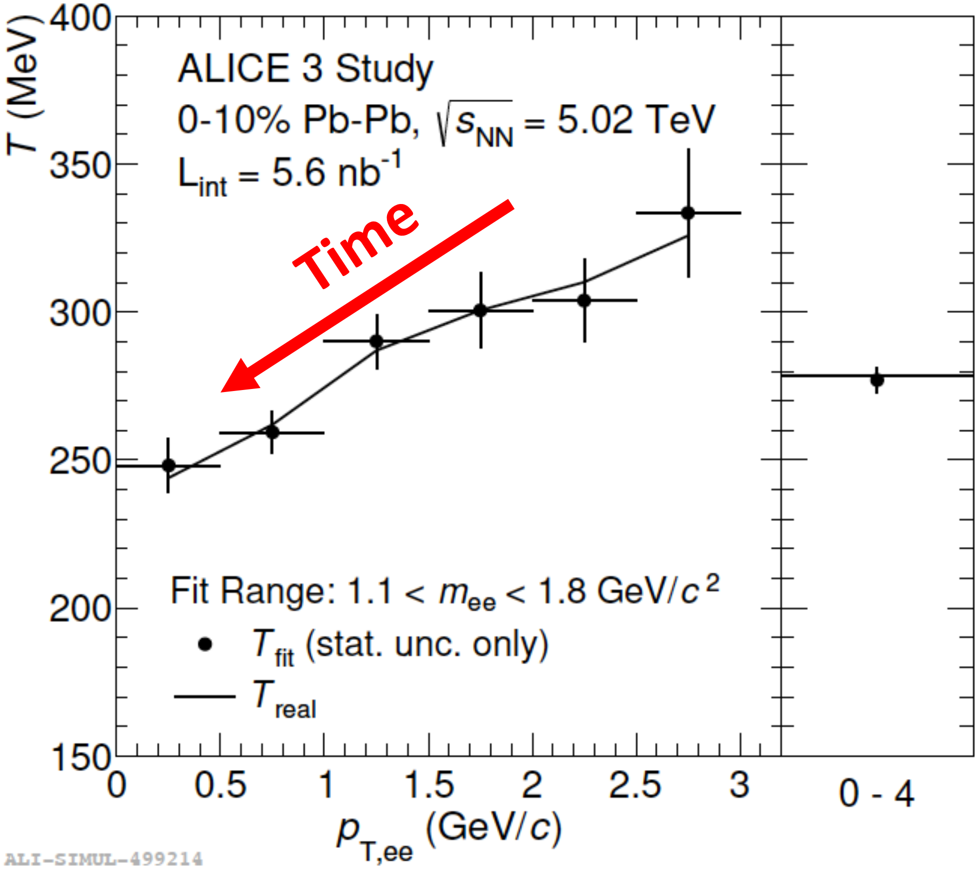

Complementary measurements with real photons.

Different systematic uncertainties → reduce overall uncertainties

R. Rapp, Adv. High Energy Phys. 2013 (2013) 148253
P.M Hohler and R. Rapp, Phys. Lett. B 731 (2014) 103
ALICE CERN-LHCC-2022-009

Heavy flavour transport

Λ_c v_2 performance

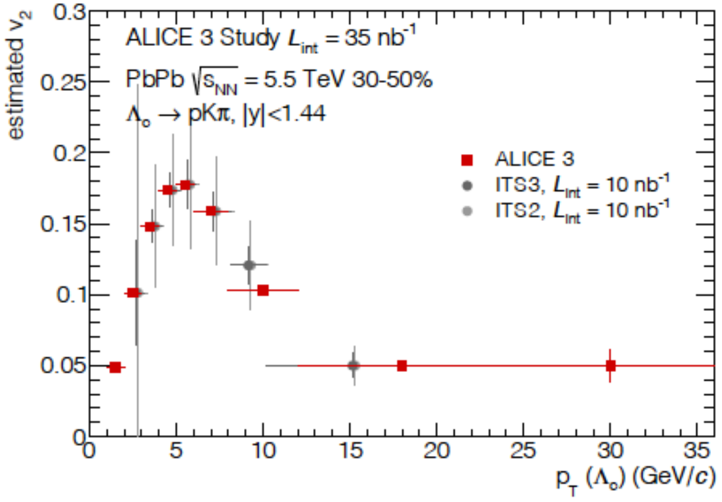

Extension to beauty

Λ_b v_2 performance

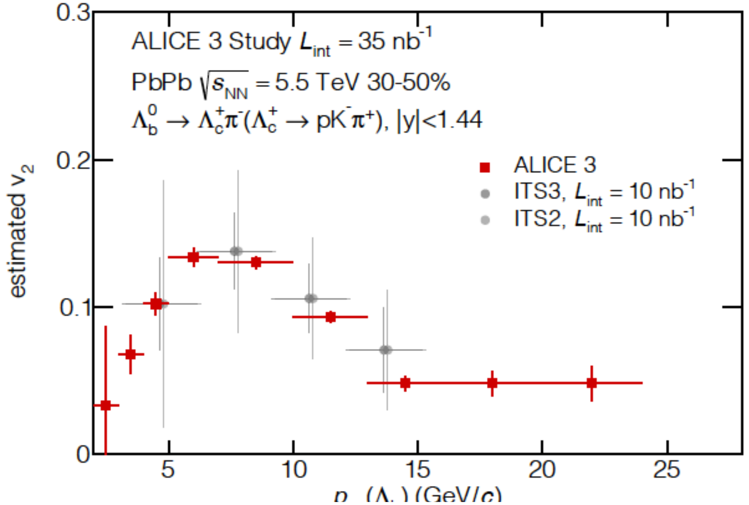

Extension to multi-charm

Ξ_{cc}^{++} v_2 performance

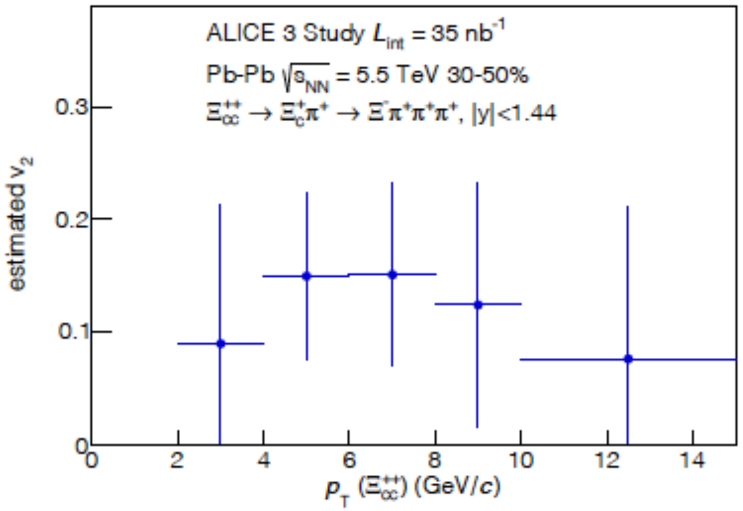

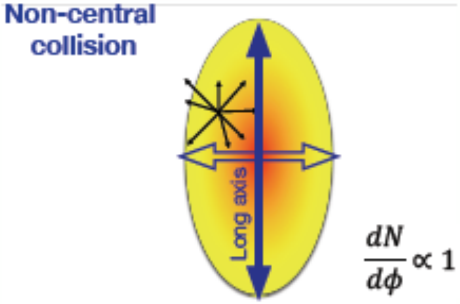

$$\frac{dN}{d\phi} \propto 1 + 2v_2\cos 2(\varphi - \psi)$$

Interactions with the plasma generate azimuthal anisotropy v2:

Relaxation time
τ_Q = (m_Q /T) D_S

Understanding of transport properties of the QGP requires heavy-flavor probes
Expect beauty thermalization slower than cham→ smaller v_2

Need ALICE 3 performance (pointing resolution , acceptance) for precision measurement of e.g. Λ_c, Λ_b, and multi-charm v_2

Mechanisms of hadron formation

Multi-charm baryons: test how independently produced quarks form hadrons

- Contribution from single parton scattering is very small
- Very large enhancement predicted by Statistical hadronization model in Pb-Pb collisions
- Progress relies on the reconstruction of complex decay chains

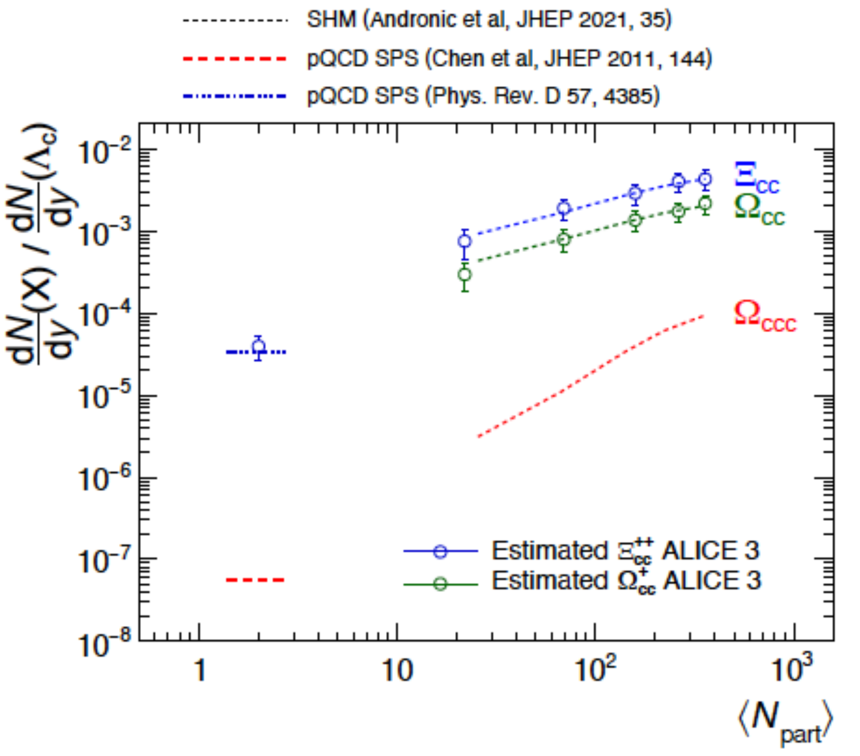

Large enhancements: unique sensitivity to
thermalisation and hadronisation dynamics

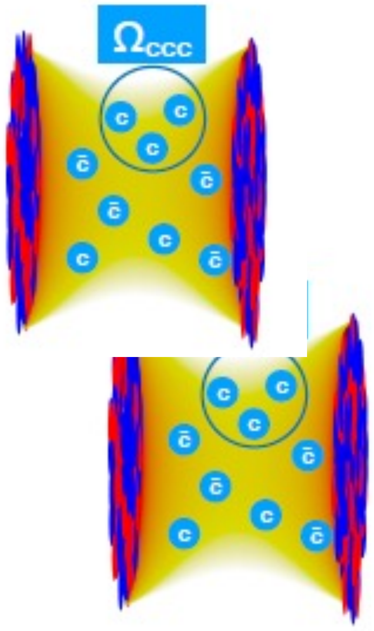

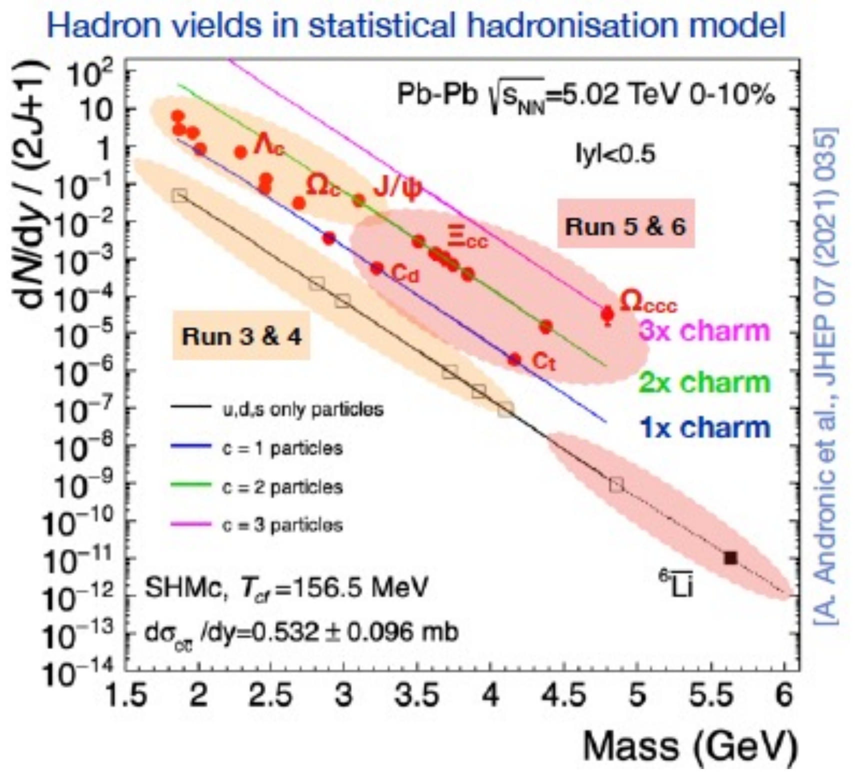

Multi-charm baryon reconstruction in ALICE 3

$$\Xi_{cc}^{++} \rightarrow \Xi_c^{+} + \pi^{+} \rightarrow \Xi^{-} + 3\,\pi^{+}$$

First ALICE 3 tracking layer at 5 mm

- Track Ξ^- before it decays, Ξ^- pointing resolution

Unique access with ALICE 3 in Pb-Pb collisions

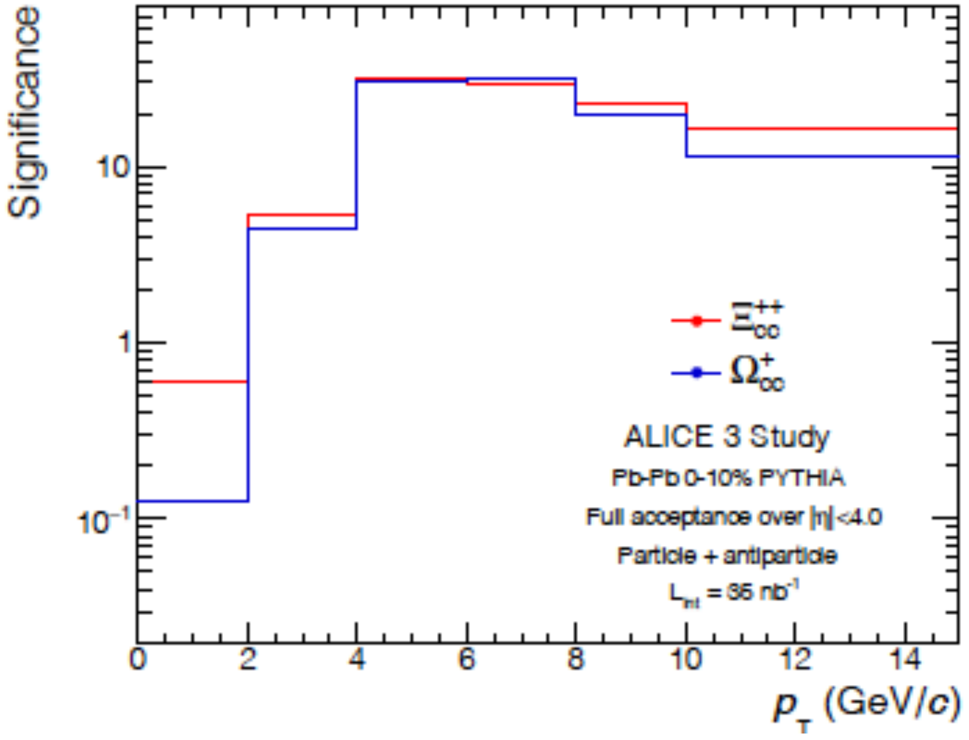

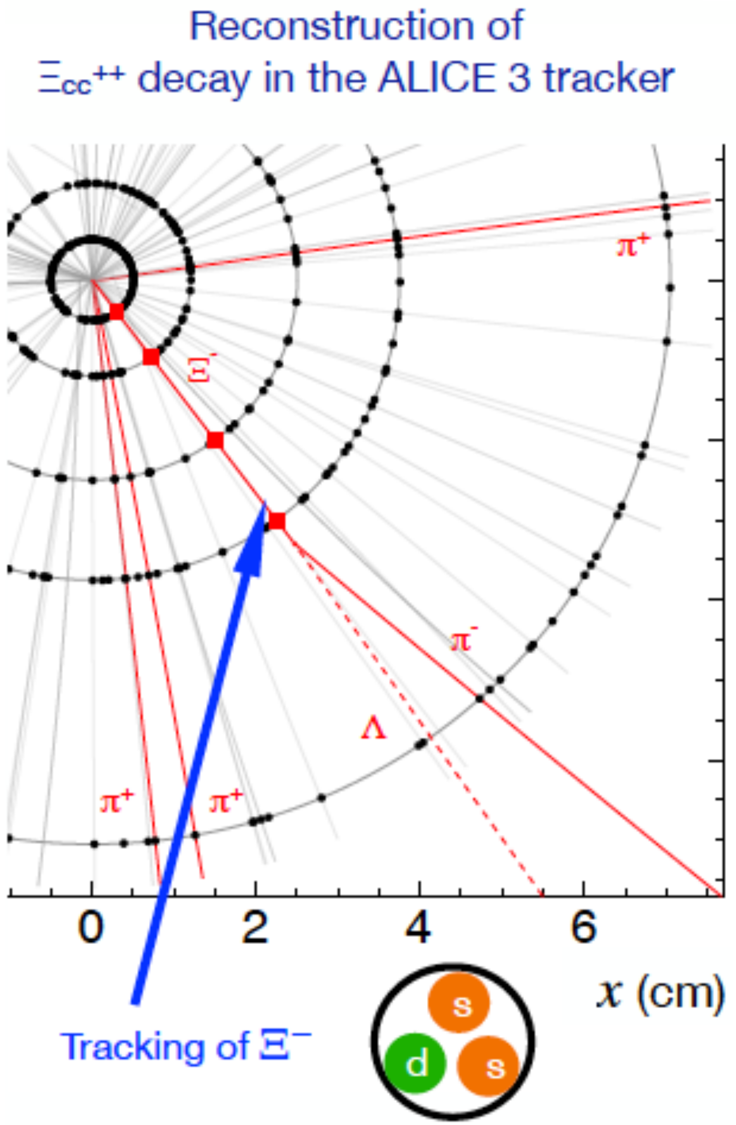

Blast-wave model parameters

A hydrodynamic inspired description of spectra

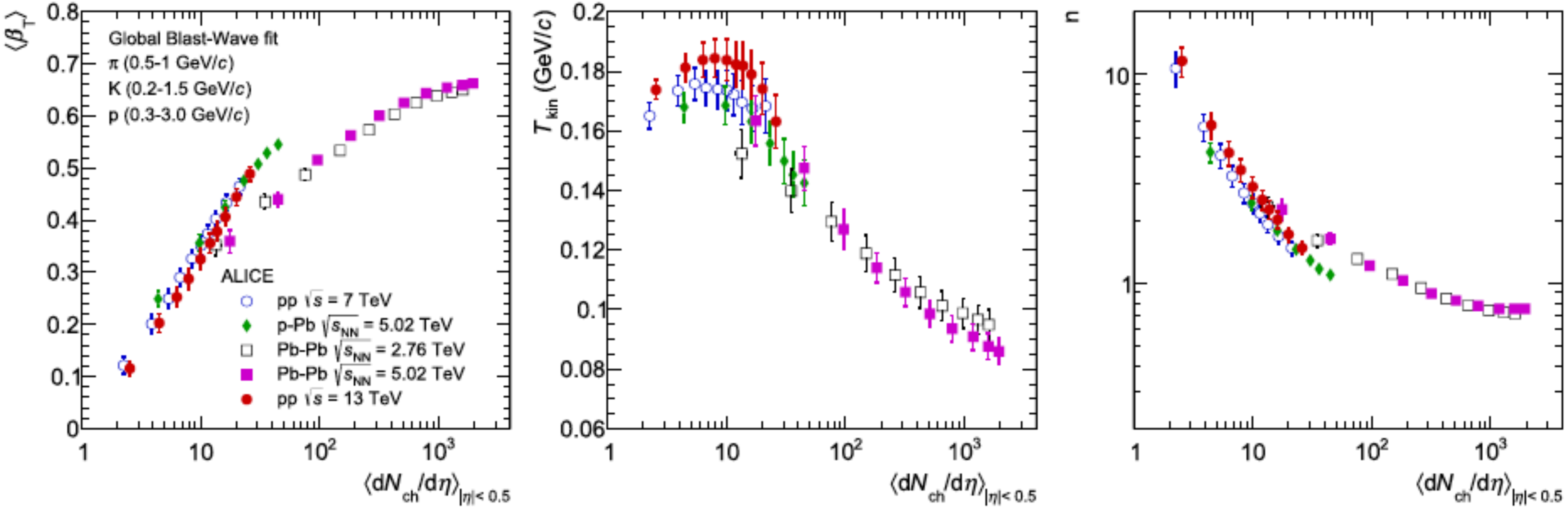

π^0 and η mesons

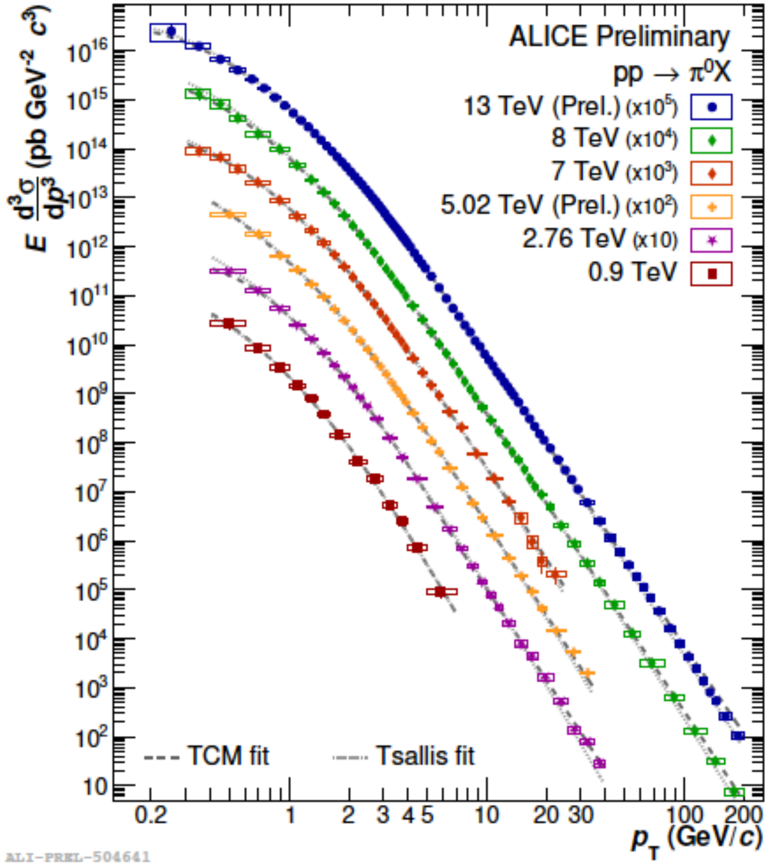

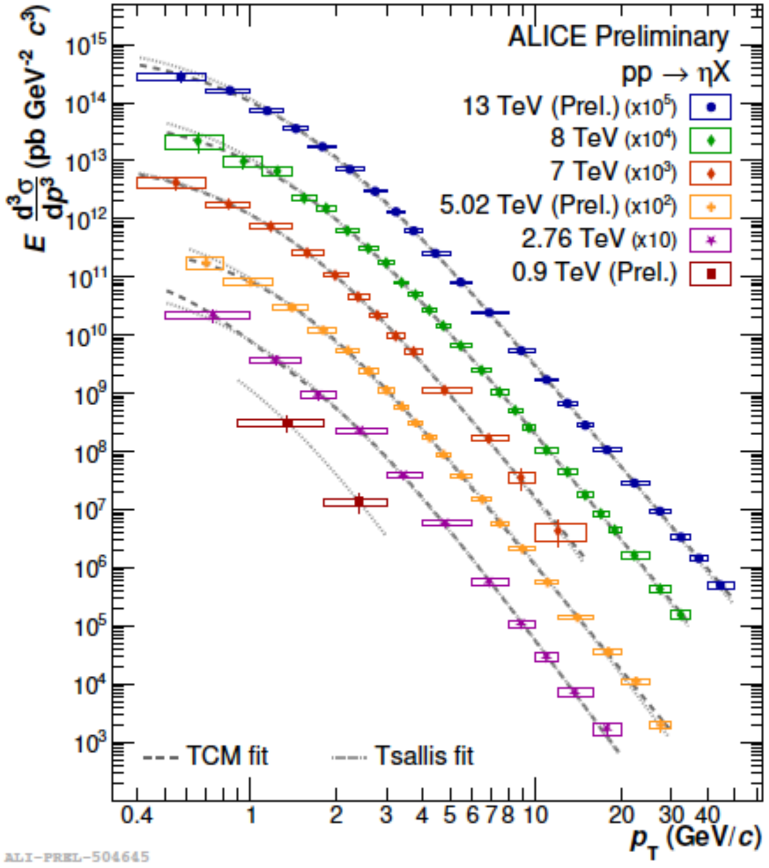

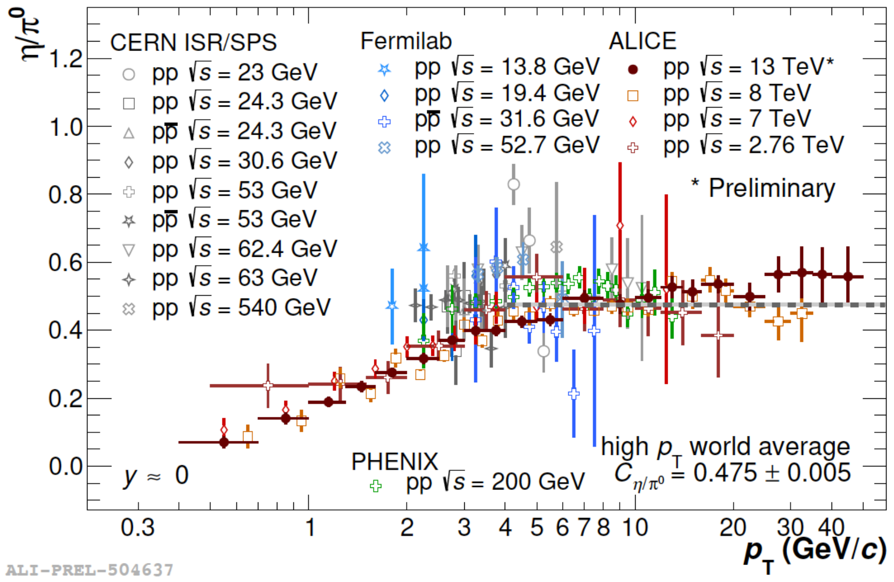

Universal behavior for all collision energies →

World data at high p_T: $\eta/\pi^0 = 0.475 \pm 0.005$

π^0: $0.2 \le p_T < 200$ GeV/c

η: $0.4 \le p_T < 50$ GeV/c

π^0 and η mesons

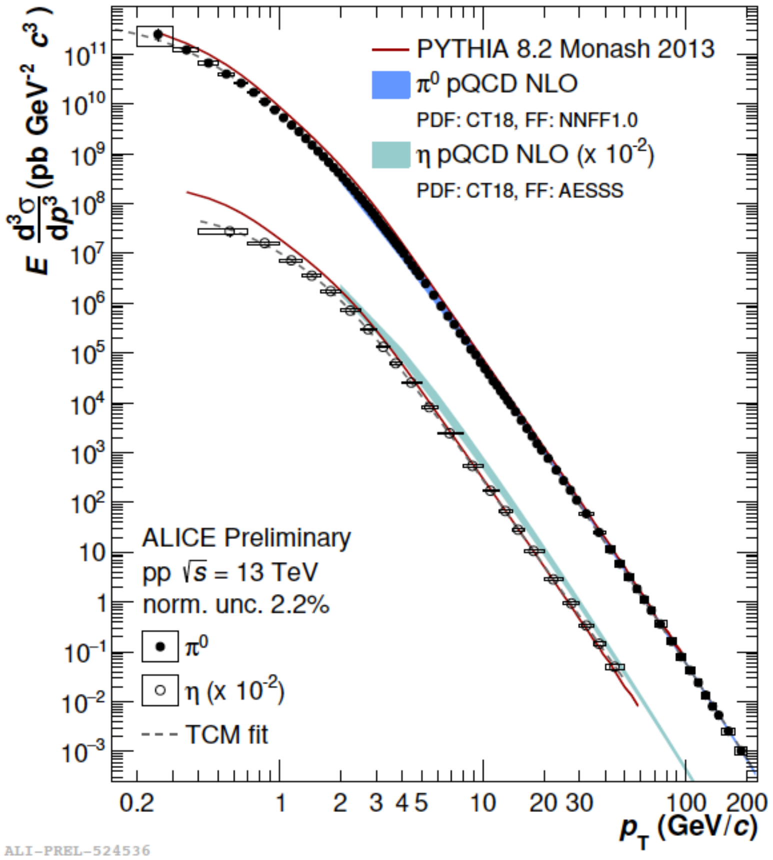

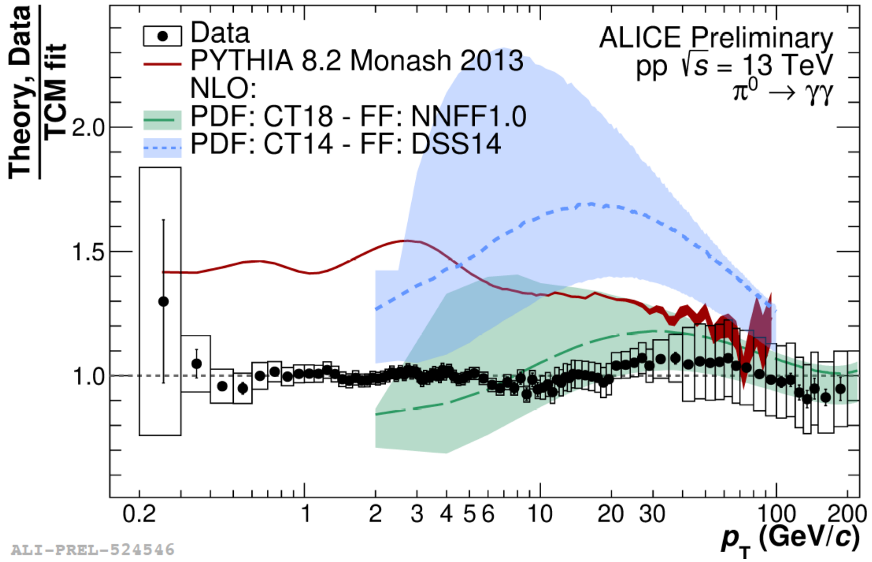

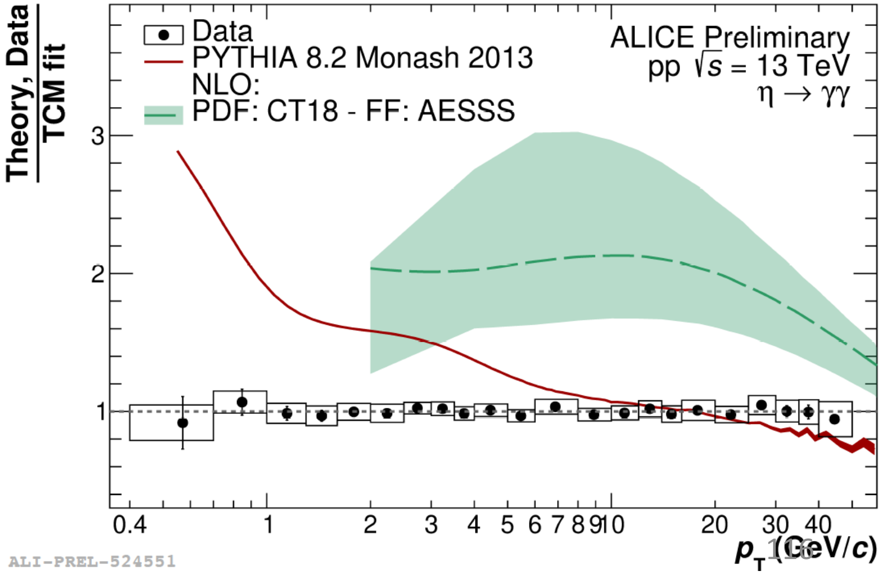

- NLO using NNFF1.0 FF describes the π^0 spectrum
- PYTHIA overshoots data and does not describe shape of spectra
- New FF are needed for the η meson

π^0 and η mesons

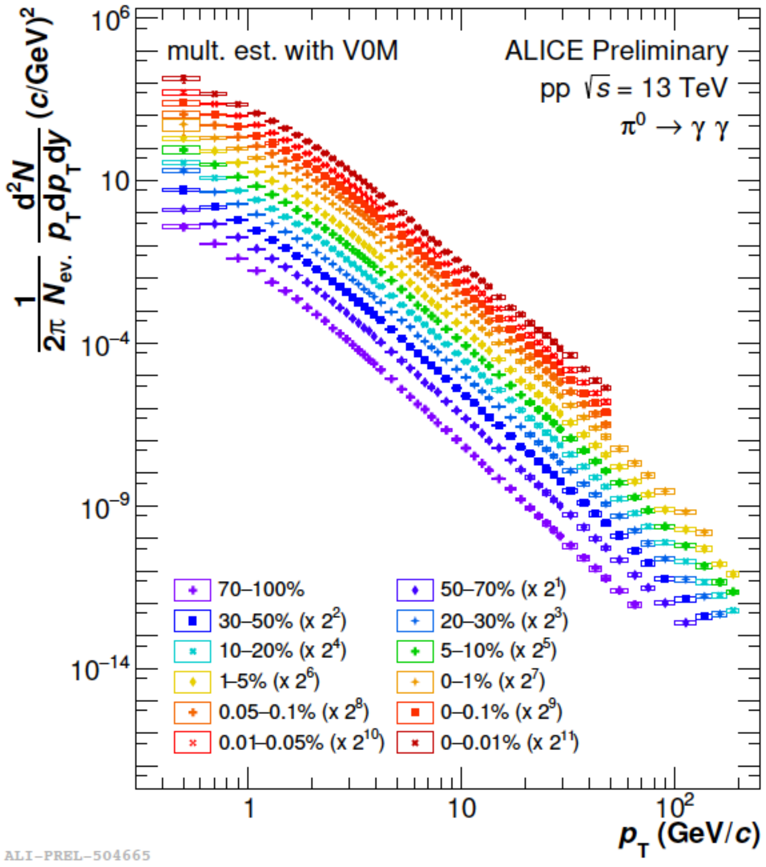

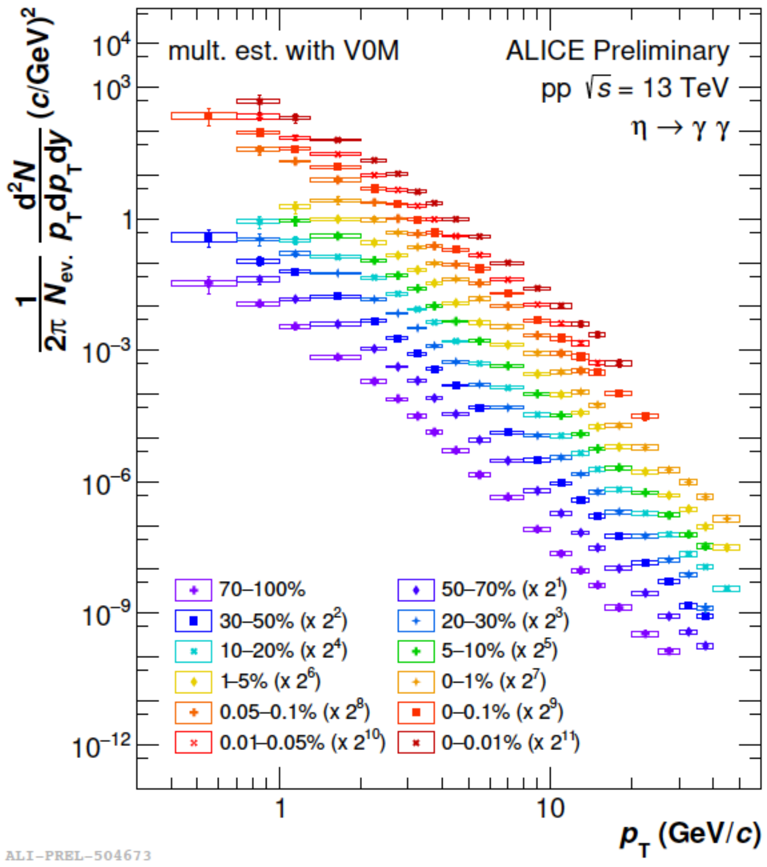

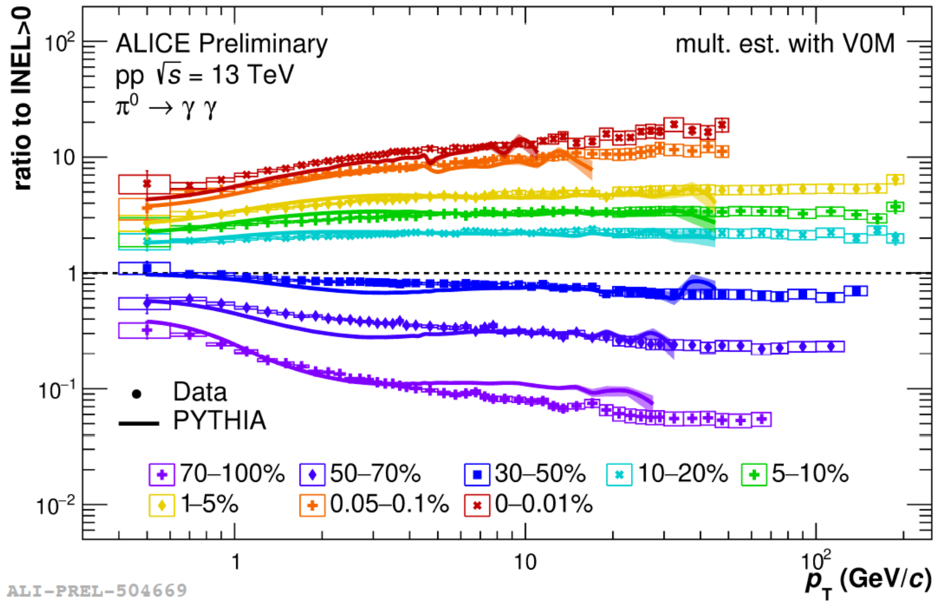

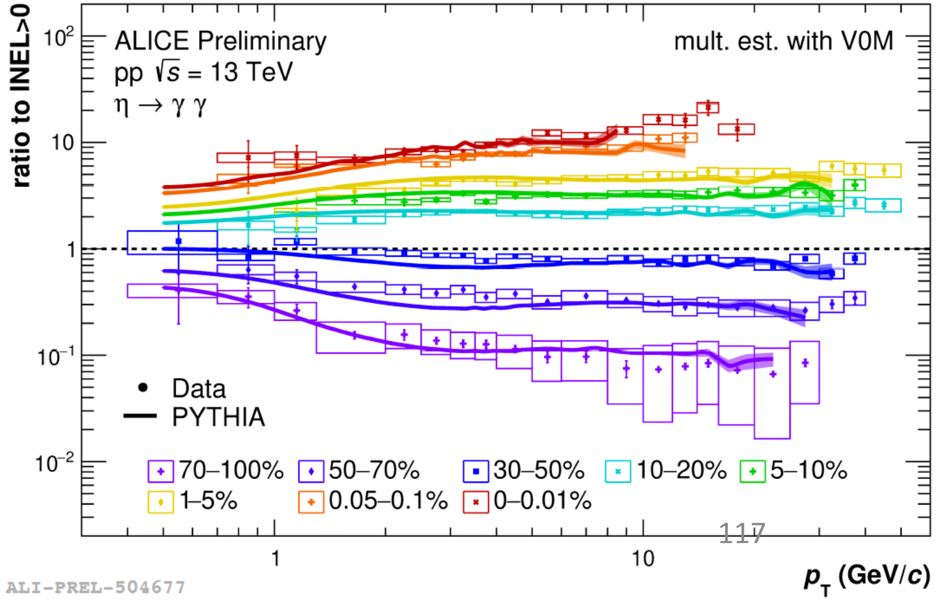

Hardening of p_T spectra with rising multiplicity

- General ordering and magnitude described by PYTHIA
- Slightly different p_T dependence

Production of charmonia

Table 1 Masses, binding energies, and radii of the lowest $c\bar{c}$ and $b\bar{b}$ bound states [3]; the listed radii are $1/2\sqrt{\langle r_i^2 \rangle}$, given by Eq. (3)

State	J/ψ	χ_c	ψ'	Υ	χ_b	Υ'	χ_b'	Υ''
Mass (GeV)	3.10	3.53	3.68	9.46	9.99	10.02	10.36	10.36
ΔE (GeV)	0.64	0.20	0.05	1.10	0.67	0.54	0.31	0.20
Radius (fm)	0.25	0.36	0.45	0.14	0.22	0.28	0.34	0.39

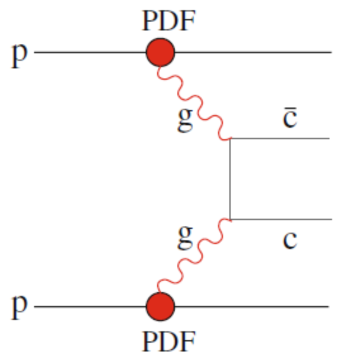

Fig. 10 Lowest order Feynman diagram for $c\bar{c}$ production through gluon fusion

- ccbar production
- color octet to color single (color neutralization)
- physical bound state (J/Ψ)

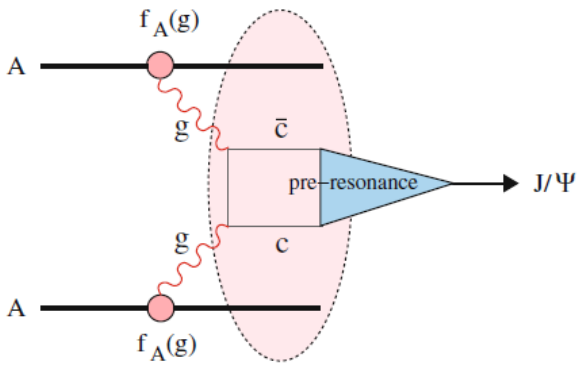

Fig. 12 J/ψ production in a nuclear medium

- Posible modifications of PDF due to other nucleons
- ccbar pair can suffer absorption while traversing nuclear matter

Hadronization of charm quarks from pp…

PRD 105 (2022) L011103

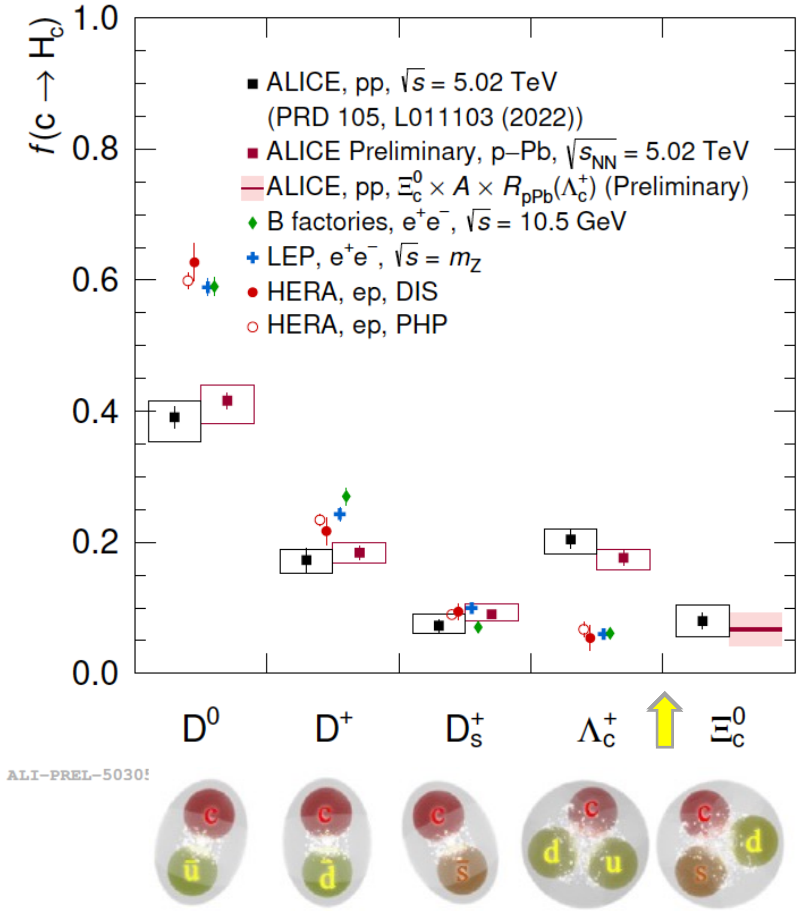

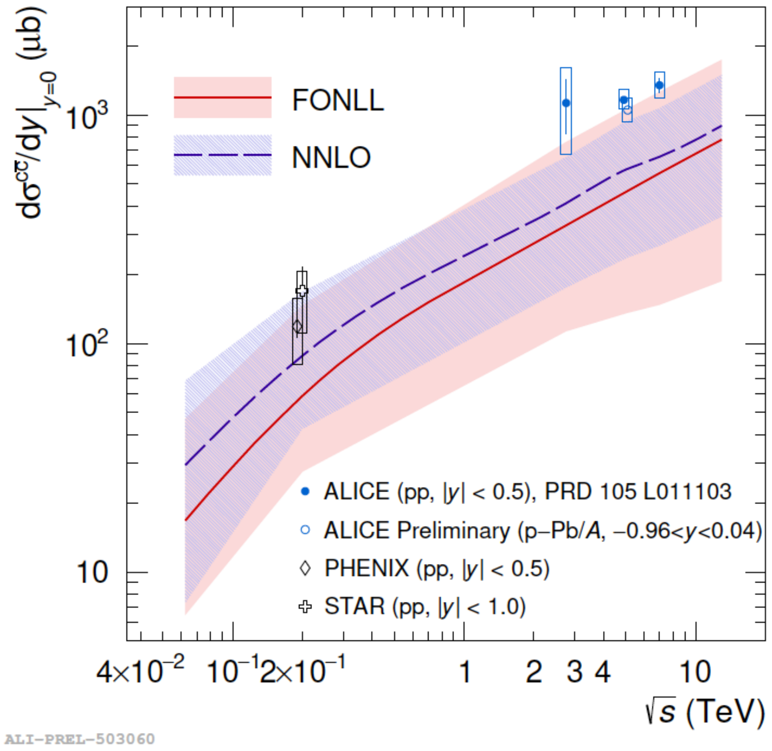

~40% increase driven by observed baryon enhancement

Data on the upper edge of FONLL and NNLO calculations

Significant baryon enhancement with respect to e^+e^- or e^-p

~30% c --> baryons in pp and pPb

Charm fragmentation functions are not universal

Hadronization of charm quarks from pp

H_c	$f(c \to H_c)[\%]$
D^0	$39.1 \pm 1.7(\mathrm{stat})^{+2.5}_{-3.7}(\mathrm{syst})$
D^+	$17.3 \pm 1.8(\mathrm{stat})^{+1.7}_{-2.1}(\mathrm{syst})$
D_s^+	$7.3 \pm 1.0(\mathrm{stat})^{+1.9}_{-1.1}(\mathrm{syst})$
Λ_c^+	$20.4 \pm 1.3(\mathrm{stat})^{+1.6}_{-2.2}(\mathrm{syst})$
Ξ_c^0	$8.0 \pm 1.2(\mathrm{stat})^{+2.5}_{-2.4}(\mathrm{syst})$
D^{*+}	$15.5 \pm 1.2(\mathrm{stat})^{+4.1}_{-1.9}(\mathrm{syst})$

Charm baryon/meson enhancement: pp→Pb-Pb

arXiv:2112.08156

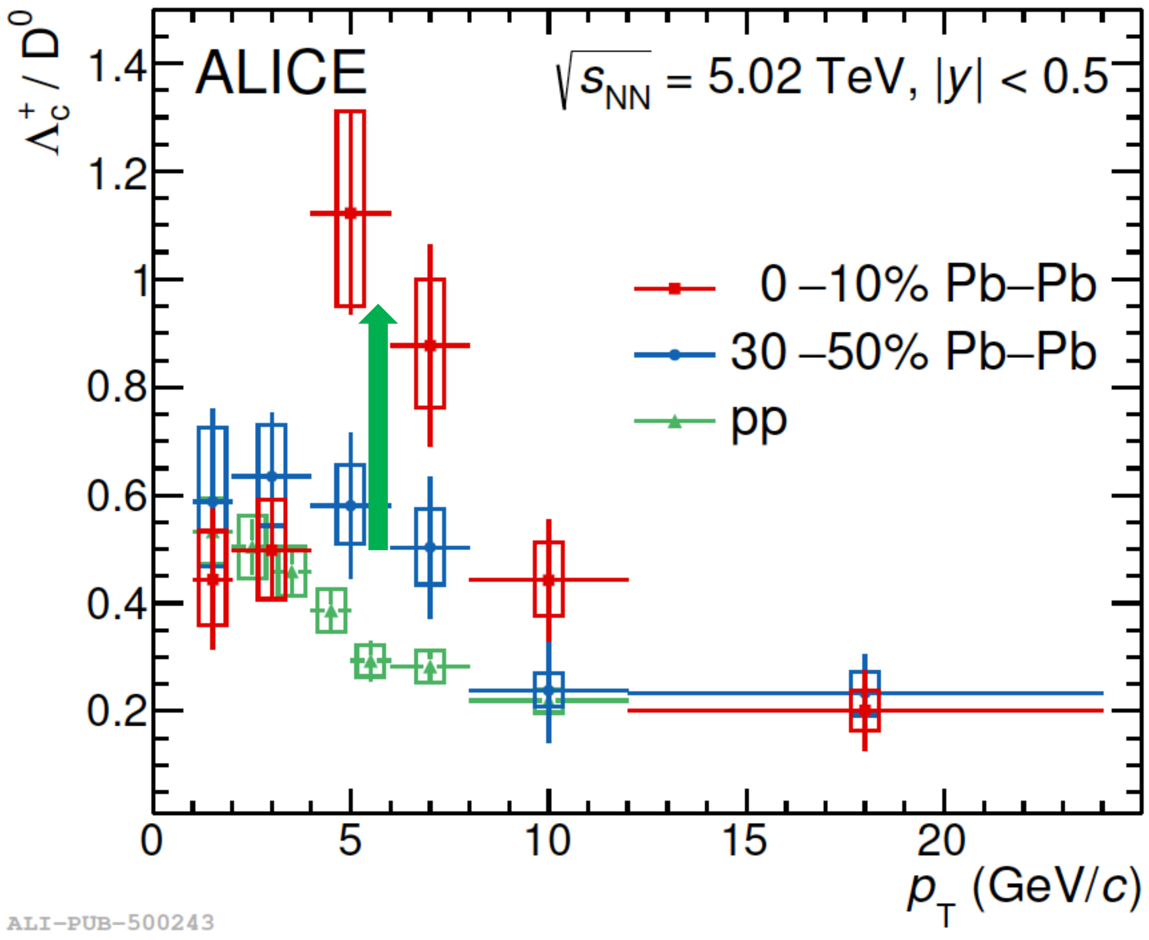

Additional dynamics in QGP

Λ_c / D^0 enhancement at intermediate p_T relative to pp

- similar to light flavor hadrons
- parton recombination at play also for c quarks
- mass-dependent p_T shift from collective flow

CERES dilepton spectrum

Phys. Lett. B666 (2008) 425

mass resolution 3.8%

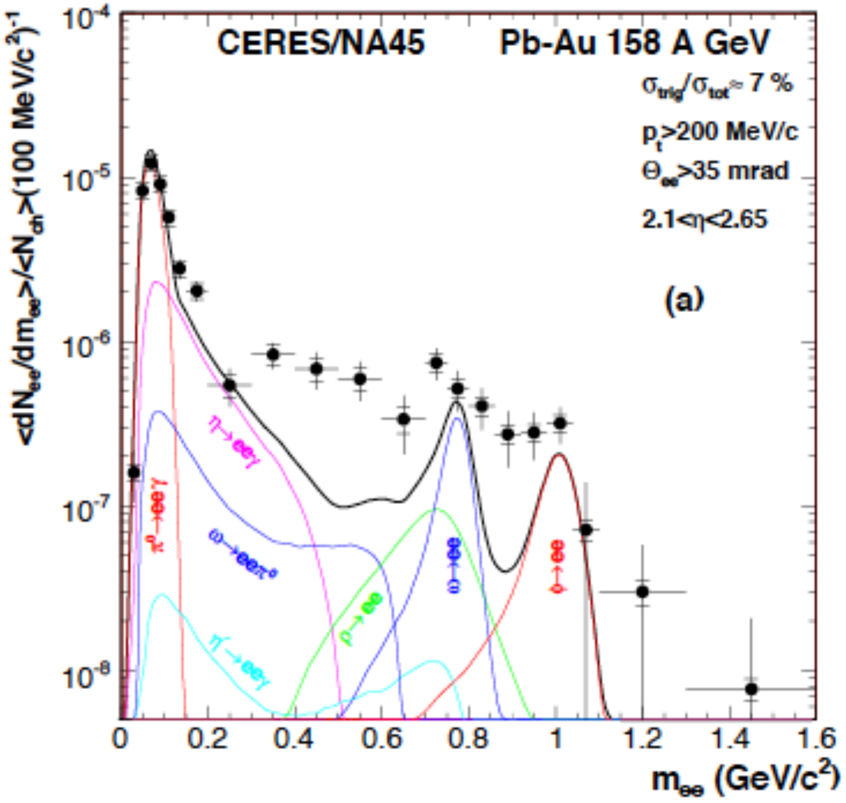

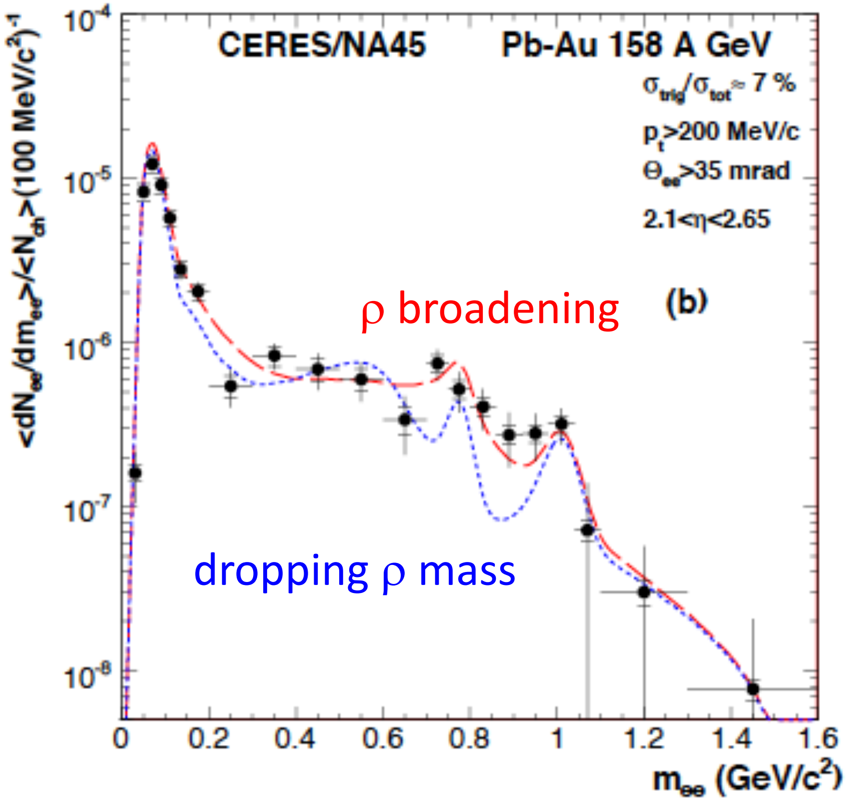

dilepton enhancement at
$0.2<m_{ee}<1.1$ GeV/c^2 :

2.45 ± 0.21 (stat.)
± 0.35 (syst.)
± 0.58 (cocktail)

Data favour ρ broadening
Most evident between ω - φ

CERES excess spectrum

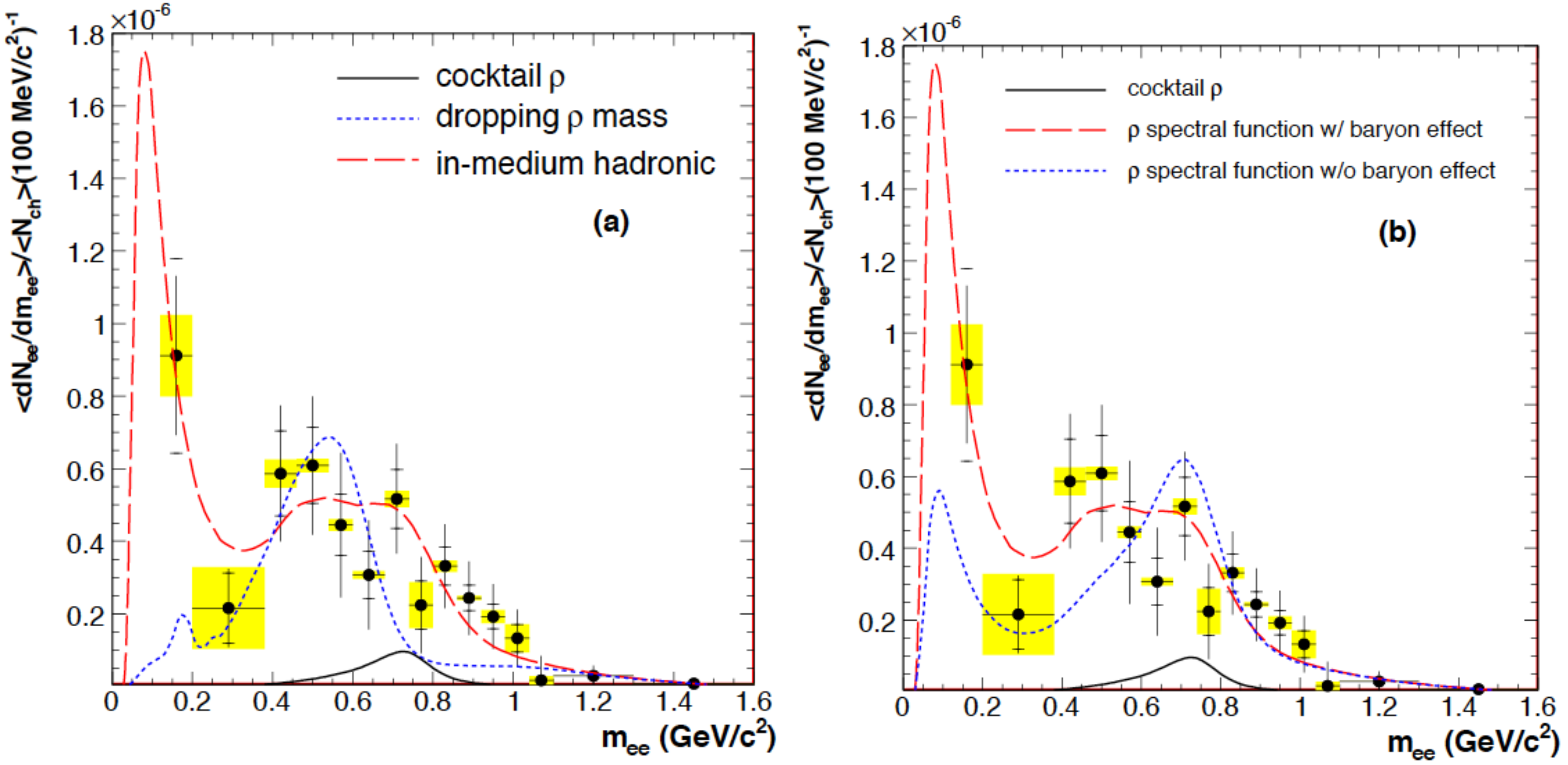

- contribution of ⍰ at freeze-out totally negligible, medium dominates by more than order of magnitude in central PbPb
- points at 0.7-1 GeV exclude dropping mass

Sensitive to role of baryons in modification

Production of e+e- pairs in Pb+Au 40AGeV

D. Adamova et al., Phys. Rev. Lett. 91(2003) 42301

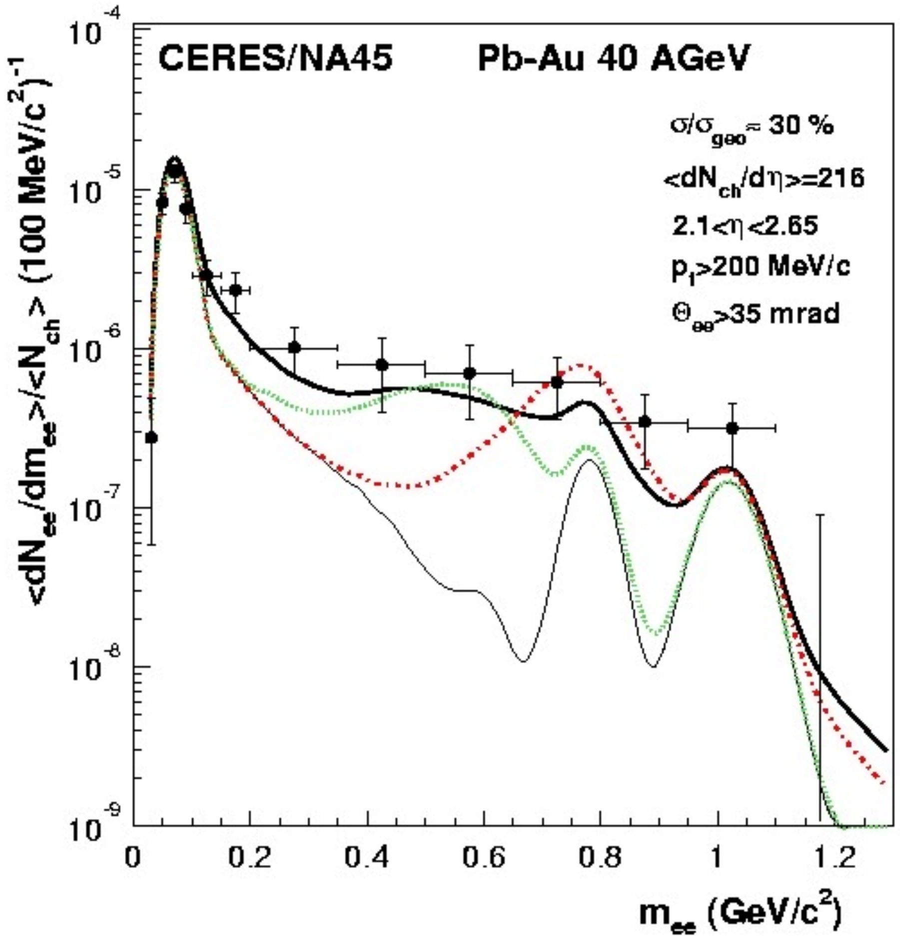

Calculations Rapp/Wambach

Including pion annihil. only

In-medium ρ modification

Dropping ρ mass

Enhancement even stronger at lower beam enery
5.9 ± 1.5 (stat) ± 1.2 (syst data) ± 1.8 (decays)
effect of baryon density?

NA60: Excess spectrum

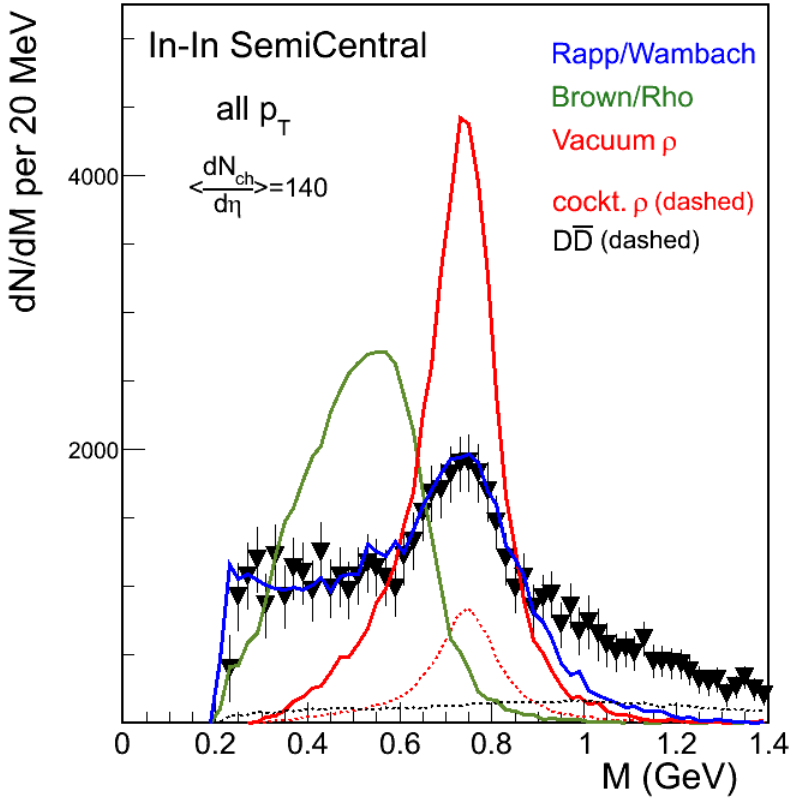

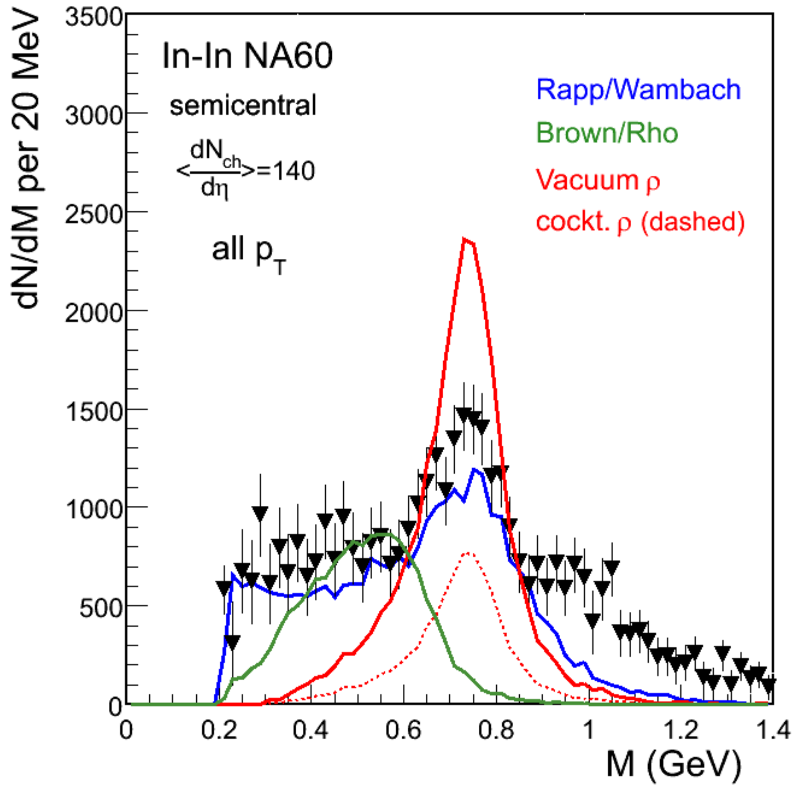

Models for contributions from hot medium (mostly $\pi\pi$ from hadronic phase)

- Vacuum spectral functions
- Dropping mass scenarios
- Broadening of spectral function

Data rule out mass drop of ρ meson

Dielectron production in central Pb—Pb at $\sqrt{s_{NN}}$ = 5.02 TeV

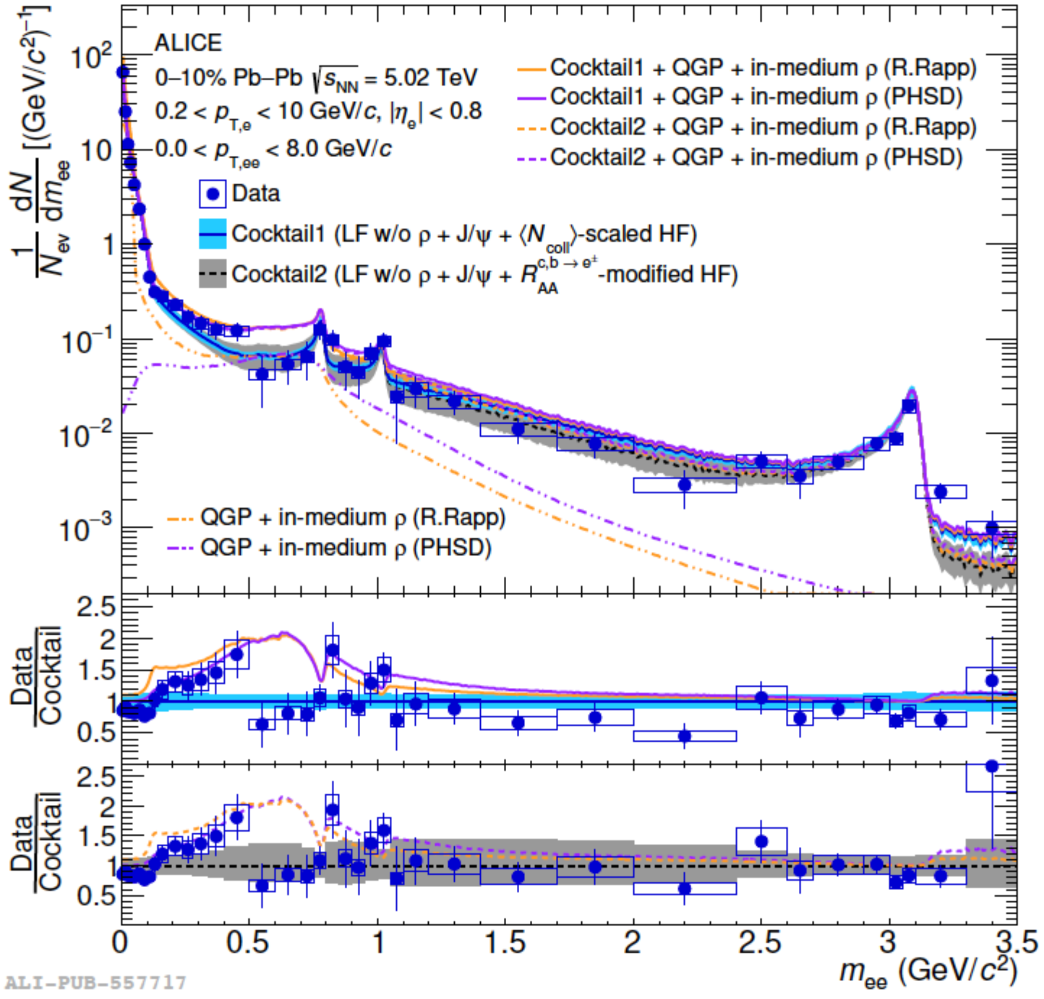

Comparison to hadronic cocktail, including:

- N_{coll} -scaled HF measured in pp at $\sqrt{s}$ = 5.02 TeV

Phys. Rev. C 102 (2020) 055204

⟶ Vacuum baseline

- Include measured R_{AA} of $c/b \to e^{\pm}$

Phys. Lett. B 804 (2020) 135377

⟶ Modified-HF cocktail

Intermediate-mass region (IMR) from 1.1 < m_{ee} < 2.7 GeV/c^2

⟶ Consistent with HF suppression & therm. radiation from QGP

Indication for an excess at lower mass

⟶ Compatible with thermal radiation from HG

Chiral Symmetry Restoration

- Spontaneous symmetry breaking gives rise to a nonzero 'order parameter'
  - QCD: quark condensate $\langle\bar{q}q\rangle \approx -250$ MeV^3
  - many models (!): hadron mass and quark condensate are linked
- Numerical QCD calculations
  - at high temperature and/or high baryon density
    → deconfinement and $\langle\bar{q}q\rangle \rightarrow 0$
  - approximate chiral symmetry restoration (CSR)
    → constituent mass approaches current mass
- Chiral Symmetry Restoration
  - expect modification of hadron spectral properties (mass m, width Γ)
- QCD Lagrangian → parity doublets are degenerate in mass